



OpenAIR@RGU

The Open Access Institutional Repository at Robert Gordon University

<http://openair.rgu.ac.uk>

Citation Details

Citation for the version of the work held in 'OpenAIR@RGU':

BAHMED, A., 2015. The design and synthesis of novel pro-drugs for the treatment of nephropathic cystinosis. Available from *OpenAIR@RGU*. [online]. Available from: <http://openair.rgu.ac.uk>

Copyright

Items in 'OpenAIR@RGU', Robert Gordon University Open Access Institutional Repository, are protected by copyright and intellectual property law. If you believe that any material held in 'OpenAIR@RGU' infringes copyright, please contact openair-help@rgu.ac.uk with details. The item will be removed from the repository while the claim is investigated.

THE DESIGN AND SYNTHESIS OF NOVEL PRO-DRUGS FOR THE TREATMENT OF NEPHROPATHIC CYSTINOSIS

AMINA BAHMED

Thesis submitted in partial fulfilment of the requirements of the
Robert Gordon University for the degree of Doctoral of
Philosophy

May 2015

DECLARATION

This thesis has been composed by myself, except where otherwise acknowledged. The work that is documented was carried out by myself. All verbatim extracts have been distinguished by quotation marks and the source of information specifically acknowledged.

Amina Bahmed

ACKNOWLEDGEMENTS

I would like to thank my principal supervisor Professor Donald Cairns for all his guidance, support, calmness, friendship and expert knowledge.

My sincere thanks must go to my second supervisor Dr Graeme Kay for his time, encouragement and for proof reading my thesis and providing me with invaluable advice.

I must also thank my co-supervisor Dr Phil Cox for his help with the crystallography.

Special thanks must go to Dr Rachel Knott for her help with the biology.

I would like to express my gratitude to Dr Hector Williams for his expert help with statistics.

I offer my sincere thanks to Professor Paul Kong for his expert advice.

I must thank John Wood and Kirstin Enright for their technical help and assistance.

Finally to my fellow PhD students for their camaraderie in particular Jessie, Evie, and Radisti.

For Yasmine and Aymen

Amina Bahmed

PhD

The design and synthesis of novel pro-drugs for the treatment of nephropathic cystinosis

ABSTRACT

Cystinosis is a metabolic disorder characterised by the abnormal accumulation of the amino acid cystine in cells leading to a slow destruction of all major organs. If patients diagnosed with cystinosis are untreated, death due to kidney failure ensues in the second decade of life. A number of studies have shown the ability of the drug cysteamine (Cystagon[®]) to lower cystine accumulation within cells resulting in reduced organ and tissue damage. Cysteamine therapy however, is associated with a number of side effects involving the gastrointestinal tract and the central nervous system. Most of these arise due to the large amount of cysteamine present in the stomach and gut following administration. In addition, cysteamine possesses an unpleasant taste and smell, resulting in poor patient compliance. In an attempt to overcome these problems, a number of pro-drug derivatives of cysteamine and cystamine, the disulfide analogue of cysteamine, have been synthesised and evaluated. Pro-drugs were synthesised using a route established in our laboratories. Briefly, cystamine dihydrochloride was basified and allowed to react with a number of cyclic anhydrides under basic conditions. The resulting di-acids were reacted with carbonyldiimidazole and monoBoc-cystamine to yield the desired pro-drugs. Removal of the tBoc-protecting group was achieved in a facile manner by use of trifluoroacetic acid to yield product. The efficacy of the synthesised pro-drugs was determined by incubation of 50 μ M compound in a suspension of cultured cystinotic fibroblasts, with 50 μ M cysteamine as control. Cell growth was measured at 72 h and the level of thiol determined.

All except one of the pro-drugs tested were significantly more effective than the control at lowering the cystine burden of the cells.

Further work will concentrate on repeating these studies and evaluating a more robust Structure Activity Relationship for these compounds.

The overall aim of all this work remains the production of an odourless, tasteless and orally active treatment for cystinosis and, if possible, improve on the current dosing regimen of every 6h. By using pro-drugs, cysteamine will be chemically camouflaged and hence, the side effects associated with its administration will be minimised or even entirely abolished.

Keywords: Nephropathic Cystinosis, Cystagon[®], cysteamine, cystamine, pro-drugs, multicomponent crystals, peptide synthesis.

ABBREVIATIONS

ACE	angiotensin converting enzyme
BBB	blood-brain barrier
BSA	bovine serum albumin
Ca	calcium
CDI	carbonyldiimidazole
CHCl₃	chloroform
CIP	Cahn-Ingold-Prelog
CNS	central nervous system
CPS	convergent peptide synthesis
CSD	cystine storage disease
DCC	dicyclohexylcarbodiimide
DCM	dichloromethane
dH₂O	distilled water
DIC	diisopropylcarbodiimide
DIPEA	N,N-diisopropylethylamine
DMSO-d₆	deuterated dimethyl sulfoxide
DMF	dimethylformamide
DSC	differential scanning calorimetry
EDTA	ethylenediaminetetraacetic acid
EMEM	Eagle's minimum essential media
ESRD	end stage renal disease
FBS	foetal bovine serum
Fmoc	fluorenylmethyloxycarbonyl chloride
Fmoc-OSu	9-fluorenylmethyl succinimidyl carbonate
GGT	gamma-glutamyl transpeptidase
GI	gastrointestinal
HCl	hydrochloride acid
Kg	kilogram
IR	infra-red spectroscopy
L-BAPNA	Na-Benzoyl-L-arginine p-nitroanilide hydrochloride
LMW	low-molecular weight

LSD	lysosomal storage disease
MeOH	Methanol
MgSO₄	magnesium sulphate
Mp	melting point
MS	mass spectrometry
NaBH₄	sodium borohydride
NaOH	sodium hydroxide
NMR	nuclear magnetic resonance
PBS	phosphate buffer saline
PO₄	phosphate
PPI	proton pump inhibitor
Ppm	parts per million
Rpm	revolutions per minute
RT	room temperature
SPPS	solid phase peptide synthesis
Tboc	Di-ter-butyl dicarbonate
TBTU	N, N,N',N'-Tetramethyl-O-(benzotriazol-1-yl)uroniumtetrafluoroborate
TFA	trifluoroacetic acid
WBC	White Blood Cells

CONTENTS

Declaration	2
Acknowledgements	3
Dedication	4
Abstract	5
Abbreviations	7
CHAPTER 1 Introduction	15
1.1. Nephropathic cystinosis	16
1.1.1. Background and Historical Aspects	16
1.1.2. Epidemiology of Cystinosis	22
1.1.3. Aetiology of Cytinosis	22
1.1.4. Cystinosis sub-categories	23
1.1.5. Symptoms of Cystinosis	24
1.1.6. Impact of the disease on the kidneys	26
1.1.7. Impact of the disease on the eyes	28
1.2. Genetics	29
1.3. Diagnosis	31
1.4. Treatment and prevention of early manifestations	31
1.4.1. Cysteamine	33
1.4.2. Problems associated with cysteamine treatment	37
1.5. Pro-drug approach	39
1.6. Research Progress	48
1.7. Aims of Project	50
CHAPTER 2 Multicomponent Crystals	52
2.1. Multicomponent crystals	53
2.1.1. Introduction	53
2.2. Materials and Instrumentation	59
2.2.1. Materials	59
2.2.2. Instrumentation	59

2.3. Methods	59
2.3.1. Slow Evaporation Technique	59
2.3.1.a. General Preparation Method for Cystamine Adipate, Cystamine 2,6-Dihydroxybenzoate, Cystamine Glutarate, and Cystamine 3-Nitrobenzoate from Cysteamine	59
2.3.1.b. General Preparation of Cysteamine Bitartrate Monohydrate (Cysteamine Hydrogen Tartrate) [1] from Cysteamine	60
2.3.1.c. General Preparation of Cystamine Tartrate [2] and Cystamine Bitartrate Dihydrate (Cystamine Hydrogen Tartrate Dihydrate) [3]	60
2.3.2. Melting Point Determination	61
2.3.3. Differential Scanning Calorimetry (DSC)	61
2.3.4. Infra-Red (IR) Spectroscopy	61
2.3.5. X- Ray Crystallography	62
CHAPTER 3 Experimental	64
3.1. Synthesis of Novel Cystamine Pro-drug Derivatives	65
3.1.2. Materials	65
3.1.2.1. Instrumentation	65
3.1.3. Methods	67
3.1.3.1. Synthesis of Cystamine Pro-drugs Derivatives [1-4]	67
3.1.3.1.1. Synthesis of Cystamine - Succinate (Pro-drug 1)	67
3.1.3.1.1.a. Synthesis of N,N'-Disuccinoylcystamine - Diamide (A)	68
3.1.3.1.1.b. Synthesis of Imidazolide Derivative (1)	68
3.1.3.1.1.c. Deprotection of Pro-drug (1)	69
3.1.3.1.2. Synthesis of Cystamine Glutarate – Pro-drug (2)	69
3.1.3.1.2.a. Synthesis of N,N'-Diglutaroylecystamine - Diamide (B)	70
3.1.3.1.2.b. Synthesis of Imidazolide Derivative (2)	70
3.1.3.1.2.c. Deprotection of Pro-drug (2)	70
3.1.3.1.3. Synthesis of Cystamine Citraconate – Pro-drug (3)	71
3.1.3.1.3.a. Synthesis of N,N'-Citraconoylcystamine - Diamide (C)	71
3.1.3.1.3.b. Synthesis of Imidazolide Derivative (3)	71
3.1.3.1.4. Synthesis of Cystamine Maleioate – Pro-drug (4)	72
3.1.3.1.4.a. Synthesis of N,N'-Maleioylecystamine - Diamide (D)	72
3.1.3.1.4.b. Synthesis of Imidazolide Derivative (4)	72

3.2. Synthesis of Novel Cystamine Pseudo-Peptides	73
3.2.1. Materials	73
3.2.2. Methods	75
3.2.3. Characterisation and Identification of Novel Pseudo-Peptides	75
3.2.4. Solid Phase Peptide Synthesis using 1, 3-Diaminopropane trityl resin (DAP)	75
3.2.4.1. Synthesis of Fmoc-2[cystamine-succinic]-DAP	75
3.2.4.1.1. Resin swelling	75
3.2.4.1.2. Method A: Peptide Coupling	75
3.2.4.1.3. Method B: Kaiser Test	76
3.2.4.1.4. Method C: Amino Group Deprotection	76
3.2.4.1.5. Method D: Peptide Cleavage	76
3.2.4.2. Synthesis of Fmoc-3[cystamine-succinic]-DAP	77
3.2.4.3. Synthesis of Fmoc-[cystamine-glutaric]-DAP	77
3.2.4.4. Synthesis of Fmoc-2[cystamine-glutaric]-DAP	78
3.2.4.5. Attempted Synthesis of Fmoc-3[cystamine-glutaric]-DAP	78
3.2.4.6. Synthesis of Fmoc-4[cystamine-glutaric]-DAP	79
3.2.4.7. Synthesis of Fmoc-[cystamine-succinic-cystamine-glutaric]-DAP	79
3.2.5. Solid Phase Peptide Synthesis using H-D-Alanine-2 chlorotrityl resin	80
3.2.5.1. Synthesis of Fmoc-2[cystamine-succinic]-Alanine	80
3.2.5.2. Synthesis of Fmoc-2[cystamine-glutaric]-Ala	80
3.2.5.3. Synthesis of Fmoc-2[cystamine-succinic-cystamine-glutaric]-Ala	81
3.2.6. Solid Phase Peptide Synthesis using Lysine (Boc) ₂ chlorotrityl resin	81
3.2.6.1. Synthesis of Fmoc-2[cystamine-succinic]-(Boc-Lys)	81
3.2.6.2. Synthesis of Fmoc-2[cystamine-glutaric]-(Boc-Lys)	82
3.2.6.3. Synthesis of Fmoc-[cyst-succinic-cystamine-glutaric]-(BocLys)	82
3.2.7. Convergent Peptide Synthesis (CPS)	83
3.2.7.1. Synthesis of Fmoc-cystamine-succinic-DAP-succinic-cystamine-Fmoc	83
3.2.7.2. Synthesis of Fmoc-cystamine-glutaric-DAP-glutaric cystamine-Fmoc	83

3.2.7.3. Attempted synthesis of Fmoc-cyst-glutaric-DAP succinic-cystamine-Fmoc	84
3.2.7.4. Attempted synthesis of Fmoc-cyst-glutaric x 2-DAP glutaric-cystamine-Fmoc	84
3.2.7.5. Synthesis of Fmoc x2[cystamine-succinic] Lysine(Boc)Fmoc	85
3.2.7.6. Attempted synthesis of Fmoc x2[cyst-succinic]Lys(Boc) glutaric-cyst-Fmoc	85
3.2.7.7. Synthesis of Fmoc-cystamine-succinic-DAP (Fmoc(CS)-DAP)	86
3.3. Cell culture	87
3.3.1. Materials	87
3.3.2. Human cystinotic fibroblasts (GM00008)	87
3.3.2.1. Cell growth conditions	87
3.3.2.2. Routine subculture	88
3.3.3. Cell viability and proliferation	88
3.3.3.1. Trypan blue dye exclusion staining protocol	88
3.3.3.2. Alamar blue cell growth assay	89
3.3.4. Quantitative Determination of Cysteine in Samples	89
3.3.4.1. Thiol assay	89
3.3.4.2. Bradford protein determination in samples	91
CHAPTER 4 Results and Discussion	92
4.1. Multicomponent crystals	93
4.1.1. Results	93
4.1.1.1. Morphology of Novel Salts	93
4.1.1.1.a. Cystamine Adipate	93
4.1.1.1.b. Cystamine 2,6 Dihydroxybenzoate	94
4.1.1.1.c. Cystamine 3-Nitrobenzoate	94
4.1.1.1.d. Cystamine Glutarate	95
4.1.1.1.e. Cysteamine Tartrate Monohydrate	95
4.1.1.1.f. Cystamine Tartrate	96

4.1.1.2. Melting Point	97
4.1.1.3. Differential Scanning Calorimetry (DSC)	98
4.1.1.3.a. Cystamine Adipate	98
4.1.1.3.b. Cystamine 2,6 Dihydroxybenzoate	99
4.1.1.3.c. Cystamine Glutarate	99
4.1.1.3.d. Cystamine 3-Nitrobenzoate	100
4.1.1.3.e. Cysteamine Tartrate Monohydrate	100
4.1.1.3.f. Cystamine Tartrate	101
4.1.1.4. Principal IR absorbance bands	101
4.1.1.4.a. IR spectra of Cystamine Adipate	103
4.1.1.4.b. IR spectra of Cystamine 2,6 Dihydroxybenzoate	103
4.1.1.4.c. IR spectra of Cystamine Glutarate	104
4.1.1.4.d. IR spectra of Cystamine 3-Nitrobenzoate	104
4.1.1.4.e. IR spectra of Cysteamine Tartrate	105
4.1.1.4.f. IR spectra of Cystamine Tartrate	105
4.1.1.5. X-Ray Crystallography Data of Novel Salts	106
4.1.1.5.a. X-Ray Crystallography Data for Cystamine Adipate [1:1]	106
4.1.1.5.b. X-ray crystallographic data for Cystamine 2,6 Dihydroxybenzoate [1:2]	108
4.1.1.5.c. X-Ray Crystallography Data for Cystamine Glutarate [1:1]	110
4.1.1.5.d. X-ray crystallography data for Cystamine 3 Nitrobenzoate [2:4]	112
4.1.1.5.e. The crystal data for samples cysteamine tartrate monohydrate [1], cystamine tartrate [2], and cystamine bitartrate dehydrate [3]	114
4.1.1.6. Other carboxylic acids used as co-formers for co-crystal synthesis	119
4.1.2. Discussion	120
4.1.2.1. Cystamine Adipate	120
4.1.2.2. Cystamine 2,6 Dihydroxybenzoate	120
4.1.2.3. Cystamine Glutarate	121
4.1.2.4. Cystamine 3- Nitrobenzoate	121
4.1.2.5. Cysteamine Tartrate Monohydrate (1)	122
4.1.2.6. Cysteamine Tartrate Mixture	123

4.1.2.6.a. Cystamine Tartrate (2)	123
4.1.2.6.b. Cystamine Bitartrate Dihydrate (3)	123
4.2. Synthesis of novel cystamine Pro-drugs derivative	125
4.2.1. Instrumental Techniques for Identification and Characterisation of Derivatives	129
4.2.2. General synthesis Cystamine pro-drug derivatives 3, 7, 11, 14	130
4.2.2.1. Synthesis of Pro-drug (3)	135
4.2.2.2. Synthesis of Pro-drug (7)	136
4.2.2.3. Synthesis of Pro-drug (11)	137
4.2.2.4. Synthesis of Pro-drug (14)	140
4.3. Synthesis of Cystamine Pseudo-Peptides	141
4.3.1. General Synthesis	141
4.3.1.1. Synthesis using Solid Phase Peptide Synthesis (SPPS) and Convergent Peptide Synthesis (CPS)	143
4.3.1.2. Attempted synthesis using Convergent Peptide Synthesis (CPS)	148
4.4. Biological studies	149
4.4.1. Cytotoxicity	149
4.4.2. Effect of synthetic pro-drugs on levels of cystine	152
CHAPTER 5 Conclusions	156
5.1. Conclusion and future work	157
CHAPTER 6 References	159
Presentations and Publications	178
Publications	179
Conference Proceedings	179
APPENDICES	180

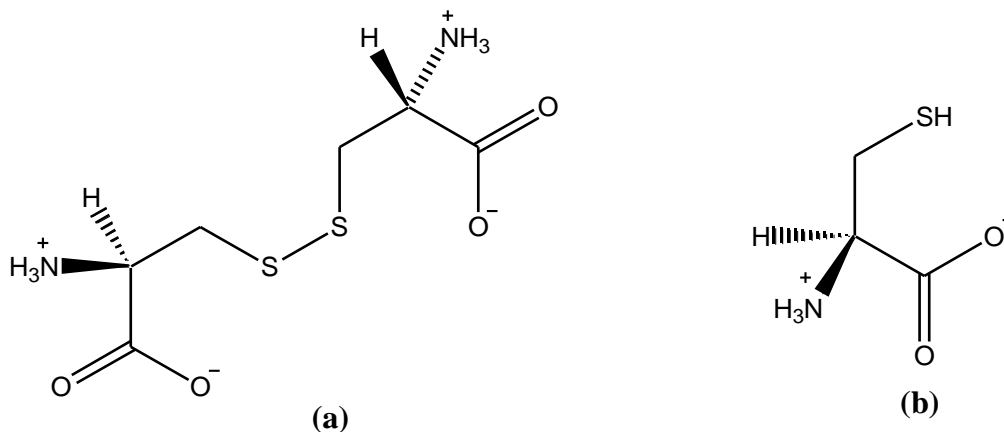
CHAPTER 1
INTRODUCTION

1.1. Nephropathic Cystinosis

1.1.1. Background and Historical Aspects

Cystinosis is a rare inherited autosomal recessive disorder, characterised by a high accumulation of the amino acid cystine in various organs and tissues, resulting in severe organ dysfunction.^{1,2}

Cystine is a non-essential amino acid for human development and was first discovered by Wollaston in 1810.³ The disulfide derivative cystine **(a)** is produced by the oxidation of two molecules of cysteine **(b)**. Sulfur bridges of this type occur naturally both within and between polypeptides, often found in extracellular proteins.³



Human proteins are composed of natural amino acids known as L-series amino acids (Figure 1). This is because the NH_3^+ group positioned on the left-hand side of the Fisher projection makes their configuration comparable to that of L-(-)-glyceraldehyde, where the most oxidised carbon is drawn at the top.⁴ (Figure 2) Furthermore, in the Cahn-Ingold-Prelog (CIP) convention, "all the common L-series amino acids are (S) unless the side-chain contains a sulfur atom."⁴ This is the case for the amino acid L-cysteine where one sulfur atom in the side-chain takes priority over the two

oxygens in the COO^- group. The CIP convention of L-cysteine is therefore (R).⁴ (Figure 3)

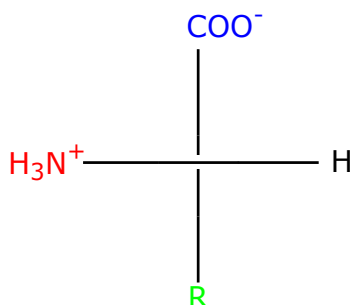


Figure 1.: Fisher projection of L-series amino acids

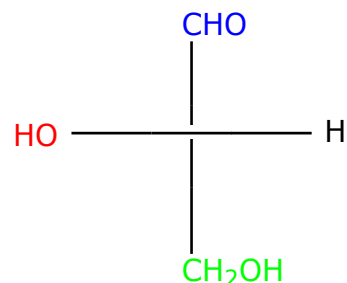


Figure 2.: L-(-)-Glyceraldehyde

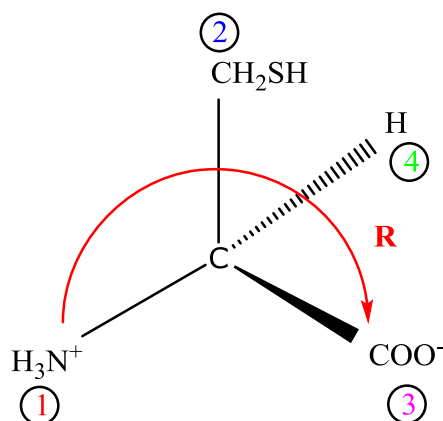


Figure 3.: Cahn-Ingold-Prelog convention for L-Cysteine.

Cystinosis was first reported in 1903 by the scientist Emil Abderhalden, following an autopsy performed on a child with severe growth failure. Abderhalden's findings revealed the presence of cystine crystals in the liver and spleen.⁵ In 1924, the observations made by Abderhalden were further developed by Lignac who identified frequent cases of children with profound rickets.⁶ Clinical understanding of the disease only matured in the early 1930s when cystinosis was first classified as a cystine storage disease (CSD) by the paediatrician Guido Fanconi^{7,8,9}, where an increase in the lysosomal cystine level to almost 100 fold was discernible in isolated fibroblasts and lymphocytes from cystinosis patients compared to normal individuals.^{7,10}

Cystine, unable to cross the cell membrane accumulates as crystals in various tissues excluding leucocytes.^{7,11}

Initially, it was anticipated that the severity of the phenotype would be relatively proportional to the content of intracellular cystine.^{7,12} However, an *in vitro* cystine loading replica of cystinosis failed to demonstrate this relationship between the build up of intracellular cystine level and renal tubular dysfunction.^{7,13}

Furthermore, irregularities in energy production in patients with cystinosis seemed to be linked to lysosomal cystine storage.⁷ This reduction in intracellular ATP levels^{14,15} which originates from a decrease in intracellular glutathione within the proximal tubule, triggers hypoxic stress followed by apoptosis, resulting in the progressive lesion of the glomerulotubular junction.^{16,17} The latter, described as the “swan-neck deformity” (Figure 4) is another common hallmark of cystinosis.¹⁸

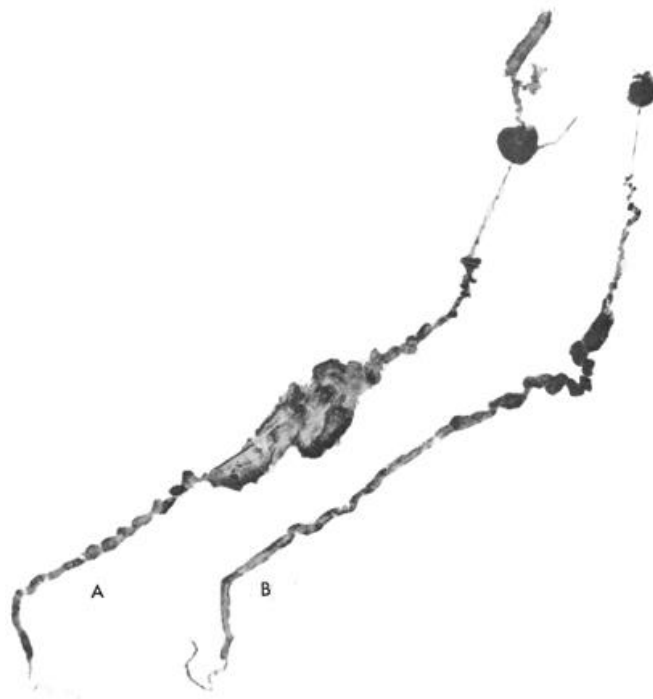


Figure 4.: Image illustrating a marked atrophy of proximal tubules (**A** and **B**) of microdissected nephrons removed from a cystinosis patient.^{19,20}

In normal physiological conditions, certain substances such as glucose and sodium are reabsorbed by the renal tubules and returned to the blood. However, Fanconi point out that in cystinosis the renal tubules fail to reabsorb these substances causing them to pass into the urine.⁶

Generally, this progressive renal tubular dysfunction will eventually lead to interstitial nephritis and ultimate necrosis²¹ resulting in only small quantities of dietary vitamin D from being reabsorbed. This in turn will prevent reabsorption of calcium and potassium ions.²²⁻²⁸

This tubulopathy was further confirmed by Debre *et al.* and De Toni who reported urinary secretion of organic acids and phosphates also known as rickets.^{6,29,30} Subsequently, Fanconi referred to cystinosis as "nephrotic-glycosuric dwarfism with hypophosphatemic rickets." (1936)^{6,31}

By 1952 Bickel *et al.* noted a relationship between Fanconi's syndrome and progressive kidney damage in a large number of cystinotic children.⁶

Ion exchange chromatography was first used in 1967 for amino acid analysis. This technique allowed the detection of infinitesimal amounts of cystine present in tissue samples of young cystinosis patients.^{8,32}

Subsequent studies such as the one by Schneider *et al.* reported an abnormality in heterozygotes. These findings were demonstrated by the measurements of the free cystine concentration in leucocytes of patients' parents which was about 6 times normal.³³

Moreover, Terec *et al.* noted a renal tubulopathy following a microdissection from two male siblings. The results suggested that the progression of the abnormality was inevitable.³⁴

In 1970 a medical innovation dramatically altered the course of research on cystinosis when Mahoney *et al.* not only proved an excellent renal allograft survival in four cystinotic children but clear evidence that glomerular and tubular cellular changes of cystinosis did not progress or recur.⁶ As a result of this outcome, the natural history of cystinosis was transformed.

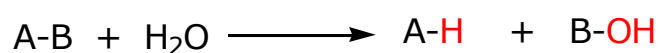
Up until the early 1970s when renal transplantation was first recognised for its health given, the prognosis of a child with cystinosis was poor with a lifespan of only 10 years. As a result of the progress in medical and surgical interventions, infantile cystinosis was no longer considered as a fatal disease.³⁵

Cystinosis was also classified as the first lysosomal storage disease (LSD) owing to a defective lysosomal membrane transport.⁷

Consequently, increased cystine concentration within cellular lysosomes will result in crystal formation causing organ and tissue damage including; the central nervous system (CNS), eyes, pancreas, thyroid, and principally tubular cell destruction, leading to Fanconi's syndrome.³⁶

As previously stated, Fanconi's syndrome will eventually lead to an increased damage to the renal tubules, preventing them from performing their normal reabsorptive function^{37,38} of sodium, bicarbonate, potassium, phosphate, glucose, amino acids, uric acid, low-molecular-weight proteins and peptides.³⁹ These losses will contribute to severe dehydration in infants.³⁶ Nevertheless, LSD was the first group of progressive disorder to be identified as a treatable disease.^{21,40} One of the characteristics of LSDs is the absence of signs of abnormality at birth. The first symptoms of glomerular dysfunction are displayed in children between the ages of 6-12 months to 2 years⁴¹ and if untreated, these children will develop an end-stage renal failure before their 10th birthday.²¹

Crystals of cystine (**a**) accrue predominantly within cellular lysosomes which are defined as small sacs each delimited by a single lipoprotein membrane. Their core functions are to digest, process and arrange cellular components. Lysosomes are found in virtually every living cell and contain several dozen different enzymes principally acid hydrolases catalysing reactions of the type:



These enzymes produced from the Golgi apparatus are responsible for the breakdown of virtually all large cellular molecules including nucleic acids, proteins, polysaccharides, and lipids, to low-molecular-weight products.^{42,43} Lysosomes (Figure 5) are also described as intracellular hydrolytic organelles where materials to be digested are incorporated within the same membrane-bounded compartments as the lysosomal enzymes. As result of this compartmentation, a low-pH environment needed for efficient activity of the enzymes hydrolases can be established.^{43,44}

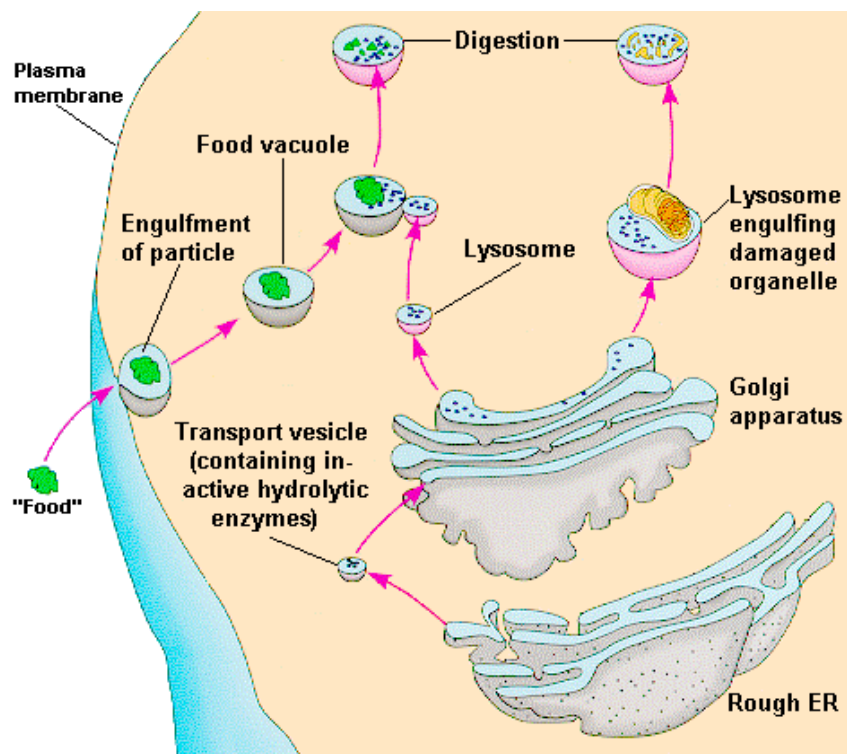


Figure 5.: Lysosome⁴⁵

1.1.2. Epidemiology of Cystinosis

The worldwide incidence of cystinosis is approximately 1:100,000 to 1:200,000 live births.^{8,46,47} These cases have been reported amongst all ethnic groups.^{7,48} A higher rate of 1 in 26,000 was found in the Western French Province of Brittany due to a founder effect. The incidence in the rest of France is 1 case per 326,440 population.^{7,48,49}

In particular, nephropathic cystinosis accounts for more than 95% of the cases, with an incidence of 1 case per 100,000 to 200,000 live births in North America.^{7,50,51,52} In the United States (U.S.) alone, around 15 new cases are diagnosed each year.² In Europe, cystinosis has been estimated to affect between 1:115,000 and 1:179,000 live births, with an estimate of 200 cystinotic patients in the United Kingdom (UK).^{7,50,51}

1.1.3. Aetiology of Cystinosis

Race

The physical characteristics in patients of European descent include blonde hair, blue eyes, and short stature. Cystinosis also occurred in other races around the globe including blacks and Hispanics.³⁵ (Figure 6)



Figure 6.: Patients with Nephropathic Cystinosis.⁸

Sex

A ratio of 1:4 male to female has been reported amongst cystinotic children.³⁵

Age

Children affected by this disease appear normal at birth but 6 to 12 months later progressively develop signs and symptoms of dehydration, acidosis, polydipsia, polyuria, failure to thrive, photophobia and rickets.^{53,54}

Poor muscular development has also been noted. Infants will display signs of renal tubular Fanconi syndrome in their first six months of life.²³

In the intermediate (adolescent) form, symptoms become obvious by age 8-12 years. Moreover, in this category, the disease progresses at a much slower pace.

The benign (adult) form of cystinosis is referred to as the ocular form due to the presence of crystals in the cornea. In this form kidneys are spared from the disease.^{35,52}

1.1.4. Cystinosis sub-categories

Cystinosis has been categorised into 2 general phenotypes, nephropathic and non-nephropathic cystinosis.^{35,52}

Based on both the severity of the symptoms and the age of onset, cystinosis has been further subdivided into three clinical forms.

(i) The late-onset or intermediate form is the more indolent form of the disease and affects only a minority of patients (~5%).^{8,55,56}

This nephropathic juvenile form of the disease is characterised by photophobia and mild proximal tubulopathy which slowly progress to chronic renal failure⁵⁷ after the age of 15.³⁵ The onset of the latter commonly occurs at the age of adolescence, regardless of displaying all the signs of the nephropathic form.⁷ Patients affected by this form of the disease display symptoms which are only limited to kidneys manifested by proteinuria and a milder form of the Fanconi syndrome.³⁵

(ii) The non-nephropathic cystinosis or the benign (ocular) form which generally occurs in adulthood is characterised by isolated photophobia with the absence of renal anomalies.⁵⁷ In this category, cystinosis is commonly detected in patients receiving treatment for photophobia. Fortunately for this group of patients, photophobia is less debilitating than in the nephropathic form.³⁵ The presence of corneal crystal deposits is confirmed by a routine slit-lamp examination. Additionally, cystine crystals have also been located in the bone marrow and leucocytes but were absent in both the retina and the kidney.^{35,55,58,5}

(iii) Nephropathic or classic infantile cystinosis is the most severe variant, where terminal renal failure is inevitable. In general, patients with infantile cystinosis are born from uncomplicated pregnancies with normal birth weight and length and do not display any clinical symptoms regardless of cystine being present in the uterus.⁷

The most common characteristics of nephropathic cystinosis are; poor growth, renal glomerular failure, and tissue and organ impairment such as the pancreas, CNS and thyroid.³⁶ Nephropathic cystinosis is also considered the major identifiable cause of renal Fanconi syndrome⁸; a clinical feature resulting from the accumulated cystine in the kidneys.³⁶

1.1.5. Symptoms of Cystinosis

The most common symptoms of cystinosis are summarised in Table 1.

Table 1.: Common symptoms of cystinosis

Organ/System	Symptoms
Kidney	Polyurea Polydipsia Renal failure
Hepatic	Hepatomegaly
Ocular	Photophobia Retinal blindness Visual impairment
Endocrine	Hypothyroidism Diabetes mellitus
Musculo-skeletal	Muscle wasting Rickets Swallowing difficulties Inter-costal muscle weakness
Reproductive	Male hypogonadism Azoospermia
CNS	Epilepsy mental deterioration Cerebella and pyramidal signs Stroke-like episodes
Other	Short stature

In nephropathic cystinosis certain factors responsible for multi-organ symptoms to progress from mild to severe include; patient's age at the time of diagnosis, age of patient when treatment is first initiated, and genetic

factors. In the past, clinical symptoms of nephropathic cystinosis would always follow a predicted chronological pattern.

At the age of 1 year infants display symptoms of poor growth, proximal tubular and Fanconi's syndrome followed by end stage renal disease (ESRD) at 10 years.^{8,35,53,55} However, the rate at which ESRD develops varies from one patient to another. Some patients will experience rapid deterioration of their renal function, whereas others reach a plateau.^{7,8}

Patients with nephropathic cystinosis experience other symptoms of constipation, poor/loss of appetite, craving of salty and hot and spicy foods, recurrent bouts of fever and manifestations of heat intolerance. These patients also go through failure in thriving which is due to secondary symptoms, namely; vomiting, anorexia, and difficulties in feeding. Infants between 6 to 12 months will experience growth deficit, and only 60% of the normal growth rate is seen after the age of 1 year.^{7,35,60}

1.1.6. Impact of the disease on the kidneys

Increased sodium chloride concentration resulting from impaired proximal tubules has been identified as a possible contributing factor to glomerular failure. The latter occurs when the activation of glomerular-tubular feedback mechanism is triggered causing the rate of glomerular filtration to decrease.^{7,61,62} This irreversible damage in the proximal tubules prevents water, electrolytes, bicarbonate, calcium, glucose, phosphate, carnitine, amino acids and tubular proteins and many other solutes from being reabsorbed in this nephron segment.^{5,7} This in turn has led to a number of pathological complications namely:

Hyperaminoaciduria has been recognised as the hallmark of Fanconi's syndrome.^{7,55,63,64,65} In general, over 98% of amino acids are reabsorbed by the proximal tubules. However, in children with cystinosis hyperaminoaciduria occurs as a result of a considerable loss of amino acids (6-16 times) greater than in normal children, whose daily excretion is only 1 to 6 mg per kilogram (kg) of body weight.⁶⁶

Glycosuria is also indicative of renal damage as normal serum glucose concentration suggests an abnormally low renal glucose threshold.⁶⁶

Additionally, owing to similarities in the urine output, the diagnosis of cystinosis can be masked by diabetes insipidus.⁵⁰

Metabolic acidosis is caused by a fall in serum bicarbonate concentrations due to a reduced threshold for bicarbonate reabsorption. The resulting bicarbonate excess in the distal tubule augments potassium excretion causing severe hypokalemia, leading to subsequent risks of developing cardiac dysfunction.^{7,63} Additionally, in children with cystinosis, this metabolic acidosis is partly accountable for their poor growth.^{7,63}

Hypovolemia occurs as a result of profound polyuria, polydipsia, dehydration and hypochloremic metabolic acidosis. Patients affected by this condition will require urgent medical treatment.⁷

Vitamin D-resistant hypophosphatemic rickets and **Osteomalacia** are conditions affecting children and adults respectively. These arise from a lack of reabsorption of calcium and phosphate by the proximal tubule.^{7,66}

Nephrocalcinosis and **renal stones** are likely to develop as a result of hyperphosphaturia and hypercalciuria.^{55,67,68}

Alpha-1-microglobulin, retinol-binding protein and beta-2-microglobulin are all low-molecular weight (LMW) proteins and are mainly excreted by cystinotic patients.^{7,55,65,69,57} Others such as large molecular proteins known as glomerular proteins have been found in the urine of patients with severe end stage glomerular function.⁶⁶ The presence of enzymes, hormones and immunoglobulins in the urine of patients suffering from Fanconi's syndrome has also been reported⁷ as well as a deficit in both plasma and muscle creatinine in children.^{7,71}

1.1.7. Impact of the disease on the eye

Cystine crystals were first identified by Burki in 1941, following a slit-lamp examination of the eye of a cystinosis patient.⁷² The crystals were described as crystalline deposits, evenly distributed in both the posterior sections (optic nerve and retina) and the anterior ophthalmic fragments (conjunctiva, iris, ciliary body and cornea).^{73,74,75,76} The crystals become visible at the age of 1 year and will continue to deposit progressively with age, becoming more dense and prominent especially in the cornea part of the eye with a ground glass opaque appearance.

(Figure 7).^{73,77,78}



Figure 7.: Corneal cystine crystals from patients with Cystinosis during slit-lamp examination ⁷⁹

This crystal growth results in major ocular complications mainly photophobia and, ultimately, blepharospasm causing great discomfort when in direct sunlight which in children can be very troublesome and debilitating.⁴¹

1.2. Genetics

The inheritance of an autosomal recessive disorder such as cystinosis will occur in a child when both parents are carriers of the abnormal gene. Due to the recessive nature of the gene, parents do not exhibit the disease but have the potential to pass it onto their offspring as shown in Figure 8.⁸⁰

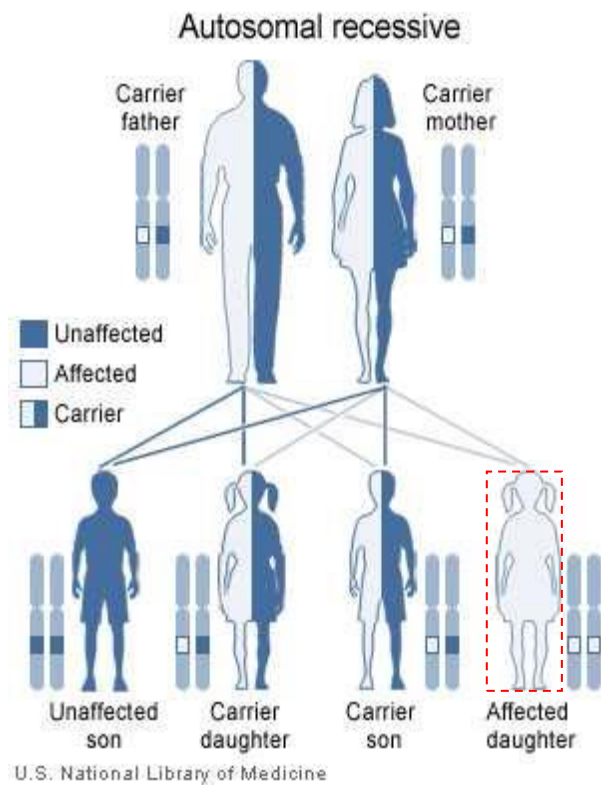


Figure 8.: Inheritance pattern of Cystinosis.⁸¹

This metabolic disorder arises due to mutations occurring in the *CTNS* gene found on chromosome 17p13 (Figure 9) coding for the lysosomal transport protein cystinosin.^{82,83}

These mutations have been reported in all cystinotic patients with the most common mutation being a 57-Kb deletion present in approximately 50% of cystinotic patients of Western European ancestry.^{83,84} In the United States of America and the Northern European population, this deletion present in the homozygous state, has been reported in almost 40% of cystinosis patients.⁸⁵ In 2004, the development of a fluorescent *in situ* hybridisation

test assisted in the detection of the 57-kb deletion with 100% specificity and 100% sensitivity.⁸⁶

Samples of chorionic villi or cultured amniocytes can be used to perform prenatal diagnostic tests.⁸⁶

Patients affected by the most severe form of the disease possess mutations on both alleles status of the *CTNS* gene and display multiple manifestations. The detection of these mutations in all forms of the disease confirmed their allelic status.⁸⁷ The normal function of this gene is to provide directions for the manufacture of the transport protein cystinosin which is situated inside the lysosomal membrane.

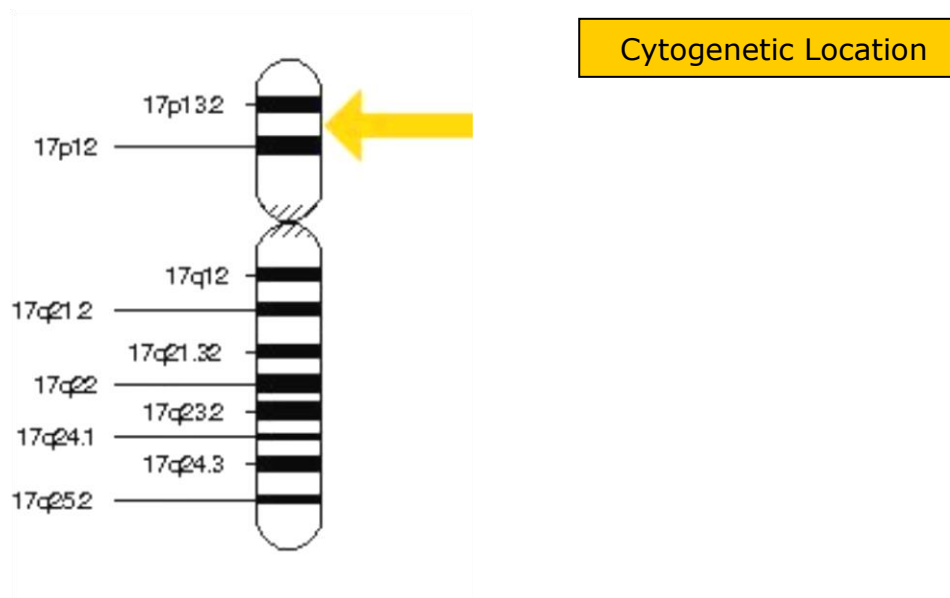


Figure 9.: Cytogenetic Location of chromosome 17p13 (*CTNS*)⁸⁸

Cystinosin (Figure 10) is a 367-amino acid protein with seven transmembrane domains and two lysosomal targeting motifs.⁸⁹ Cystinosin is specifically responsible for the export of the amino acid cystine across the lysosomal membrane and into the cytoplasm.^{11,90} This transport process is defective in cystinosis sufferers resulting in an accumulation of the poorly soluble cystine in the lysosomes.

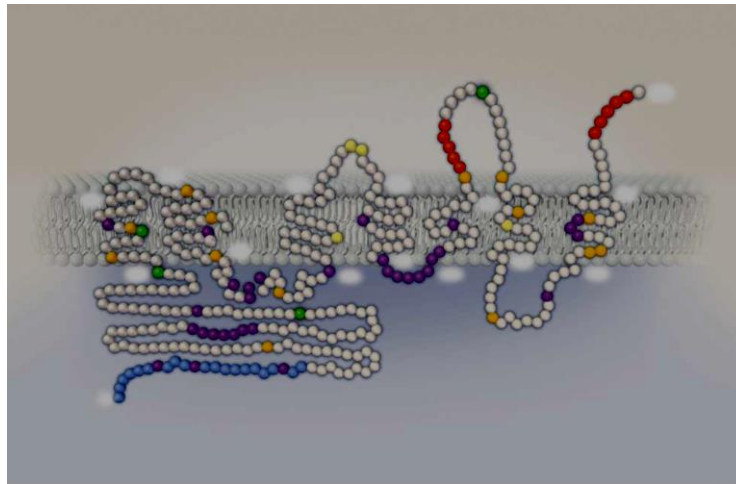


Figure 10.: Cystinosin in the lysosomal membrane ⁸

1.3. Diagnosis

The normal physiological values of cystine are ≤ 0.2 nmol half-cystine/mg protein, whereas the abnormal values range between 3.0 to 23 nmol half-cystine/mg protein.¹¹ Therefore, the markedly elevated levels of the intracellular leucocyte cystine play an important role in the definitive diagnosis of cystinosis. The detection of renal tubular Fanconi syndrome between the ages of 6 and 12 months, followed by photophobia and hypothyroidism by the age of 10 and finally renal failure by the age of 12 can also assist in the diagnosis of nephropathic cystinosis.⁹¹

In addition, the detection of corneal crystals by slit-lamp examination of the cornea is another diagnostic test for cystinosis.⁹² Tissue accumulation of cystine remains the diagnostic trademark of cystinosis.

1.4. Treatment and prevention of early manifestations

The goals of therapy in the management of nephropathic cystinosis seek to relieve the symptoms and to treat the underlying pathology. If patients diagnosed with cystinosis are untreated, death ensues in the second decade

of their life. The care of cystinosis patients involves the use of a number of therapeutic modalities:

Primarily and most importantly, excessive loss of fluids and electrolytes resulting from defective renal absorption (renal Fanconi syndrome) are replenished through adequate amounts of water, and supplementation with salts and minerals in particular citrate in order to alkalinise the blood.^{7,51,93,94}

Acidosis is controlled by a daily use of anions mainly bicarbonates, acetate or citrate salts (2-10 mEq/kg/day).^{7,71}

Metabolic acidosis can only be managed by either bicarbonate or citrate; supplementation with potassium is also required.^{7,95} Phosphate replacement therapy is also required with a daily supplementation of 1-3 g of neutral phosphate complemented with vitamin D for better absorption.⁷¹ Although thiazide diuretics have been successfully used in the past for the treatment of Fanconi's syndrome in order to increase proximal tubular reabsorption of bicarbonates, however, patients with cystinosis have not benefited from this therapy.⁷

Cystinosis patients often suffer from feeding difficulties and caloric intake can be problematic, nevertheless, the provision of essential nutrients for growth development has been made possible *via* a gastric tube. However, early withdrawal from this nutritional support is always recommended and has been proven possible with successful cystine depletion therapy.^{7,96}

Growth hormone therapy is also used to correct poor growth^{51,93,94,97} and has benefited children with cystinosis as it helped enhance their development.⁹⁸ These hormones are not usually required for those who are well-treated as they have shown good growth. It has also been reported that the use of these hormones assisted in the increase of phosphate reabsorption.^{7,63}

Severe glomerular proteinuria can be alleviated with the use of angiotensin converting enzyme (ACE) inhibitors, but caution should be shown when using this class of drugs due to blocking volume compensation mechanisms.^{7,96} Patients with ESRD who are awaiting renal transplantation will temporarily undergo both hemodialysis and peritoneal dialysis.^{7,96}

A typical treatment regimen in cystinosis will involve an exhaustive list of medication including, levothyroxine used for the treatment of hypothyroidism, glibenclamide and insulin to control diabetes, sodium valproate for epilepsy, ciclosporin, and prednisolone.⁵¹

These conditions occur secondary to cystinosis due to cystine accumulation in the thyroid, pancreas, and central nervous system.

Most children will also be supplemented with solutions of calcium (Ca) and phosphate (PO₄) in order to prevent rickets.

Worldwide, a few female cystinosis patients have had successful pregnancies, but there have been no reports of males cystinosis patients known to have the ability to cause pregnancy. A study, in which seven male cystinosis patients (19-43 years) were treated with cysteamine, was carried out in order to analyse the fertility status in adults.⁹⁹

The findings of semen analysis performed on five patients displayed azoospermia, and the biopsy of one patient's testis revealed spermatogenesis which may offer male cystinosis patients the prospect of producing their own progeny *via in vitro* fertilisation.⁹⁹

1.4.1. Cysteamine

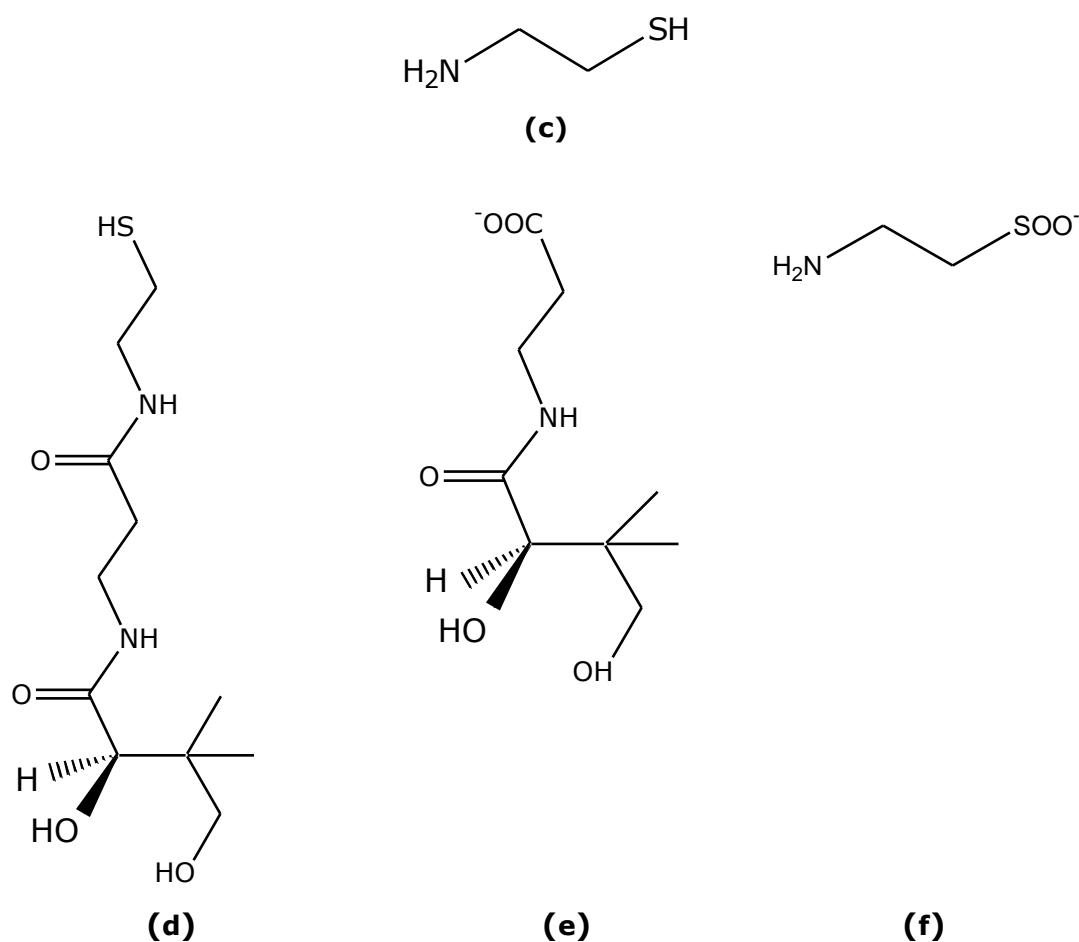
Currently the only treatment used to deplete cystine is the oral administration of cysteamine bitartrate (Cystagon®); the only commercially marketed drug for the treatment of cystinosis and has been used effectively since the 1970s.

In the early 1980s, studies have shown that the introduction of cysteamine for the treatment of cystinosis has helped not only to reduce the decline in renal function but also to improve linear growth in diseased children even with a deficiency in renal tubule transport.³⁵ As a result these patients have reached adulthood and even had children.^{21,100}

In 1987 a study involving 93 children treated with cysteamine was conducted in order to demonstrate and support these findings. The results were conclusive and demonstrated that cysteamine was also very effective at depleting intracellular cystine.⁹⁴

In 1994, Cystagon[®] was also approved by the Food and Drug Administration in the USA.¹⁰¹

Cysteamine also known as mercaptamine or β -mercaptoethylamine, MEA **(c)** occurs naturally from the breakdown of pantotheine **(d)** to pantothenic acid **(e)** and cysteamine which then undergoes oxidation by the enzyme cysteamine oxidase to produce hypotaurine **(f)**.¹⁰²



Cysteamine present as the bitartrate salt is a very stable, water-soluble drug available in capsules containing the equivalent of 50 mg or 150 mg of cysteamine free-base.¹⁰¹ The amino-thiol cysteamine works by lowering intracellular cysteine levels due to the formation of a disulfide bond between cysteamine and cysteine giving rise to a cysteamine-cysteine mixed disulfide.¹⁰³ (Figure 11) The resulting compound is isosteric with lysine and

may egress the lysosome using the lysine transport protein which remains intact in cystinosis.¹⁰³ Cysteamine-cysteine exits the lysosomes within a cell *via* the lysine excretion pathway hence, removing almost all the lysosomal cysteine from cystinotic cells.^{7,10,104}

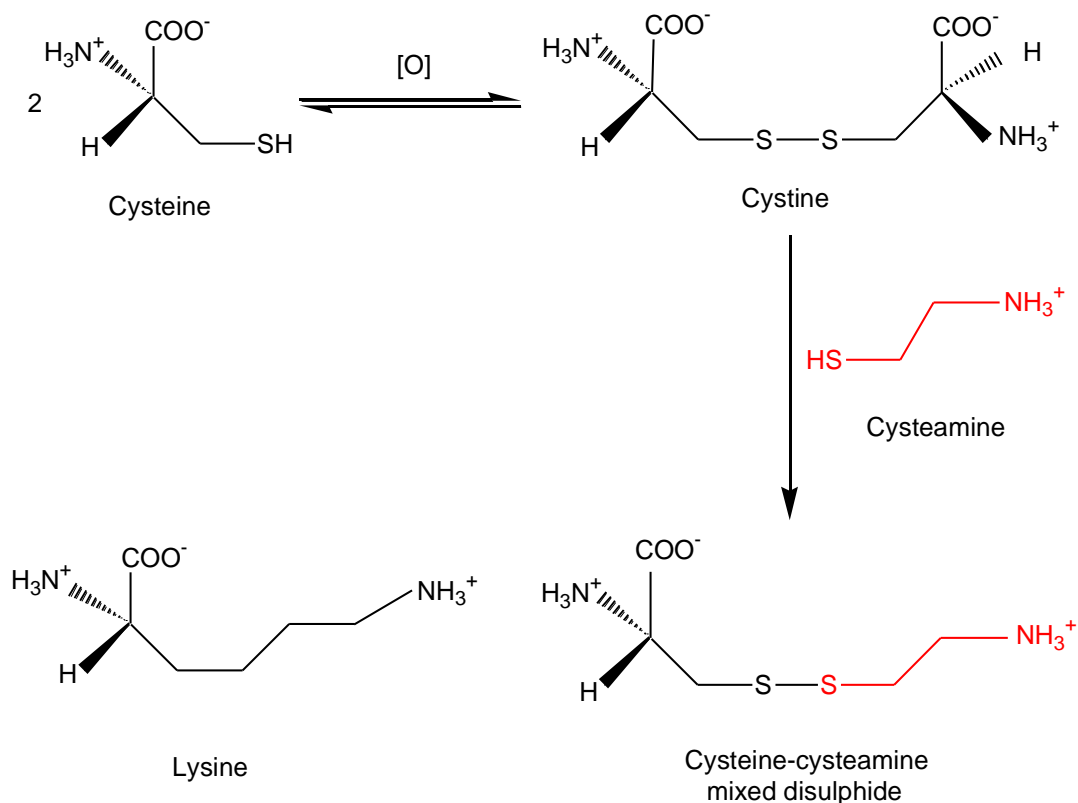
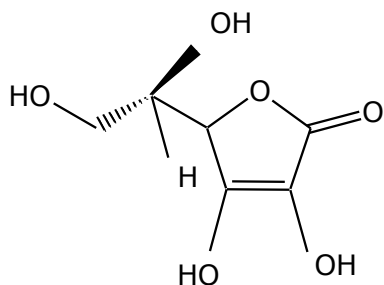


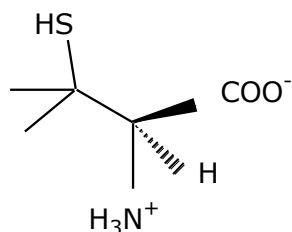
Figure 11.: The mode of action by which cysteamine exists the lysosomes *via* the lysine transporter.

Cysteamine has a half-life of 1.88 hours,¹⁰⁵ reaching high blood level peaks at 1h, and a subsequent rapid decline.²¹ As a result of this a nightly oral dose should not be omitted, however, this can have an impact on the quality of life of both the patients and their families.¹⁰⁰

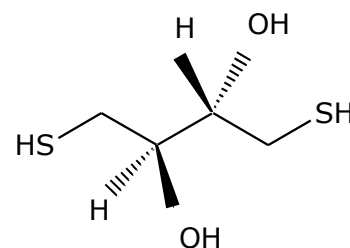
Studies have shown that cysteamine can also successfully deplete up to 95% of cystine from cells in the kidneys, liver, pancreas, lung and spleen¹⁰⁴ when compared to ascorbic acid (**g**)^{106,107}, penicillamine (**h**)^{108,109,110} and dithiothreitol (**i**).¹¹¹



(g)



(h)

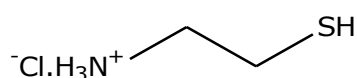


(i)

The ability for this drug to remove almost 90% of the cystine content from the cystinotic cells fails to prevent or reverse the Fanconi syndrome but reduces glomerular damage, and delays the onset of renal failure (ESRD)^{41,53} as well as the necessity for renal allograft^{7,53}. In order to prevent renal failure, hypothyroidism and a host of non-renal complications, early lifelong and diligent cysteamine therapy should be considered immediately after diagnosis and should be initiated to all patients regardless of their age and transplantation status.^{7,53,105,112}

In cystinosis the treatment is only effective if cysteamine is frequently administered (every six hours) to children and adults in a capsule form and at a dose of 60-90mg/kg/day. Adults can take a dose of 500mg every six hours and up to a maximum dose of 750mg.¹¹³

In infants cysteamine is also given every six hours as a solution of cysteamine hydrochloride **(K)** at a dose of 50mg/ml.⁷



(k)

The regular use of cysteamine is also of a paramount importance as this will enhance growth as well as depleting cystine in muscle parenchyma.^{94,112,114,115}

Following an oral dose of cysteamine (5-6 hours) leucocyte cystine levels are measured so that they can be used to help evaluate the efficacy of the treatment and to establish appropriate dosing regimen.⁷

Children with cystinosis who have received early and diligent treatment have demonstrated a development in their renal capacity up to age of 3 years, and did not require renal transplantation. Increased life expectancy for up to 20 years has also been reported.^{7,8} Moreover, the growth profile of the children has too been improved which gave a good incentive to the importance of an early provision of diagnosis and treatment as well as a regular and compliant regimen.

Topical cysteamine hydrochloride eye drops have been used as an add on therapy and must be applied every 1 to 2 hours due to a very short residence time.^{116,117} Their

use was first introduced in 1987 by both Gahl *et al* and Dufier *et al*.^{118,119}

This topical therapy is required to dissolve corneal crystals³⁰ and is usually initiated for school age children and has been proven effective in improving photophobia within few weeks of commencing the treatment.^{7,73}

1.4.2. Problems associated with cysteamine treatment

One of the major problems associated with the administration of cysteamine is the extensive loss of the drug due to first-pass metabolism. Cysteamine and can also be bound to circulating proteins preventing it from being absorbed.^{100,120} However, a successful treatment outcome will require high blood levels of cysteamine which can only be achieved by high doses of the administered drug. In addition, the low molecular weight thiol has raised a number of pharmaceutical challenges because of its offensive taste, smell and a variety of unpleasant gastrointestinal (GI) side effects caused by a large production of gastric acid resulting in nausea, and vomiting which regularly occurs following drug ingestion.^{51,100,121,122,123,124} Loss of appetite has also being noted.^{51,121,122,123}

Nausea is the most frequent side effect and can be successfully alleviated however, by the use of antiemetics and should be initiated as early as possible into the treatment. Other drugs such as H₂ blockers or a proton pump inhibitor (PPI) have also been used to combat GI side effects.^{7,112}

Other problems associated with the treatment are the excretory pathways of cysteamine from the body which include the breath and sweat, resulting in halitosis and an unpleasant body odour. In addition to the side effects of cysteamine and its malodorous metabolites (H₂S, CH₃SH), frequent administration (every 6 hours) of Cystagon[®] can impact upon patient compliance especially when patients reach adolescence.⁵¹ However, it has been reported that a third of cystinosis patients rigorously comply with this dosage regimen.^{7,112}

Unfortunately this treatment is not curative of the disease as it will progressively cause death due complications including, diabetes, and difficulties in swallowing, cardiovascular disease, muscular wasting and damage in both the cornea and retina but in most cases sepsis or respiratory problems will be the main cause of death.^{8,21,125,126} The development of these serious complications arises from cystine accumulation in various non-renal organs such as the eye, pancreas, liver, brain, thyroid, and muscles.

Despite the difficulties that these patients face, their life expectancy has been improved however, and some even survive into their fifth decade of life with the ability to engage in a normal fulfilling lifestyle.³⁵

A continual cysteamine treatment is imperative post kidney transplant due to a build up of crystals in other tissues and organs^{40,100}, by host macrophages. As a result of this overabundance in crystals, multiple organ systems are damaged, causing major complications including difficulty in swallowing occurring due to generalised muscular wasting, diabetes, and cardiovascular disease. Crystal overload in both the cornea and retina have also caused problematic complications to the patients especially to their quality of life.^{125,127,128}

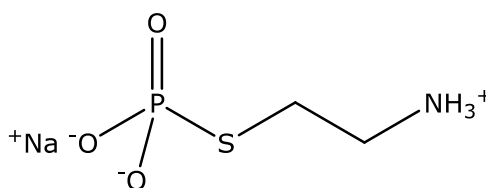
Signs of cerebral deterioration were noted in patients reaching their twenties, displaying a mental decline, pyramidal signs and severe visual

memory loss but only for a short-term.⁴⁰ Other symptoms include severe impairment of spatial processing functions.¹²⁹ In addition, it has been reported that cystinosis patients are more likely to have a lower IQ than their parents and siblings.¹³⁰ Academically, these patients experience difficulties, particularly in the areas of mathematic and spelling.¹³¹

1.5. Pro-drug approach

In order to overcome the problems associated with the oral administration of cysteamine, numerous studies have been undertaken, in which a number of cysteamine pro-drug derivatives have already been designed, synthesized and currently evaluated for their ability to deplete cysteine or cystine in cultured cystinotic cells.⁵¹ These pro-drugs work by masking the thiol functional group responsible for the unpleasant taste and smell of the drug, increasing the molecular weight of cysteamine thus reducing its volatility and also by improving its lipophilicity.

An example of this type of studies was the one conducted by Gahl *et al.* in 1988, when the pro-drug phosphocysteamine **(I)** was considered as a potential alternative to cysteamine.¹³²



(I)

The study examined the comparison of a typical cysteamine treatment and phosphocysteamine. The findings showed that by masking the thiol group responsible for the offensive taste and smell, the side effects were reduced. An increase in bioavailability was also reported as a result of reduced protein binding. It was suggested that the pro-drug phosphocysteamine becomes active by intracellular dephosphorylation, thus directly targeting the lysosomal cystine stores. In conclusion, this study demonstrated a degree

of similarity between cysteamine and the pro-drug in terms of treatment efficacy.

Pro-drugs are pharmacologically inactive compounds, converted in the body either spontaneously or by metabolic biotransformation to release the parent drug. This conversion is often carried out by enzyme-controlled metabolic reactions and can either occur before, during or after absorption.⁵¹

Pro-drugs are extremely valuable composites to use when the parent drug is ineffective, toxic or defective at reaching its site of action. In addition, enhanced efficacy and reduced toxicity can both be achieved by pro-drugs through control of absorption, blood levels, metabolism, distribution and cellular uptake.

“Pro-drugs are designed to overcome pharmaceutically and/or pharmacokinetically based problems associated with the parent drug molecule that would otherwise limit the clinical usefulness of the drug.”¹³³

The underlying principles of the pro-drug approach are to:¹³⁴

- Increase chemical or biological stability of a drug.
- Reduce drug toxicity.
- Make the drug more patient compatible by improving the taste.
- Achieve site specific delivery.
- Alleviate pain caused by parenteral administration of a drug.
- Modify the length of the time of the drug’s duration of action.
- Increase lipid or water solubility.

Pro-drugs are broadly classified into two groups, namely, *bioprecursor* and *carrier* pro-drugs. Bioprecursor pro-drugs are converted into their active compounds involving a variety of metabolic reactions including, oxidation, reduction and phosphorylation. Figures 12 and 14 illustrate a summary of the overall process.

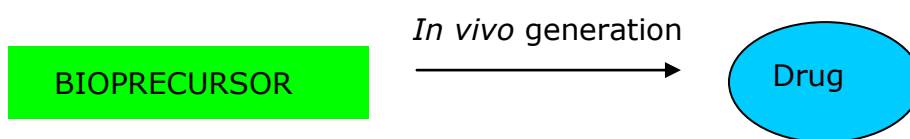


Figure 12.: Bioprecursor Pro-drugs.¹³⁴

Levodopa (**m**) is an antiparkinsonian agent used in the treatment of Parkinson's disease, a condition caused by a deficiency in Dopamine (**n**). This dopaminergic drug is a classic example of a bioprecursor pro-drug. Unlike levodopa dopamine is less likely to cross the blood-brain barrier (BBB) due to its insufficient lipophilicity. Levodopa is more able to cross the BBB, not only because it is polar, but because it is an amino acid and able to be transported across the blood-brain barrier and into the site of action (brain) by amino acid transporters. Subsequent enzymatic decarboxylation of levodopa will result in the release of active dopamine.¹³⁵ (Figure 13)

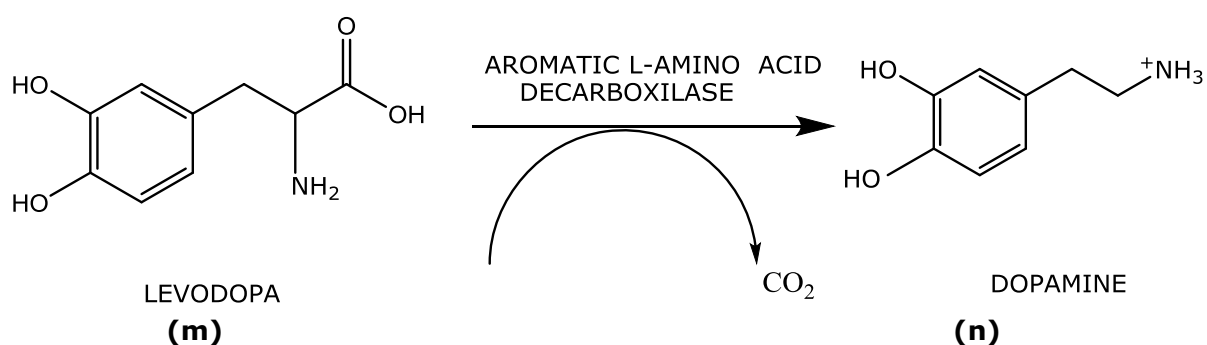


Figure 13.: Metabolic pathway for Dopamine formation

Carrier pro-drugs differ from bioprecursor pro-drugs in that they are formed by combining an active drug with a carrier species creating a compound with the desired chemical and biological characteristics.¹³⁴ (Figure 14)

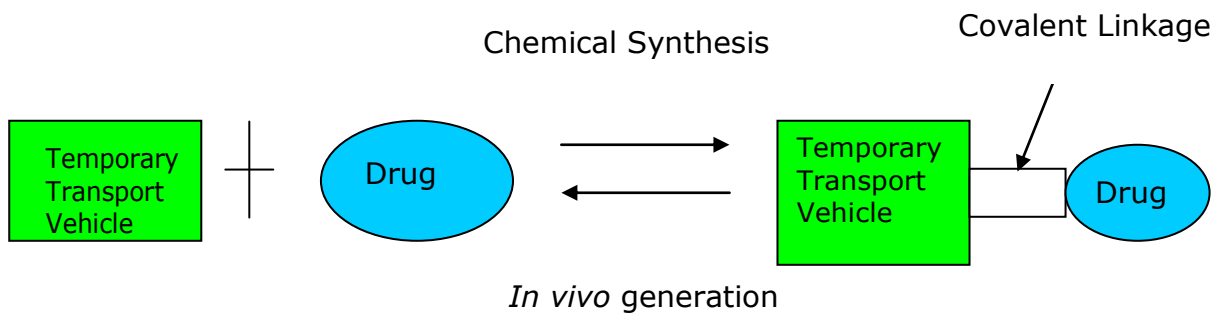


Figure 14.: Carrier Pro-drugs

Ideally all carrier pro-drugs should: ¹³⁴

- Be less toxic than the parent drug.
- Have an improved bioavailability when orally administered.
- Be site specific.
- Be inactive or significantly less active than the parent drug.
- Have a rate of drug formation rapid enough to maintain the drug's concentration within its therapeutic window.

The pro-drug concept has been adopted for a number of years and in various therapeutic areas such as in the treatment of ulcers, antibiotics and antihistamines.⁵¹ A study by Nolen *et al.* demonstrated a typical example of such therapy which involved the pro-drug Budesonide-beta-D-glucuronide used orally for the potential treatment of colonic inflammatory bowel disease. The management of this condition which usually involves the use of budesonide, a topically active glucocorticosteroid with low oral bioavailability (15%), is substituted by the oral administration of glucuronide pro-drug and should provide localised high concentration of the active drug. Once the parent drug budesonide has been delivered and absorbed, inactivation of the large fraction should be expected owing to hepatic metabolism.¹³⁶

Antibiotic therapy is another area where wide arrays of pro-drugs have been used to afford a better bioavailability, minimise toxicity or to resolve organoleptic problems associated with certain drugs.¹³⁷

Ampicillin (**o**) is a broad spectrum antibiotic used for the treatment of a wide range of infections such as urinary-tract-infections (UTIs), otitis media, sinusitis, oral infections and many more. Despite ampicillin's large bactericidal activity and reduced toxicity, only 30% to 50% is absorbed in the gut.¹³⁷ Bacampicillin (**p**), displays a greater bioavailability (95%) than the parent Ampicillin. An average oral dose of 400mg of Bacampicillin will achieve a high plasma concentration of 7µg/ml which is equivalent to 1000mg of Ampicillin. As a result of these pharmacokinetic characteristics, Bacampicillin plasma concentration can be rapid and elevated when compared to the one achieved from the same doses of the parent drug. Furthermore, only 18% of the pro-drug is bound to plasma proteins allowing a high concentration of free and therapeutically active Ampicillin.¹³⁷

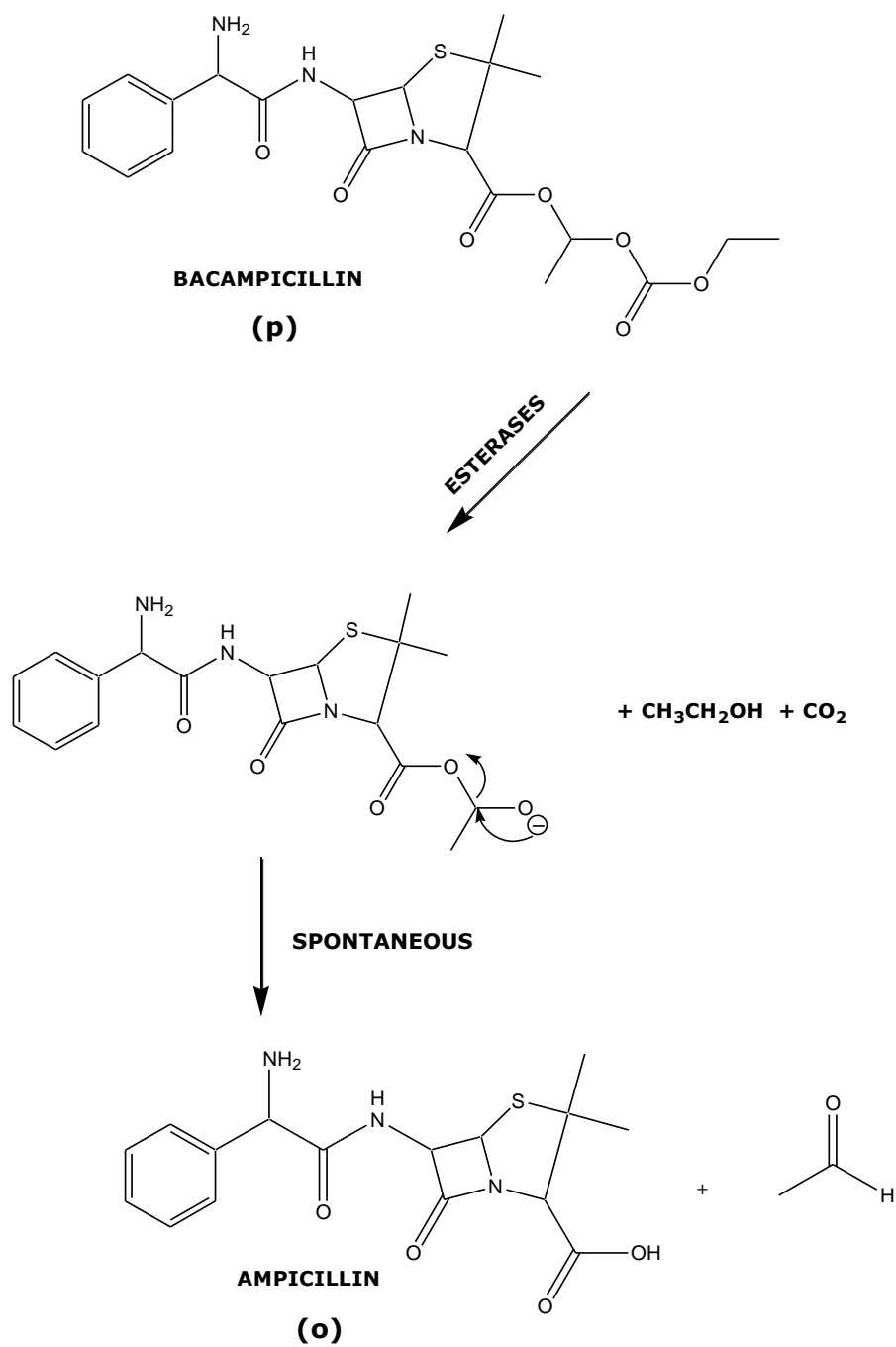


Figure 15.: Activation of Bacampicillin

This sophisticated approach has been considered, because it demonstrates both the enhanced pharmacodynamic and pharmacokinetic properties of the pro-drug, when compared to the parent drug. These properties encompass the most favourable interaction of the pro-drug with the target, and the

improvement of the drug's ability to reach its target and to have an acceptable lifetime.¹³⁴ (i.e. make the molecule more 'druggable').

Besides the uses and effectiveness of pro-drugs in other diseases, they are also being investigated for the treatment of cystinosis. As part of the work carried out to improve the treatment of this genetic disease, three generations of cysteamine and cystamine pro-drugs derivatives have been synthesised and biologically evaluated by a team of researchers based at Robert Gordon University.

Fatty amide derivatives of cystamine (**q**) were the first generation pro-drugs to be synthesised.¹³⁸ (Figure 16)

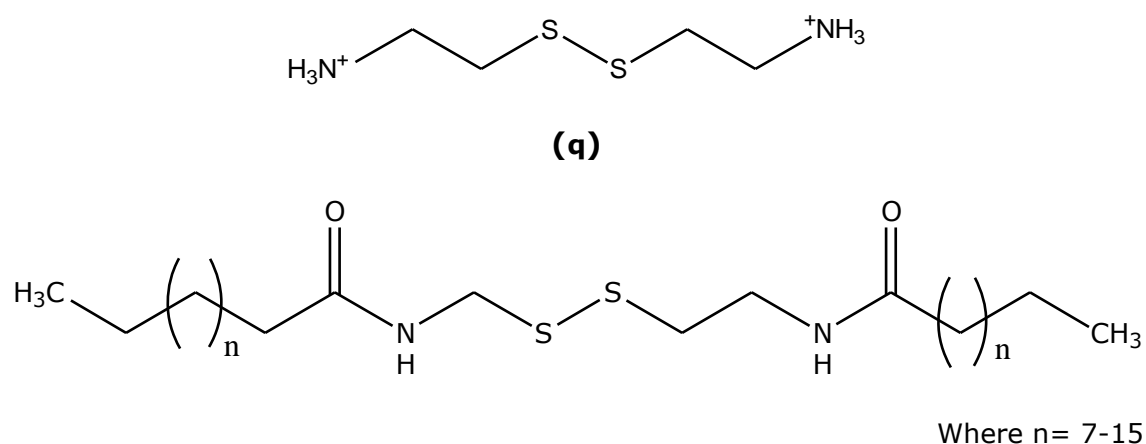
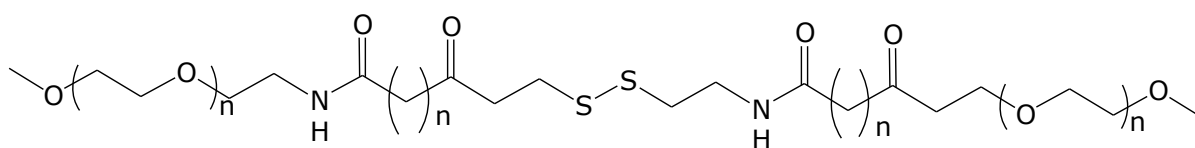


Figure 16.: Fatty amide derivatives of cystamine

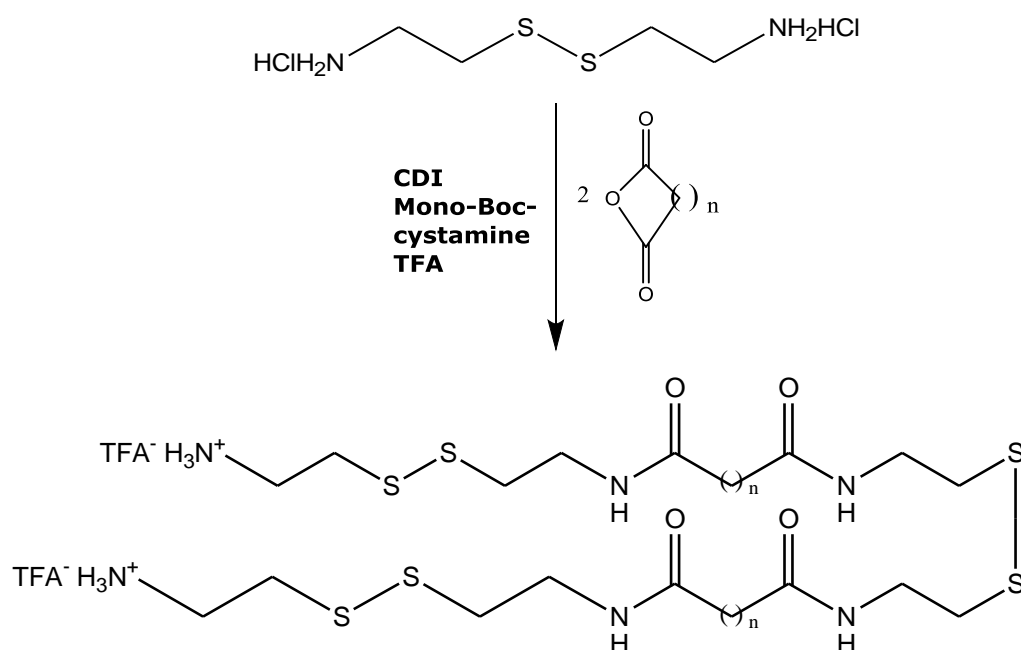
The second generation of pro-drugs were the PEGylated pro-drugs (Figure 17) derived from the activation of their carboxylate terminals with excess carbonyldiimidazole (CDI), followed by a coupling with amino polyethylenglycol. These compounds were synthesised with acceptable yields 40%-60%.¹³⁹



Where n = 2

Figure 17.: PEGylated Pro-drugs

The third generation of pro-drugs were synthesised using a route established in our laboratories. Briefly, cystamine dihydrochloride the disulfide derivative of cysteamine was basified and allowed to react with a number of cyclic anhydrides under basic conditions. The resulting di-acids were reacted with carbonyldiimidazole (CDI) and monoBoc-cystamine to yield the desired pro-drugs. Removal of the tBoc-protecting group was achieved in a facile manner by use of trifluoroacetic acid (TFA).¹⁴⁰ (Figure 18).



Where n=2, 3

Figure 18.: Succinic and Glutaric Cystamine Pro-drugs Derivatives

Additionally a folate pro-drug derivative of cystamine was also synthesised (Figure 19). This new pro-drug was non cytotoxic and displayed the greatest ability to reduce intralysosomal cystine seen so far in our studies, when compared to previous pro-drugs.¹⁴¹

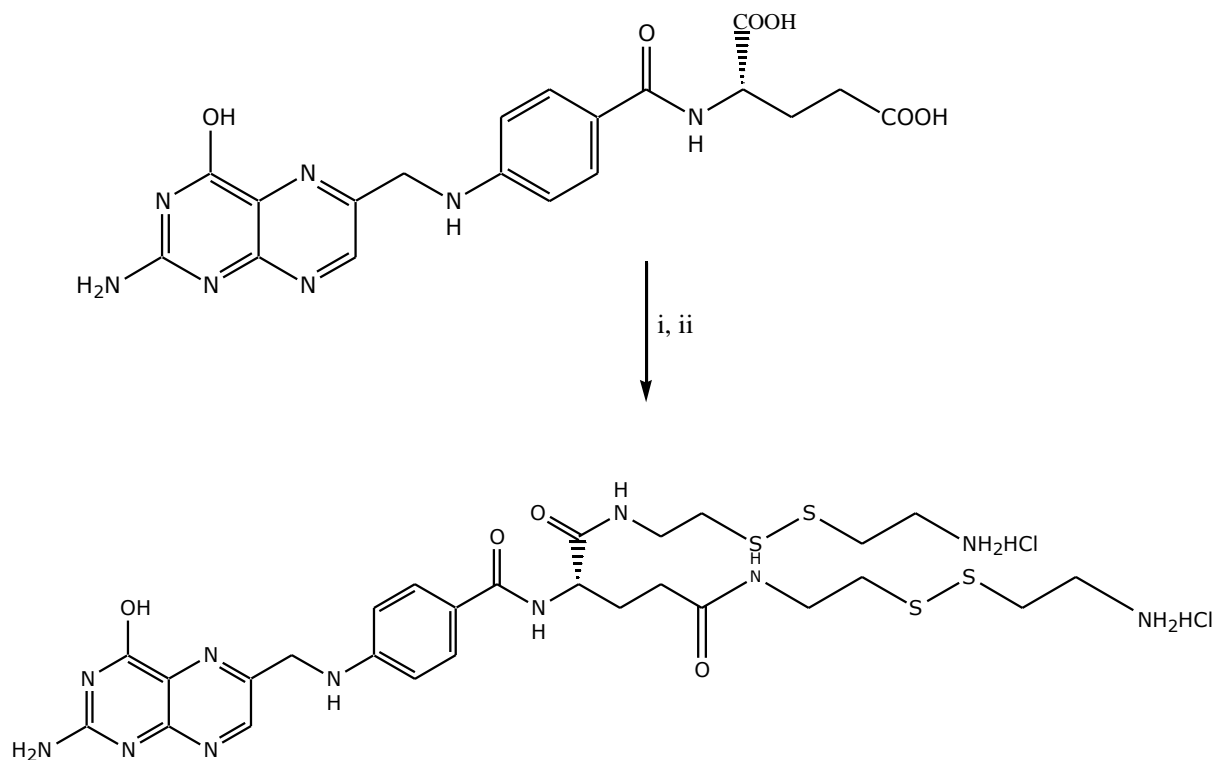


Figure 19.: Chemical synthesis of the Folate Pro-drug Derivative of Cystamine. Reagents and Conditions: **(i)** *tert*-butyl 2-(2-(aminoethyl) disulfanyl) ethylcarbamate (2.5 equiv), DEC (4 equiv), 12h, rt. **(ii)** 4 N HCl in dioxan, 30 min, rt.

Further work on pro-drugs has also been carried out by a team of researchers at the University of Sunderland and generated a group of pro-drug involving the derivatisation of both the amino and thiol functional group responsible for the unpleasant taste and smell of cysteamine. By developing γ -glutamyl pro-drug derivatives the properties of the parent drug (cysteamine) are altered and the problems of taste and smell reduced to negligible levels.

These pro-drugs are known to resist proteolytic degradation and can only be hydrolysed in the presence of the enzyme gamma-glutamyl transpeptidase (GGT) which is specific to γ -glutamyl pro-drugs.

GGT is required for the glutathione cycle and can be found in high concentrations on the surface of most cells including the kidney, liver, skin, and pancreas, allowing it to interact with γ -glutamyl-cysteamine pro-drugs. This in turn will result in the intracellular release of both glutamate and cysteamine.¹⁴²

To date, the work in pro-drugs has been fruitful and generated a considerable number of non cytotoxic compounds which displayed significantly greater ability to deplete the level of intralysosomal cystine in cultured cells when compared to the parent drug. The advantages of using cysteamine pro-drugs in the treatment of cystinosis are three fold, namely masking the unpleasant taste and smell, achieving desirable kinetics by avoiding release during passage through the gut and thus reducing the frequency of drug administration and finally efficient and complete release of multiple molecules of cysteamine (up to six molecules) once in the blood. With this approach patient compliance will be enhanced leading to an improved quality of life.^{51,140,141,143}

1.6. Research Progress

Recent advances have demonstrated that kidney function can be saved if early diagnosis and initiation of a diligent cysteamine therapy are undertaken. The earlier patients receive treatment ideally before the age of 2 years the more likely they will be to retain their kidney function. Commencement of early cysteamine therapy also reduces the chances of developing cystinosis – related complications at a later age.²¹

In 1998 it was reported that cysteamine should not be recommended during pregnancy and breastfeeding due to its teratogenic and fetotoxic effects.¹⁰⁵ These studies have shown that these side effects are linked to the production of hydroxyl radicals.¹⁴⁴ Therefore, treatment with cysteamine

should be suspended during the period of gestation and nursing. However, in order to prevent ill health, advice should be given to those wishing to conceive about the potential risks associated when stopping cysteamine therapy.

Other recent studies have reported a new side effect on the elbow and knees (Figure 20). The reports describe the side effect as lesions similar to Ehlers-Danlos syndrome occurring due to high doses cysteamine resulting from altering a typical four times a day regime to larger doses of three times daily. This treatment regimen is purposely used by patients to suit their daily routine.¹⁴⁵ Nevertheless the symptoms can be alleviated by a dose reduction.



Figure 20.: Skin manifestations of cysteamine toxicity.¹⁴⁶

A group of researchers at King's College in London have engineered a drug solution for use in renal transplantation. It has been anticipated that this novel drug will help increase graft survival time ¹⁴⁷ as well as maintaining effective kidney function during transfer from donor to recipient. The launch of this drug solution is scheduled for 2015.¹⁴⁷

In the world of formulation, topical cysteamine treatment has been dramatically improved by the development of a bioadhesive ophthalmic gel which could potentially replace the current eye drops, thus reducing the frequency of administration from 10-14 times a day to twice or even once daily. The novel gel has been formulated to slowly release the drug owing to its pseudoplastic property allowing a longer and painless (neutral pH) retention time when compared to the current eye drops.

The impermeable nature of the eye allows only 1% of cysteamine dose to reach the site of action (cornea) when used in the form of eye drops. Cysteamine eye drops have shown to clear crystals entirely from the cornea but only for a short time period, as result a multi-dose (15 times/day) is necessary. This innovative product will not only improve compliance amongst cystinosis patients but will also prevent ophthalmic morbidity such as blindness.¹⁴⁸

Further formulation research resulted in 2013, in the launch of a new enteric coated formula of cysteamine bitartrate (trade name Procysbi™, Raptor Pharmaceutical Corp, USA). This product was designed to reduce the number of cysteamine administration (every 6 hours) to only twice a day.¹⁴⁹

As previously mentioned, frequent administration of cysteamine is necessary in order to maintain White Blood Cells (WBC) cystine levels below 1.0 nmol ½ cystine/mg protein.¹⁵⁰ This new formulation has been designed so that the drug (cysteamine) can be administered directly into the small intestine resulting in increased plasma levels.¹⁵¹

Recent clinical trials, in which a sequential treatment with Cystagon® and Procysbi™ was offered to patients for a period of 3 weeks gave clear evidence that Procysbi™ displayed similar efficacy in lowering WBC cystine levels when compared to Cystagon®.¹⁵² A safety extension study is currently underway.

1.7. Aims of Project

In an attempt to overcome the problems of palatability and the GI related side effects associated with the administration of cysteamine, the aim of this project was to synthesise, characterise and biologically evaluate a series of novel odourless and tasteless oral therapies for cystinosis. It is anticipated that these compounds would enhance patient compliance resulting in an improved quality of life.

Two approaches were adopted, the synthesis, characterisation and evaluation of novel pro-drugs of cysteamine and cystamine and the attempted synthesis of novel co-crystal forms of cysteamine and cystamine.

This study was undertaken to complement and further previous studies on pro-drugs ¹⁴⁰ and focused on the synthesis of a small library of novel cystamine pro-drugs derivatives based on synthetic methods developed in house and pioneered by Omran *et al.* 2011.

These compounds will be evaluated *in vitro* using human cystinotic fibroblasts (GM00008), to help establish a structure-activity relationship and to determine the biological activity of the new pro-drugs on cellular uptake and distribution. It is hoped that these compounds will display significantly greater efficacy than cysteamine.

In addition, both solid phase peptide synthesis (SPPS) and convergent peptide synthesis (CPS) techniques will be employed to generate a number of "pseudo-peptides pro-drugs". The new compounds will be composed of repeating units of cystamine with succinic and glutaric acids.

Cell culture techniques developed in house will be used to evaluate both the cytotoxicity and the efficacy of the novel compounds.

Finally, as part of our expanded synthetic work and our desire to produce odourless and tasteless oral therapies for cystinosis, there may be the possibility of the manufacture of co-crystals of cysteamine and cystamine.

CHAPTER 2

MULTICOMPONENT CRYSTALS

2.1. Multicomponent Crystals

2.1.1. Introduction

The concept of multicomponent crystals has been adopted for a number of years and in 1844 a Quinhydrone prototype was first reported.¹⁵³

Co-crystals have been broadly defined as mixed crystals or crystals comprising of two different molecules.^{154,155,156}

Desiraju described the concept as "the understanding of intermolecular interactions in the context of crystal packing and the utilisation of such understanding in the design of new solids with desired physical and chemical properties".¹⁵⁷

In 1955 Pepnisky established the hypothesis of crystal engineering.¹⁵³

The creation of a supramolecular assembly can be achieved through crystal engineering which involves using design to generate crystals.¹⁵⁵ The concept of supramolecular synthesis or crystal engineering, aims to form new molecules in a solid state without breaking or forming covalent bonds.¹⁵⁴

Crystal engineering facilitates the study of the way molecules are packed together in the crystal lattice where intermolecular interactions are directed by hydrogen bonding.¹⁵³

Due to advances in technology, crystal engineering became a commonly used technique in the pharmaceutical industry.¹⁵⁵

This approach has also been applied to improve the pharmacokinetic properties of weakly soluble drugs without altering the stability of their physicochemical properties.^{156,157}

On the basis of intermolecular interactions, crystal engineering aims to create unfailing links between molecular and supramolecular structure.^{157,158}

Polymorphism has been studied for a number of years and was first described in 1965 by McCrone, as "solid crystalline phase of a given compound resulting from the possibility of at least two different arrangements of the molecules of that compound in the solid state".¹⁵³ The same molecule can display different polymorphs (Figure 21) resulting in different solubility and melting points, and an example is that of the

barbiturates where 70% are present in various polymorphic forms with the most stable one exhibiting the lowest free energy.^{159,160}

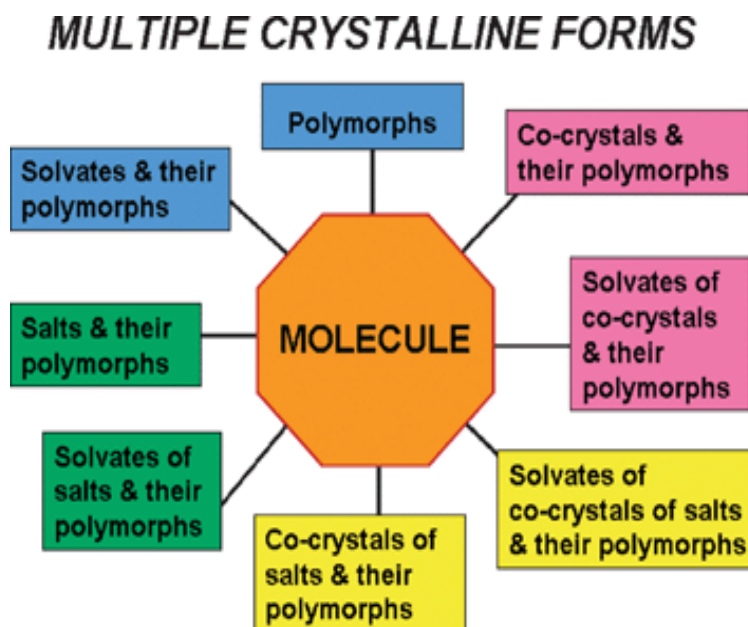


Figure 21.: Multiple polymorphic forms generated from the same molecule. ¹⁶⁰

In order to determine if hydrogen bonding has occurred, the study of the Lewis structure of a molecule must be carried out. Hydrogen bonding occurs between hydrogen atoms and electronegative atoms such as oxygen or nitrogen. This occurs due to an excess in electron density around the electronegative species.¹⁵⁸

Hydrogen bonds between OH...N and CH...O with energies of 2-20 kJmol⁻¹ are termed weak bonds, whereas bonds between OH...O and NH...O with energies of 20-40 kJmol⁻¹ are termed strong bonds.¹⁶¹

The bond length between a hydrogen donor (D) and an acceptor (A) is between 1.80 Å to 2.00Å for NH...O bonds, and between 1.60 Å to 1.80 Å for OH...O bonds.¹⁶¹

Multicomponent crystals are formed when intermolecular interactions take place between two or more components and these can be molecules, atoms or ions.¹⁶² Co-crystals, salts, solvates, hydrates and clathrates are types of multi-components crystals^{163,164} as shown in Figure 22.

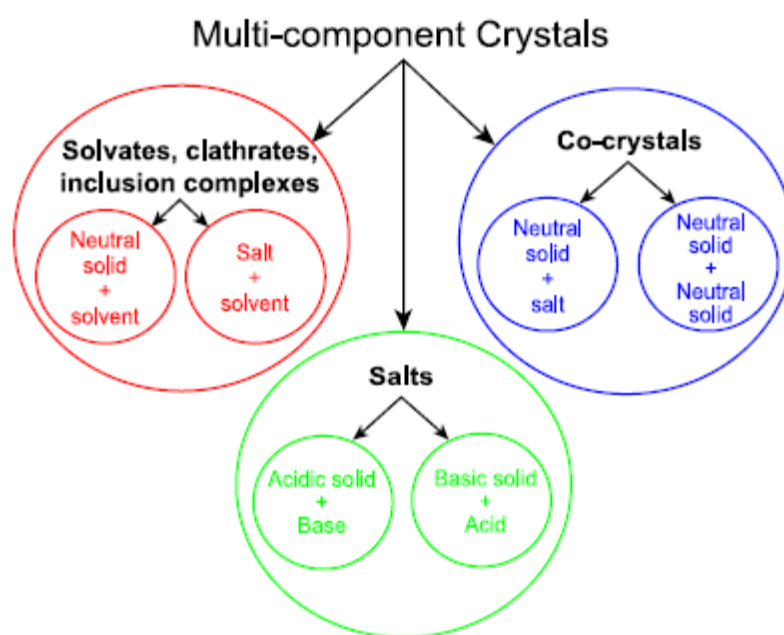


Figure 22.: Types of multicomponent crystals.¹⁶⁴

Salts form due to a proton transfer between an acid and a base¹⁵⁸ and are commonly manufactured with most active pharmaceutical compounds, usually to increase aqueous solubility or to provide a stable, crystalline species for formulation.¹⁶⁵

To produce a stable salt the pKa of each component should vary by at least two (log) units.¹⁶⁶ pKa is a term used to express the strengths of acids and bases and is defined as the negative logarithm, to the base 10, of the dissociation or ionisation constant. Solvates occur if one of the components is a liquid at room temperature.¹⁵⁴ Hydrates arise when water has been incorporated into the crystal structure.¹⁶⁷

Co-crystals have been described as crystalline materials consisting of two or more components that are solids at ambient temperature held together in a crystal lattice *via* hydrogen bonds.^{168,169} This is shown in Figure 23.¹⁷⁰

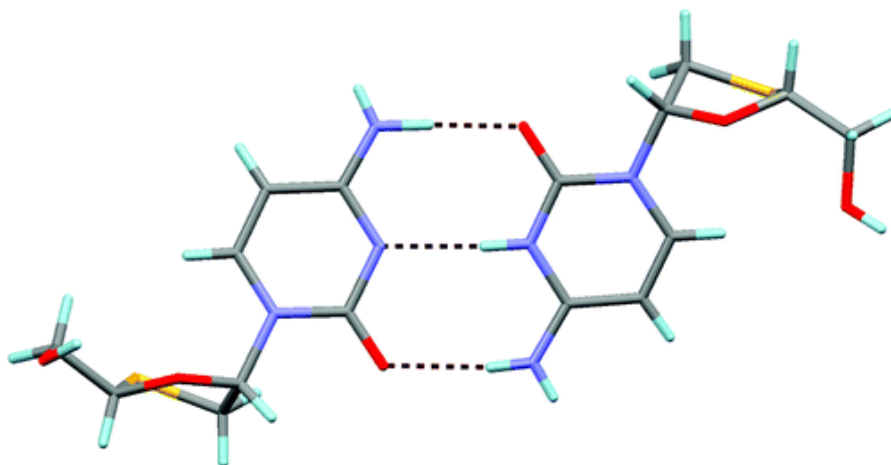


Figure 23.: Non-covalent bonds between the drugs Lamivudine and Zidovudine.¹⁷⁰

In contrast to salts, there is no proton transfer taking place between the constituents of a co-crystal.¹⁶⁵

The design of co-crystals has been based on the crystal engineering approach which provides an insight on the molecular interactions between functional groups in particular hydrogen bonding interactions.¹⁷¹

The recent advances in the area of drug formulation enabled the opportunity to manufacture pharmaceutical materials by design. Particularly, the development of co-crystals symbolises a prospective way to produce pharmaceutical compounds with improved physicochemical properties of interest.^{171,172, 173}

Indeed, these properties are of paramount importance for the safe, efficient and cost-effective delivery of a drug to a patient, as schematically illustrated in Figure 24.¹⁷²

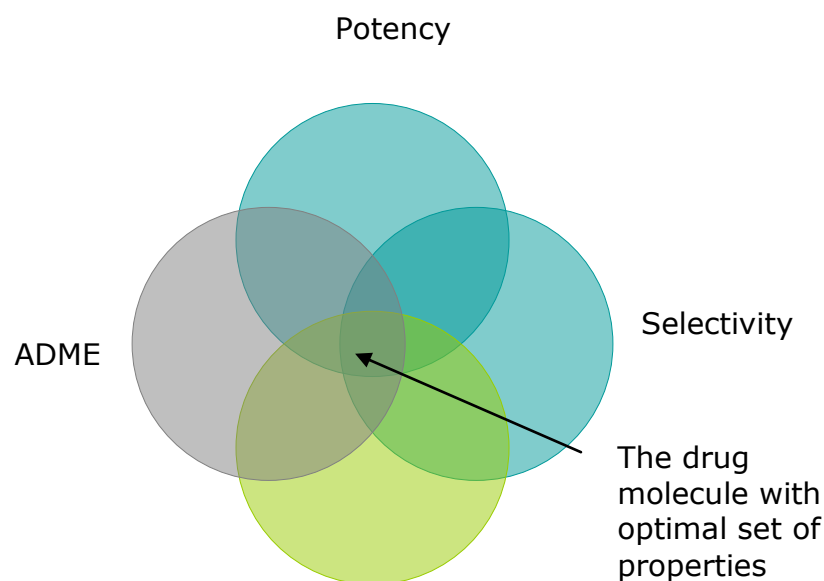


Figure 24.: Properties vital for a successful drug candidate.¹⁷²

Crystal engineering or supramolecular synthesis aims to produce pharmaceutical co-crystals in the form of a supramolecular synthon.¹⁷⁴ This process is aided by the presence of carboxylic acid functional groups which represent a good foundation for the process of crystal engineering of pharmaceutical co-crystals.¹⁷⁴

Figure (25) represents the creation of a supramolecular homosynthon favoured by complementary carboxylic acid hydrogen bond donor and acceptor sites.¹⁵³

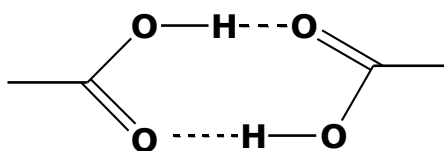


Figure 25.: Supramolecular Homosynthon.

A number of factors such as functional group position, geometry, and steric hindrance can control the process of co-crystallisation.

Subsequently, a chemical structure on its own does not represent the sole basis of co-crystal formation.¹⁷¹

The most commonly used method in co-crystallisation is the slow evaporation technique which requires a solvent. To prevent solvates forming, the grinding method whereby the solvent is omitted is often employed as the method of choice. (Figure 26)



Figure 26.: Crystallisation of single crystals by the process of grinding.¹⁷⁵

This method simply involves two solid starting materials placed in a ballmill. However, this solid state approach results in the reduction of the particle size of the solid making the product unsuitable for structure elucidation by single crystal diffraction.¹⁶⁸

Other methods of co-crystallisation include; sublimation, slurries, and growth from melt.¹⁵⁵

As stated in the introduction, the objectives of the present work are to develop colourless and tasteless oral therapies for Nephropathic Cystinosis. It was envisaged that co-crystals of cysteamine or cystamine with biologically acceptable organic acids provide a solution to this problem.

2.2. Materials and Instrumentation

2.2.1. Materials

One-step chemical reactions were performed with laboratory grade reagents purchased from Sigma-Aldrich, UK unless otherwise stated, and were used without further purification.

2.2.2. Instrumentation

A Metler AE 240-S analytical balance was used to record the weights of products.

The chemical structure and purity of the products were determined by Melting Point (MP), Differential Scanning Calorimetry (DSC), Fourier Transform Infra-Red (FTIR), and Single-Crystal X-Ray Diffraction.

The melting points were determined on a Stuart Scientific SMP1 apparatus and are uncorrected. The Infra-Red (IR) spectra were recorded on a Nicolet Avatar 360 FTIR and Nuclear Magnetic Resonance (NMR) spectra were obtained from a Bruker 400 ultarshield using Dimethyl Sulfoxide-d₆ (DMSO-d₆) as solvent.

2.3. Methods

2.3.1. Slow Evaporation Technique

2.3.1.a. *General Preparation Method for Cystamine Adipate, Cystamine 2,6-Dihydroxybenzoate, Cystamine Glutarate, and Cystamine 3-Nitrobenzoate from cysteamine.*

Millimolar amounts (1:1) ratio of cysteamine and each co-former were weighed. Both materials were transferred to a 25 ml conical flask and 5 ml of hot ethanol was added. The flask containing the mixture was then placed on a water bath at a temperature of 50°C and small aliquots of solvent were added until a clear solution was obtained. The solution was then filtered,

loosely covered with parafilm and left in the fume cupboard to allow crystallisation to occur by slow evaporation.

Following a few days, crystals formed. These were collected by gravity filtration and allowed to dry on a filter paper.

2.3.1.b. *General Preparation of Cysteamine Bitartrate Monohydrate (Cysteamine Hydrogen Tartrate) [1] from Cysteamine.*

Millimolar amounts (1:1) ratio of cysteamine and *L*-(+)-tartaric acid were weighed and transferred into a 50 ml conical flask. A small amount (5 ml) of hot ethanol was added to the mixture, and the flask and contents were placed in a water bath, with swirling, at 50°C. After 10 minutes (min) both starting materials remained solid, and so to aid dissolution the flask was stirred and heated to 60°C on a hot plate. Further quantities of solvent were added drop-wise to the mixture until a clear solution was obtained. The whole process lasted for about an hour and a total volume of 15 ml of ethanol was used. The solution was then filtered, loosely covered with Parafilm and left in the fume cupboard for crystallization to take place by slow evaporation. After 5 days, clear rod shaped crystals of (I) separated from the product mixture. The crystals were then collected by gravity filtration and allowed to dry on filter paper.

2.3.1.c. *General Preparation of Cystamine Tartrate [2] and Cystamine Bitartrate Dihydrate (Cystamine Hydrogen Tartrate Dihydrate) [3] from cystamine.*

For [2] and [3] same millimolar amounts (1:1) ratio of cystamine and *L*-(+)-tartaric acid were weighed and transferred into a 50 ml conical flask. 5 ml of hot ethanol was added which resulted in the formation of a white precipitate. The flask was then placed in a 50°C water bath with swirling. Small aliquots of solvent were added drop wise until a clear solution was achieved. A total volume of 20ml of ethanol was used. The solution was then filtered, loosely covered with parafilm and left in the fume cupboard for crystallization to take place by slow evaporation. The following day crystals were formed.

The crystals (blades [2] and needles [3]) were then collected by gravity filtration and allowed to dry on a filter paper.

Product [3] also formed as a non-crystalline mass in the preparation of product [1]. Attempts to obtain high quality crystals of product [3] were only partially successful.

2.3.2. Melting Point Determination

Prior to undertaking slow evaporation, the Stuart Scientific SMP1 apparatus was used to record the melting point of each starting material. The melting point was recorded from the start of phase change and until complete liquification of the sample. The same procedure was also carried out for all crystalline products.

2.3.3. Differential Scanning Calorimetry (DSC)

Approximately 5mg of the sample to be analysed was weighed using the Metler AE50 balance, and hermetically sealed with an aluminium lid. The Universal Analysis Software was used to process all the results.

2.3.4. Infra-Red (IR) Spectroscopy

An IR spectrum was collected for all starting materials prior to commencing crystal preparation. A small amount of the sample to be analysed was placed directly into contact with the diamond point after which all generated spectra including the ones from the newly formed crystals were analysed using OMNIC software (Trademark of Nicolet Instrument Corporation, Madison, U.S.A.). A comparison of all spectra was then achieved. The diamond accessory was the method of choice as it only required a small amount of the sample to be analysed. Additionally, a dried mixture of Potassium Bromide (KBr) and the sample was used to achieve a better quality spectrum.

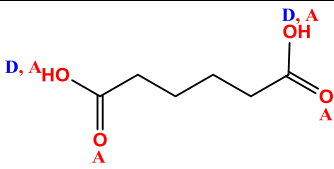
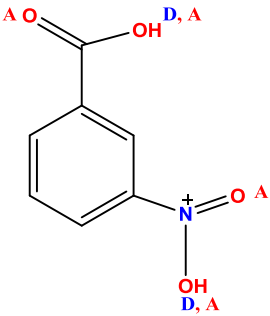
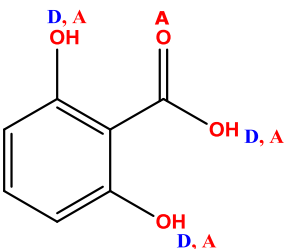
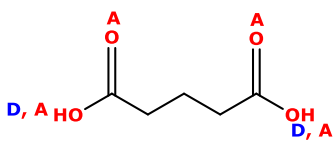
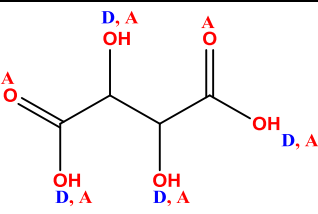
2.3.5. X-Ray Crystallography

The collection of X-Ray data for the newly synthesised crystals was carried out by the Engineering and Physical Sciences Research Council (EPSRC) National X-Ray Crystallography Service at Southampton University.⁷⁵

The WingGX system was used to solve, refine and analyse the molecular structure.⁷⁶

Hydrogen bond acceptors and donors of acid co-formers were obtained with the Marvin computer software.⁸⁵ (Table 2)

Table 2.: Hydrogen bond acceptors and donors

Compound	Structure	Number of hydrogen donors/ acceptors
Adipic acid		Donor sites : 2 Donor count: 2 Acceptor sites: 6 Acceptor count: 4
3 - Nitrobenzoic acid		Donor sites : 2 Donor count: 2 Acceptor sites: 6 Acceptor count: 4
2, 6 - Dihydroxybenzoic acid		Donor sites : 3 Donor count: 3 Acceptor sites: 5 Acceptor count: 4
Glutaric acid		Donor sites : 2 Donor count: 2 Acceptor sites: 6 Acceptor count: 4
L (+)- Tartaric acid		Donor sites : 4 Donor count: 4 Acceptor sites: 8 Acceptor count: 6

CHAPTER 3

EXPERIMENTAL

3.1. Synthesis of Novel Cystamine Pro-drug Derivatives

In this chapter the aim of the experimental work was to synthesise and characterise a small library of cystamine derivatives using a number of dicarboxylic acids.

3.1.2. Materials

All chemicals were purchased from Sigma Aldrich, UK unless otherwise stated, and were used without further purification.

Silica gel 60 F₂₅₄ gel.....Merck (Germany)

Dimethyl Sulfoxide-D6 (DMSO-d6).....Goss Scientific (UK)

Dichloromethane (DCM).....Fisher Scientific (UK)

Chloroform (CHCl₃).....Fisher Scientific (UK)

Dimethylformamide (DMF).....Fisher Scientific (UK)

3.1.2.1. Instrumentation

Thin layer chromatography (TLC) was performed on silica gel 60 F₂₅₄ Aluminium plates (2cm x 5cm) (Merck, Germany) in a mobile phase of ethylacetate:methanol (1:1 or 9:1) mobile phase. Spots were visualized with short wavelength UV-light (254 nm) or if no chromophore was present, with iodine vapour.

TLC determination involved a stationary phase consisting of a silica gel aluminium plate onto which a small spot of the reaction mixture was spotted using a micro pipette. The silica plate was allowed to dry, and subsequently placed vertically in a TLC development tank containing the solvent as the mobile phase. This system allows the solvent to travel by capillary action which separates the mixture into distinct spots

corresponding to the components contained within the solution. Once the plate is dry, the spots are visualised under UV-light.

Mass spectra were obtained on a Thermofisher LTQ orbitrap XL (low resolution) mass spectrometer. MS works on the basic principle of generating and separating charged molecules according to their mass-to-charge ratio (m/z) defined as the charge of an anion using an electric and/or magnetic field.

ESI allows the production of negatively charged ions through atomisation. These fragments are then accelerated, detected and translated into a mass spectrum.¹⁷⁹

Nuclear Magnetic Resonance (NMR) spectra were recorded on a Bruker 400 ultrashield spectrometer operating at 400.1 MHz for proton (^1H). Samples were dissolved in DMSO- d_6 .

Wilmad 5 mm Economy NMR Tubes (N51 glass, WG-1228-8) were purchased from Goss Scientific Ltd, UK. The NMR solvent, Dimethyl Sulfoxide- D_6 (DMSO- d_6) was used for analysis of both intermediate and final compounds. The compounds obtained from the synthetic process were concentrated, dried and residual solvent removed. The samples were subsequently dissolved in an appropriate deuterated solvent, such as Dimethyl Sulfoxide- D_6 (DMSO- d_6). Approximately 1-2 ml of the sample were transferred to a NMR tube, capped and introduced into the NMR instrument. Once the sample was lowered into the NMR probe, it underwent rotation, locking and shimming, before being processed by the Bruker Topspin 1.3 software, to give an NMR spectrum.

Magnetic resonance occurs due to magnetic properties exhibited by specific nuclei, in particular, proton (^1H or hydrogen). ^1H NMR can be viewed at frequency of 400.1. Protons can be detected by ^1H NMR.

3.1.3. Methods

3.1.3.1. Synthesis of Cystamine Pro-drugs Derivatives

Mono-Boc-Cystamine (starting material) was prepared from cystamine dihydrochloride (5g; 22mmol) dissolved in dH₂O (10 mL). The resulting solution was basified with NaOH to pH 14. Cystamine free base (2.25g; 15mmol) was dissolved in chloroform (10mL) at 0 °C and a solution of Di-ter-Butyl dicarbonate (Boc)₂O (1.09g; 5mmol) in 50mL CHCl₃ added drop wise over three hours. The reaction mixture was stirred at room temperature for a further 12 hours. The resulting product was extracted with DCM, dried over MgSO₄ to afford a yellow solid.

This was purified by flash chromatography (elution with 90% DCM/MeOH) and 1% NH₄OH to yield a yellow oil.¹⁸⁰

Boc-Cystamine (0.38g; 30%). LR-MS for C₉H₂₀N₂O₂S₂ [Mass: 252], found: 253 (M + H⁺) (100%), 375 (M + Na⁺) (20%).

¹H NMR (400 MHz, DMSO-d₆) δ (ppm): 1.45 (s, 9H, CH₃), 1.55 (s, NH₂), 2.77 (t, 2H, CH₂S), 2.79 (t, 2H, CH₂S), 3.02 (t, 2H, CH₂NH₂), 3.44 and 3.46 (2t, 2H, CHHNHBoc), 4.95 (s, NH).

3.1.3.1.1. Synthesis of Pro-drug Cystamine - Succinate

[2-(2-{4-[2-(2-{4-[2-(2-tert-Butoxycarbonylaminoethyl)disulfanyl]-ethylcarbamoyl]-propionylamino}-ethyl)disulfanyl]-ethylcarbamoyl]-propionylamino}-ethyl)disulfanyl]-ethyl]-carbamic acid-tert-butyl ester. (**1**)

Compound 1 was synthesised from intermediates (2) and (3) as described in sections **3.1.3.1.1.a.** and **3.1.3.1.1.b.** respectively.

(**1**) (1.94g; 83%), LR-MS for C₃₀H₅₆N₆O₈S₆ [Mass: 820], found: 821 (M + H⁺) (100%), 843 (M + Na⁺) (10%), 865 (M + FA - H⁺) (100%).

¹H NMR (400 MHz, DMSO-d₆) δ (ppm): 1.37 (s, 18H, CH₃), 2.30 (s, 8H, BocCH₂), 2.74(t, 12H, COCH₂CH₂), 3.19 (t, 4H, CH₂CH₂S), 3.30(m, 8H, CH₂CH₂NH), 6.99(t, 2H, NH₂CH₂), 8.04 (t, 4H, CH₂NHCO). Figure A.1; Appendix 2

3.1.3.1.1.a. Synthesis of N,N'-Disuccinoylcystamine - Diamide (A)

N-{2-[2-(3-Carboxy-propionylamino)-ethyl]disulfanyl}-ethyl}-succinamicacid. (2)

Cystamine dihydrochloride (1.0g; 44mmol) was dissolved in 150 mL of distilled water (dH₂O). The resulting solution was basified with 4M NaOH to pH 10. To this solution (3.33g; 132.9 mmol) of succinic acid anhydride were added, and the pH maintained between 7 and 10 with additional NaOH. The solution was stirred for 30 minutes, at room temperature, then the pH was reduced to 1 by addition of 6M hydrochloric acid (HCl), whereupon, a white precipitate formed. The latter was carefully washed with distilled water (200 mL) and dried under reduced pressure.

(2) (0.456g; 92%), mp 162 °C - 164 °C.

LC-MS for C₁₂H₂₁N₂O₆S₂ [Mass: 352], found: 353 (M + H⁺) (100%). Other major peaks 375 (M + Na⁺) (75%), 351 (M + Cl⁻) (100%).

¹H NMR (400 MHz, DMSO-d₆) δ (ppm): 1.65 (t, 2H, CH₂CH₂CO); 2.30 (t, 2H, COCH₂CH₂); 2.42 (t, 2H, CH₂CH₂S); 2.72 (m, 2H, NHCH₂CH₂); 8.0 (t, 2H, CH₂NHCO); 9.2 (s, 1H, CH₂COOH). Figure A.2; Appendix 2

3.1.3.1.1.b. Synthesis of the Imidazolidine Derivative

[2-(2-{4-[2-(2-{4-[2-(2-tert-Butoxycarbonylaminoethyl)disulfanyl]-ethyl}carbamoyl]-propionylamino}-ethyl)disulfanyl]-ethyl}carbamoyl]-propionylamino}-ethyl)disulfanyl]-ethyl]-carbamicacid-tert-butyl ester. (3)

To a solution of N, N'-disuccinoylcystamine (1.0 g; 2.8 mmol) in 10 mL of anhydrous DMF, was added CDI (1.05 g; 6.5 mmol) resulting in a rapid formation of a white precipitate. The reaction mixture was stirred at room temperature for 3 hours, after which time a small aliquot was used for analysis, and a solution of mono-substituted cystamine (1.13g; 4.5mmol) in 5 mL of anhydrous DMF was added, without isolating the product intermediate (3). The reaction mixture was stirred for a further 12 hours, at room temperature. Following solvent evaporation, 25 mL of distilled water was added to the residue and the white precipitate (compound 1) was then filtered off, washed with small amounts of aqueous 0.1M HCl and ethylacetate, then dried in vacuo at 70°C.

(3)-crude LR-MS for $C_{18}H_{24}N_6O_4S_2$ [Mass: 452], found: 453 ($M + H^+$).

3.1.3.1.1.c. Deprotection of compound (1) *N1,N1'-(disulfanediy)bis(ethane-2,1-diy))bis(N4-(2-((2-aminoethyl)disulfanyl)ethyl)succinamide)*. **(4)**

Compound **1** (0.5g; 0.6mmol) was dissolved in 5 mL of trifluoroacetic acid, and the solution was stirred for 30 minutes at room temperature, after which ethanol (20 mL) was added (**i**).

The solution was allowed to stand for 15 minutes at room temperature (**ii**) then residual solvent was evaporated using the rotary evaporator (**iii**). Steps (**i-iii**) were repeated 3 times. To the resulting solution, 5 mL of diethyl ether was added to give a white precipitate (compound **4**). This was collected by filtration and dried at 50° C, under *vacuo*.

(4) (0.36g; 72%), LR-MS for $C_{20}H_{40}N_6O_4S_6$ [Mass: 621], found: 623 ($M + 2H^+$) (15%). Other major peak, 311 ($M + 2H$)/2 (100%).

1H NMR (400 MHz, DMSO- d_6) δ (ppm): 2.31 (s, 8H, NH_2CO), 2.76 (m, 4H, Boc CH_2CH_2), 2.94 (t, 8H, $COCH_2CH_2$), 3.11(t, 4H, CH_2CH_2S), 3.31(m, 8H, $NHCH_2CH_2$), 8.11(t, 10H, CH_2NHCO).

3.1.3.1.2. Synthesis of Pro-drug Cystamine Glutarate

[2-(2-{4-[2-(2-{4-[2-(2-tert-Butoxycarbonylamino-ethyl)disulfanyl]-ethyl)carbamoyl]-butyrylamino}-ethyl)disulfanyl]-ethyl)carbamoyl]-butyrylamino}-ethyl]disulfanyl)-ethyl]-carbamic acid tertbutyl ester. **(5)**

This compound was prepared using the method for compound 1.

(5) (1.64g; 73%), LR-MS for $C_{32}H_{60}N_6O_8S_6$ [Mass: 848], found: 849 ($M + H^+$) (35%), 871 ($M + Na^+$) (100%), 883 ($M + Cl^-$) (100%), 893 ($M + FA - H$) (40%). Other peaks of interest; 619 ($M/2 + 2tboc$) (40%).

1H NMR (400 MHz, DMSO- d_6) δ (ppm): 1.36 (s, 18H, CH_3); 1.77 (m, 4H, $CH_2CH_2CH_2$) 2.12 (t, 12H, $COCH_2CH_2$), 2.80(m, 4H, $NHCH_2CH_2$), 3.20(t, 8H, CH_2CH_2S), 3.38(m, 8H, $NHCH_2CH_2S$), 7.07- 8.20 (t, 6H, $CONHCH_2$). Figure A.3; Appendix 2

3.1.3.1.2.a. Synthesis of N,N'-Diglutaroylcystamine - Diamide (B)

5,5'-((disulfanediy)bis(ethane-2,1-diyl))bis(azanediyl))bis(5-oxopentanoic acid). (6)

This compound was prepared from glutaric anhydride (1.53g; 13.42mmol) using the method for diamide A.

(6) (1.34g; 90%), mp 121 °C - 128 °C. LR-MS for C₁₄H₂₄N₂O₆S₂ [M: 380], found: 381 (M + H⁺) (45%), 403 (M + Na⁺) (100%), 379 (M - H⁺) (100%).

¹H NMR (400 MHz, DMSO-d₆) δ (ppm): 1.69 (m, 2H, CH₂CH₂CH₂); 2.10 (t, 2H, CH₂CH₂CO); 2.22 (t, 2H, CH₂CH₂COOH); 2.73 (t, 2H, CH₂CH₂S); 3.28 (q, 2H, NHCH₂CH₂); 8.0 (t, 2H, CH₂CONH). Figure A.4; Appendix 2

3.1.3.1.2.b. Synthesis of the Imidazolide Derivative

N,N'-(disulfanediy)bis(ethane-2,1-diyl))bis(5-(1H-imidazol-1-yl)-5-oxopentanamide). (7)

This compound was prepared from N,N'-diglutaroylcystamine (1.0 g, 2.6 mmol) using the method described in section **3.1.3.1.1.b.**

(7)-crude LR-MS calculated for C₂₀H₂₈N₆O₄S₂, found: 481 (M + H⁺) 481.

3.1.3.1.2.c. Deprotection of compound (5)

Compound **5** (0.82g; 0.97mmol) was deprotected using the method described in section **3.1.3.1.1.c.** to yield a white precipitate (compound **8**) *N1,N1'(disulfanediy)bis(ethane-2,1-diyl))bis(N5-(2aminoethyl)disulfanyl)ethyl)glutaramide).*

(8) (0.49g; 60%), LR-MS for C₂₂H₄₄N₆O₄S₆ [Mass: 648], found: 325 (M/2 + H) (100%). Other peaks of interest; 519 (M/2 + tBoc)⁺ (95%), 671 (M + Na⁺) (75%)

¹H NMR (400 MHz, DMSO-d₆) δ (ppm): 1.70 (s, 4H, TFANH₃⁺CH₂), 2.07 (m, 8H, CH₂CH₂CH₂), 2.78(m, 8H, COCH₂CH₂), 2.95(m, 4H, NHCH₂CH₂), 3.08 (m, 4H, CH₂CH₂S), 3.32 (m, 8H, NHCH₂CH₂S), 8.09 (m, 10H, CONHCH₂).

3.1.3.1.3. Synthesis of Pro-drug Cystamine Citraconate

di-tert-butyl ((9Z,21Z)-10,21-dimethyl-8,11,20,23-tetraoxo-3,4,15,16,27,28-hexathia-7,12,19,24-tetraazatriaconta-9,21-diene-1,30-diyl)dicarbamate. **(9)**

This compound was prepared using the same method for compounds (1) and (5).

(9) (0.19g; 38%), LR-MS for $C_{32}H_{56}N_6O_8S_6$ [Mass: 844], found: 845 (M + H) (15%), 879 (M + Cl⁻) (75%). Other peaks; for $C_9H_{20}N_2O_2S_2$ [Mass: 252], found: 253 (M + H) (35%) corresponding to Monoboc cystamine, and unidentifiable peak at 667 (100%).

3.1.3.1.3.a. Synthesis of N,N'-Citraconoylcystamine - Diamide (C)

(2Z,2'Z)-4,4'-((disulfaneylbis(ethane-2,1-diyl))bis(azanediyl))bis(3-methyl-4-oxobut-2-enoic acid). **(10)**

This compound was prepared from anhydrous citraconic acid (2.0g; 17.85 mmol) using the method for diamides **A** and **B**.

(10) (1.6g; 27%), mp 145 °C - 151 °C. HR-MS (ESI): calculated for $C_{14}O_{19}N_2O_6S_2$, 375.0690, found: 375.0682 [M - H]⁻ (100%). Figure B.1; Appendix 3

¹H NMR (400 MHz, DMSO-d₆) δ (ppm): 1.8 (s, 6H, CH₃); 2.9 (t, 4H, CH₂CH₂S); 3.1 (q, 4H, CH₂CH₂NH); 6.9 (s, 2H, CHCO); 7.1 (t, 2H, CH₂NHCO); 9.1 (s, 2H, CHCOOH).

3.1.3.1.3.b. Synthesis of the Imidazolidine Derivative

(Z)-N-(2-(((2-((Z)-4-(1H-imidazol-1-yl)-2-methyl-4-oxobut-2-enamido)ethyl)disulfanyl)ethyl)-4-(1H-imidazol-1-yl)-3-methyl-4-oxobut-2-enamide). **(11)**

This compound was prepared from N,N'-Citraconoylcystamine (0.4 g; 1.07 mmol) using the method described in section **3.1.3.1.1.b.** but was not isolated. Over time, a colour change from pale pink to dark red was observed. A red residue (9) was obtained following a solvent extraction with H₂O and DCM (3 x 200mL).

(11)-crude LR-MS for $C_{20}H_{24}N_6O_4S_2$ [Mass: 476], found: 477 ($M + H^+$) (85%), 239 ($M/2 + H^+$) (100%), 511 ($M + Cl^-$) (100%).

3.1.3.1.4. Synthesis of Pro-drug Cystamine Maleioate

di-tert-butyl((9Z,21Z)-8,11,20,23-tetraoxo-3,4,15,16,27,28-hexathia-7,12,19,24-tetraazatriaconta-9,21-diene-1,30-diyl)dicarbamate. **(12)**

This compound was prepared using the same method for compounds 1, 5, and 9.

(12) (0.37g, 41%) LR-MS for $C_{30}H_{52}N_6O_8S_6$ [Mass: 816], found: 419.5 ($M + Na^+$)/2 (100%); other peaks 815 ($M - H^+$) (10%).

3.1.3.1.4.a. Synthesis of N,N'-Maleioylcystamine - Diamide (D)

(2Z,2'Z)-4,4'-((disulfanediy)bis(ethane-2,1-diyl))bis(azanediyl))bis(4-oxobut-2-enoic acid). **(13)**

This compound was prepared from maleic anhydride (1.30g; 13.26 mmol) using the method for Diamides **A**, **B**, and **C**.

(13) (0.27g, 59%). mp 160°C - 175°C. HR-MS (ESI): calculated for $C_{12}H_{16}N_2O_6S_2$, 347.0377 found: ($M - H$)⁻ 347,0371 (100%). Figure B.2; Appendix 3

¹H NMR (400 MHz, DMSO-d₆) δ (ppm): 2.8 (t, 4H, CH₂CH₂S); 3.4 (q, 4H, NHCH₂CH₂); 6.2 (d, 2H, CHCHCO); 6.3 (d, 2H, CH-COOH); 7.9 (br, 2H, CONHCH₂); 9.2 (t, 2H, CHCOOH).

3.1.3.1.4.b. Synthesis of the Imidazolidine Derivative

(2Z,2'Z)-N,N'-((disulfanediy)bis(ethane-2,1-diyl))bis(4-(1H-imidazol-1-yl)-4-oxobut-2-enamide). **(14)**

This compound was prepared from N,N'-Maleinoylcystamine (0.5 g; 1.43mmol) using the method described in section **3.1.3.1.1.b.** and was not isolated. A colour change from pale pink to dark red was also observed. A red residue (**12**) was obtained by solvent extraction with H₂O and DCM (3 x 200mL).

(14)-crude LR-MS for C₁₈H₂₀N₆O₄S₂ [Mass: 448], found: 449 (M + H⁺) (25%), 225 (M + Na⁺)/2 (48%), 471 (M + Na⁺) (85%), 481 (M + CH₃OH + H⁺) (48%).

3.2. Synthesis of Novel Cystamine Pseudo-Peptides

3.2.1. Materials

All chemicals were purchased from Sigma Aldrich, UK unless otherwise stated, and were used without further purification.

Dimethylformamide (DMF).....	Fisher Scientific (UK)
Dioxane.....	Fisher Scientific (UK)
Piperidine.....	Fisher Scientific (UK)
H-Lys(Boc)-2-Cl-trt resin.....	Novabiochem (UK)
1, 3-Diaminopropane trityl resin.....	Novabiochem (UK)
H-Ala-2 Cl-trt resin.....	Novabiochem (UK)

Fmoc-cystamine succinic and glutaric acids (**15** and **16**) were prepared by first dissolving cystamine dihydrochloride (2.25g; 10mmol) in H₂O (30mL) and stirred in dioxane (100 mL). The solution was then cooled in an ice bath to 0 °C for 10 minutes and succinic (1g; 10mmol) or glutaric anhydride (1.14g; 10mmol) was added. The reaction mixture was stirred overnight at room temperature.

After this time, DIPEA (3.3mL) and Fmoc-OSu (3.373g; 10mmol) in 10mL of DMF were successively added to the stirred solution in the ice bath at 0 °C and stirring continued for a further 2 hours. The reaction product was collected by gravity filtration. The filtrate was concentrated to a viscous liquid and H₂O (200mL) was added producing a white precipitate, which was then collected by filtration, washed with H₂O (2 x 200mL) and dried under vacuum.

Flash chromatography was performed using 5-10% Methanol in DCM. The organic layer was dried with MgSO_4 , filtered and reduced to produce a white solid.¹⁸¹

Fmoc N-protected cystamine succinic acid (15).

Yield: 1.5g, 40%.

LR-MS for $\text{C}_{23}\text{H}_{26}\text{N}_2\text{O}_5\text{S}_2$ [Mass: 474], found: 475 ($\text{M} + \text{H}^+$) (100%), 497 ($\text{M} + \text{Na}^+$) (85%), 473 ($\text{M} - \text{H}^+$) (100%).

^1H NMR (400 MHz, DMSO-d_6) δ (ppm): 2.3 (t, 2H, COCH_2CH_2), 2.4 (t, 2H, COCH_2CH_2), 2.74 (t, 4H, $\text{CH}_2\text{CH}_2\text{S}$), 3.3 (m, 4H, $\text{CH}_2\text{CH}_2\text{NH}$), 4.2 (t, 1H, CHCH_2), 4.3 (d, 2H, CHCH_2O), 7.3 (m, 2H, Ar-H), 7.4 (t, 4H, Ar-H), 7.6 (d, 2H, Ar-H), 7.87 (d, 2H, CH_2NHCO), 8.0 (t, 1H, CH_2COOH) Figure A.5; Appendix 2

Fmoc N-protected cystamine glutaric acid (16)

Yield: 1.7g, 35%.

LR-MS for $\text{C}_{24}\text{H}_{28}\text{N}_2\text{O}_5\text{S}_2$ [Mass: 488], found: 489 ($\text{M} + \text{H}^+$) (100%), 511 ($\text{M} + \text{Na}^+$) (70%), 487 ($\text{M} - \text{H}^+$) (100%).

^1H NMR (400 MHz, DMSO-d_6) δ (ppm): 1.5 (m, 2H, $\text{CH}_2\text{CH}_2\text{CH}_2$), 2.0 (t, 2H, $\text{CH}_2\text{CH}_2\text{CO}$), 2.3 (t, 2H, COCH_2CH_2), 2.58 (m, 4H, NHCH_2CH_2), 3.1 (m, 4H, $\text{CH}_2\text{CH}_2\text{NHCO}$), 4.1 (m, 1H, CHCH_2O), 4.15 (d, 2H, CHCH_2), 7.1 (d, 2H, Ar-H), 7.2 – 7.3 (m, 4H, Ar-H), 7.5 (d, 2H, Ar-H), 7.7 (d, 2H, CH_2NHCO), 7.8 (t, 1H, CH_2COOH). Figure A.6; Appendix 2

3.2.2. Methods

3.2.3. Characterisation and Identification of Novel Pseudo-Peptides

All synthetic products were analysed for purity by Thin Layer Chromatography (TLC) and Mass Spectrometry (MS). Solvent system used for thin layer chromatography (TLC), Dichloromethane: methanol (9:1).

3.2.4. Solid Phase Peptide Synthesis (SPPS) using 1, 3-Diaminopropane trityl resin (DAP).

3.2.4.1. Synthesis of Fmoc-2[cystamine-succinic]-DAP (Fmoc2CSDAP)

(9H-fluoren-9-yl)methyl (27-amino-8,11,20,23-tetraoxo-3,4,15,16-tetrathia-7,12,19,24-tetraazaheptacosyl)carbamate. (**17**)

3.2.4.1.1. Resin swelling

0.2g (0.16mmol) of diaminopropane resin was transferred into a vessel and 10mL of DCM was added. The vessel was left in the fridge overnight. The next day DCM was flushed out and the resin was washed with DMF (3x10mL).

3.2.4.1.2. Method A: Peptide coupling

HOBT (0.085g; 0.63mmol; 3.92 equivalents), TBTU (0.2g; 0.62mmol; 3.94 equivalents) were dissolved in DMF (10mL) and added to the vessel containing the resin.

DIPEA (110 μ L; 0.65mmol; 4 equivalents) was also added and the mixture left for 10 minutes at room temperature. Compound **15** (0.3g; 0.66mmol; 4 equivalents) was dissolved in DMF (5mL) and added to the mixture last. The mixture was mounted onto a Stuart Flash shaker (SF1) and shaken for

2 hours at a speed of 700 osc/min. Additional coupling reactions were carried out using similar amounts of reagents and **15** and/or **16**.

3.2.4.1.3. Method B: Kaiser Test

After each cycle of coupling and deprotection, the reaction mixture was flushed out and washed with DMF (3x 10mL). A few beads of dry resin were transferred into a micro-test tube and ninhydrin (6 drops), molten phenol solution (6 drops) and potassium cyanide solution (6 drops) were added. The test tube was heated with a heat gun for 20 seconds. Colourless beads would indicate that coupling had taking place, whereas a purple colour would indicate a presence of a primary amine in the sample.

3.2.4.1.4. Method C: Amino Group Deprotection

A mixture of DMF and piperidine (4:1, 20mL) was added to the washed resin and shaken for 2 hours.

3.2.4.1.5. Method D: Peptide Cleavage

After the second coupling, the reaction mixture was flushed out and washed with DCM (10mL). A solution of TFA in DCM (1% v/v; 10mL) was added and the reaction mixture was shaken for 2 hours, flushed out and washed with DCM (3 x 10mL). The resulting filtrate was evaporated under vacuum to yield a viscous, hygroscopic residue which was treated with ethanol (3 x 15mL) and re-evaporated to dryness.

Yield: 0.1g, 10%. HR-MS (ESI): calculated for $C_{34}H_{49}N_6O_6S_4$ 765.2591, found: 765.2583 $[M + H]^+$ (100%). Figure B.3; Appendix 3

Other major peaks, $(M + Cl^-)$ 799 (85%), $(M + FA - H^+)$ 809 (100%), $(M + TFA - H^+)$ 877 (72%).

3.2.4.2. Synthesis of Fmoc-3[cystamine-succinic]-DAP (Fmoc3CSDAP)

(9H-fluoren-9-yl)methyl (39-amino-8,11,20,23,32,35-hexaoxo-3,4,15,16,27,28-hexathia-7,12,19,24,31,36-hexaazanonatriacontyl) carbamate (**18**).

This compound was prepared from diaminopropane resin (0.5g; 0.4mmol), HOBT (0.211g; 1.55mmol; 3.92 equivalents), TBTU (0.506g; 1.57mmol; 3.94 equivalents), DIPEA (275 μ L; 1.59mmol; 4 equivalents) and **15** (0.76g; 1.60mmol; 4 equivalents) using Method **A**. The same amounts of reagents and **15** were used for all couplings.

A Kaiser test and deprotection were performed using Method **B** and **C** respectively and the resulting oily product was obtained using Method **D**.

Yield: 0.55g, 11%.

HR-MS (ESI): Calculated for C₄₂H₆₃N₈O₈S₆ 999.3088 [M + H]⁺, found: 999.3070 [M + H]⁺ (55%). Figure B.4; Appendix 3

3.2.4.3. Synthesis of Fmoc-[cystamine-glutaric]-DAP (FmocCGDAP)

(9H-fluoren-9-yl)methyl (2-((2-(5-((3-aminopropyl)amino)-5-oxopentanamido)ethyl)disulfanyl)ethyl)carbamate. (**19**)

This compound was prepared from diaminopropane resin (0.2g; 0.16mmol), HOBT (0.085g; 0.63mmol; 3.92 equivalents), TBTU (0.2g; 0.62mmol; 3.94 equivalents), DIPEA (110 μ L; 0.65mmol; 4 equivalents), and compound **16** (0.313g; 0.64mmol) using Method **A**.

A Kaiser test was performed using Method **B**. The peptide cleavage was carried out using Method **D** to yield a yellow viscous, oily product.

Yield: 0.1g; 29%.

HR-MS (ESI): calculated for C₂₇H₃₅N₄O₄S₂ 545.2251 [M + H]⁺, found: 545.2255

[M + H]⁺ (100%). Figure B.5; Appendix 3

(173.17) non identifiable contaminant (100%), other peaks, (M + Na)⁺ 567 (15%),

657 (M + TFA - H)⁻ (100%), 589 (M + FA - H)⁻ (60%)

3.2.4.4. Synthesis of Fmoc-2[cystamine-glutaric]-DAP (Fmoc2CGDAP)

(9H-fluoren-9-yl)methyl (29-amino-8,12,21,25-tetraoxo-3,4,16,17-tetrathia-7,13,20,26-tetraazanonacosyl)carbamate. (**20**)

This compound was prepared from diaminopropane resin (0.5g; 0.4mmol), HOBT (0.211g; 1.55mmol; 3.92 equivalents), TBTU (0.506g; 1.57mmol; 3.94 equivalents), DIPEA (275 μ L; 1.59mmol; 4 equivalents) and **16** (0.8g; 1.60mmol; 4 equivalents) using Method **A**. The same amounts of reagents and **16** were used for all couplings. A Kaiser test and deprotection were performed using Method **B** and **C** respectively, and the resulting oily product was obtained using Method **D**.

Yield: 0.4g, 15%.

HR-MS (ESI): calculated for C₃₆H₅₃N₆O₆S₄ 793.2904 [M + H⁺]⁺, found: 793.2900 (100%). Figure B.6; Appendix 3

Other major peaks, (M + Na⁺) 815 (92%), (M/2 + H⁺) 397 (50%), (M + Cl⁻) 827 (60%), (M + TFA - H⁺) 837 (80%).

3.2.4.5. Attempted Synthesis of Fmoc-3[cystamine-glutaric]-DAP (Fmoc3CGDAP). (9H-fluoren-9-yl)methyl(42-amino-8,12,21,25,34,38-hexaoxo-3,4,16,17,29,30-hexathia-7,13,20,26,33,39-hexaazadotetracontyl)carbamate. (**21**)

This compound was prepared from diaminopropane resin (0.2g; 0.16mmol), HOBT (0.085g; 0.63mmol; 3.92 equivalents), TBTU (0.2g; 0.62mmol; 3.94 equivalents), DIPEA (110 μ L; 0.65mmol; 4 equivalents), and compound **16** (0.31g; 0.64mmol; 4 equivalents) using Method **A**.

A Kaiser test and amino deprotection were performed using Method **B** and **C** respectively. Peptide cleavage was carried out using Method **D**.

Yield: 0.3g, 15%.

LR-MS for C₄₅H₆₈N₈O₈S₆ [Mass: 1014], no recognisable peak obtained.

3.2.4.6. Synthesis of Fmoc-4[cystamine-glutaric]-DAP (Fmoc4CGDAP)

(9H-fluoren-9-yl)methyl(55-amino-8,12,21,25,34,38,47,51-octaoxo-3,4,16,17,29,30,42,43-octathia-7,13,20,26,33,39,46,52-octaazapentapentacontyl)carbamate. (**22**)

This compound was prepared from diaminopropane resin (0.3g; 0.24mmol), HOBT (0.127g; 0.94mmol; 3.92 equivalents), TBTU (0.303g; 0.2.93mmol; 3.94 equivalents), DIPEA (165 μ L; 0.96mmol; 4 equivalents), and compound **16** (0.47g; 0.0.96mmol; 4 equivalents) using Method **A**. A Kaiser test and amino deprotection were performed using Method **B** and **C** respectively. Peptide cleavage was carried out using Method **D**.

Yield: 0.25g, 5%

LR-MS for C₅₄H₈₄N₁₀O₁₀S₈ [Mass: 1288], found: 1289 (M + H⁺) (25%), 1310 (M + Na⁺) (100%), 1287 (M - H⁺) (65%), 1323 (M + Cl⁻) (60%).

3.2.4.7. Synthesis of Fmoc-[cystamine-succinic-cystamine-glutaric]-DAP (FmocCSGDAP)

(9H-fluoren-9-yl)methyl (28-amino-8,11,20,24-tetraoxo-3,4,15,16-tetrathia-7,12,19,25-tetrazaooctacosyl)carbamate (**23**)

This compound was prepared from diaminopropane resin (0.2g; 0.16mmol), HOBT (0.085g; 0.63mmol; 3.92 equivalents), TBTU (0.2g; 0.62mmol; 3.94 equivalents), DIPEA (110 μ L; 0.65mmol; 4 equivalents), compounds **15** (0.30g; 0.66mmol; 4 equivalents) and **16** (0.31g; 0.64mmol; 4 equivalents) using Method **A**. A Kaiser test and amino deprotection were performed using Method **B** and **C** respectively. Peptide cleavage was carried out using Method **D** to yield a colourless and viscous oily product.

Yield: 0.076g, 8%.

HR-MS (ESI): calculated for C₃₅H₅₁N₆O₆S₄ 779.2747 [M + H]⁺, found: 779.2738 [M + H]⁺ (80%). Figure B.7; Appendix 3

Other major peaks, (M + Na⁺) 801 (70%), (M + K⁺)/2 + H⁺ 407 (65%), (M + Cl⁻) 813 (70%), (M + FA - H⁺) 823 (55%).

3.2.5. Solid Phase Peptide Synthesis using H-D-Alanine-2-chlorotrityl resin.

3.2.5.1. Synthesis of Fmoc-2[cystamine-succinic]-Alanine (Fmoc-2CS-Ala)(1-(9H-fluoren-9-yl)-3,12,15,24-tetraoxo-2-oxa-7,8,19,20-tetrathia-4,11,16,23-tetraazaheptacosan-27-oyl)alanine. (24)

This compound was prepared from alanine trityl resin (0.2g; 0.11mmol), HOBT (0.058g; 0.43mmol; 3.92 equivalents), TBTU (0.139g; 0.43mmol; 3.94 equivalents), DIPEA (76 μ L; 0.44mmol; 4 equivalents), and compound **15** (0.21g; 0.44mmol; 4 equivalents) using Method **A**. A Kaiser test and amino deprotection were performed using Method **B** and **C** respectively. Peptide cleavage was carried out using Method **D** producing a colourless oily product.

Yield: 0.09g, 13%

HR-MS (ESI): calculated for C₃₄H₄₆N₅O₈S₄ 780.2224 [M + H]⁺, found: 780.2226 [M + H]⁺ (55%). Figure B.8; Appendix 3

3.2.5.2. Synthesis of Fmoc-2[cystamine-glutaric]-Ala (Fmoc-2CG-Ala)

(1-(9H-fluoren-9-yl)-3,12,16,25-tetraoxo-2-oxa-7,8,20,21-tetrathia-4,11,17,24-tetraazanonacosan-29-oyl)alanine. (25)

This compound was prepared from alanine trityl resin (0.2g; 0.11mmol), HOBT (0.058g; 0.43mmol; 3.92 equivalents), TBTU (0.139g; 0.43mmol; 3.94 equivalents), DIPEA (76 μ L; 0.44mmol; 4 equivalents), and compound **16** (0.22g; 0.44mmol; 4 equivalents) using Method **A**. A Kaiser test and amino deprotection were performed using Method **B** and **C** respectively. Peptide cleavage was carried out using Method **D** to yield a colourless and viscous product.

Yield: 0.07g, 10%.

HR-MS (ESI): calculated for C₃₆H₅₀N₅O₈S₄ 808.2537 [M + H]⁺, found: 808.2537 [M + H]⁺ (100%). Figure B.9; Appendix 3

3.2.5.3. Synthesis of Fmoc-2[cystamine-succinic-cystamine-glutaric]-Ala (Fmoc-CS-CG-Ala)

(1-(9H-fluoren-9-yl)-3,12,15,24-tetraoxo-2-oxa-7,8,19,20-tetrathia-4,11,16,23-tetrazaoctacosan-28-oyl)alanine. (**26**)

This compound was prepared from alanine trityl resin (0.2g; 0.11mmol), HOBT (0.058g; 0.43mmol; 3.92 equivalents), TBTU (0.139g; 0.43mmol; 3.94 equivalents), DIPEA (76 μ L; 0.44mmol; 4 equivalents), and compounds **15** (0.21g; 0.44mmol; 4 equivalents) and **16** (0.22g; 0.44mmol; 4 equivalents) using Method **A**. A Kaiser test and amino deprotection were performed using Method **B** and **C** respectively. Peptide cleavage was carried out using Method **D** to yield a colourless and viscous product.

Yield: 0.08g, 11%.

HR-MS (ESI): calculated for C₃₅H₄₈N₅O₈S₄ 794.2380 [M + H]⁺, found: 794.2383 (65%). Figure B.10; Appendix 3

3.2.6. Solid Phase Peptide Synthesis using Lysine (Boc)₂ – chlorotrityl resin.

3.2.6.1. Synthesis of Fmoc-2[cystamine-succinic]-(Boc-Lys) (Fmoc-2CS-BocLys)

N²-(1-(9H-fluoren-9-yl)-3,12,15,24-tetraoxo-2-oxa-7,8,19,20-tetrathia-4,11,16,23-tetrazaheptacosan-27-oyl)-N⁶-(tert-butoxycarbonyl)lysine. (**27**)

This compound was prepared from lysine 2-chlorotrityl trityl resin (0.2g; 0.15mmol), HOBT (0.079g; 0.58mmol; 3.92 equivalents), TBTU (0.190g; 0.59mmol; 3.94 equivalents), DIPEA (103 μ L; 0.60mmol; 4 equivalents), and compound **15** (0.28g; 0.60mmol; 4 equivalents) using Method **A**.

A Kaiser test and amino deprotection were performed using Method **B** and **C** respectively. Peptide cleavage was carried out using Method **D** to yield a colourless, oily product.

Yield: 0.15g, 13%.

HR-MS (ESI): calculated for C₄₂H₆₁N₆O₁₀S₄ 937.3327 [M+H]⁺, found: 937.3330.

Calculated for 959.3146 [M+Na]⁺, found: 959.3147 [M+Na]⁺. Figure B.11;

Appendix 3. Other peaks, (M - ^tBoc) 837 (15%), (M - H⁺) 935 (45%).

3.2.6.2. Synthesis of Fmoc-2[cystamine-glutaric]-(Boc-Lys) (Fmoc-2CG-BocLys)

N2-(1-(9H-fluoren-9-yl)-3,12,16,25-tetraoxo-2-oxa-7,8,20,21-tetrathia-4,11,17,24-tetraazanonacosan-29-oyl)-N6-(tert-butoxycarbonyl)lysine. (**28**)

This compound was prepared from lysine 2-chlorotrityl trityl resin (0.3g; 0.225mmol), HOBT (0.119g; 0.88mmol; 3.92 equivalents), TBTU (0.285g; 0.89mmol; 3.94 equivalents), DIPEA (0.155μL; 0.90mmol; 4 equivalents), and compound **16** (0.44g; 0.90mmol; 4 equivalents) using Method **A**. A Kaiser test and amino deprotection were performed using Method **B** and **C** respectively. Peptide cleavage was carried out using Method **D** to yield a colourless, oily product.

Yield: 0.2g, 11%

HR-MS (ESI): calculated for $C_{44}H_{65}N_6O_{10}S_4$ 965.3640 $[M + H]^+$, found: 965.3636 (100%). Figure B.12; Appendix 3

Other major peaks, $(M + Na^+)$ 987 (85%), $(M - H^+)$ 963 (100%).

3.2.6.3. Synthesis of Fmoc-[cystamine-succinic-cystamine-glutaric]-(BocLys) (Fmoc-CS-CG-BocLys)

N2-(1-(9H-fluoren-9-yl)-3,12,15,24-tetraoxo-2-oxa-7,8,19,20-tetrathia-4,11,16,23-tetrazaoctacosan-28-oyl)-N6-(tert-butoxycarbonyl)lysine. (**29**)

This compound was prepared from lysine 2-chlorotrityl trityl resin (0.3g; 0.225mmol), HOBT (0.119g; 0.88mmol; 3.92 equivalents), TBTU (0.285g; 0.89mmol; 3.94 equivalents), DIPEA (0.155μL; 0.90mmol; 4 equivalents), **15** (0.43g; 0.90mmol; 4 equivalents) and **16** (0.44; 0.90mmol; 4equivalents) using Method **A**. A Kaiser test and amino deprotection were performed using Method **B** and **C** respectively. Peptide cleavage was carried out using Method **D** to produce a colourless, oily product.

Yield: 0.18g, 10%

HR-MS (ESI): calculated for $C_{43}H_{61}N_6O_{10}S_4$ 949.3337 $[M - H]^-$, found: 949.3283

$[M - H]^-$ (100%). Figure B.13; Appendix 3

$(M + Cl^-)$ 985 (100%).

3.2.7. Convergent Peptide Synthesis (CPS)

3.2.7.1. Synthesis of Fmoc-cystamine-succinic-DAP-succinic-cystamine-Fmoc (Fmoc-CS-DAP-SC-Fmoc) .

bis((9H-fluoren-9-yl)methyl) (8,11,17,20-tetraoxo-3,4,24,25-tetrathia-7,12,16,21-tetraazaheptacosane-1,27-diyl)dicarbamate. (**30**)

36 (0.053g; 0.1mmol), HOBT (0.014g; 0.10 mmol; 1.1 equivalents), and TBTU (0.033g; 0.10mmol; 1.1 equivalents) were dissolved in a small volume of DMF (5 mL) and after 10 minutes DIPEA (52 μ L; 0.31mmol; 3.2 equivalents) was added. The mixture was left for a further 10 minutes at room temperature and **15** (0.05g; 0.10mmol; 1.1 equivalents) was added last. The reaction mixture was stirred for two days at room temperature and monitored by TLC.

Liquid-liquid extraction was carried out with H₂O and DCM (3 x 200 mL). The organic layer was dried with MgSO₄, filtered and reduced to produce compound **30**.

Yield: 0.2g, 18 %.

LR-MS for C₄₉H₅₈N₆O₈S₄ [Mass: 988], found: 987 (M + H⁺) (20%), 1025 (M + K⁺) (55%).

3.2.7.2. Synthesis of Fmoc-cystamine-glutaric-DAP-glutaric-cystamine-Fmoc (Fmoc-CG-DAP-GC-Fmoc).

bis((9H-fluoren-9-yl)methyl) (8,12,18,22-tetraoxo-3,4,26,27-tetrathia-7,13,17,23-tetraazanonacosane-1,29-diyl)dicarbamate. (**31**)

To a solution of (**19**) (0.1g; 0.18mmol), HOBT (0.049; 0.36mmol; 2 equivalents), TBTU (0.12g; 0.37mmol; 2 equivalents), and DIPEA (183 μ L; 1.06mmol; 5.8 equivalents) in 5 mL of DMF was added **16** (0.18g; 0.37mmol; 2 equivalents). The mixture was stirred for 24 hours at room temperature and monitored by TLC. The same amounts of coupling reagents were added to the stirred solution and stirring continued for a further 24 hours at room temperature.

Liquid-liquid extraction was carried out with H₂O and DCM (3 x 200 mL). The organic layer was dried with MgSO₄, filtered and reduced to produce a yellow solid (**31**).

Yield: 0.13g, 23%

LR-MS for C₅₁H₆₂N₆O₈S₄ [Mass: 1014], found: 1015 (M + H⁺) (15%), 1037 (M + Na⁺) (30%), 1049 (M + Cl⁻) (85%), 1059 (M + FA - H⁺) (100%).

3.2.7.3. Attempted synthesis of Fmoc-cystamine-glutaric-DAP-succinic-cystamine-Fmoc (Fmoc-CG-DAP-SC-Fmoc).

bis((9H-fluoren-9-yl)methyl) (8,11,17,21-tetraoxo-3,4,25,26-tetrathia-7,12,16,22-tetrazaooctacosane-1,28-diyl)dicarbamate. (**32**)

To a solution of (**19**) (0.086g; 0.16mmol) in 5 mL DMF was added HOBT (0.13mmol; 2 equivalents), TBTU (0.102g; 0.32mmol; 2 equivalents), and DIPEA (157μl; 0.9mmol; 5.8 equivalents). **15** (0.15g; 0.32mmol; 2 equivalents) was then added to the mixture and the reaction mixture stirred for 2 days at room temperature and monitored by TLC. Liquid-liquid extraction was carried out with H₂O and DCM (3 x 200 mL). The organic layer was dried with MgSO₄, filtered and reduced to produce a yellow oily product **32**.

Yield: 0.05g, 11 %

LR-MS for C₅₀H₆₀N₆O₈S₄ [Mass: 1000.34], found 1000.34. No identifiable peaks were obtained.

3.2.7.4. Attempted synthesis of Fmoc-cystamine-glutaric x 2-DAP-glutaric-cystamine-Fmoc. (Fmoc-CG-DAP2GC-Fmoc-cystamine).

bis((9H-fluoren-9-yl)methyl) (8,12,21,25,31,35-hexaoxo-3,4,16,17,39,40-hexathia-7,13,20,26,30,36-hexaazadotetracontane-1,42-diyl)dicarbamate (**33**).

This compound was prepared with **20** (0.1g; 0.126mmol), HOBT (0.019g; 0.14 mmol; 1.1 equivalents), TBTU (0.044g; 0.13mmol; 1.1 equivalents), DIPEA (69μL; 0.4mmol; 3.2 equivalents), and **16** (0.11g; 0.22mmol; 1.1 equivalents). The reaction mixture was stirred for two days at room temperature and monitored by TLC. The solution was partitioned between

DCM and water (3 x 200mL). The organic layer was removed, dried with MgSO₄, filtered and reduced to give a colourless oily product **33**.

Yield: 0.06g, 13%

LR-MS for C₆₀H₇₈N₈O₁₀S₆ [Mass: 1262.42]. No product peaks could be identified by m/s. Other peaks of interest Fmoc-cystamine-glutaric acid [C₂₄H₂₈N₂O₅S₂] (M + Cl⁻) 523 (20%).

3.2.7.5. Synthesis of Fmoc- x 2 [cystamine-succinic]- Lysine (Boc) – Fmoc. (Fmoc-2CS-Lys(Boc)-Fmoc-cystamine)

bis((9H-fluoren-9-yl)methyl) (9-(4-((tert-butoxycarbonyl)amino)butyl)-8,11,14,23,26-pentaoxo-3,4,18,19,30,31-hexathia-7,10,15,22,27-pentaazatritriacontane-1,33-diyl)dicarbamate. (**34**)

This compound was prepared using HOBT (0.028g; 0.27mmol; 2 equivalents), TBTU (0.068g; 0.21mmol; 2 equivalents), Fmoc-cystamine (0.079g; 0.21mmol; 2 equivalents), DIPEA (105μL; 0.61mmol; 5.8 equivalents), and ^tBoc protected compound **27** (0.99g; 1.06mmol). The reaction mixture was stirred overnight at room temperature. Subsequent amounts of **27** and coupling reagents (double the equivalence) were added to the stirred solution and stirring continued for a further 24 hours, while the reaction was monitored by TLC. The solution was partitioned between DCM and water (3 x 200mL). The organic layer was removed, dried with MgSO₄, filtered and reduced to give a yellow viscous, oily product **34**.

Yield: 0.09g, 10%.

LR-MS for C₆₁H₈₀N₈O₁₁S₆ [Mass: 1292], found: 1294 (10%), 1294 (M + 2H⁺) (10%).

3.2.7.6. (Fmoc-2CS-Lys(Boc)-GC-Fmoc) Attempted synthesis of Fmoc- x 2 [cystamine-succinic] –Lys(Boc)-glutaric – cystamine-Fmoc.

29-(1-(9H-fluoren-9-yl)-3,12,16-trioxo-2-oxa-7,8-dithia-4,11,17-triazahenicosan-21-yl)-1-(9H-fluoren-9-yl)-3,12,15,24,27-pentaoxo-2-oxa-7,8,19,20-tetrathia-4,11,16,23,28-pentaazatriacontan-30-oic acid. (**35**)

Refer to **3.2.7.4**. This compound was prepared with HOBT (0.028g; 0.20 mmol; 3.92 equivalents), TBTU (0.065g; 0.20mmol; 3.94 equivalents), **16** (0.13g; 0.27mmol; 4 equivalents), DIPEA (36 μ L; 0.21mmol; 4 equivalents), and ^tBoc deprotected compound **27** (0.044g; 53mmol) using the method described for **34**. A yellow viscous, oily product (**35**) was obtained.

Yield: 0.075g, 19%.

LR-MS for C₆₁H₇₈N₈O₁₂S₆ [Mass: 1306.41]. No product peaks could be identified by m/s. Other peaks, (Fmoc-cystamine-glutaric) [C₃₇H₅₂N₆O₈S₄, Mass: 488], found: 489 (M + H⁺) (90%), 977 (2M + H⁺) (25%), 245 (M/2 + H⁺), 487 (M - H⁺) (100%).

3.2.7.7. Synthesis of Fmoc-cystamine-succinic-DAP (Fmoc(CS)-DAP)

9H-fluoren-9-yl) methyl (2-((2-(4-((3-aminopropyl)amino)-4-oxobutanamido)ethyl)disulfanyl)ethyl)carbamate. (**36**)

This compound was prepared from diaminopropane resin (0.2g; 0.16mmol), HOBT (0.085g; 0.63mmol; 3.92 equivalents), TBTU (0.2g; 0.62mmol; 3.94 equivalents), DIPEA (110 μ L; 0.65mmol; 4 equivalents), and Fmoc N-protected cystamine-succinic (**15**) (0.3g; 0.66mmol; 4 equivalents) using Method **A**. A Kaiser test and amino deprotection were performed using Method **B** and **C** respectively. Peptide cleavage was carried out using Method **D**.

Yield: 0.05g; 15%

LC-MS for C₂₆H₃₄N₄O₄S₂ [Mass: 530], found: 531 (M + H⁺) (100%), 553 (M + Na⁺) 553 (67%).

3.3. Cell culture

3.3.1. Materials

All cell culture reagents were purchased from Invitrogen (Paisley, UK), all plastics and glassware from FisherScientific UK Ltd. (Loughborough, UK) and all chemicals from Sigma-Aldrich (Poole, UK) unless otherwise stated and were used without further purification.

3.3.2. Human cystinotic fibroblasts (GM00008)

Human cystinotic fibroblasts were purchased from Coriell Cell Repositories (NJ, USA) and were used to carry out all *in vitro* investigations.

3.3.2.1. Cell growth conditions

Cell growth was carried out using under aseptic conditions in an Aura laminar flow air hood (Bioair Instruments, UK) using sterile plastics, glassware and solutions.

Routine cells culture was carried out using Eagle's minimum essential media (EMEM) supplemented with 15% foetal calf serum (FBS), 200 U mL⁻¹ Penicillin, 200 µg mL⁻¹ Streptomycin and 2 mM Glutamine. Growth conditions were sustained at 37°C in a humidified atmosphere of 5% CO₂ /95% room air in a Hera cell 150 incubator (Heraeus, UK). Cells multiplied in 75cm² tissue culture flasks and cell confluence was monitored by visualisation using an inverted light Leica DMIL microscope (Microscopesystems Limited).

The media was changed twice weekly and replaced with 12mL of fresh growth medium.

3.3.2.2. Routine subculture

Cells were collected by decanting the growth medium from the monolayer which was rinsed 3 times with sterile phosphate buffer saline (PBS). A solution of 0.05% Trypsin (5mL) was added to the monolayer and incubated for 5 minutes. The cell monolayer was removed by gently rocking the flask, and an equal volume of medium containing FBS was added to neutralise the enzymatic action of the Trypsin. The cell suspension was transferred into a sterile universal tube and the cell pellet was collected by centrifugation at 1200 rpm for 6 minutes. After carefully removing the supernatant, the cell pellet was resuspended with 1mL of fresh medium. The cell suspension was divided using a ratio of 1 to 3, and an equal volume of 333 μ L of cell suspension was introduced to sterile 75cm² flasks and supplemented with 12mL of fresh growth medium. The flasks were placed in an incubator under aseptic conditions as previously described, and left undisturbed to allow cell adherence and growth. Cell growth was checked regularly under a microscope. Once reaching 80% confluence, the cells were prepared for experimental procedures, frozen in liquid nitrogen and stored as pellets at -80°C.

3.3.3. Cell viability and proliferation

3.3.3.1. Trypan blue dye exclusion staining protocol

Cystinotic fibroblasts were harvested from a 75cm² flask using method 3.3.2.2, and cell count was performed using method 3.3.3.1.

A 1:1 dilution of the cell suspension (500 μ L) was prepared using 0.4% trypan blue solution and left to stand for 1-2 minutes to allow non viable cells to take up the colouring agent. A small aliquot of the cell suspension was loaded into the counting chambers of a haemocytometer where the area under the cover slip was covered by means of capillary action. Cell counting (viable and non viable) was performed visually using a microscope in the 25 squares. The total number of viable cells was calculated using the formula below.

$$\text{Number of cells/mL} = \frac{\text{Cell count per large square} \times \text{Dilution factor} \times 10^{-4} \text{ cm}^3}{\text{(Volume of large square)}}$$

3.3.3.2. Alamar blue cell growth assay

Following cell count described in **3.3.2.1**, the cell suspension was diluted to 25,000 cells mL⁻¹ using growth media. Cells were seeded in a 96 well sterile cell culture plates, at a density of 0.025 x 10⁶ cells mL⁻¹. 200µL of the diluted cell suspension was applied to the subsequent wells (i.e. 5000 cells/well).

The plates were transferred in an incubator under the same aseptic conditions described in section **3.3.2.1**, and were allowed to adhere overnight. The next day, cell adherence and initial growth were confirmed by microscopy. Fresh growth medium supplemented with 10% (v/v) alamar blue (Serotec) was used and the plates were incubated in the presence of 50µM either cysteamine, or novel compounds. Vehicle control (0.5% DMSO) and untreated cell control were also used in the assay. The assay was performed in triplicates and cell growth was measured at 0, 24, 48, and 72 hours, by measuring the absorbance at 570nm using a Synergy/HT FL6000 microplate reader (Biotek).¹⁴⁰

3.3.4. Quantitative Determination of Cysteine in Samples

3.3.4.1 Thiol assay

The assay was carried out using a method developed in house using freshly prepared buffers and solutions.

Buffer **A** (5mM sodium acetate, 50mM NaCl, 0.5mM EDTA, pH 4.7).

Buffer **B** (40mM sodium phosphate, 2mM EDTA, pH 7.6).

Buffer **C** (5mM sodium acetate, pH 4.0).

Cells were harvested from a 75cm² flask using method **3.3.2.2**.

A 10 mM stock solution (DMSO) for each of the compounds to be analysed and the controls (cysteamine and vehicle) was prepared in 0.5% DMSO (1mL). From the stock solution a 50 μ M working solution (Growth Media) was then prepared for each sample.

The cell pellets were removed from -80°C freezer and immediately transferred to ice and resuspended in 200 μ L of 1mM N-ethylmaleimide prepared in phosphate buffer solution (pH 7.6). Gentle pipetting was applied to break down the cell pellets. Cell lysis was achieved by sonication in a sonic water bath for 10 seconds (step **a**) followed by 20 seconds of cooling on ice (step **b**). Steps **a.** and **b.** were repeated a further 2 times. The solution was centrifuged (Biofuge primo R Heraeus centrifuge) at 15000 rpm for 10 minutes at 4°C. A portion of 100 μ L of each cell lysate was removed and 10 μ L of 4M NaBH₄ in 0.1 M NaOH:DMSO was added. To a 96 well plate, 3 μ L of buffer **A** was added, followed by a similar volume of the reduced sample lysates (prepared in cell lysis), followed by 100 μ L of 0.6mgmL⁻¹ of papain-SSCH₃ which was prepared by mixing equal volumes of 1.2mgmL⁻¹ papain-SSCH₃ working solution with buffer **B**. The plate was gently mixed and left to incubate for 1 hour at room temperature. After this time, 100 μ L of 4.9 mM L-BAPNA solution in buffer **C** was added to each well and the plate was gently mixed and left to incubate for a further 1 hour at room temperature. The principle of the assay is summarised in diagram 1. The absorbance was measured at 410 nm using the plate reader. The cysteine levels were recorded by comparison to known cysteine standards.¹⁴⁰

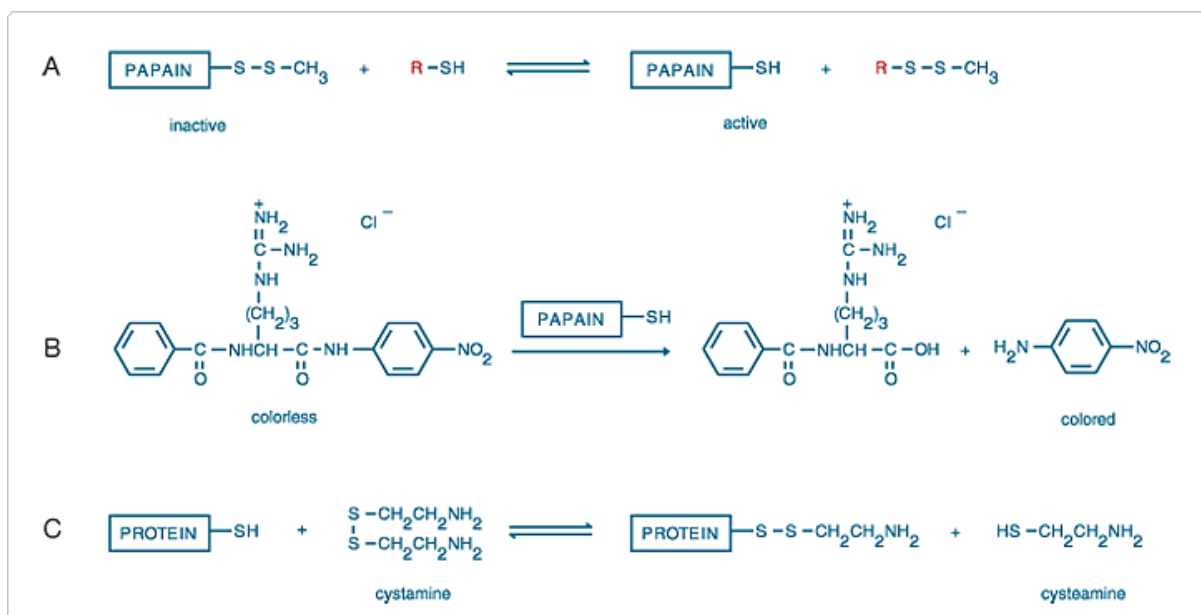


Diagram 1 was obtained from www.lifetechnologies.com

3.3.4.2. Bradford protein determination in samples

This assay was performed according to the Bradford method on the same day as the cysteine quantity.¹⁴⁰ A calibration using Bovine Serum Albumin (BSA prepared by dissolving 10mg of BSA in 10mL of dH₂O) was also carried out. The cell supernatant (40 μL) was diluted in 20 μL of dH₂O and 10 μL of the diluted cell supernatant (1:20) was added to a 96 wells plate. 200 μL of Bradford reagent was added to each well containing the diluted samples and the plate was left to incubate for 5 minutes at room temperature. The absorbance was measured at 595 nm using a plate reader. The protein concentration was recorded by comparison to known BSA standards.¹⁴⁰

CHAPTER 4

RESULTS AND DISCUSSION

4.1. Multicomponent crystals

4.1.1. Results

All of the crystals produced in this study used cysteamine as a starting material. Notwithstanding this, the results showed that all new crystals formed were salts of cysteamine except for cysteamine tartrate monohydrate. These findings were only revealed when X-ray diffraction analysis of the novel salts was carried out. This is due to the tendency for cysteamine to oxidise to cystamine (the disulfide form of the compound) at room temperature in solution.

4.1.1.1. Morphology of Novel Salts

4.1.1.1.a. Cystamine Adipate

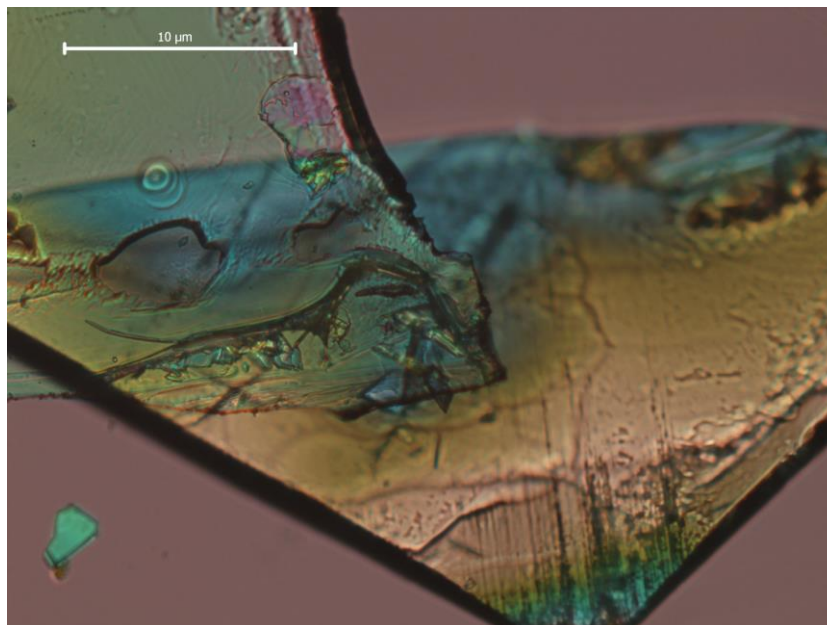


Figure 27.: Image of crystals of Cystamine Adipate taken at 200x magnification using crossed polarizers

4.1.1.1.b. Cystamine 2,6 Dihydroxybenzoate

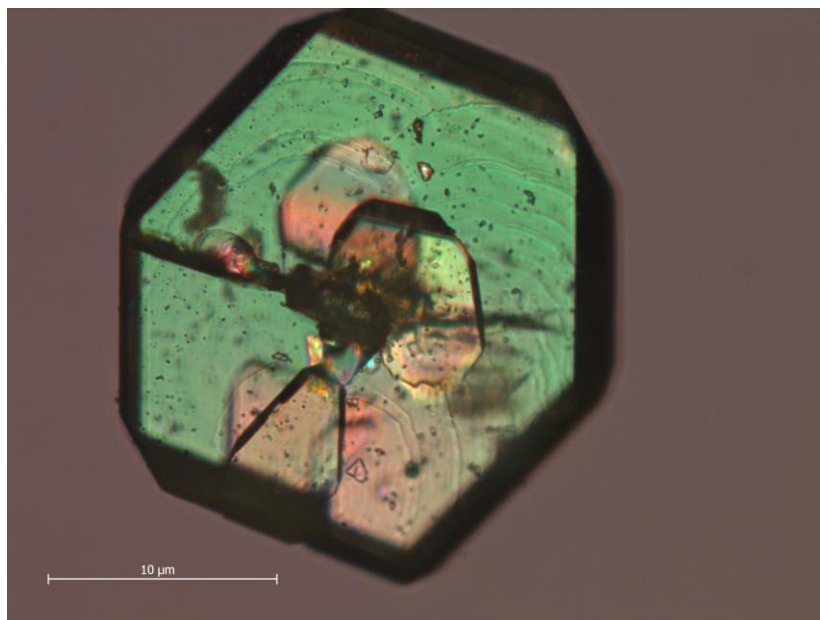


Figure 28.: Image of crystals of Cystamine 2,6 Dihydroxybenzoate taken at 200x magnification using crossed polarizers

4.1.1.1.c. Cystamine 3-Nitrobenzoate

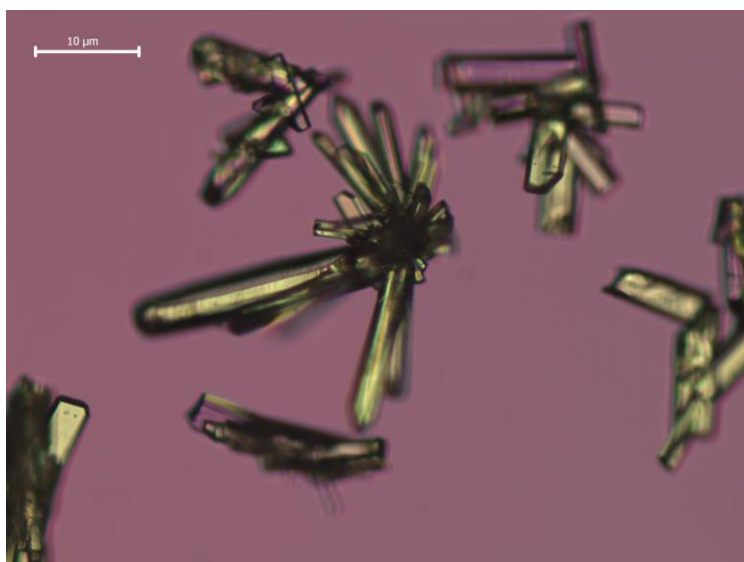


Figure 29.: Image of crystals of Cystamine 3-Nitrobenzoate taken at 100x magnification using crossed polarizer

4.1.1.1.d. Cystamine Glutarate

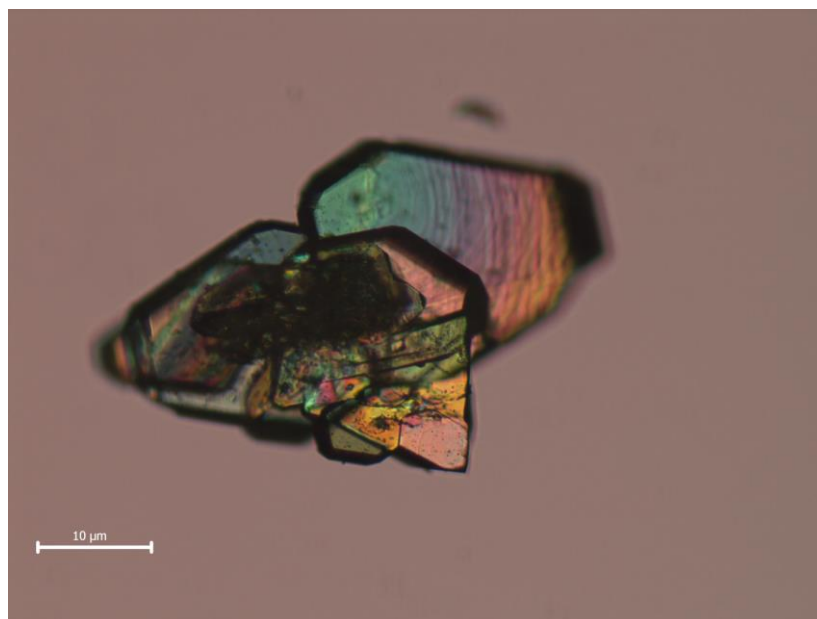


Figure 30.: Image of crystals of Cystamine Glutarate taken at 100x magnification using crossed polarizers

4.1.1.1.e. Cysteamine Tartrate Monohydrate

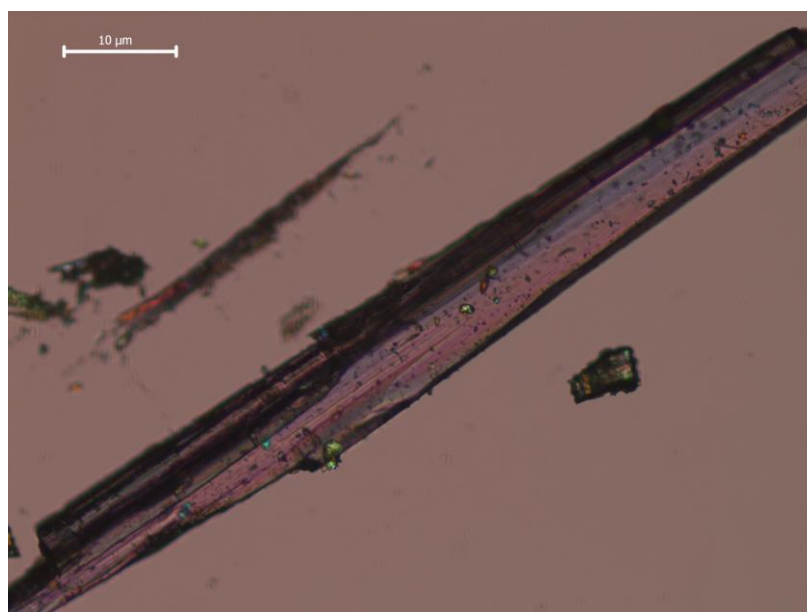


Figure 31.: Image of crystals of Cysteamine Tartrate Monohydrate taken at 100x magnification using crossed polarizers

4.1.1.1.f. Cystamine Tartrate

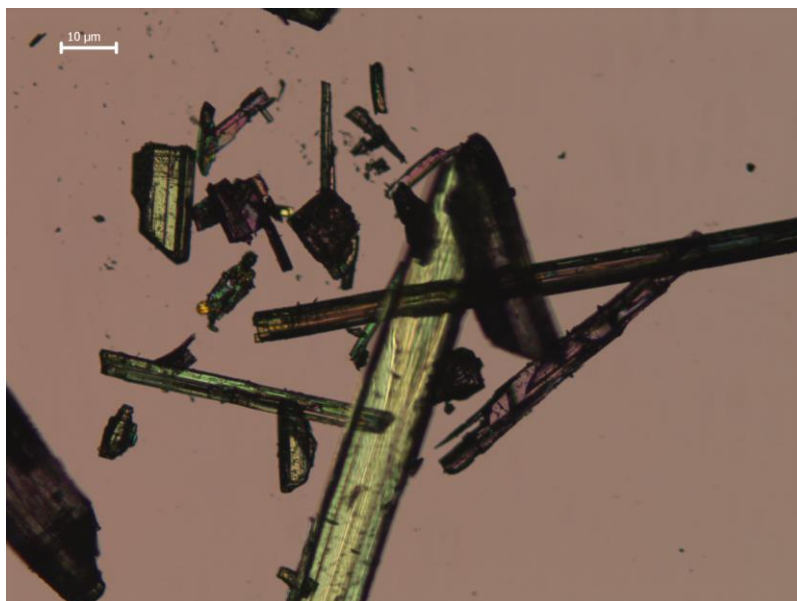


Figure 32.: Image of crystals of Cystamine Tartrate taken at 50x magnification using crossed polarizers

4.1.1.2. Melting Point

Table 3.: Melting Points for Starting Material, Co-Formers and Novel Salts

Compound	Literature Melting Point (°C)	Actual Melting Point (°C)	Novel Salts	Melting Point of Novel Salts (°C)
Cysteamine	90-96	94-96	-----	-----
Cystamine	203-214	200-206	-----	-----
Adipic acid	151-154	151-154	Cystamine adipate	160
2,6 Dihydroxybenzoic acid (2,6 DHBA)	165-168	165-168	Cystamine 2,6 Dihydroxybenzoate	219-220
Glutaric acid	95-98	94-98	Cystamine Glutarate	143
3-Nitrobenzoic acid (3-NBA)	139-141	130	Cystamine 3-Nitrobenzoate	215-224
L-Tartaric acid	168-170	169	Cysteamine Tartrate	75
L-Tartaric acid	168-170	169	Cystamine Tartrate	114

4.1.1.3. Differential Scanning Calorimetry (DSC)

4.1.1.3.a. Cystamine Adipate

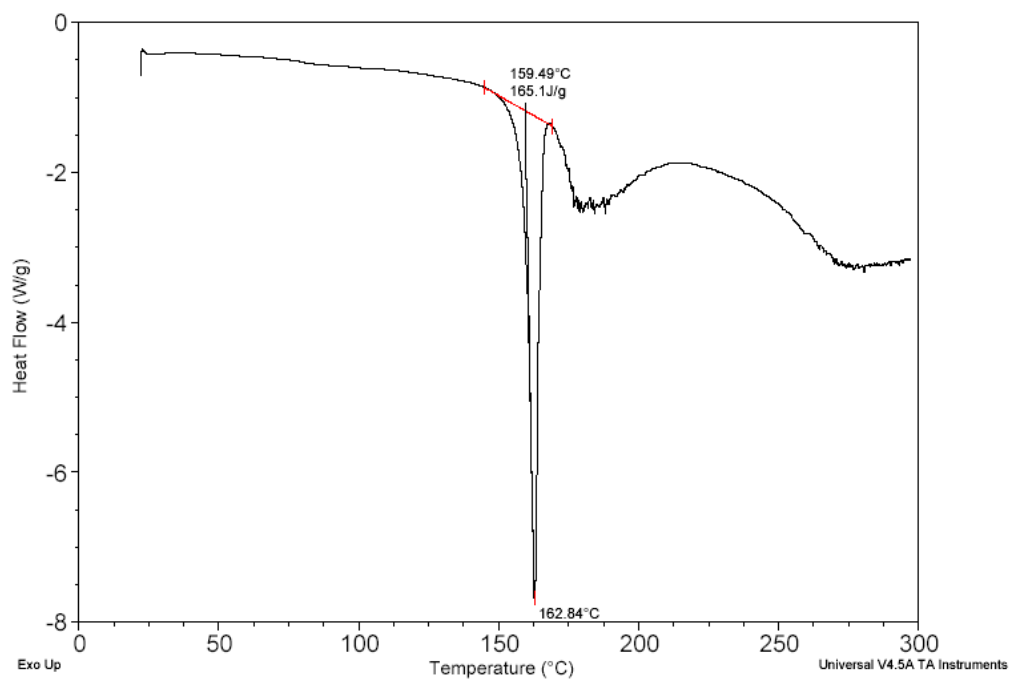


Figure 33.: Graph showing DSC results for Cystamine Adipate

4.1.1.3.b. Cystamine 2,6 Dihydroxybenzoate

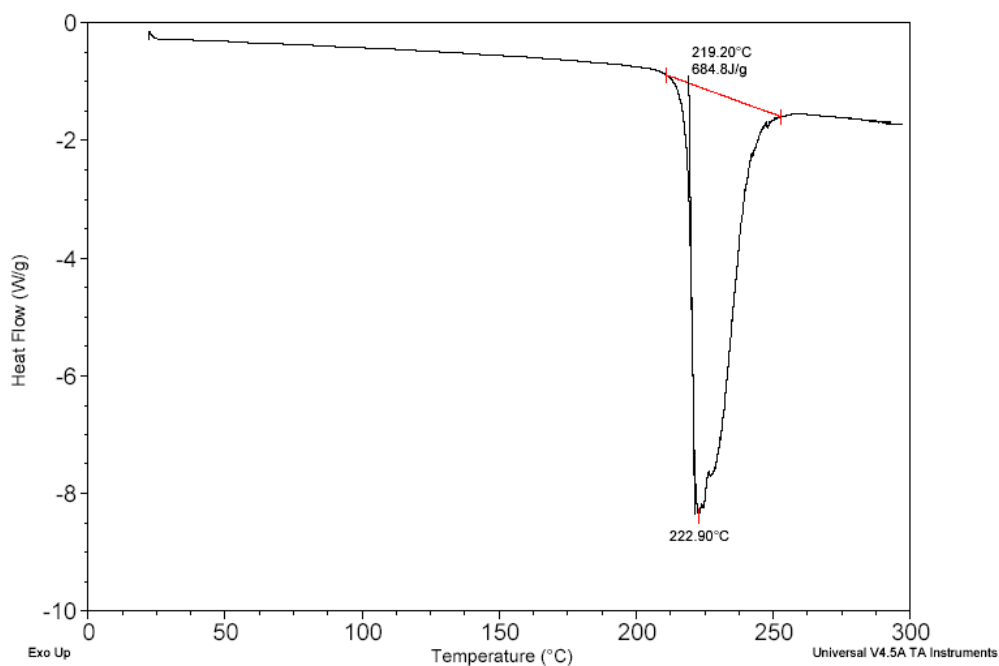


Figure 34.: Graph showing DSC results for Cystamine 2,6 Dihydroxybenzoate

4.1.1.3.c. Cystamine Glutarate

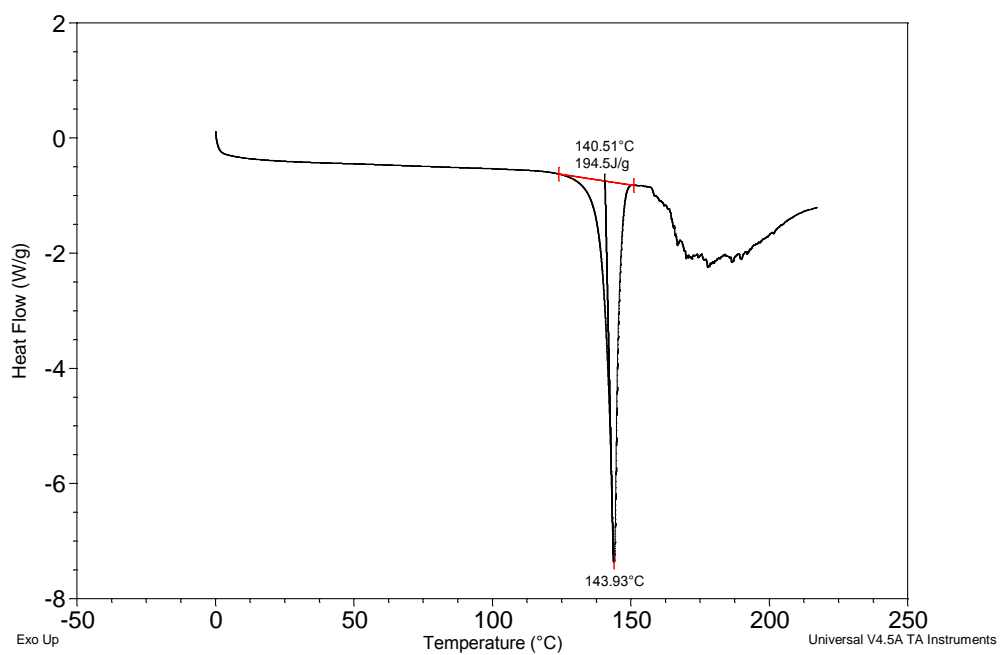


Figure 35.: Graph showing DSC results for Cystamine Glutarate

4.1.1.3.d. Cystamine 3-Nitrobenzoate

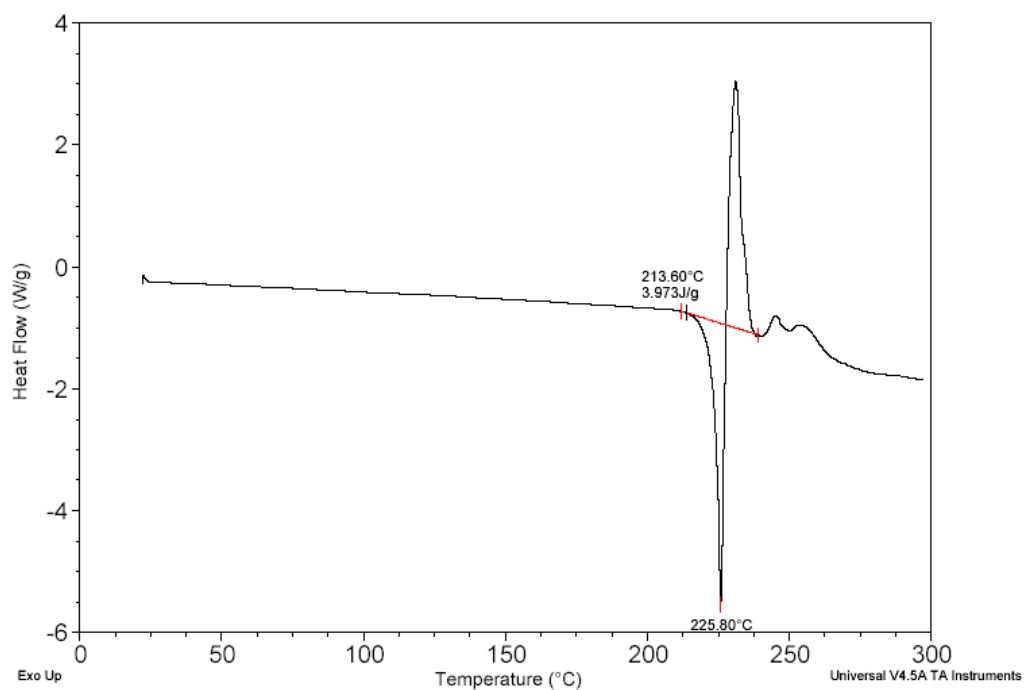


Figure 36.: Graph showing DSC results for Cystamine 3-Nitrobenzoate

4.1.1.3.e. Cysteamine Tartrate Monohydrate

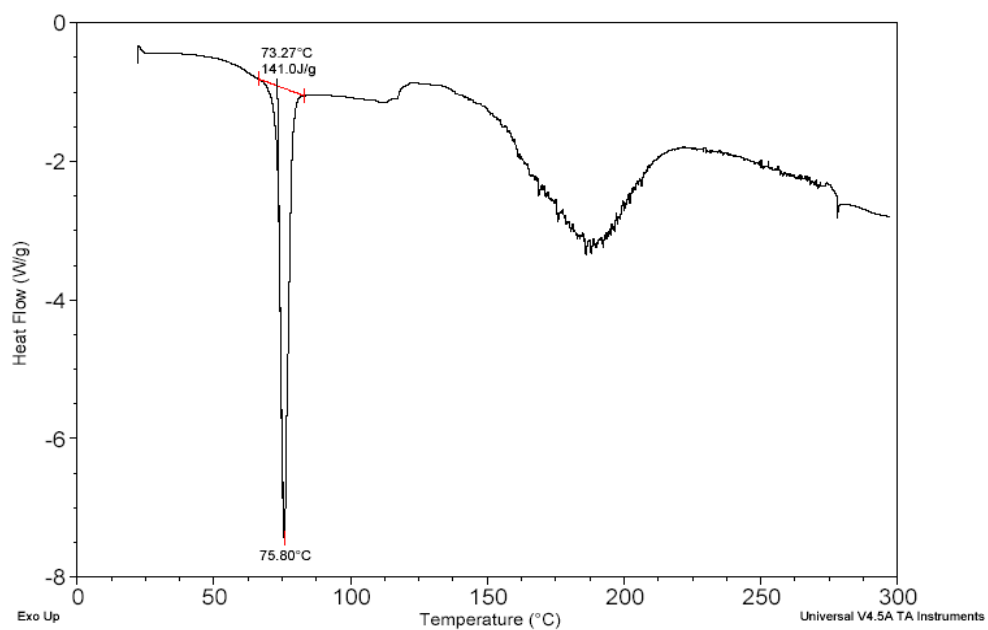


Figure 37.: Graph showing DSC resultss for Cysteamine Tartrate Monohydrate

4.1.1.3.f. Cystamine Tartrate

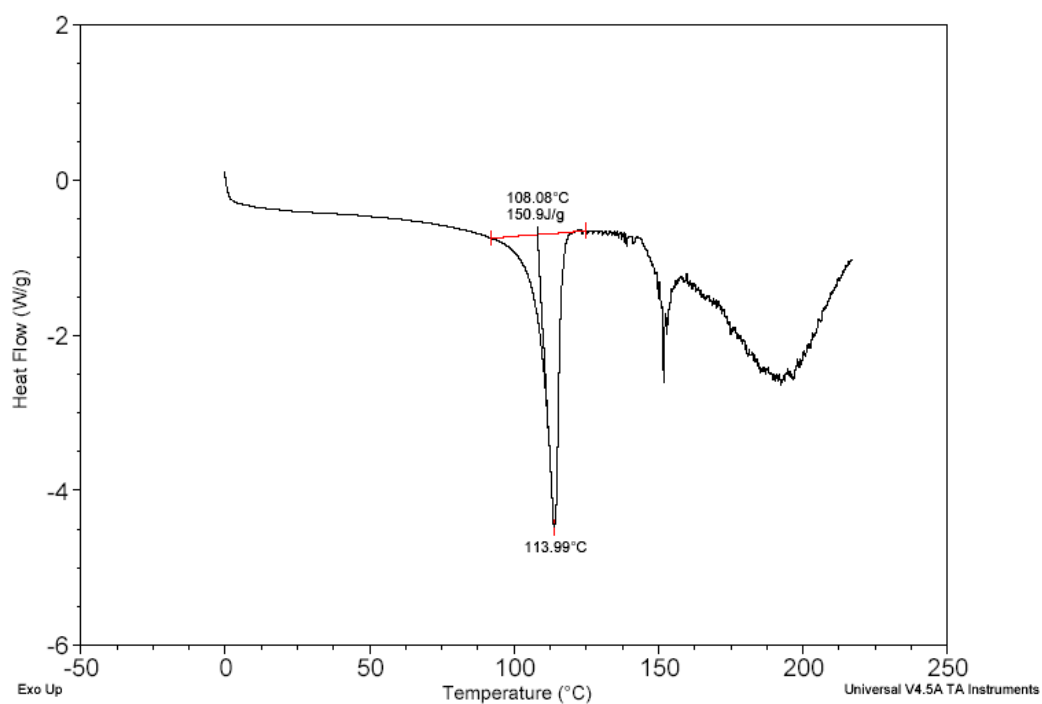
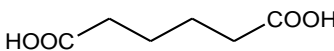
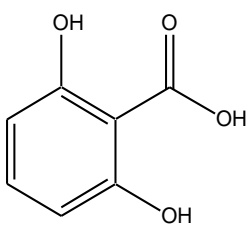
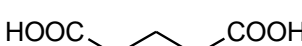
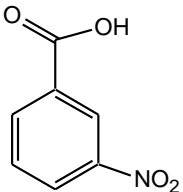
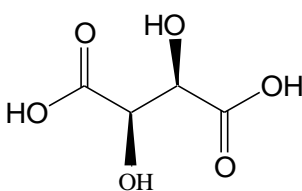


Figure 38.: Graph showing DSC results for Cystamine Tartrate

4.1.1.4. Principal IR absorbance bands

Principal (IR) wavenumbers for all co-formers are shown in Table (4)

Table 4.: Principal IR wavenumbers for all co-formers.

Compound	Principal Bands wave number (cm ⁻¹)	Due to	Group
 Adipic Acid	1681.03 1189.82-1273.15	C=O Stretching =C-O-C Stretching	Carboxylic acid
 2,6 Dihydroxybenzoic Acid	3075.81 1627-1471.24 1276.67	C-H Stretching Ring Vibrations O-H Bending	Aromatic Aromatic Aromatic
 Glutaric Acid	1681.03	C=O Stretching	Carboxylic acid
 3- Nitrobenzoic Acid	1529.22-1448.94 1290.83	Ring vibrations C-O Stretching	Aromatic C=C stretching Carboxylic Acid
 L- Tartaric Acid	3403.27 1736.52 1252.38	O-H Stretching C=O Stretching C-O Bending	Hydroxyl Carboxylic Acid Carboxylic Acid

4.1.1.4.a. IR spectra of Cystamine Adipate

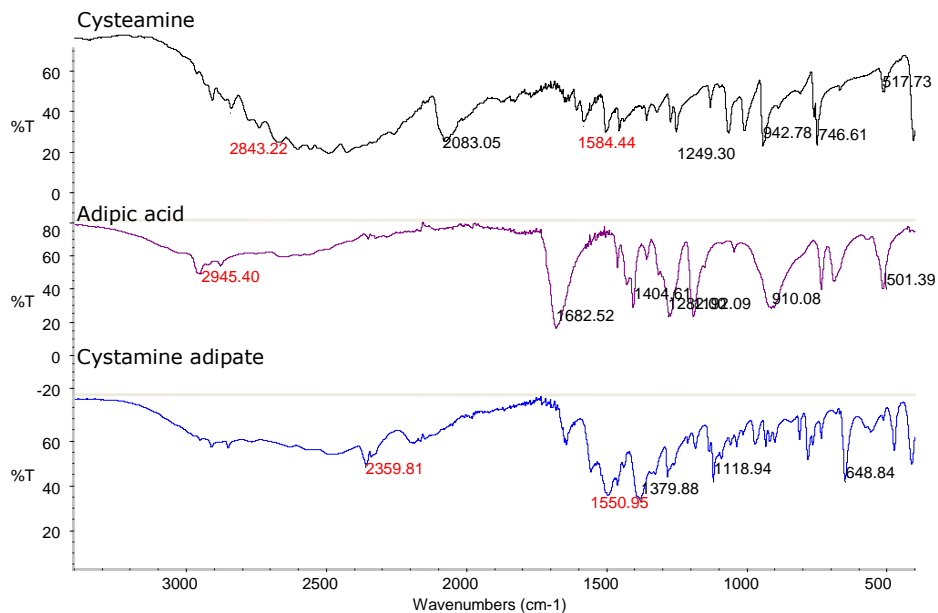


Figure 39.: IR spectra of sample Cystamine Adipate

4.1.1.4.b. IR spectra of Cystamine 2,6 Dihydroxybenzoate

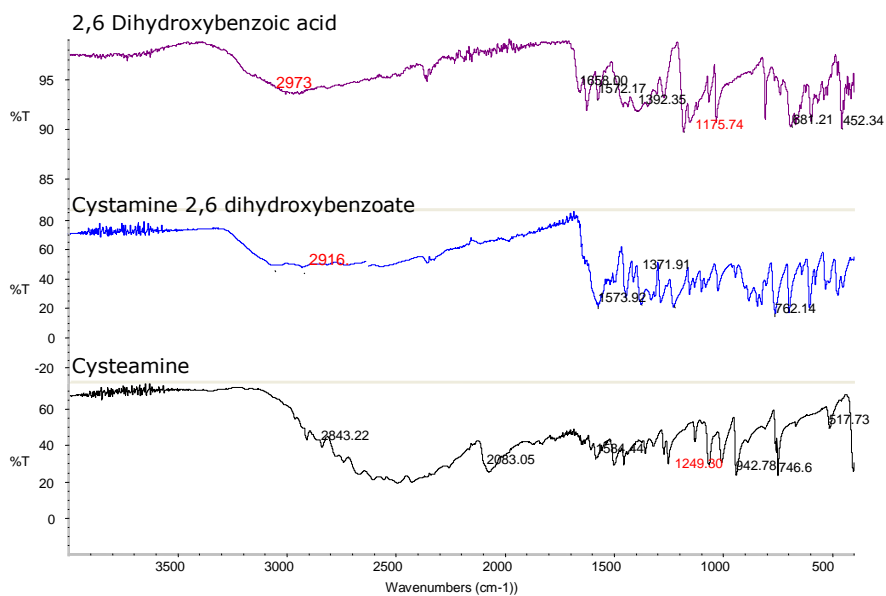


Figure 40.: IR spectra of sample Cystamine - 2,6 Dihydroxybenzoate

4.1.1.4.c. IR spectra of Cystamine Glutarate

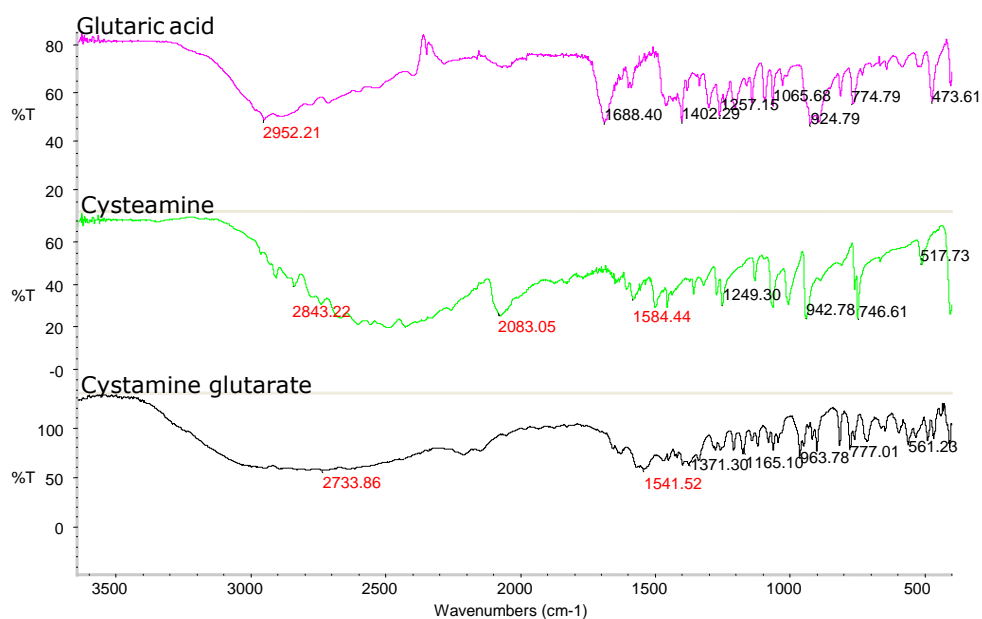


Figure 41.: IR spectra of sample Cystamine Glutarate

4.1.1.4.d. IR spectra of Cystamine 3-Nitrobenzoate

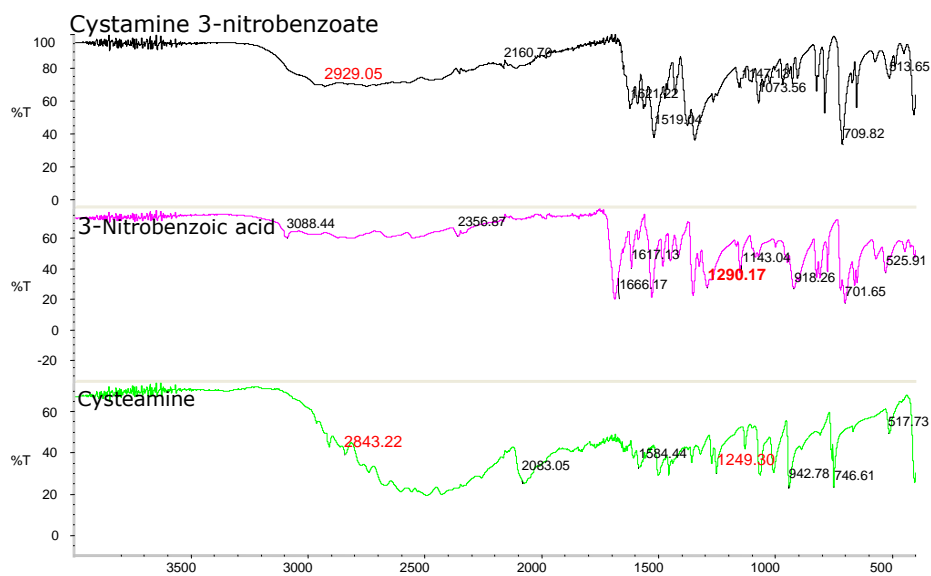


Figure 42.: IR spectra of sample Cystamine 3-Nitrobenzoate

4.1.1.4.e. IR spectra of Cysteamine Tartrate

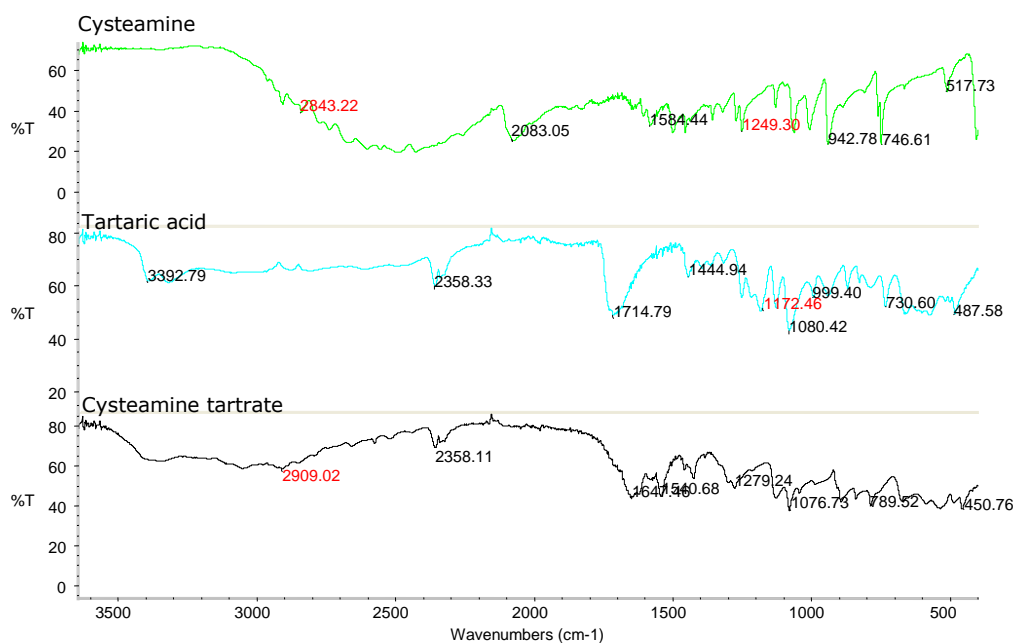


Figure 43.: IR spectra of sample Cysteamine Tartrate

4.1.1.4.f. IR spectra of Cystamine Tartrate

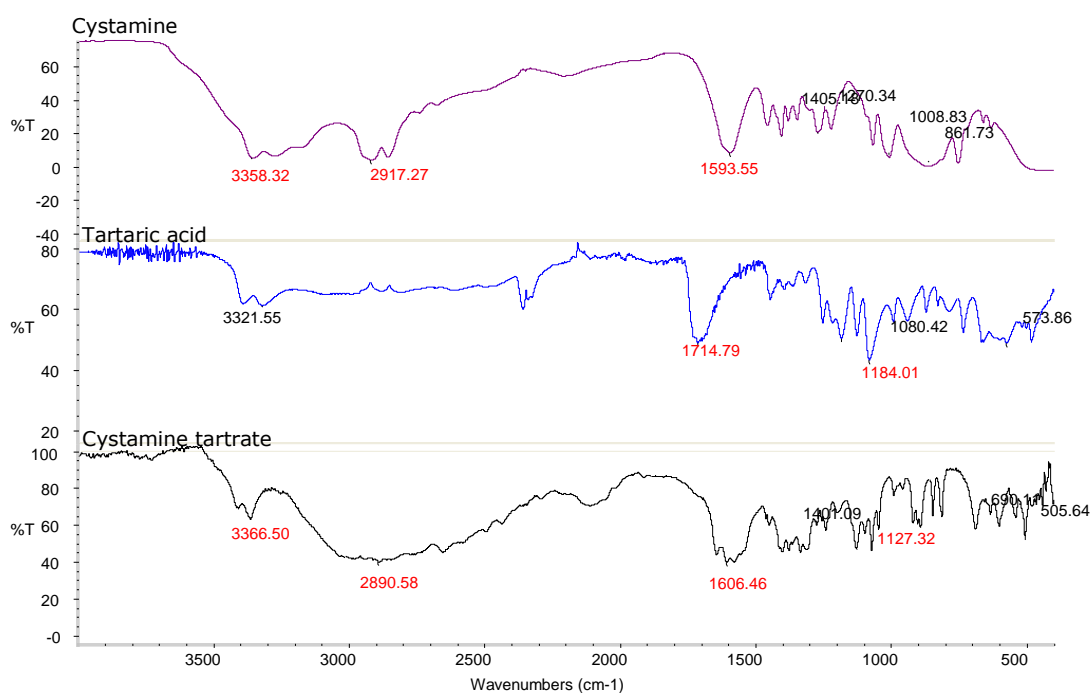


Figure 44.: IR spectra of sample Cystamine Tartrate

4.1.1.5. X-Ray Crystallography Data of Novel Salts

4.1.1.5.a. X-Ray Crystallography Data for Cystamine Adipate [1:1]

Table 5.: Crystal data and structure refinement for Cystamine Adipate

Formula	$C_4H_{14}S_2N_2^{2+} \cdot C_6H_8O_4^{2-}$	
Formula weight	298.42	
Temperature	150(2) K	
Wavelength	0.71073 Å	
Crystal system	Orthorhombic	
Space group	P ca2 ₁	
Unit cell dimensions	a = 7.7274(3) Å	α = 90°.
	b = 16.7038(6) Å	β = 90°.
	c = 10.9188(3) Å	γ = 90°.
Volume	1409.37(8) Å ³	
Z	4	
Density (calculated)	1.406 Mg/m ³	
Absorption coefficient	0.387 mm ⁻¹	
F(000)	640	
Crystal size	0.22 x 0.16 x 0.02 mm ³	
Theta range for data collection	3.45 to 27.46°.	
Index ranges	-10 ≤ h ≤ 7, -20 ≤ k ≤ 21, -14 ≤ l ≤ 10	
Reflections collected	8762	
Independent reflections	2874 [R(int) = 0.0424]	
Completeness to theta = 27.46°	99.5 %	
Max. & min. transmission	0.9923 and 0.9198	
Refinement method	Full-matrix least-squares on F ²	
Data / restraints / parameters	2874 / 1 / 166	
Goodness-of-fit on F ²	1.087	
Final R indices [I > 2σ(I)]	R1 = 0.0344, wR2 = 0.0815	
R indices (all data)	R1 = 0.0368, wR2 = 0.0836	
Final weighting scheme	calc w = 1/σ ² [(Fo ²) + (0.0289P) ² + 1.1609P]	
where P = (Fo ² + 2Fc ²)/3		
Absolute structure parameter	0.03(8)	
Largest diff. peak and hole	0.256 and -0.207 e.Å ⁻³	

Table 6.: Hydrogen bonds for Cystamine Adipate [\AA and $^\circ$].

D-H...A	d(D-H)	d(H...A)	d(D...A)	$\angle(\text{DHA})$
N(1)-H(1A)...O(1)	2.09		2.853(3)	141.2
N(1)-H(1B)...O(2)#1	0.91	1.89	2.767(3)	162.2
N(1)-H(1C)...O(1)#2	0.91	1.84	2.743(3)	173.3
N(1)-H(1C)...O(2)#2	0.91	2.65	3.234(3)	122.7
N(2)-H(2A)...O(4)#3	0.91	1.90	2.787(3)	165.2
N(2)-H(2B)...O(3)#4	0.91	1.79	2.693(3)	171.7
N(2)-H(2C)...O(4)#5	0.91	1.83	2.737(3)	175.8
N(2)-H(2C)...O(3)#5	0.91	2.62	3.191(3)	121.1

Symmetry transformations used to generate equivalent atoms:

#1 $-x+3/2, y, z+1/2$ #2 $x-1/2, -y+2, z$ #3 $-x+1, -y+1, z+1/2$

#4 $x-1/2, -y+1, z$ #5 $-x+1/2, y, z+1/2$

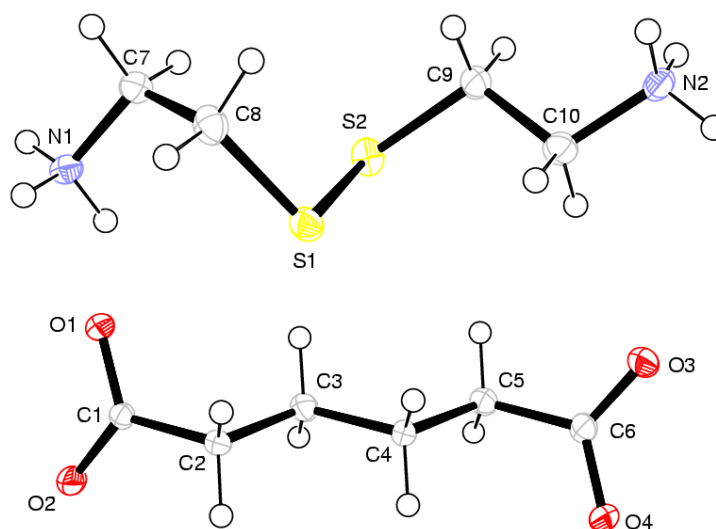


Figure 45.: Atomic arrangement in Cystamine Adipate

Figure 45 shows that the product is a salt where one hydrogen ion from each carboxylic group C1 and C6 has been transferred to the N1 and N2 nitrogens of cystamine molecule.

4.1.1.5.b. X-ray crystallographic data for Cystamine - 2,6-Dihydroxybenzoate [1:2]

Table 7.: Crystal data and structure refinement for Cystamine - 2,6-Dihydroxybenzoate

Formula	$C_{14}H_{10}O_8^{2-} \cdot C_4H_{14}N_2S_2^{2+}$	
Formula weight	460.52	
Temperature	120(2) K	
Wavelength	0.71073 Å	
Crystal system	Monoclinic	
Space group	C2/c	
Unit cell dimensions	$a = 21.0281(10)$ Å	$\alpha = 90^\circ$.
	$b = 8.5309(5)$ Å	$\beta = 123.002(3)^\circ$.
	$c = 12.8186(7)$ Å	$\gamma = 90^\circ$.
Volume	$1928.49(18)$ Å ³	
Z	4	
Density (calculated)	1.586 Mg/m ³	
Absorption coefficient	0.329 mm ⁻¹	
F(000)	968	
Crystal size	0.40 x 0.32 x 0.20 mm ³	
Theta range for data collection	3.61 to 27.48°.	
Index ranges	-27 <= h <= 25, -11 <= k <= 10, -14 <= l <= 16	
Reflections collected	10776	
Independent reflections	2211 [R(int) = 0.0672]	
Completeness to theta = 27.48°	99.6 %	
Max. and min. transmission	0.9372 and 0.8797	
Refinement method	Full-matrix least-squares on F ²	
Data / restraints / parameters	2211 / 0 / 139	
Goodness-of-fit on F ²	1.059	
Final R indices [I > 2sigma(I)]	R1 = 0.0408, wR2 = 0.0945	
R indices (all data)	R1 = 0.0666, wR2 = 0.1072	
Final weighting scheme	calc $w = 1/[\sigma^2(F_o^2) + (0.0508P)^2 + 1.3325P]$	
where $P = (F_o^2 + 2F_c^2)/3$		
Largest diff. peak and hole	0.315 and -0.366 e.Å ⁻³	

Table 8.: Hydrogen bonds for Cystamine 2,6-Dihydroxybenzoate
[Å and°]

D-H...A	d(D-H)	d(H...A)	d(D...A)	<(DHA)
N(1)-H(1A)...O(2)#1	0.91	2.17	3.040(2)	158.6
N(1)-H(1A)...O(1)#2	0.91	2.48	2.992(2)	116.0
N(1)-H(1B)...O(2)#3	0.91	2.03	2.913(2)	164.1
N(1)-H(1C)...O(4)#4	0.91	2.04	2.921(2)	161.8
O(1)-H(1D)...O(2)	0.84	1.82	2.570(2)	147.7
O(4)-H(4)...O(3)	0.84	1.75	2.500(2)	148.2

Symmetry transformations used to generate equivalent atoms:

#1 $-x, y, -z+1/2$ #2 $x, y, z+1$ #3 $x, -y+1, z+1/2$

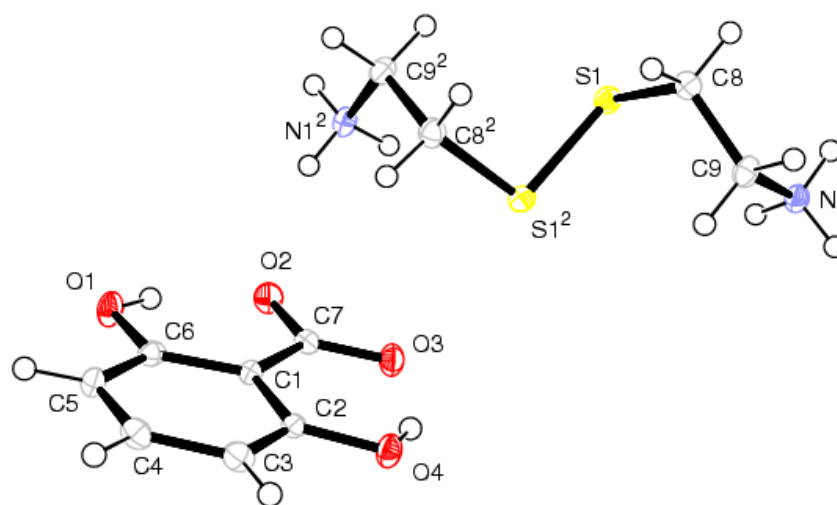


Figure 46.: Atomic arrangement in Cystamine 2, 6 Dihydroxybenzoate

Figure 46 shows that the product is a salt where one hydrogen ion from each carboxylic group has been transferred to the nitrogens N1 and N1² of cystamine molecule.

4.1.1.5.c. X-Ray Crystallography Data for Cystamine Glutarate [1:1]

Table 9.: Crystal data and structure refinement for Cystamine Glutarate.

Formula	$C_2H_{10}NS^{2+} \cdot C_5H_{10}O_2^{2-}$	
Formula weight	284.39	
Temperature	120(2) K	
Wavelength	0.71073 Å	
Crystal system	Monoclinic	
Space group	P2 ₁ /c	
Unit cell dimensions	a = 8.4519(2) Å	$\alpha = 90^\circ$.
	b = 17.3693(6) Å	$\beta = 92.498(2)^\circ$.
	c = 8.8427(2) Å	$\gamma = 90^\circ$.
Volume	1296.91(6) Å ³	
Z	4	
Density (calculated)	1.457 Mg/m ³	
Absorption coefficient	0.416 mm ⁻¹	
F(000)	608	
Crystal size	0.59 x 0.40 x 0.12 mm ³	
Theta range for data collection	3.29 to 27.45°.	
Index ranges	-10 ≤ h ≤ 10, -22 ≤ k ≤ 21, -11 ≤ l ≤ 11	
Reflections collected	15899	
Independent reflections	2954 [R(int) = 0.0351]	
Completeness to theta = 27.45°	99.8 %	
Max. and min. transmission	0.9518 and 0.7913	
Refinement method	Full-matrix least-squares on F ²	
Data / restraints / parameters	2954 / 0 / 154	
Goodness-of-fit on F ²	1.061	
Final R indices [I > 2σ(I)]	R1 = 0.0299, wR2 = 0.0739	
R indices (all data)	R1 = 0.0345, wR2 = 0.0771	
Final weighting scheme	calc w = 1/[σ ² (F _o ²) + (0.0360P) ² + 0.7531P]	
where P = (F _o ² + 2F _c ²)/3		
Largest diff. peak and hole	0.383 and -0.310 e.Å ⁻³	

Table 10.: Hydrogen bonds for Cystamine Glutarate [\AA and $^\circ$].

D-H...A	d(D-H)	d(H...A)	d(D...A)	$\angle(\text{DHA})$
N(1)-H(1A)...O(1)#1	0.91	1.88	2.7512(15)	158.8
N(1)-H(1B)...O(2)	0.91	1.92	2.7743(15)	154.7
N(1)-H(1C)...O(3)#3	0.91	1.96	2.8419(15)	164.2
N(2)-H(2A)...O(2)	0.91	1.82	2.6799(15)	155.9
N(2)-H(2B)...O(4)#4	0.91	1.91	2.8212(14)	176.4
N(2)-H(2C)...O(4)#5	0.91	1.98	2.8638(15)	164.6

Symmetry transformations used to generate equivalent atoms:

#1 $-x+1, -y, -z+1$ #2 $x, y, z+1$ #3 $x+1, -y+1/2, z+1/2$

#4 $x+1, -y+1/2, z-1/2$ #5 $x+1, y, z$

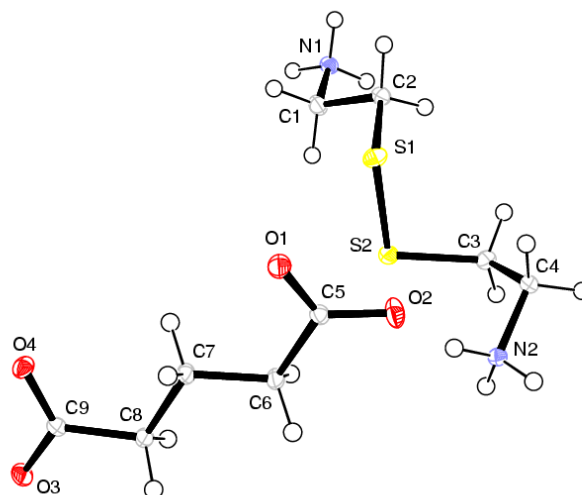


Figure 47.: Atomic arrangement in Cystamine Glutarate

Cystamine glutarate (Figure 47) is a salt formed by transfer of both hydrogen ions from the two carboxylic acid groups C5 and C9 in the tartaric acid molecule to the two amino groups N1 and N2 in cystamine.

4.1.1.5.d. X-ray crystallography data for Cystamine 3-Nitrobenzoate [2:4]

Table 11.: Crystal data and structure refinement for cystamine 3-Nitrobenzoate

Formula	$C_4H_{14}N_4S_2^{2+} \cdot C_{14}H_{15}O_8^{2-}$	
Formula weight	3892.13	
Temperature	120(2) K	
Wavelength	0.71073 Å	
Crystal system	Monoclinic	
Space group	P 2 ₁ /c	
Unit cell dimensions	a = 13.6477(3) Å	α = 90°.
	b = 24.3527(5) Å	β = 116.9700(10)°.
	c = 14.7148(2) Å	γ = 90°.
Volume	4358.70(14) Å ³	
Z	4	
Density (calculated)	1.483 Mg/m ³	
Absorption coefficient	0.298 mm ⁻¹	
F(000)	2032	
Crystal size	0.38 x 0.25 x 0.21 mm ³	
Theta range for data collection	2.95 to 27.50°.	
Index ranges	-16 ≤ h ≤ 17, -31 ≤ k ≤ 31, -19 ≤ l ≤ 19	
Reflections collected	43615	
Independent reflections	9973 [R(int) = 0.0494]	
Completeness to theta = 27.50°	99.7 %	
Max. and min. transmission	0.9401 and 0.8952	
Refinement method	Full-matrix least-squares on F ²	
Data / restraints / parameters	9973 / 0 / 581	
Goodness-of-fit on F ²	1.036	
Final R indices [I > 2σ(I)]	R1 = 0.0474, wR2 = 0.1176	
R indices (all data)	R1 = 0.0770, wR2 = 0.1321	
Final weighting scheme	calc w = 1/[σ ² (Fo ²) + (0.0587P) ² + 2.0386P]	
where P = (Fo ² + 2Fc ²)/3		
Largest diff. peak and hole	0.633 and -0.422 e.Å ⁻³	

Table 12.: Hydrogen bonds for Cystamine 3-Nitrobenzoate [\AA and $^\circ$].

D-H...A	d(D-H)	d(H...A)	d(D...A)	$\angle(\text{DHA})$
N(1)-H(1A)...O(6)#1	0.91	1.85	2.742(2)	165.7
N(1)-H(1B)...O(14)#2	0.91	2.01	2.825(2)	148.8
N(1)-H(1B)...O(4)#2	0.91	2.56	3.154(2)	123.7
N(1)-H(1C)...O(10)#3	0.91	1.86	2.767(2)	175.0
N(2)-H(2A)...O(13)#4	0.91	1.79	2.692(2)	170.1
N(2)-H(2B)...O(2)#5	0.91	1.94	2.829(2)	164.7
N(2)-H(2C)...O(2)#6	0.91	1.95	2.788(2)	151.9
N(3)-H(3C)...O(1)#5	0.91	1.76	2.655(2)	167.0
N(3)-H(3D)...O(6)#5	0.91	1.95	2.833(2)	163.3
N(3)-H(3E)...O(14)	0.91	1.96	2.813(2)	154.7
N(4)-H(4C)...O(9)#4	0.91	1.87	2.758(2)	166.3
N(4)-H(4D)...O(9)#3	0.91	2.03	2.819(2)	143.8
N(4)-H(4D)...O(16)#6	0.91	2.60	3.239(2)	127.7
N(4)-H(4E)...O(5)#7	0.91	1.83	2.728(2)	169.5

Symmetry transformations used to generate equivalent atoms:

#1 $-x+1, y-1/2, -z+3/2$ #2 $x, y, z+1$ #3 $x+1, y, z+1$

#4 $-x+1, -y, -z+1$ #5 $-x+1, y-1/2, -z+1/2$ #6 $x, -y+1/2, z+1/2$

#7 $x+1, -y+1/2, z+1/2$

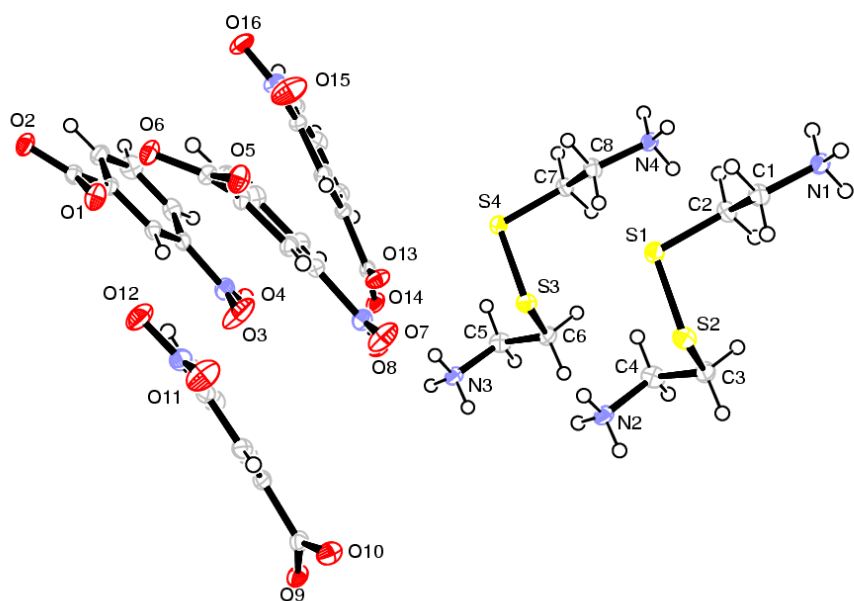


Figure 48.: Atomic arrangement in Cystamine 3-Nitrobenzoate

This product (Figure 48) is a salt formed by transfer of both hydrogen ions from eight carboxylic acid groups in four molecules of tartaric acid to the four amino groups N1, N2, N3, and N4 in two molecules of cystamine.

4.1.1.5.e. The crystal data for samples cysteamine tartrate monohydrate **[1]**, cystamine tartrate **[2]**, and cystamine bitartrate dehydrate **[3]**

Table 13. X-ray crystallographic data for **1**, **2**, and **3**.

Compound	1	2	3
Formula	C ₂ H ₈ NS.C ₄ H ₅ O ₆ .H ₂ O	C ₄ H ₁₄ N ₂ S ₂ ²⁺ . C ₄ H ₄ O ₆ ²⁻	C ₄ H ₁₄ N ₂ S ₂ ²⁺ . 2C ₄ H ₅ O ₆ ⁻ . .2H ₂ O
Formula weight	245.25	302.36	488.48
Crystal size (mm)	0.84 x 0.12 x 0.10	0.36 x 0.14 x 0.03	0.22 x 0.02 x 0.02
Crystal shape	Rod	cut blade	Needle
Crystal colour	Colourless	Colourless	Colourless
Space group	<i>P</i> 2 ₁ 2 ₁ 2 ₁	<i>P</i> 2 ₁ 2 ₁ 2 ₁	<i>P</i> 2 ₁ 2 ₁ 2 ₁
Unit cell dimensions:			
<i>a</i> [Å]	7.0630(2)	5.7281 (3)	7.3425 (5)
<i>b</i> [Å]	10.3833(5)	9.3699 (5)	10.5227 (8)
<i>c</i> [Å]	14.8591(7)	24.6770 (14)	26.983 (2)
<i>α</i> [°]	90	90	90
<i>β</i> [°]	90	90	90
<i>γ</i> [°]	90	90	90
<i>V</i> [Å ³]	1089.73(8)	1324.46 (12)	2084.8 (3)
<i>Z</i>	4	4	4
<i>D</i> _{calc} [g cm ⁻³]	1.495	1.516	1.556
Absorption coefficient <i>μ</i> [mm ⁻¹]	0.31	0.423	0.329
<i>F</i> (000)	520	640	1032
Scan mode	φ - ω scans	φ - ω scans	φ - ω scans
θ range [°]	2.91 – 27.48	2.91 – 27.48	2.91 – 27.48
Index ranges	-9 ≤ <i>h</i> ≤ 8 -13 ≤ <i>k</i> ≤ 13 -17 ≤ <i>l</i> ≤ 19	-7 ≤ <i>h</i> ≤ 7 -12 ≤ <i>k</i> ≤ 12 -32 ≤ <i>l</i> ≤ 29	-8 ≤ <i>h</i> ≤ 8 -12 ≤ <i>k</i> ≤ 12 -32 ≤ <i>l</i> ≤ 30
Reflections collected	9253	9158	12189
<i>R</i> _{int}	0.0509	0.0830	0.0841
Data/restraints/parameters	2485/ 0/143	3020/0/165	3527/6/291
Goodness of fit on <i>F</i> ²	1.064	1.046	1.093
Absolute structure parm.	-0.04(9)	0.20(13)	-0.1(2)
<i>R</i> [<i>I</i> ≥ 2σ(<i>I</i>)] / <i>R</i> (all data)	0.0387 / 0.0873	0.0601 / 0.1268	0.0783 / 0.1309
w <i>R</i> [<i>I</i> ≥ 2σ(<i>I</i>)] / w <i>R</i> [all data]	0.0510 / 0.0932	0.0879 / 0.1393	0.01259 / 0.1517
Max/Min residual electron density [eÅ ⁻³]	0.268 / -0.254	0.553 / - 0.430	0.421 / - 0.392

Molecular plots for **(1)**, **(2)** and **(3)** are shown in Figures (49), (50) and (51) respectively.

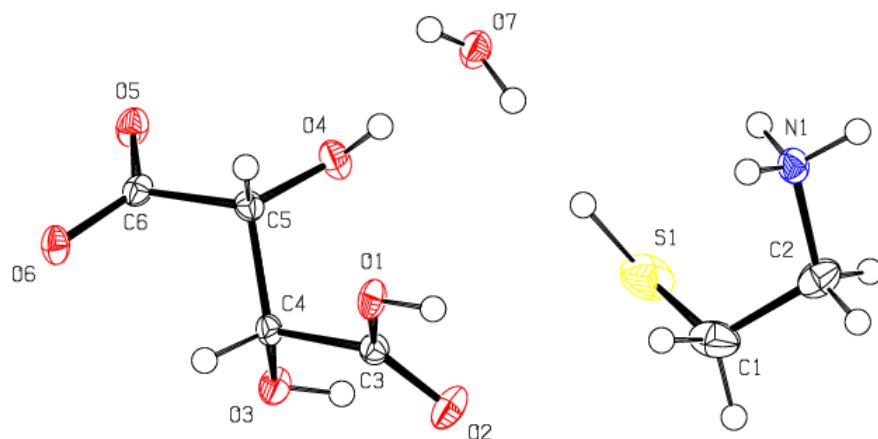


Figure 49.: Atomic arrangement in Cysteamine Tartrate Monohydrate (1).

For (1) the salt formation results from the transfer of a proton from one of the two carboxylic acid groups in the tartaric acid molecule to the amino group N1 in cysteamine.

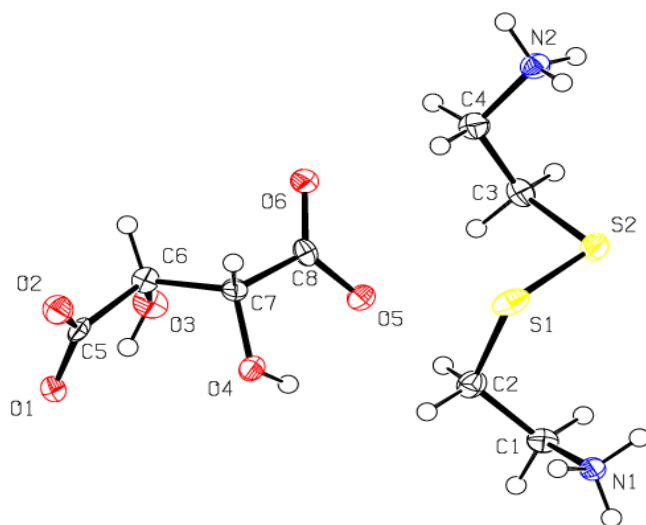


Figure 50.: Atomic arrangement in Cystamine Tartrate (2)

Product (2) is an anhydrous salt formed by transfer of both hydrogen ions from the two carboxylic acid groups in tartaric acid to the two amino groups N1 and N2 in cystamine

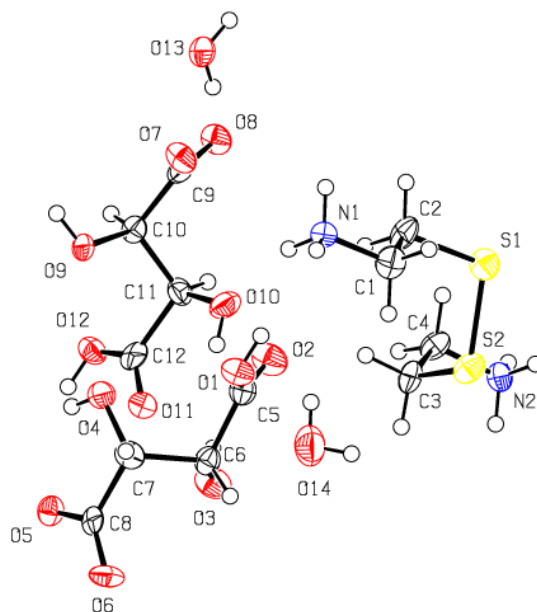


Figure 51.: Atomic arrangement in Cystamine Bitartrate Dihydrate (3)

As in (2) both amino groups N1 and N2 have acquired an additional hydrogen ion. This proton transfer occurred from separate tartaric acid molecules leaving a single charge on each bitartrate anion.

Table 14.: Hydrogen bonding for **(1)**

D-H...A	d(D-H)	d(H...A)	d(D...A)	<(DHA)
O(1)-H(1).....O(6)#1	0.84	1.66	2.4885(18)	169.3
O(3)-H(3).....O(7)#2	0.84	2.13	2.819(2)	139.0
O(4)-H(4).....O(7)	0.84	1.90	2.742(2)	177.2
N(1)-H(1A)...O(3)#3	0.91	2.00	2.813(2)	148.2
N(1)-H(1B)....O(2)#4	0.91	1.92	2.814(2)	165.9
N(1)-H(1C)....O(5)#1	0.91	1.89	2.772(2)	161.8
N(1)-H(1C)...O(4)#1	0.91	2.30	2.850(2)	118.4
O(7)-H(7A)...O(5)#1	0.87	1.89	2.7455(19)	168.1
O(7)-H(7B)...O(6)#5	0.77	2.14	2.8910(19)	166.4

Symmetry transformations used to generate equivalent atoms:

#1 $x+1,y,z$ #2 $-x+1,y-1/2,-z+1/2$ #3 $-x+1,y+1/2,-z+1/2$

#4 $-x+2,y+1/2,-z+1/2$ #5 $x+1/2,-y+1/2,-z+1$

Table 15.: Hydrogen bonding for **(2)**

D-H...A	d(D-H)	d(H...A)	d(D...A)	<(DHA)
N(1)-H(1A)...O(1)#1	0.91	1.88	2.786(4)	174.9
N(1)-H(1B)...O(2)#2	0.91	1.82	2.705(4)	162.2
N(1)-H(1C)...O(1)#3	0.91	1.99	2.892(4)	170.2
N(2)-H(2A)...O(3)#4	0.91	1.99	2.871(4)	161.3
N(2)-H(2B)...O(6)#5	0.91	1.77	2.684(4)	177.1
N(2)-H(2C)...O(5)#6	0.91	1.87	2.727(4)	155.3
O(3)-H(3)...O(1)	0.84	2.09	2.588(4)	117.4
O(3)-H(3)...S(1)#7	0.84	2.92	3.703(3)	156.4
O(4)-H(4)...O(5)	0.84	2.13	2.613(4)	116.1
O(4)-H(4)...O(2)#8	0.84	2.20	2.889(4)	139.4

Symmetry transformations used to generate equivalent atoms:

#1 $x-1,y+1,z$ #2 $x-3/2,-y+1/2,-z$ #3 $x-1/2,-y+1/2,-z$

#4 $x,y+1,z$ #5 $-x+2,y+1/2,-z+1/2$ #6 $-x+1,y+1/2,-z+1/2$

#7 $x,y-1,z$ #8 $x-1,y,z$

Table 16.: Hydrogen bonding for **(3)**

D-H...A	d(D-H)	d(H...A)	d(D...A)	<(DHA)
N(1)-H(1A)...O(11)#1	0.91	1.90	2.789(8)	164.4
N(1)-H(1B)...O(2)	0.91	2.32	2.861(8)	118.1
N(1)-H(1B)...O(5)#1	0.91	2.34	2.983(8)	127.1
N(1)-H(1C)...O(10)	0.91	1.97	2.860(7)	164.2
N(2)-H(2A)...O(5)#2	0.91	1.87	2.742(8)	159.8
N(2)-H(2B)...O(7)#3	0.91	2.16	2.948(8)	144.7
N(2)-H(2B)...O(9)#3	0.91	2.27	2.987(8)	135.7
N(2)-H(2C)...O(4)#3	0.91	1.87	2.766(7)	169.0
O(1)-H(1).....O(6)#1	0.84	1.73	2.555(7)	167.4
O(3)-H(3).....O(14)	0.84	2.39	2.818(8)	112.6
O(4)-H(4).....O(5)	0.84	2.07	2.577(7)	118.3
O(4)-H(4).....O(13)#4	0.84	2.23	2.942(8)	142.6
O(9)-H(9).....O(13)#5	0.84	1.85	2.683(7)	170.6
O(10)-H(10)..O(11)	0.84	2.05	2.572(7)	119.3
O(12)-H(12)..O(8)#4	0.84	1.66	2.476(7)	164.9
O(13)-H(13A).O(7)	0.85(2)	1.99(4)	2.743(7)	148(7)
O(13)-H(13B)..O(9)#1	0.85(2)	2.00(2)	2.833(7)	170(7)
O(14)-H(14A)...O(10)	0.86(2)	2.51(6)	3.171(9)	135(7)
O(14)-H(14B)...O(6)#6	0.87(2)	1.97(4)	2.787(8)	156(9)

Symmetry transformations used to generate equivalent atoms:

#1 $x+1, y, z$ #2 $x+1, y-1, z$ #3 $x, y-1, z$ #4 $x-1, y, z$

#5 $x-1/2, -y+3/2, -z$ #6 $-x, y-1/2, -z+1/2$

4.1.1.6. Other acids used as co-formers for co-crystal synthesis

Acids such as benzoic acid; 2,5 dihydroxybenzoic acid, oxalic acid; paracetamol; phenol; saccharin; sulfamethoxazole; and salicylic acid were used as co-formers to synthesise co-crystals of cysteamine. However, these co-formers did not generate any novel products. The results were confirmed by mp and IR spectra which indicated the presence of starting materials, i.e. the corresponding acids.

4.1.2. Discussion

4.1.2.1. *Cystamine Adipate*

The melting point for this compound was higher than both the starting material and its co-former as shown in Table (3). This was confirmed by DSC (Figure 33). The IR spectrum (Figure 39) of cystamine adipate displayed different absorbances when compared to both starting materials. The peak at 2843 cm^{-1} present on the cysteamine spectrum corresponding to an N-H stretching band had disappeared on the cystamine adipate spectra. The peak corresponding to the O-H stretching band at 2945.50 cm^{-1} present on the adipic acid spectrum had also disappeared and a new peak at 2359.81 cm^{-1} was present. In addition, the N-H bending band at 1584.40 cm^{-1} in cysteamine had slightly shifted to 1550.95 cm^{-1} due to hydrogen bonding within the new compound. Moreover, the results in Table (6) show that these crystals are held together by extensive intermolecular hydrogen bonding with $d(\text{D-H}) = 0.91\text{ \AA}$, and an angle (DHA) of almost 180° . These two parameters are indicative of strong intermolecular hydrogen bonding between the donor and the acceptor site.

Additionally, Figure (45) typically shows salt formation by transfer of both hydrogen atoms from the two carboxylic acid groups of adipic acid to the two amine nitrogen atoms of cystamine. This is confirmed by bond character in the carboxylate groups shown by $\text{C}(1)\text{-O}(1) = 1.268(3)\text{ \AA}$, $\text{C}(1)\text{-O}(2) = 1.261(3)\text{ \AA}$, $\text{C}(6)\text{-O}(3) = 1.258(8)\text{ \AA}$ and $\text{C}(6)\text{-O}(4) = 1.268(3)\text{ \AA}$.

4.1.2.2. *Cystamine 2,6 Dihydroxybenzoate*

By displaying a different melting point to both starting materials as shown in Table (3), a change in the physical properties indicates the potential for a newly formed compound; this was also confirmed by DSC (Figure 34). IR spectral interpretation (Figure 40) indicated a shift of the O-H stretching band from 2973 cm^{-1} in 2, 6 dihydroxybenzoic acid to 2916 cm^{-1} in the newly formed compound resulting from hydrogen bonding between the co-former and the new compound. This was confirmed by transfer of the hydrogen atom from the carboxylic acid groups of 2, 6 dihydroxybenzoic acid to the

two amine nitrogen atoms of cystamine (Figure 46). Bond character in the carboxylate groups was shown by C(7)-O(2) = 1.279(2)Å, C(7)-O(3) = 1.263(2)Å. Extensive hydrogen bonding is also present. (Table 8)

4.1.2.3. Cystamine Glutarate

The melting point for this compound was found to be much higher than both the starting material and its co-former as shown in Table (3). This was confirmed by DSC (Figure 35). IR spectra (Figure 41) of cystamine glutarate displayed different peaks when compared to those of both starting materials. The peak at 2843 cm⁻¹ present on the cysteamine spectrum corresponding to N-H stretching band had disappeared on the compound spectrum. The peak corresponding to the O-H stretching band at 2952 cm⁻¹ present in the glutaric acid spectrum had also disappeared and a new peak at 2733 cm⁻¹ was formed. In addition, the N-H bending band at 1584 cm⁻¹ in cysteamine had slightly shifted to 1541 cm⁻¹ due to hydrogen bonding with the new compound. The above results confirm that a new crystal compound had been formed. Transfer of the hydrogen atom from the carboxylic acid group of glutaric acid to the two amine nitrogen atoms of cystamine (Figure 47) also confirms the formation of a novel salt, where bond character in the carboxylate groups is shown by C(5)-O(1) = 1.2447(17)Å, C(5)-O(2) = 1.2669(16)Å, C(9)-O(3) = 1.2512(16)Å, C(5)-O(2) = 1.2729(16)Å. Table (10) confirms that these crystals are held together by very strong hydrogen bonding.

4.1.2.4. Cystamine 3- nitrobenzoate

The melting point for this compound was found to be considerably higher than both the starting material and its co-former as shown in Table (3). This was confirmed by DSC (Figure 36). IR spectra (Figure 42) of cystamine 3-nitrobenzoate displayed different absorbances when compared to those of both starting materials. Hydrogen bonding with cysteamine has caused the peak at 2843.22 cm⁻¹ present on the cysteamine spectrum corresponding to N-H stretching band to shift to 2929.06 cm⁻¹ on the compound spectrum. A

shift of the C-O stretching band in 3-Nitrobenzoic acid from 1290.17 cm^{-1} to 1229.99 cm^{-1} was also noted.

In this compound (Figure 48) both nitrogen atoms in cystamine molecule have also acquired an additional hydrogen atom resulting in ionisation. Evidence of this proton transfer is based on the bond character in the carboxylate group and is shown by $\text{C}(15)\text{-O}(1) = 1.253(2)\text{Å}$, $\text{C}(15)\text{-O}(2) = 1.1263(2)\text{Å}$, $\text{C}(22)\text{-O}(5) = 1.255(2)\text{Å}$, $\text{C}(22)\text{-O}(6) = 1.1266(2)\text{Å}$, $\text{C}(29)\text{-O}(9) = 1.265(2)\text{Å}$, $\text{C}(29)\text{-O}(12) = 1.253(2)\text{Å}$, $\text{C}(36)\text{-O}(13) = 1.249(2)\text{Å}$, $\text{C}(36)\text{-O}(14) = 1.263(2)\text{Å}$

As with all novel salts mentioned above, this crystal material also displayed strong hydrogen bonding. (Table 12)

Compounds **(1)**, **(2)** and **(3)** described in the sections below were formed from the same reaction using cysteamine and tartaric acid as the starting materials.

4.1.2.5. Cysteamine Tartrate Monohydrate (1)

The melting point compound **(1)** was found to be between both the starting material and its co-former as shown in Table (3). This was confirmed by DSC (Figure 37).

IR spectra (Figure 43) of compound **(1)** displayed different absorbances when compared to those of both starting materials. Hydrogen bonding with cysteamine has caused the peak at 2843.22 cm^{-1} present on the cysteamine spectrum corresponding to N-H stretching band to shift to 2909.02 cm^{-1} on spectrum. A shift of the C-O stretching band in tartaric acid from 1172.46 cm^{-1} to 1249.30 cm^{-1} was also noted.

The above results confirm that a new crystal compound had been formed.

For compound **(1)** (Figure 49) the product is clearly seen to possess a hydrogen atom attached to the sulfur with a sulfur-hydrogen bond length of $1.31(3)\text{ Å}$. Only one of the hydrogen atoms from the two carboxylic acid groups has transferred to the nitrogen. The single bond character of $\text{C}3\text{-O}1 = 1.301(2)\text{ Å}$ compares with the double bond for $\text{C}3\text{-O}2 = 1.224(2)\text{ Å}$ and with the bonds in the carboxylate group, i.e., $\text{C}6\text{-O}5 = 1.240(2)\text{ Å}$ and $\text{C}6\text{-O}6 = 1.240(2)\text{ Å}$

O6 = 1.280(2) Å. The crystals are held together by extensive hydrogen bonding (Table 14). A water molecule is present in the crystal and this is hydrogen bonded to the carboxylate group and to the hydroxyl groups at O3 and O4.

4.1.2.6. Cystamine Tartrate Mixture

4.1.2.6.a. Cystamine Tartrate (2)

The resulting melting point (Table 3) for the crystal compound (**2**) was lower than the starting material and its co-former. These results were confirmed by DSC (Figure 38). In addition, IR spectra (Figure 44) showed a shift of the N-H stretching band of cystamine from 2917.27 cm⁻¹ to 2890.58 cm⁻¹ due to hydrogen bonding with the new compound. Hydrogen bonding with cystamine has also caused the peak at 1593.55 cm⁻¹ present on the cystamine spectrum corresponding to N-H stretching band to shift to 1606.46 cm⁻¹ on the compound spectra. A shift of the C-O stretching band from 1184.01 cm⁻¹ to 1127.32 cm⁻¹ was also noted.

Molecule (**2**) (Figure 50) is a typical anhydrous salt formed by transfer of both hydrogen atoms from the two carboxylic acid groups to the two amine nitrogen atoms (i.e. full ionisation). Bond character in the carboxylate groups is shown by C(5)-O(1) = 1.257(5)Å, C(5)-O(2) = 1.244(5)Å, C(8)-O(5) = 1.258(5)Å and C(8)-O(6) = 1.251(5)Å. The sulfur-sulfur bond length is 2.038(2)Å. As in compound (**1**) extensive hydrogen bonding is present (Table 15).

4.1.2.6.b. Cystamine Bitartrate Dihydrate (3)

The quality of the data set related to the crystal for compound (**3**) (Figure 51) was not as good as those obtained for compounds (**1**) and (**2**) and discussion of the fine details of the molecular structure needs to be approached with caution. As in **2** both nitrogen atoms have acquired an additional hydrogen atom resulting in ionisation. Each of these two protons appears to have transferred from separate tartaric acid molecules leaving a single charge on each anion. Evidence for this is again based on bond

lengths such that for the carboxylic acid group C(5)-O(1) = 1.292(9)Å, C(5)-O(2) = 1.191(9)Å and in the same anion the carboxylate group has C(8)-O(5) = 1.261(8)Å and C(8)-O(6) = 1.231(8)Å.

In the second anion the bond character is less obvious but it appears the carboxylic acid group has C(12)-O(11) = 1.220(9)Å and C(12)-O(12) = 1.274(9)Å and in the carboxylate group these bonds are C(9)-O(7) = 1.229(9)Å and C(9)-O(8) = 1.278(8)Å. As in compound **(1)** and **(2)** extensive hydrogen bonding is present (Table 16).

Other models were tried, i.e. proton transfer from a single tartaric acid molecule and the possibility of H₃O⁺ formation, however, the refinement of these models were less satisfactory than the one presented. The sulfur – sulfur bond length is 2.038(3)Å. These values are in good agreement with the literature values of 2.00Å.¹⁶¹

4.2. Synthesis of novel cystamine Pro-drugs derivatives

The objectives of the work described in this thesis were the design, synthesis and *in vitro* evaluation of novel pro-drugs for the treatment of Nephropathic Cystinosis. The current treatment (Cystagon[®]), although effective is known to cause both gastric irritation when taken orally and possesses a foul taste and smell. These side effects associated with its administration are caused by the presence of both an amine and a thiol functional group in the molecule.^{140,141,143}

In order to minimise the side effects and to improve patient compliance, previous work undertaken in our laboratories concentrated on the design and production of pro-drugs designed to decompose to release cysteamine *in vivo*, while at the same time being completely odourless and tasteless. If the compounds could be designed to allow once daily dosing (instead of the current 6h dosing of cysteamine) this would also be advantageous. A number of pro-drugs have been successfully produced and evaluated by a team of researchers at the Robert Gordon University.^{138,139,140,141,143}

The first class (or first generation) pro-drugs synthesised in this programme were a number of long chain fatty acid amide derivatives of cysteamine and cystamine.¹³⁸ These compounds were deliberately designed to be poorly water soluble. This strategy was adopted in an attempt to neutralise the unpleasant taste of cysteamine. For a substance to be tasted, it must first dissolve in saliva in the mouth. Compounds with low aqueous solubility are unable to dissolve in the mouth and so are not tasted.¹³⁸ This approach has been widely used to mask the unpleasant taste of antibiotics, such as chloramphenicol¹⁸² and other therapeutic agents. A second generation of polyethylene glycol (PEG) derivatives of cystamine (pegylated pro-drugs) were then produced. These compounds extended the pro-drug concept by the use of a more water-soluble aliphatic linker as a spacer moiety. PEG is a non-toxic, non-immunogenic, non-antigenic polymer which is highly soluble in water. Importantly, modification of a compound by attachment to PEG greatly extends the half life of the compound¹⁸³. It was envisaged that this extension to half life may allow the possibility of less frequent oral

dosing in the treatment of cystinosis. PEG also had the advantage of a long track history of safety in pharmaceutical use.¹³⁹

These novel pro-drugs were non toxic and were shown to deplete intracellular cystine levels, in some cases even with greater ability than the parent drug, cysteamine.^{138,139} The problem with the first and second generation pro-drugs, however, was a lack of potency. The compounds were as active (or slightly more active) than cysteamine itself, and were therefore not sufficiently potent to be considered for further development as therapies for cystinosis.^{138,139}

In an attempt to increase the potency of the compounds, and to utilise completely the existing library of non-toxic building blocks, a third generation of 'multi dose' pro-drugs was designed and synthesised in house.¹⁴⁰ These compounds used succinic and glutaric acids as simple, biologically acceptable linkers and were designed to incorporate multiple cysteamine molecules in their structure. It was anticipated that alternate organic acid – cysteamine amides could be built up sequentially to yield a long chain molecule which would release multiple copies of cysteamine if hydrolysed completely. These derivatives were produced in good yield and displayed little or no cytotoxicity when tested *in vitro*.¹⁴⁰ When the efficacy of the compounds was determined, they were found to be slightly more potent than cysteamine, but did not provide the desired increase in effect. Even though they had been designed to yield up to 4 molecules of cysteamine when hydrolysed, they proved to be only 1.5 times more potent. This drop in activity was attributed to incomplete hydrolysis of the parent pro-drug within the time scale of the assay.¹⁴⁰

As part of the project to improve the delivery of cysteamine to cystinotic cells, a folic acid derivative of cysteamine was synthesised and evaluated. This compound was designed to utilise the existing folate uptake mechanism which remains functional in cystinosis.¹⁴¹ The folate pro-drug was evaluated in cultured cystinotic fibroblasts and displayed the greatest ability to reduce intralysosomal cystine seen so far in our studies.¹⁴¹

Chemical structures of each of the pro-drugs mentioned above can be found in Chapter 1, section 1.5.

The work described herein continues the programme of pro-drug synthesis and the production of novel 'multi dose' pro-drugs designed to release multiple cysteamine molecules when hydrolysed (see Figure 52). The overall aim of all of the work remains the design of an odourless and tasteless oral therapy for the treatment of cystinosis.

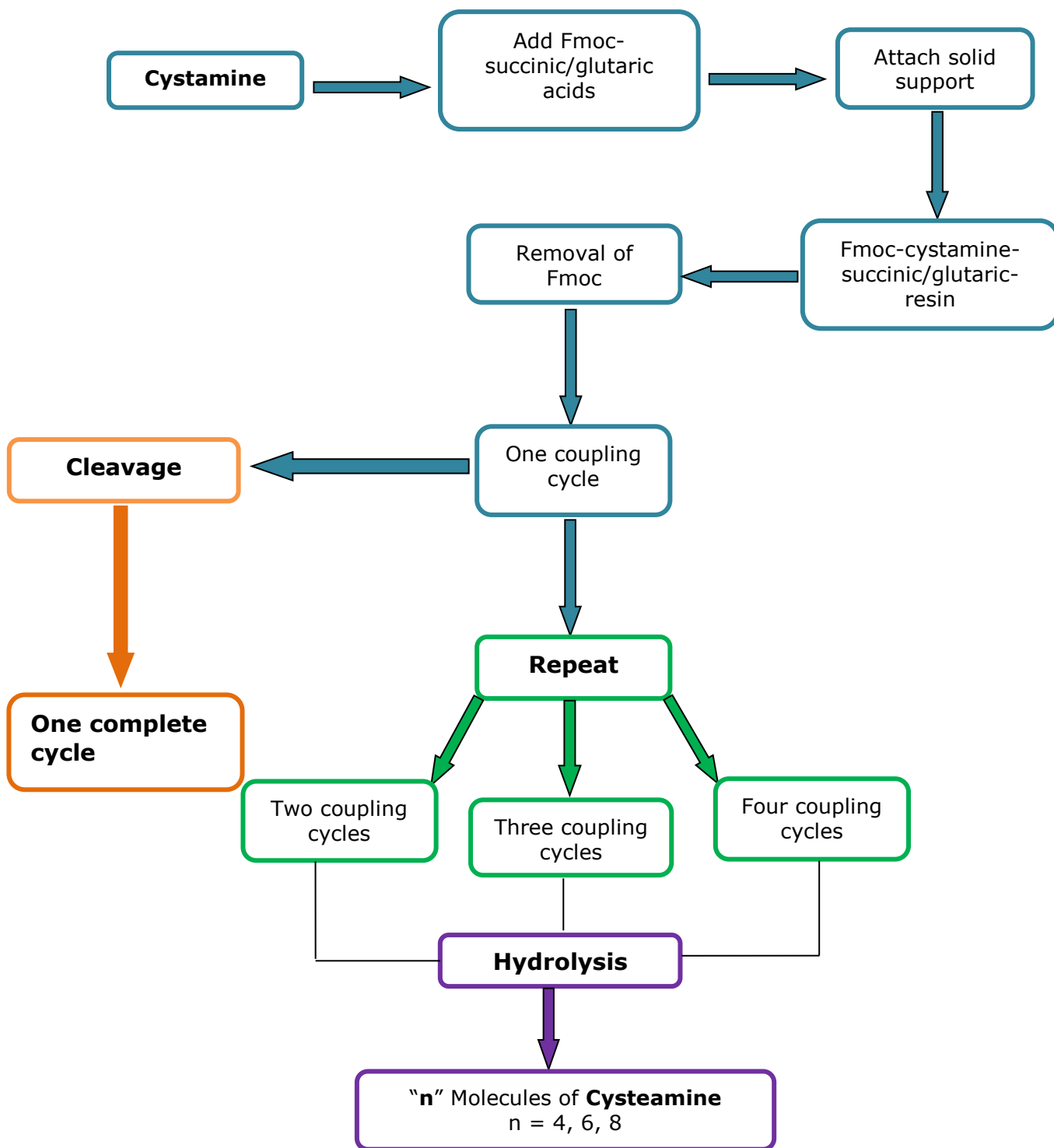


Figure 52.: Peptide synthesis of " multi-dose" pro-drugs

4.2.1. Instrumental Techniques for Identification and Characterisation of Derivatives

Mass Spectrometry (MS) and Nuclear Magnetic Resonance (NMR) were the instrumental techniques employed to identify and characterise the compounds at each stage of the synthesis.

Electron Ionisation Mass Spectrometry (EI-MS) was also employed since it is an important technique for the elucidation of unknown structures and, if a molecular ion radical is identified, MS provides a rapid method to determine the relative molecular mass of the product and hence the number of coupling reactions achieved. Low resolution MS was undertaken to determine fully the structure of the synthesised compounds, whereas high resolution MS was used to obtain an accurate mass.

Additionally, ^1H NMR was used to obtain a complete structure elucidation of the final products and their intermediates. The resonance of expected protons was not found in several spectra. This was due to the repeating nature of the molecular units used to build up the novel pro-drugs as shown in Figure 53. The signals due to individual protons tended to become superimposed, and this led to complex and over-lapping spectra which reduced the usefulness of the technique for the analysis of structures.

Thin Layer chromatography (TLC), was also used to allow a rapid determination of reaction progress as well as providing a simple estimation of the purity of compounds produced.¹⁸⁴

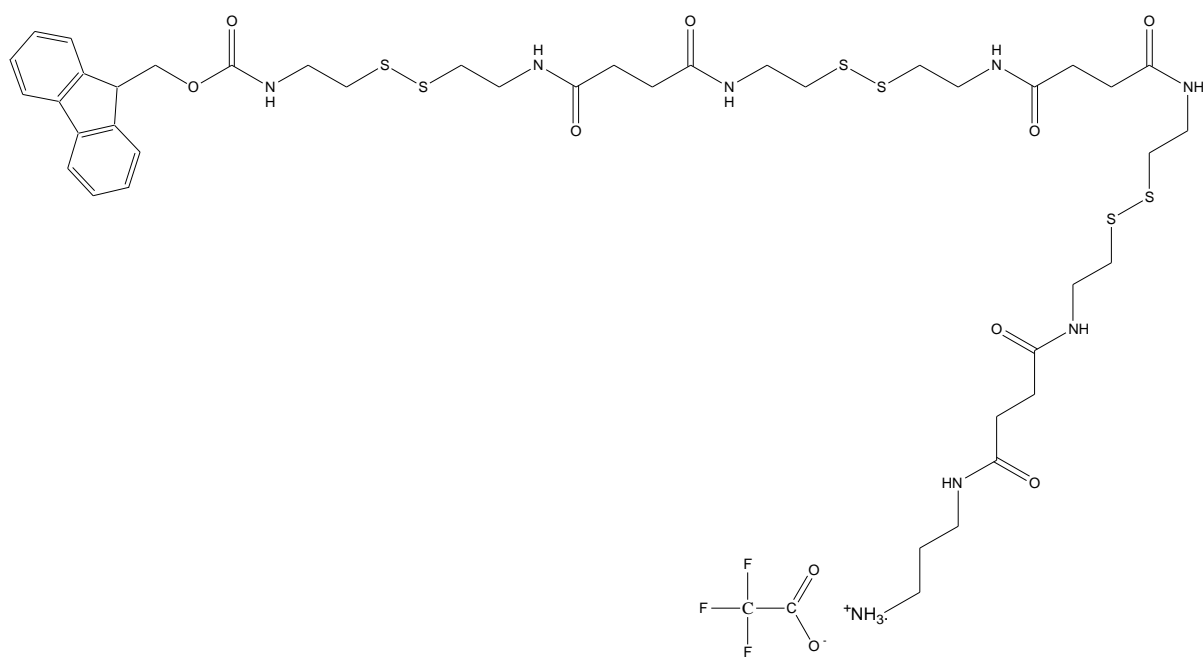


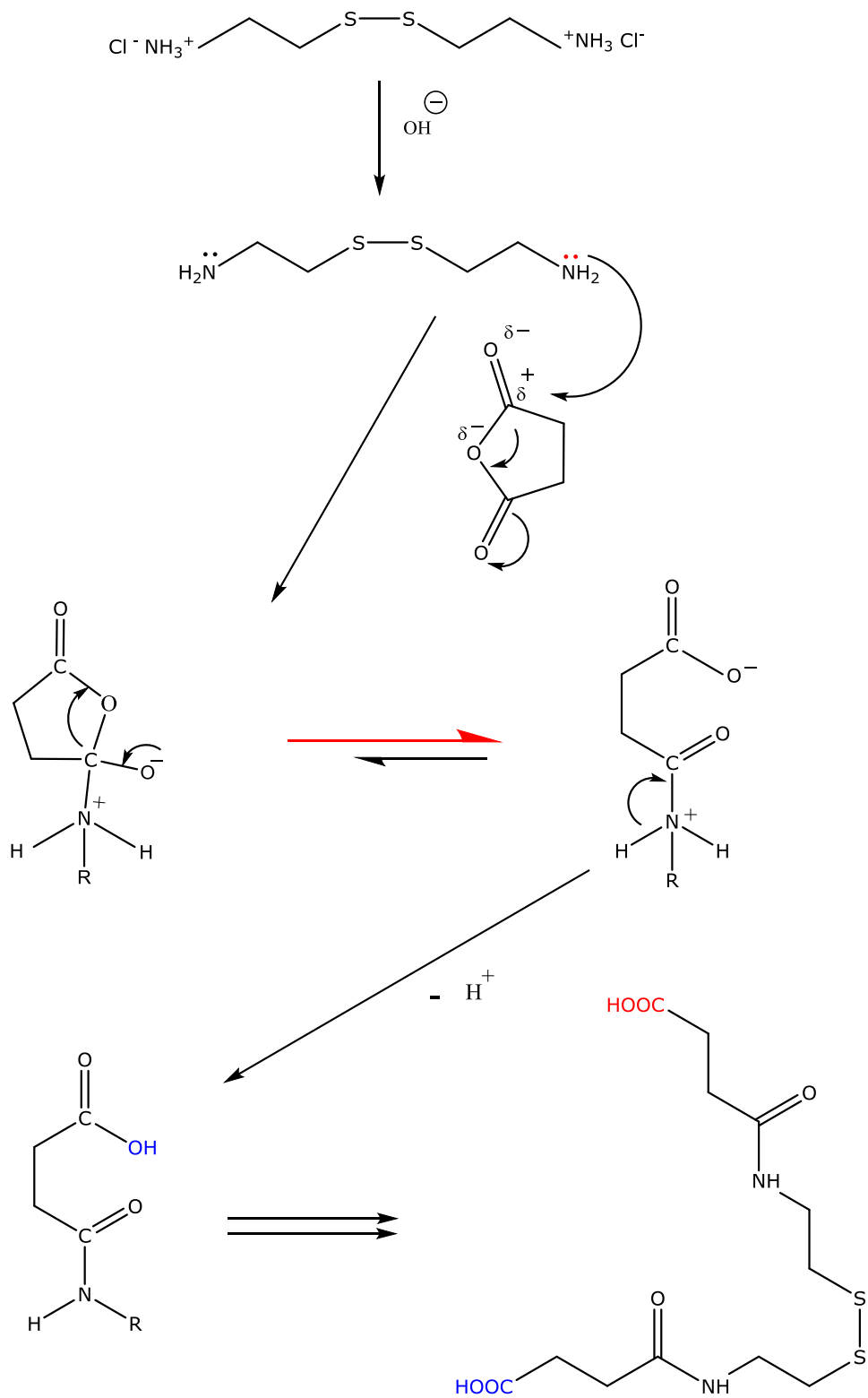
Figure 53.: Structure of repeating units of cystamine –succinic pro-drug

4.2.2. General synthesis Cystamine pro-drug derivatives **3, 7, 11, 14.**

The strategy to synthesise all pro-drugs was adopted from the synthetic method employed by Omran *et al.* (2011). Scheme **1** shows the synthetic route to the pro-drugs.^{140,185}

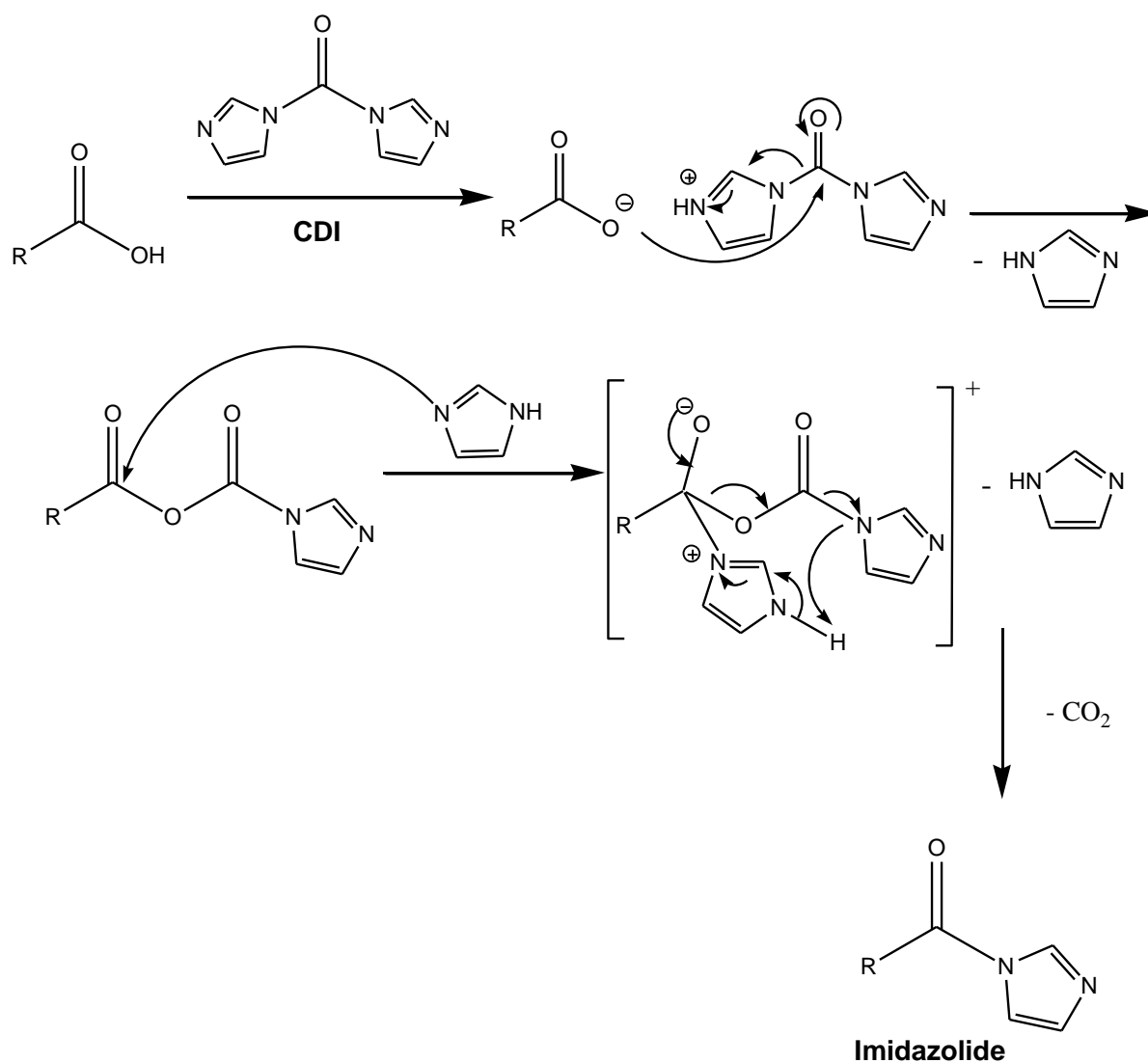
The synthesis of the pro-drugs was carried out using peptide coupling techniques with tert-butyloxycarbonyl (tBoc) as the protecting group for one of the free cystamine nitrogen atoms. This meant that mono Boc-cystamine became a key synthetic intermediate for all subsequent synthesis. During the synthesis, carbonyldiimidazole (CDI) was used as an activating agent for the coupling reaction.

CDI incorporates an electron deficient carbon atom making it useful in nucleophilic substitution reactions where the carbon can be readily attacked as shown in scheme 2.¹⁸⁶



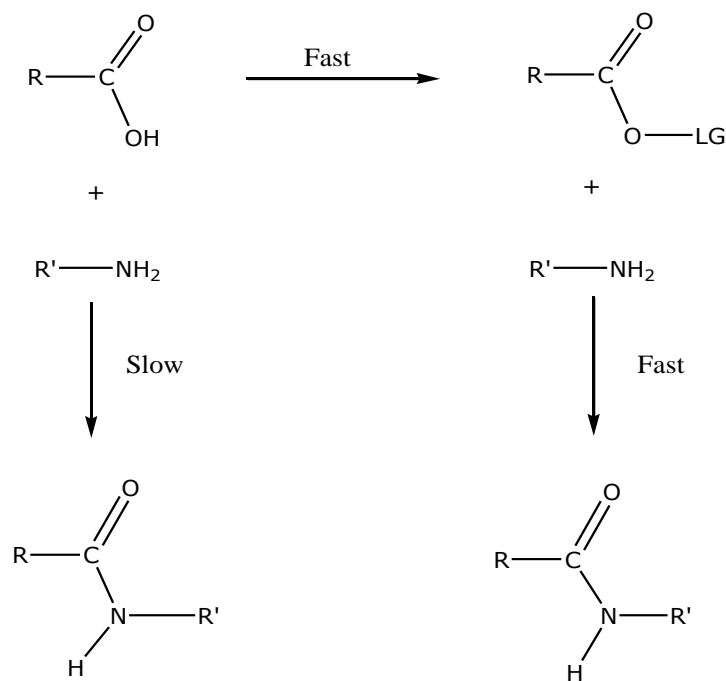
Scheme 2.: Nucleophilic substitution at the carbonyl group of succinic anhydride

The resulting imidazolide acts as a good leaving group in the synthesis of the pro-drug. This occurs because the carboxylic anhydride reacts with CDI to produce a corresponding imidazole derivative and carbon dioxide (CO₂) as illustrated in Scheme 3. The CO₂ produced is lost from the reaction and this drives the equilibrium to the right hand side.



Scheme 3.: Mechanism for synthesis of imidazolide derivative

Incorporation of CDI as a leaving group necessitates an additional step over the published Omran synthesis, but overcomes the slow rate of reaction between carboxylic acids and amines as outlined in scheme 4 below.



Scheme 4.: Reaction mechanism of Carbonyldiimidazole (CDI)

4.2.2.1. Synthesis of Pro-drug (1). [2-(2-{4-[2-(2-{4-[2-(2-tert-Butoxycarbonylaminoethyldisulfanyl)ethylcarbamoyl]propionylamino}ethyl)disulfanyl)ethylcarbamoyl]propionylamino}ethyl)disulfanyl)ethyl]carbamic acid tert-butyl ester

The terminal carboxylic acid groups of (**2**) were activated in the presence of carbonyldiimidazole (CDI) in anhydrous DMF.^{140,141} However, compared to previous studies, the imidazolide derivative (**3**) was not isolated and was coupled with 2 equivalents of mono-Boc-cystamine in anhydrous DMF *in situ* to yield the corresponding cystamine derivative (**1**). By omitting the isolation of the intermediate (**3**), the percentage yield (83%) of the reaction

was improved when compared to previous studies where the percentage yield was only (60%).

Compound (**1**) was then characterised by mass spectrometry which gave a signal at m/z 821 $[M+ 1]$ corresponding to a relative molecular mass of 820. The structure of the N-protected compound was confirmed by proton NMR spectroscopy that showed the presence of the ^tBoc-protecting group as an 18-proton singlet centred at 1.37 ppm and the amide NH as a four-proton triplet at 8.08ppm. All remaining protons were fully assigned. Deprotection of compound **1** with TFA gave the trifluoroacetate salt (**4**), the structure of which was confirmed by proton NMR spectrum and mass spectrometry which gave a signal at m/z 621 $[M + 1]$ corresponding to RNH_3^+ and a relative molecular mass of 620.

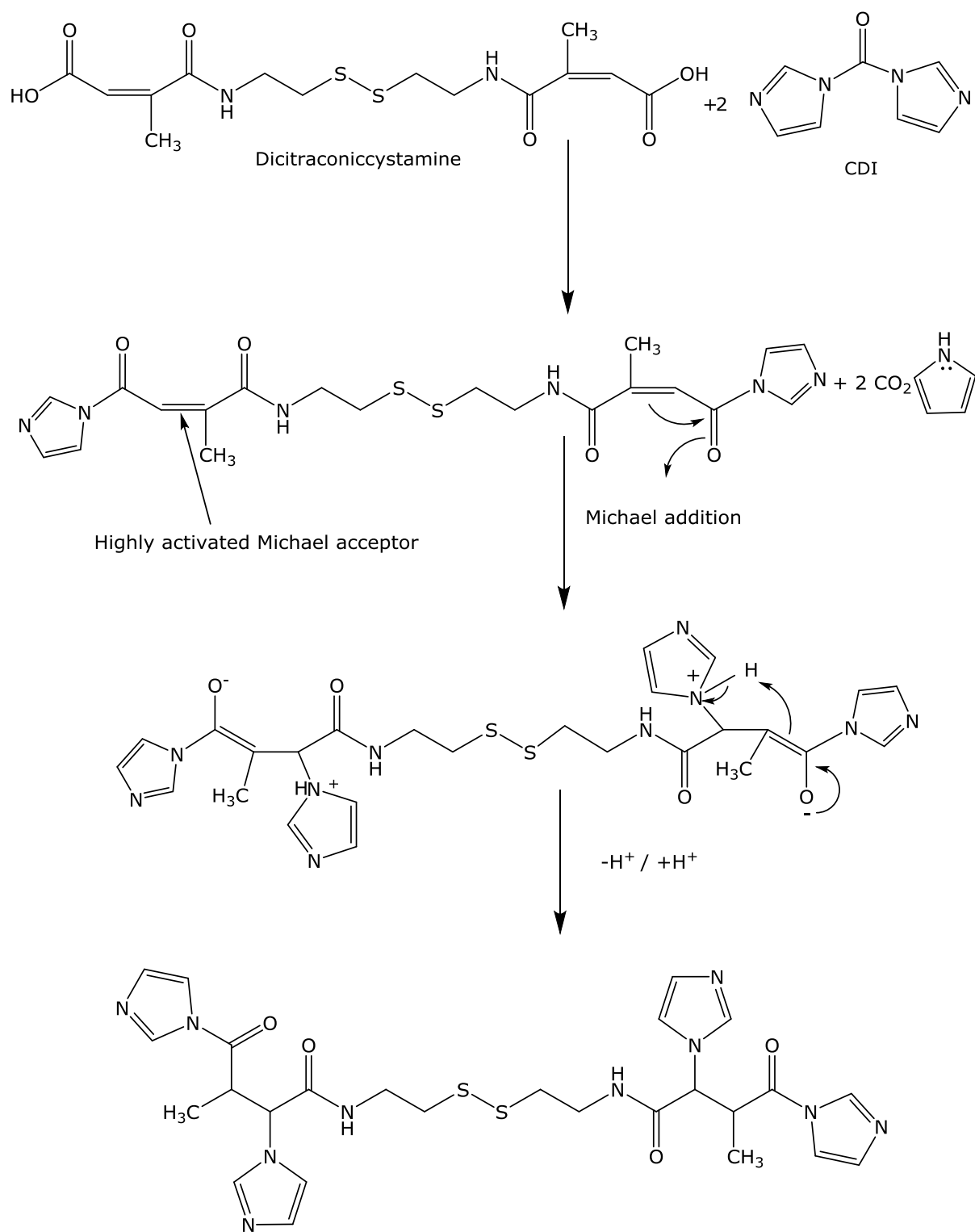
4.2.2.2. Synthesis of Pro-drug (5). [2-(2-{4-[2-(2-{4-[2-(2-tert-Butoxycarbonylaminoethyl)disulfanyl)ethyl]carbamoyl]butyrylamino}ethyl)disulfanyl)ethyl]carbamic acid tert-butyl ester

The product yield for this reaction was also improved when compared to previous studies.¹⁴⁰ The compound was characterised by mass spectrometry which gave a signal at m/z 849 $[M+ 1]$ corresponding to a relative molecular mass of 848. The structure was confirmed by proton NMR spectroscopy that showed for example an additional ethyl group in the glutaric acid molecule which was identified as a 4 proton multiplet at 1.77 ppm. All remaining protons were fully assigned.

Deprotection of compound **5** with TFA was confirmed by the absence of the ^tBoc-protecting group on the ¹H NMR spectrum. All remaining protons of the trifluoroacetate salt structure (**8**) were fully assigned and the MS showed a signal at m/z 649 $[M + 1]$ corresponding to RNH_3^+ and a relative molecular mass of 648.

4.2.2.3. Synthesis of Pro-drug (9). di-tert-butyl ((9Z,21Z)-10,21-dimethyl-8,11,20,23-tetraoxo-3,4,15,16,27,28-hexathia-7,12,19,24-tetraazatriaconta-9,21-diene-1,30-diyl)dicarbamate.

The synthesis of pro-drug **9** was complicated by the fact that the presence of a double bond in citraconic acid gives the possibility that a side reaction, could occur due to a Michael addition mechanism. The addition of CDI to the dicitraconic cystamine had the potential to form a highly activated Michael acceptor as shown in Scheme 5.



Scheme 5.: Mechanism of Michael addition

Despite the theoretical possibility for Michael addition, the desired diamide (C) was synthesised and characterised by mass spectrometry (EI/CI) which gave a signal at m/z 375 $[M - H^+]$ corresponding to a relative molecular mass of 376.

Another indication of the effect of the double bond in the synthesis was the formation of a red reaction product. This product strongly suggested the presence of a chromophore and may be due to through conjugation between the citraconic double bonds and the carbonyl imidazole.

Furthermore, the synthesis using this type of acid produced diamides **C** and **D** with a low yield when compared to diamides **A** and **B** as outlined in Table 17.

Table 17.: Effects of Michael addition on the yield of diamides C and D

Diamide	Mass of final product (G)	% Yield of final product
(A)	0.46	92
(B)	0.36	72
(C)	0.16	27
(D)	0.27	59

This suggests that the side reaction due to a Michael addition, even though the Michael product could not be isolated, may be having a detrimental effect on the final yield as shown in Table 18 below.

The final product (11) was characterised by mass spectrometry which yielded a signal at m/z 879 $[M + Cl^-]$ corresponding to a relative molecular mass of 844. Mass spectrometry also showed the presence of the starting material Monoboc cystamine which had a signal at m/z 253 $[M + H^+]$ suggesting the low yield may also be due to incomplete reaction.

4.2.2.4. Synthesis of Pro-drug (12). di-tert-butyl ((9Z,21Z)-8,11,20,23-tetraoxo-3,4,15,16,27,28-hexathia-7,12,19,24-tetraazatriaconta-9,21-diene-1,30-diyl)dicarbamate.

The synthesis of this compound was also affected by the presence of a C=C in the starting acid. Nevertheless, the synthesis produced the desired diamide (**D**) which was characterised by mass spectrometry (EI/CI) which had a signal at m/z 347 $[M - H^+]$ corresponding to a relative molecular mass of 348.

However, the yield of the final product (**12**) was also low (see Table 18) and this is attributed to the Michael addition discussed above.

Table 18.: Effects of Michael addition on the yield of final products

Compound	Mass of final product (G)	% Yield of final product
(1)	1.94	83
(5)	1.64	73
(9)	0.19	38
(12)	0.37	41

The final product (**12**) which was also coloured red and was characterised by mass spectrometry to give a signal at m/z 419.5 corresponding to a relative molecular mass of $[816 + Na]/2$. Starting material could not be identified in the mass spectrum, suggesting that this reaction did proceed to completion.

4.3. Synthesis of Cystamine Pseudo-Peptides.

In an attempt to increase the overall efficacy of the compounds, target molecules which could release multiple cysteamine residues were designed. These compounds, if hydrolysed completely *in vivo*, would release multiple molecules of cysteamine and it was envisaged this would increase the potency of the drug.

A small library of pro-drugs was synthesised using Fmoc-based solid phase peptide synthesis techniques which is now the method of choice for the routine synthesis of peptides. The hindered base-labile *N-Fmoc* group was used to protect the α -amino function of amines which is also compatible with *tert*-butyl-based side-chain protection.

The required protected amino acids were not commercially available and amino acids **15** and **16** were prepared as described in Chapter 3, section 3.2.1.

4.3.1. General Synthesis

All novel cystamine pseudo-peptides were synthesised using a cycle of reactions incorporating TBTU/HOBt activation as shown in Figure 54.

TBTU was used to convert the Fmoc amino acid into the active OBt ester in the presence of DIPEA. The aromatic ester HOBt becomes the activated ester which can be easily hydrolysed and can also react with a wide range of nucleophiles.¹⁸⁷ Under mild conditions HOBt reacts minimally with amines usually with reduced racemisation of the alpha carbon atom. In peptide synthesis, HOBt is one of the most commonly used coupling reagents because of the electron-withdrawing nature of its particular alcohol resulting in the increased electrophilicity of the carbonyl centre.¹⁸⁷

Furthermore, the presence of hydroxyl group (OH) in the carboxylic acid of amino acids 15 and 16, acted as good leaving groups in the formation of an amide bond between the two amino acid residues.

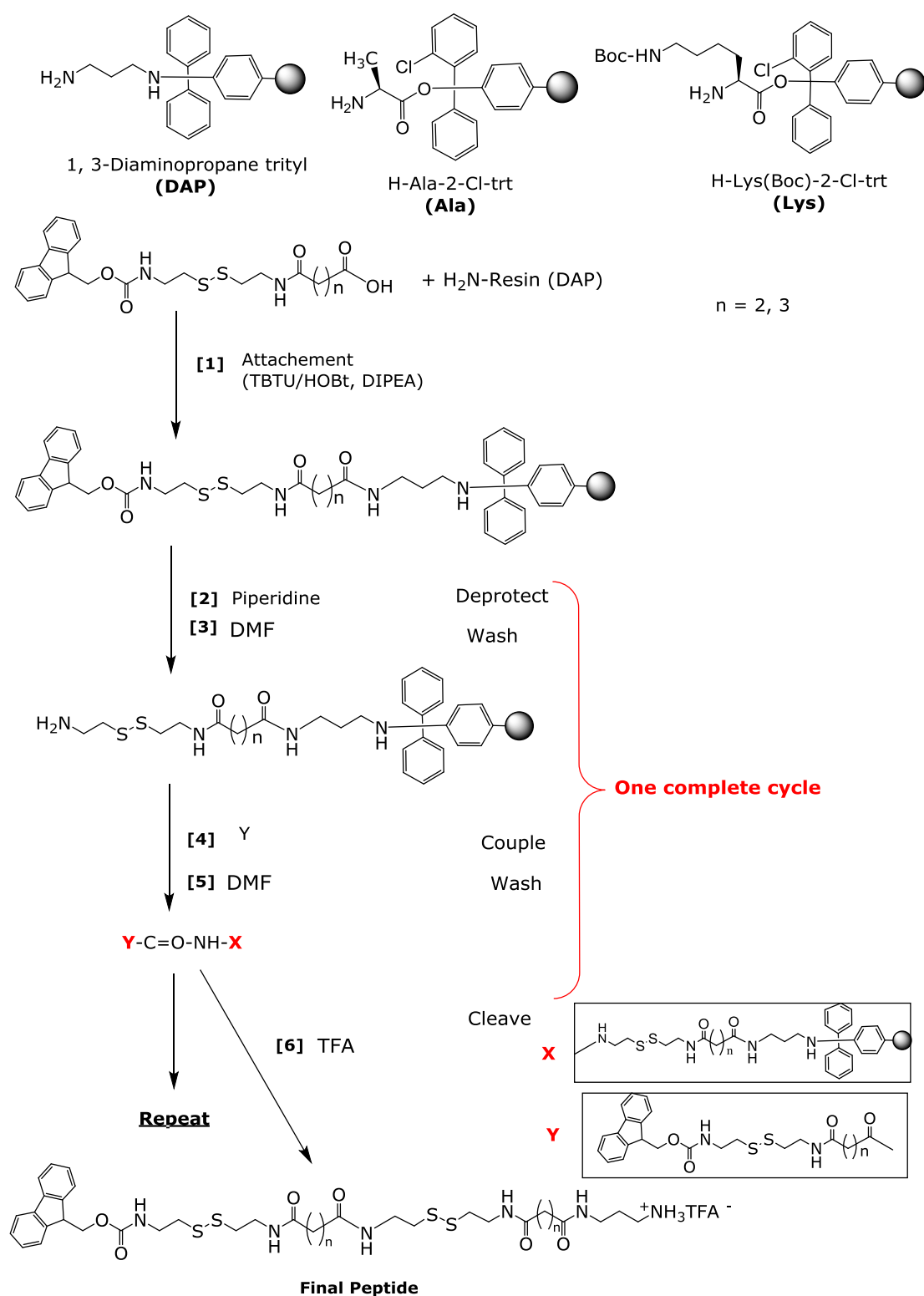
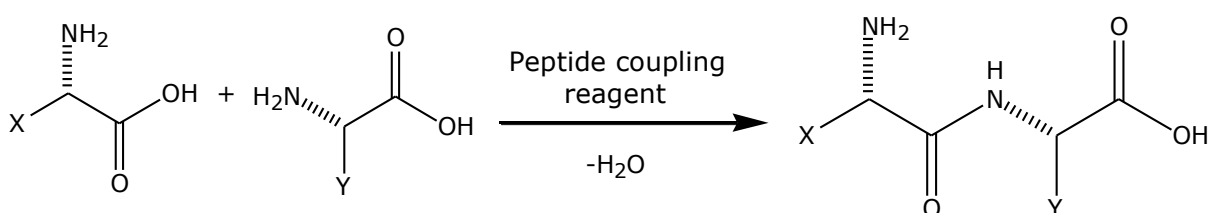


Figure 54.: Solid phase peptide synthesis (SPPS) steps with Fmoc-chemistry. Reagents and conditions: [1] HOBt, TBTU, DIPEA, DMF, RT, 2 h; [2] 20% piperidine, RT, 2 h; [3] DMF; [4] HOBt, TBTU, DIPEA, RT, 2 h; [5] DMF; [6] 1% TFA, RT, 2 h.

4.3.1.1. Synthesis using Solid Phase Peptide Synthesis (SPPS) and Convergent Peptide Synthesis (CPS).

In a typical peptide coupling reaction, the carboxylic acid moiety of the amino acid 1 is first activated by an appropriate peptide coupling reagent, and then reacted with the amine moiety of the amino acid 2 to produce a desired peptide as illustrated in Scheme 6.¹⁸⁸

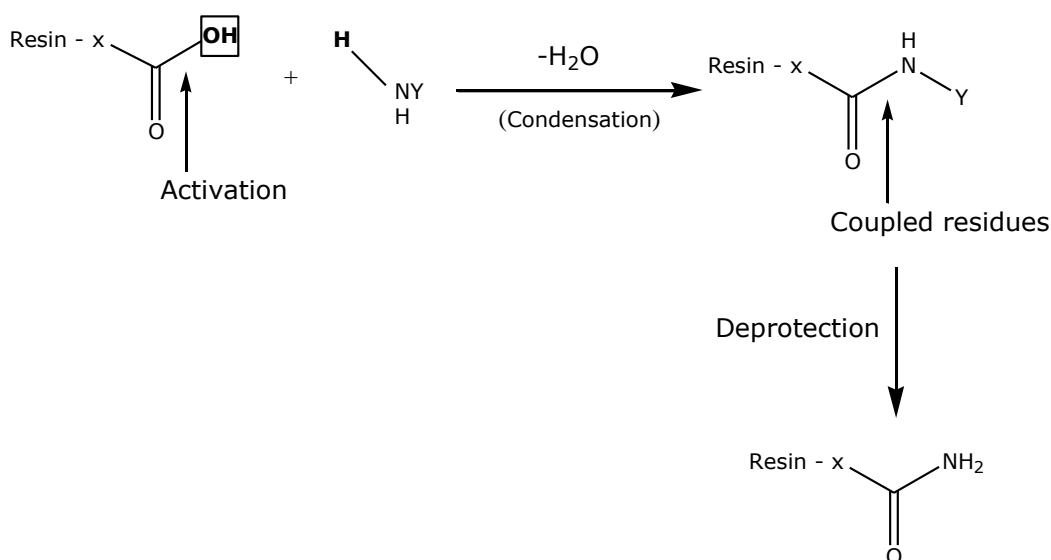


Scheme 6.: General synthesis of peptides

All peptides were synthesised in a relatively facile manner on three different solid supports (resins) using a standard protocol for TBTU/HOBt/DIPEA activation of Fmoc protected cystamine derivatives.

The synthesis followed the stepwise assembly of peptides by consecutive coupling of compound 15 or 16 which were the common starting materials in the synthesis of the peptides.

The first step in synthesis was to incorporate compound 15 or 16 onto the solid support through an ester linkage and the reaction was monitored by TLC. The N protected group was deprotected under conditions which did not cleave the resin-amino acid ester bond (see Scheme 7). Another Fmoc protected cystamine derivative 15 or 16 was coupled to the amino group of the resin bound substrate *via* an amide coupling. The resulting peptide bond was formed due to the condensation reaction usually initiated by activation of the carboxylic acid component as shown in Scheme 7.¹⁸⁹



The N^α deprotection and coupling steps were repeated until the desired sequence was assembled on the resin. The final step in the process was to cleave the resulting sequence from the support with 10% TFA giving rise to the free pseudo peptide which was characterised by mass spectrometry (see Table 19 below).

Table 19.: Mass spectrometry (MS) results

Peptide	HR-MS	LR-MS
17	(M + H ⁺) 765.2583 (100%)	
18	(M + H ⁺) 999.3070 (55%)	
19	(M + H ⁺) 545.2255 (100%)	
20	(M + H ⁺) 793.2900 (100%)	
21		No recognisable peak obtained
22		(M + H ⁺) 1289 (25%)
23	(M + H ⁺) 779.2738 (80%)	
24	(M + H ⁺) 780.2226 (100%)	
25	(M + H ⁺) 808.2537 (100%) Weak	

26	(M + H ⁺) 794.2379 (65%)	
27	(M + H ⁺) 937.3330 (15%)	
28	(M + H ⁺) 965.3636 (100%)	
29	(M - H ⁺) 949.3283 (100%)	
30		(Mass + H ⁺) 987 (20%) (M + K ⁺) 1025 (55%)
31		(M + Cl ⁻) 1049 (100%) (M + H ⁺) 1015 (15%) (M + Na ⁺) 1037 (35%)
32		No identifiable peaks were obtained
33		No identifiable peaks were obtained
34		Mass 1292 (10%)
35		No identifiable peaks were obtained
36		(M + H ⁺) 531 (100%)

H-Lys(Boc)-2-Cl-trt resin (**Lys**) and H-Ala-2-Cl-trt resin (**Ala**) consistently generated peptides with a similar yield when compared to peptides synthesised using 1, 3-Diaminopropane trityl resin (**DAP**) as shown in Table 20.

Table 20.: Peptides generated from solid phase peptide synthesis (**SPPS**) using different solid support resins and convergent peptide synthesis (**CPS**).

Resin	Peptide	Mass of final product (G)	% Yield of final product
DAP	Fmoc(2CS)-DAP (17)	0.1	10
	Fmoc(3CS)-DAP (18)	0.55	11
	Fmoc(CG)-DAP (19)	0.1	29
	Fmoc(2CG)-DAP (20)	0.4	15
	Fmoc(4CG)-DAP (22)	0.25	5
	Fmoc(CS-CG)-DAP (23)	0.076	8
	Fmoc(CS)-DAP (36)	0.05	15
Ala	Fmoc-2CS-Ala (24)	0.09	13
	Fmoc-2CG-Ala (25)	0.07	10
	Fmoc-CS-CG-Fmoc-Ala (26)	0.08	11
Lys	Fmoc-2CS-BocLys (27)	0.15	13
	Fmoc-2CG-BocLys (28)	0.2	11
	Fmoc-CS-CG-BocLys (29)	0.18	10
CPS	Fmoc-CS-DAP-SC-Fmoc (30)	0.2	18
	Fmoc-CG-DAP-GC-Fmoc (31)	0.13	23
	Fmoc-2CS-Lys(Boc)-Fmoc-cystamine (34)	0.09	10

Attempts were made to improve the yields obtained using the DAP resin by increasing the stoichiometric amounts of resin, and also the reaction temperature, however, the yield remained low. Solid phase peptide synthesis is often selected for the production of small peptides. The resulting peptides would often have a yield not exceeding 100 mg.¹⁸⁹

In addition, the longer the sequence, the greater the number of coupling cycles required and the lower the yield produced. This was seen with peptides 18 and 22 (Table 20).

Other problems which could have contributed to the low yields obtained during peptide synthesis were the formation of side reaction residues such as urea. Previous studies showed that during peptide synthesis using for example DCC as the coupling reagent, the highly reactive *O*-acylisourea is formed which in turn reacts with the amine to produce the peptide and urea derivative.¹⁹⁰

Incomplete coupling could have also been a contributing factor in obtaining peptides with low yields. This was confirmed by the production of a reddish-brown colour produced by the ninhydrin reaction as described in chapter 3, section 4.2.4.1.4, indicating a positive reaction to an incomplete coupling.

In addition, the presence of sulfur in the starting reagents could allow REDOX type reactions to reduce further the yields obtained. Previous studies by Antonkine *et al.* reported the formation of iron-sulfur clusters with relatively low yield of 17% during a standard Fmoc-synthesis. The presence of a large amount of cysteine residues may have contributed to the low yield obtained, giving that cysteine commonly undergoes a number of side reactions during peptide synthesis.¹⁹¹

In order to increase the library of compounds produced for biological evaluation, it was decided to adopt a convergent peptide synthesis.

Compounds 19 and 36, produced from sequential linear peptide synthesis were used to produce new peptides *via* a convergent approach.

The overall yield of these peptides was higher than that obtained from linear synthesis as seen in Table 20.

Moreover, using the convergent approach allowed us to carry out the chemistry with relatively small fragments.

4.3.1.2. Attempted synthesis using Convergent Peptide Synthesis (CPS)

The convergent approach was repeated with compounds 32, 33, and 35, (refer to the structure library).

Although a product was isolated, no identifiable peaks were obtained following characterisation by mass spectrometry as shown in Table 19. However, MS results for compound 33 and 35 showed the presence of both starting materials; refer to Chapter 3 section 3.2.7.4 and 3.2.7.5 respectively for details.

These results could have also been due to multiple ionisations of the product or instability in the desired product.

Throughout the synthesis of the peptides, routine TLC was used to monitor the reactions. The use of preparative HPLC was investigated as a more efficient method to purify the synthetic products. Suitable chromatographic conditions were identified using a 4.6mm, C18, reverse phase analytical column, but resolution and peak separation were reduced when the separation was scaled up to prep or semi-prep quantities. This was not unexpected and was attributed to a loss of resolution with the larger prep column. Further optimisation of the technique was becoming time consuming, and as a result, this method of separation was not pursued.

4.4. Biological studies

A small number of synthesised compounds were evaluated for cell toxicity and their ability to reduce the levels of cystine in cultured cystinotic cells. Statistical analysis of both the cytotoxicity and activity data was carried out using Paired t-tests and One-way ANOVA analysis.

4.4.1. Cytotoxicity

A small number of synthesised cystamine pseudo peptides were selected and evaluated for their growth inhibitory and cell toxicity effects on cystinotic fibroblasts. The criterion for selection comprised of the sample size and the representation of each class of compounds. This study was developed and conducted in our laboratory using the Alamar Blue cell proliferation assay as described in Chapter 3 section 3.3.3.2.

This assay was based on the use of an indicator dye developed to measure and quantify cell growth in cultured cells. The mechanism by which the Alamar Blue dye works is by an oxidation-reduction (REDOX) reaction. Live cells are able to metabolically convert the blue dye (resazurin) to a pink coloured compound (resofurin). The intensity of the resulting colour was quantified using a spectrophotometer at a wavelength of 570nm which is the λ max for the reduced compound. The values obtained were proportional to the growth of the cells in the cell culture plates and are represented graphically in Figure 55.

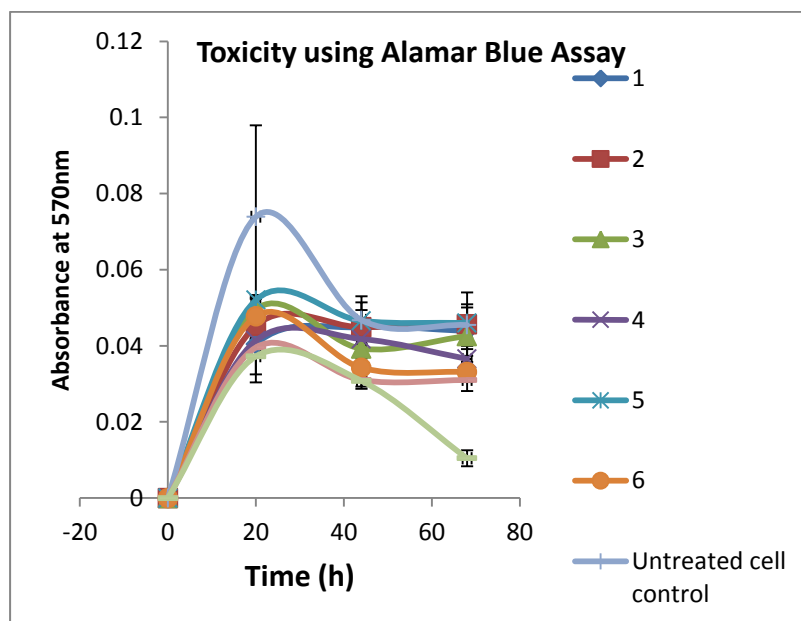


Figure 55.: Graph showing cell growth in presence of cysteamine and compounds **1-6** (50 μ M) over a 72 hour incubation. Cytotoxicity was determined by Alamar Blue Assay. Data are mean \pm SD of 3 independent experiments ($n = 3$). Each measurement was carried out in triplicate.

- Compound 1 Fmoc-3x (CystSucc)-DAP
- Compound 2 Fmoc-(CystGlut)-DAP
- Compound 3 Fmoc-(CystSucc-CystGlut)-Lysboc
- Compound 4 Fmoc-2x (CystGlut)-Ala
- Compound 5 Fmoc-2x (CystGlut)-Lysboc
- Compound 6 Fmoc-2x (CystSucc)-Lysboc

The results in Figure **55** clearly show that all of the synthesised pro-drugs (**1-6**) gave a growth profile similar to the vehicle (0.5% DMSO) and all were less toxic than cysteamine itself. As expected, the most significant period of cell growth was evident in the first 20 hours for all of the samples tested. The net increase of all samples tested was lower at 20 hours when compared to the untreated cell control. By approximately 48 hours, no drop in growth was observed as the cells would have probably reached confluence, rather than any inherent toxic effect. These results are not unexpected, since previous work in our laboratories, using similar compounds (**7**, **8**, and **9**), has not resulted in substantial levels of cytotoxicity as seen in Figure **56**.

The pro-drugs synthesised are composed of repeating units of endogenous compounds (succinic acid, glutaric acid, cystamine, etc.) which are known to be non-toxic to cells.

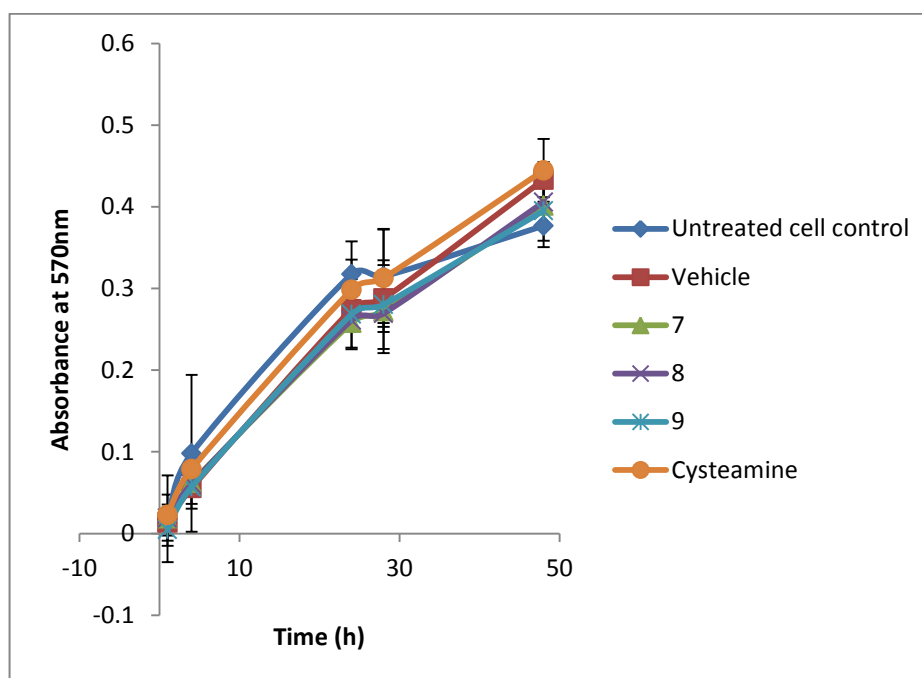


Figure 56.: Graph showing cell growth of cysteamine and compounds **7-9** (50 μ M) over a 48 hour incubation. Cytotoxicity was determined by Alamar Blue Assay. Data are mean \pm SD of 3 independent experiments ($n = 3$). Each measurement was carried out in triplicate.

Compound 7 Fmoc-x2 (CystSucc)-DAP

Compound 8 Fmoc-x2 (CystGlut)-DAP

Compound 9 Fmoc-(CystSucc-CystGlut)-DAP

4.4.2. Effect of synthetic pro-drugs on levels of cystine

A commercially available Thiol assay kit (Fisher Scientific, UK) was used along with the Bradford Protein assay to evaluate the efficacy of the novel compounds in reducing the cystine levels in cultured cystinotic fibroblasts. The assays are described in Chapter 3, sections 3.3.4.1 and 3.3.4.2 respectively.

The results of these assays are presented in Figure **57**. However, due to the small sample number (results are the average of 3 observations) these data should be regarded as preliminary. The results were analysed using independent sample unpaired t-tests which showed some differences between the samples.

Compounds **3, 4, 5, 7, 10, and 11** resulted in a significant decrease in cystine level when compared to the Vehicle Control. (Figure 56)

Compound 6 although non toxic, generated an abnormally high set of results when compared to previous studies.

Ideally, these measurements should be repeated using replicates of up to 9 observations to provide results which are statistically rigorous, however, there was insufficient sample available for some of the synthesised pro-drugs which curtailed the replicates for the experiment.

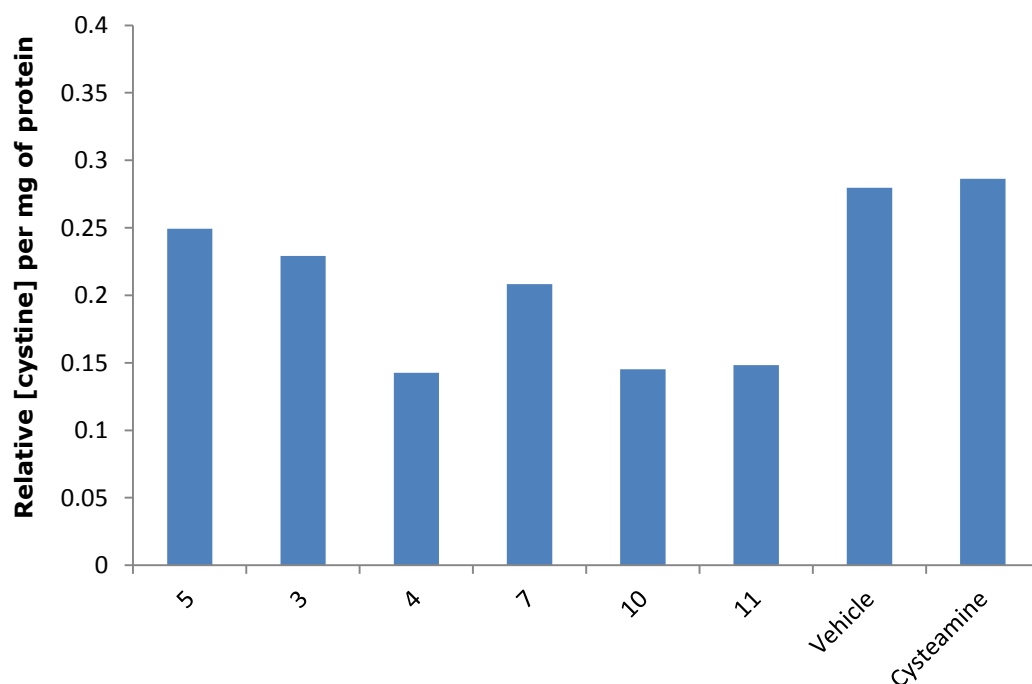


Figure 57.: Relative cystine depletion in cystinotic fibroblasts measured following a 24 hour incubation with cysteamine and compounds **3-11** (50 μ M). Data are mean \pm SD of 3 observations. Each measurement was carried out in triplicate. The level of significance was determined using independent sample unpaired t-tests.

Compound 3 Fmoc-(CystSucc-CystGlut)-Lysboc

Compound 4 Fmoc-2x (CystGlut)-Ala

Compound 5 Fmoc-2x (CystGlut)-Lysboc

Compound 6 Fmoc-2x (CystSucc)-Lysboc

Compound 7 Fmoc-2x (CystSucc)-DAP

Compound 10 Fmoc-3x (CystSucc)-DAP

Compound 11 Fmoc-(CystGlut)-DAP

The result for Compound **6** appeared completely anomalous and the cystine values (**1.115 per mg of protein**) obtained far exceed any values seen during previous work on cysteamine pro-drugs. This anomalous result is potentially attributed to poor aqueous solubility. Compound **6** displayed only limited aqueous solubility and it proved difficult to get the drug into solution. It is proposed that, once added to the cell suspension, Compound

6 may have precipitated from solution and this would have contributed to an anomalously high absorbance reading. This is particularly true if particles of drug were present in the sample, which could scatter light during the spectrophotometric assay.

Compounds 3, 5, and 7 and in particular 4, 10, and 11 displayed a significant reduction of lysosomal cystine levels when compared to the vehicle control and cysteamine. This is an encouraging result and suggests that the synthesised pro-drugs are active in reducing the cystine levels in these cells. We propose that this effect is due to intracellular hydrolysis of the pro-drugs to yield free cysteamine which is able to cleave the disulfide bond in cystine as described in the Introduction. It is possible that the pro-drugs are decomposing in the extracellular medium and released cysteamine is entering the cells to reduce the cystine burden, however, the delay in onset of action suggests that the pro-drugs are being absorbed intact and then breaking down within the cell to release the active agent. A definitive answer would require analysis of the intracellular contents to determine the presence of intact prodrug but this was not possible during this study.

Furthermore, the drug design rationale for these compounds required complete hydrolysis of the amide linkages in the pro-drug to release multiple molecules of cysteamine (6 to 8 cysteamine molecules depending on the pro-drug). These results do not show that the pro-drugs were 6 to 8 times more effective than cysteamine, which strongly suggests that hydrolysis was incomplete in the time course studies here. It is also possible that some of the amide bonds in the pro-drugs are more highly resistant to hydrolysis, by intracellular amidases and in solution, than others.

The result for cysteamine is also anomalous. This compound is clinically proven to reduce the cystine level of cells, but in this assay, the levels for cysteamine are not significantly different to the control. A possible reason for this is oxidation of cysteamine to cystamine in the course of the

experiment. The thiol group of cysteamine oxidises readily to a disulfide and this precludes formation of the mixed disulfide and a reduction in the levels of cystine. These studies would have to be repeated in the absence of oxygen (e.g. under an inert atmosphere in a glove box using degassed solutions) to allow a conclusion to be reached. Cysteamine and cystamine exist in a REDOX equilibrium¹⁹² and the proportion of the oxidised or reduced species depends on the environment in the cells.

CHAPTER 5

CONCLUSIONS

5.1. Conclusion and future work

Throughout the whole of the crystallography work described in this project, the objective has been to synthesise and evaluate novel co-crystals of cysteamine and cystamine, as part of our desire to produce odourless and tasteless oral therapies for cystinosis. Despite our best efforts we have failed to produce novel cysteamine/cystamine co-crystals, but the work has generated a series of novel cysteamine and cystamine salts which were fully characterised by melting point (mp), Differential Scanning Calorimetry (DSC), infra-red (IR) spectroscopy and Xray diffraction. However, further work is required to determine the cytotoxicity of these novel salts and assess their ability to deplete the high cystine levels associated with cystinosis. Moreover, in an attempt to resolve the problems associated with the formation of salts with cystamine, more work is required to try to synthesise co-crystals rather than salts. Salts are formed when ionisation occurs and a proton is transferred from acid to base. The possibility of proton transfer should be reduced by using weaker acids with a higher pKa and through inactivation of the amine functional group of cystamine by, for example, substitution with an electron withdrawing substituent (e.g. a phenyl ring). This reduction in basicity should favour co-crystal formation (where no proton transfer occurs) over salt formation where a proton is exchanged.

Another way of improving the analysis of co-crystals would be to analyse the product using neutron diffraction techniques, instead of beams of X-rays, allowing a more accurate location of the hydrogen atoms. However, to fully utilise this technique, a robust scientific rationale will be required and an approximate location for the hydrogen atoms should already be established. Additionally, establishing a comprehensive screening process using different co-formers may be the way ahead for co-crystal production.

This research project has also shown that a series of multicysteamine pro-drugs (i.e. pro-drugs which may hydrolyse *in vivo* to release up to six molecules of cysteamine per molecule of pro-drug) can be successfully

synthesised in good yields. Although the main synthetic route employed was not novel and followed a method pioneered by Omran *et al.* (2011), we have demonstrated that by adopting an *in-situ* approach in one of the reaction steps, the yield of the final product has been improved and the overall reaction simplified. The synthesised pro-drugs were fully characterised by NMR spectroscopy and mass spectrometry before biological evaluation using techniques of cell culture.

In addition, work has also been undertaken using other carboxylic acids such as maleic acid and citraconic acid as starting materials. However, synthesis using these particular acids produced compounds in low yields. It has been suggested that an alternative reaction mechanism *via* an undesired Michael addition could have been a factor in limiting the yield obtained. A definitive answer could be obtained by repeating the synthesis with other unsaturated carboxylic acids, isolating and fully characterising the Michael product.

In order to build up our library of compounds further, solid phase peptide synthesis was employed using three different resin supports. Although this type of approach produced good results, the yield of the final peptides was very low. Therefore, in order to improve the yield and purity of the synthesised compounds, the next logical step would be to try other solid support resins and vary the reaction conditions (e.g. replacement of TBTU by dicyclohexylcarbodiimide [DCC] or diisopropylcarbodiimide [DIC] as dehydrating agent with HOBT or hydroxysuccinimide to minimise unwanted side-reactions, could be pursued). Further work in this area should also involve the optimisation of a robust preparative or semi-prep HPLC method for the purification of synthetic products.

Finally, all the work described herein has concentrated on the design of pro-drugs able to form a mixed disulfide with cystine, which is isosteric with the amino acid lysine. It should be noted that there are a number of other amino acid transporters present in lysosomal membranes.¹⁹³ It may be that pro-drugs designed to target these transporters would provide a future source of agents active in the treatment of cystinosis.

CHAPTER 6

REFERENCES

1. Anderson RJ, Cairns D, Cardwell WA, Case MC, Groudwater PW, Hall AG, Hogarth LA, Meth-Cohn O, Suryadevara P, Tindal A, and Thoene JG. Design, Synthesis and Initial *in vitro* Evaluation of Novel Prodrugs for the Treatment of Cystinosis. *Letters in drug design and discovery*. 2006; 3:336-345
2. Thoene JG. A Review of the Role of Enhanced Apoptosis in the Pathophysiology of Cystinosis. *Molecular Genetics and Metabolism*. 2007; 92(4):292-298.
3. Budavari S. The Merck index: an encyclopaedia of chemicals, drugs, and biological. Whitehouse Station, NJ: Merck & Co; 2006
4. Cairns D. Essentials of Pharmaceutical Chemistry. Fourth edition. 2012. Pharmaceutical Press. London
5. Gahl WA, Kleta R. Cystinosis: Antibodies and Healthy Bodies. *Journal of the American Society of Nephrology*. 2002; 13:2189-2191.
6. Goudier P. The history of Cystinosis: Lessons for Clinical Management. *International Journal of Nephrology*. 2011.
7. Nesterova G, and Gahl WA. Cystinosis: the evolution of a treatable disease. *Pediatric Nephrol*. 2012
8. Gahl WA, Thoene JG, and Schneider JA. Cystinosis. *New England Journal of Medicine*. 2002; 347(2):111-121.
9. Drube J, Schiffer E, Mischak H, Kemper MJ, Neuhaus T, Pape L, Lichtinghagen R, and Ehrich JH. Urinary proteome pattern in children with renal Fanconi syndrome. *Nephrol Dial Transplant*. 2009; 24(7):2161-2169
10. Pisoni RL, Thoene JG, and Christensen HN. Detection and characterisation of carrier-mediated cationic amino acid transport in lysosomes of normal and cystinotic human fibroblasts: role in therapeutic cystine removal. *J Biol Chem*. 1985; 260:4791-4798.
11. Gahl WA, Bashan N, Tietze F, Bernardini I, and Schulman JD. Cystine transport is defective in isolated leucocyte lysosomes from patients with cystinosis. *Science*. 1982; 217:1263-1265.
12. Gahl WA, Thoene JG, O'Regan S, Kaiser-Kupfer MI, and Kuwabara T. NHI conference – Cystinosis: progress in a prototypic disease. *Ann Intern Med*. 1988; 109:557-569.

13. Park M, Helip-Wooley A, and Thoene J. Lysosomal cystine storage augments apoptosis in cultured human fibroblasts and renal tubular epithelial cells. *J Am Soc Nephrol*. 2002; 13:2878-2887
14. Thoene JG. A review of the role of enhanced apoptosis in the pathophysiology of cystinosis. *Mol Genet Metab*. 2007; 92(4):292-298.
15. Laube GF, Shah V, Stewart VC, Hargreaves IP, Haq MR, Heales SJR, and van't Hoff WG. Glutathione depletion and increased apoptosis rate in human cystinotic proximal tubular cells. *Pediatr Nephrol*. 2006; 21 (4): 503 - 509
16. Sansanwal P, Yen B, Gahl WA, Ma Y, Ying L, Wong LJ, and Sarwal MM. Mitochondrial autophagy promotes cellular injury in nephropathic cystinosis. *J Am Soc Nephrol*. 2010; 21(2):272-283.
17. Park M, and Thoene J. Potential role of apoptosis in development of the cystinotic phenotype. *Pediatric Nephrol*. 2005; 20:441-446.
18. Larsen CP, Walker PD, and Thoene J. The incidence of atubular glomeruli in nephropathic cystinosis renal biopsies. *Mol Genet Metab*. 2010; 101(4):417-420.
19. Chevalier R, and Forbes M. Generation and evolution of atubular glomeruli in the progression of renal disorders. *American Society of Nephrology*. 2008; 19:197-206.
20. Mahoney CP, and Striker GE. Early development of the renal lesions in infantile cystinosis. *Pediatric Nephrol*. 2000; 15:50-56.
21. Gahl WA. Cystinosis. *Pediatric Nephrology*. 2009; 6:1019-1038.
22. Gahl WA, Bernardini I, Dalakas M, Rizzo WB, Harper GS, Hoeg JM, Hurko O, and Bernar J. Oral caritine therapy in children with cystinosis and renal Fanconi syndrome. *Journal of Clinical Investigation*. 1988; 81(2):549-560
23. Gahl WA. Cystinosis coming of age. *Advanced Paediatrics*. 1986; 33:95-126
24. Schneider JA. Cystinosis: A defect of lysosomal cystine efflux. *Bioessays*. 1985; 2(4):162-164)

25. Bernardini I, Rizzo WB, Dalkas M, Merner J, and Gahl WA. Plasma and muscle free carnitine deficiency due to renal Fanconi syndrome. *Journal of Clinical Investigation*. 1985; 75:1124-1130.
26. Arant BS, Greifer I, Edelmann CM, and Spitzer A. Effect of chronic salt and water loading on the tubular defects of a child with Fanconi syndrome (cystinosis). *Paediatrics*. 1976, 58:370-377.
27. Jackson JD, Smith FG, Litman NN, Yuile CL, and Latta H. The Fanconi syndrome with cystinosis. Electron microscopy of renal biopsy specimen from five patients. *American Journal of Medicine*. 1962; 33:893-910
28. Worther HG, and Good RA. The De Toni-Fanconi syndrome with cystinosis. Clinical and metabolic study of two cases in a family and a critical review on the nature of the syndrome. *American Journal of Disease in Children*. 1958; 95:653.
29. Toni D. "Remarks on the relations between rickets (renal dwarfism) and renal diabetes." *Acta pædiatrica*. 1933; 16:479-484
30. Debre RMJ, Cleret F, and Messimy R. Late rickets coexisting with chronic nephritis and glycosuria. *Archives of Children Medicine*. 1934; 37:597-606.
31. Fanconi G. The early infantile nephrotic-glycosurische dwarfism with hypophosphatemic rickets. *Yearbook of Pediatrics*. 1936; 47:299-318
32. Schneider JA, Rosenbloom FM, Bradley KH, and Seegmiller JE. Increased free-cystine content of fibroblasts cultured from patients with cystinosis. *Biochem Biophys Res Commun*. 1967; 29:527-531.
33. Schneider JA, Bradley K, and Seegmiller JE. Increased cystine in leukocytes from individuals homozygous and heterozygous for cystinosis. *Science*. 1967; 157:1321-1322.
34. Terec TM, Friedman AB, Kent LM, and Fetterman GH. Cystinosis and proximal tubular nephropathy in siblings: progressive development of the physiological and anatomical lesion. *Am. J. Dis. Child*. 1970; 119:481-487.
35. Elenberg E. Cystinosis. 2013 [Online] [American Society of Nephrology](#) and [American Society of Pediatric Nephrology](#). Available from: <http://emedicine.medscape.com>. [Accessed 15 June 2013]

36. Broyer M, Tete MJ, Gubler MC. Late Symptoms in Infantile Cystinosis. *Pediatric Nephrology*. 1987; 1(3):519-524.
37. Devilliers P, Gutta R, and Szymela VF. Cystinosis, Fanconi syndrome, and odontogenic cysts. *Oral Surg Oral Med Oral Pathol Oral Radiol Endo*. 2008; 106:866-871
38. Chol M, Nevo N, Cherqui S, Antignac C, and Rustin P. Glutathione precursors replenish decreased glutathione pool in cystinotic cell lines. *Biochemical and Biophysical Research Communications*. 2004; 324:231-235
39. Orson WM, Donald W, Baum S, and Baum M. The Fanconi Syndrome. *Genetic Diseases of the Kidney*. 2009; 6:171-197
40. Syres K, Harrison F, Tadlock M, Jester JV, Simpson J, Roy S, *et al*. Successful treatment of the murine model of cystinosis using bone marrow cell transplantation. *Blood*. 2009; 114(12):2542-2552.
41. Gahl WA, Balog JZ, and Kleta R. Nephropathic Cystinosis in Adults: Natural History and Effects of Oral Cysteamine Therapy. *Annals of Internal Medicine*. 2007; 147(4):242-250.
42. Pisoni RL, Park GY, Velilla VQ, and Thoene JG. Detection and characterisation of a transport system mediating cysteamine entry into human fibroblast lysosomes. Specificity for aminoethylsulfide derivatives. *Journal of Biological Chemistry*. 1995; 270(3):1179-1184.
43. Holtzman Eric. *Lysosomes*. 1989. Plenum Press, New York
44. Ruivo R, Anne C, Sagne C, and Gasnier B. Molecular and cellular basis of lysosomal transmembrane protein dysfunction. *Biochimica et Biophysica Acta*. 2009; 1793(4):636-649
45. The Worlds of David Darling. Lysosome. [Online]. Encyclopedia of Science. Available from: <http://www.daviddarling.info/encyclopedia/L/lysosome.html> [Accessed 20 June 2013]
46. Anderson R. *Improving cystinosis treatments*. [online] Reading: Cystinosis Foundation UK. Available from: <http://www.cystinosis.org.uk/techArticle.php?id=2> [Accessed 18 February 2012]

47. Cystinosis Research Network. *About Cystinosis*. [Homepage on the Internet]. Illinois, USA: Cystinosis Research Network Available from: <http://www.cystinosis.org/aboutcystinosis.html> [Accessed 17 February 2012]
48. Anikster Y, Lucero C, Touchman JW, Huizing M, Mcdowell G, Shoteleersuk V, *et al*. Identification and detection of the common 65-kb deletion breakpoint in the nephropathic cystinosis gene (CTNS). *Mol Genet Metab*. 1999; 66:111-116.
49. Kalatzis V, Cherqui S, Jean G, Cordier B, Cochat B, Broyer M, and Antignac C. Characterisation of a putative founder mutation that accounts for the high incidence of cystinosis in Britany. *Journal of the American Society on Nephrology*. 2001; 12(10):2170-2174.
50. Gahl WA, Thoene J, Schneider JA. Cystinosis: a disorder of lysosomal membrane transport. In: Scriver CR, Beaudet AL, Sly WS, Valle D, Childs B, Kinzler KW, and Vogelstein B. (eds) *The metabolic and molecular basis of inherited disease*, Eighth edition. McGraw-Hill Companies, Inc, pp. 5085-5108
51. Cairns D, Anderson RJ, Coulthard M, and Terry J. Cystinosis and its Treatment. *Pharmaceutical Journal*. 2002; 269:615-616.
52. Nesterova G, and Gahl W. Nephropathic cystinosis: late complications of a multisystemic disease. *Pediatr Nephrol*. 2008; 23(6):863-78
53. Markello T.C, Bernadini I.M, and Gahl W.A. Improved renal function in children with cystinosis treated with cysteamine. *New England Journal of Medicine*. 1993; 328(16):1157-1162
54. Krasnewich DM, and Gahl WA. Cystinosis: a treatable lysosomal storage disease. *Endocrinologist*. 1991; 1:111-118.
55. Wilmer MJ, Schoeber JP, van den Heuvel LP, and Levtchenko EN. Cystinosis: practical tools for diagnosis and treatment. *Pediatric Nephrol*. 2011; 26(2):205-215.
56. Langman CB, Moore ES, Thoene JG, and Schneider JA. Renal failure in a sibship with late-onset cystinosis. *J Pediatr*. 1985; 107):755-756
57. Tarranta A, Palma A, and Emma F. Pathogenesis of cell dysfunction in nephropathic cystinosis. *Advances in Metabolic and Kidney Diseases. Paediatrics and Child Health*. 2008; 18:S51-S53

58. Schneider JA, Wong V, Bradley K, Seegmiller JE. Biochemical comparisons of the adult and childhood forms of cystinosis. *N Engl J Med.* 1968; 279:1253–1257
59. Anikster Y, Lucero C, Guo J, Huizing M, Shotelersuk V, Bernardini I, McDowell G, Iwata F, Kaiser-Kupfer MI, Jaffe R, Thoene J, Schneider JA, Gahl WA. Ocular nonnephropathic cystinosis: clinical, biochemical, and molecular correlations. *Pediatr Res.* 2000; 47:17–23
60. Winkler L, Offner G, Krull F, and Brodehl J. Growth and pubertal development in nephropathic cystinosis. *Pediatric Nephrol.* 1993; 152:244-249
61. Cetinkaya I, Schlatter E, Hirsch JR, Herter P, Harms E, and Kleta R. Inhibition of Na⁺ - dependent transporters in cystine-loaded human renal cells: electrophysiological studies on the Fanconi syndrome of cystinosis. *J Am Soc Nephrol.* 2002; 13:2085-2093.
62. Manz F, and Gretz N. Progression of chronic renal failure in a historical group of patients with nephropathic cystinosis. European Collaborative Study on Cystinosis. *Pediatric Nephrol.* 1994; 8:466-471.
63. Baum M. The Fanconi syndrome of cystinosis: insights into the pathophysiology. *Pediatric Nephrol.* 1998; 12:492-497
64. Brodehl J, Hagge W, Gellissen K. Changes in kidney function in cystinosis. I. Inulin, PAH and electrolyte clearance in various stages of the disease. *Ann Paediatr.* 1965; 205:131–154
65. Levtchenko E, Monnens L. Development of Fanconi syndrome during infancy in a patient with cystinosis. *Acta Paediatr.* 2006; 95:379–380
66. Roth KS, Foreman JW, and Segal S. The Fanconi syndrome and mechanisms of tubular transport dysfunction. *Kidney Int.* 1981; 20:705-716.
67. Saleem MA, Milford DV, Alton H, Chapman S, Winterborn MH. Hypercalciuria and ultrasound abnormalities in children with cystinosis. *Pediatr Nephrol.* 1995; 9:45–47
68. Theodoropoulos DS, Hhawker TH, Heinrichs C, and Gahl WA. Medullary nephrocalcinosis in nephropathic cystinosis. *Pediatric Nephrol.* 1995; 9:412-418.

69. Drube J, Schiffer E, Mischak H, Kemper MJ, Neuhaus T, Pape T et al. Urinary proteome pattern in children with renal Fanconi syndrome. *Nephrol Dial Transplant*. 2009; 24(7):2161-2169.
70. Wilmer MJ, Christensen EI, Heuvel LP, Monnens LA, and Levtchenko EN. Urinary protein excretion pattern and renal expression of megalin and cubilin in nephropathic cystinosis. *Am J Kidney Dis*. 2008; 51:893-903
71. Bernardini I, Rizzo WB, Dalakas, M, Bernar J, and Gahl WA. Plasma and muscle free carnitine deficiency due to renal Fanconi syndrome. *J Clin Invest*. 1985; 75:1124-1130.
72. Burki E. *Annales Paediatrici, Basel*. 1941; 156:324
73. Gahl WA, Kuehl EM, Iwata F, Lindblad A, and Kaiser-Kupfer MI. Corneal Crystals in Nephropathic Cystinosis: Natural History and Treatment with Cysteamine Eyedrops. *Molecular Genetics and Metabolism*. 2000; 71:100-120
74. Tsilou ET, Rubin BI, Reed GF, Iwata F, Gahl WA, and Kaiser-Kupfer MI. Age-related prevalence of anterior segment complications in patients with infantile nephropathic cystinosis. *Cornea*. 2002; 21(2):173-176
75. Kaiser-Kupfer M, Gazzo MA, Datiles MB, Caruson RC, Kuehl EM, and Gahl WA. A randomised placebo-controlled trial of cysteamine eye drops in nephropathic cystinosis. *Archives in Ophthalmology*. 1990; 108(5):689-693.
76. Wong V. Ocular manifestations in cystinosis. *Birth Defects*. 1976; 12:181-186
77. Dufier JL, Orssaud D, Dhermy P, Gubler MC, Gagnadoux MF, Kleinknecht C, and Broyer M. Ocular changes in some progressive hereditary nephropathies. *Paediatric Nephrology*. 1987; 1:525-530
78. Kaiser-Kupfer M, Caruson RC, Minkler DS, and Gahl WA. Long-term ocular manifestations in nephropathic cystinosis. *Archives in Ophthalmology*. 1986; 104(5):706-711
79. Gahl WA, Thoene JG, and Schneider JA. Medical progress. Cystinosis. *New England Journal of Medicine*. 2002; 2:111-347

80. kleta, R, and Gahl W.A. Cystinosis. [online] Seattle, WA:University of Washington. Available from: <http://www.genetest.org>. [Accessed 17 February 2012]
81. Genetics Home Reference, 2009. What conditions are related to the CTNS gene? [online] Bethesda, MA.: U.S National Library of Medicine. Available from: <http://www.ghr.nlm.nih.gov> [Accessed 20 February 2012]
82. Town M, Jean G, Cherqui S, Attard M, Forestier L, Whitmore SA, Callen DF, Gribouval O, Broyer M, Bates GP, van't Hoff W and Antignac C. A novel gene encoding an integral membrane protein is muted in nephropathic cystinosis. *Nat Genet.* 1998; 18:319-324
83. Attard M, Jean G, Forestier L, Cherqui S, van't Hoff W, Broyer M, Antignac C, and Town M. Severity of phenotype in cystinosis varies with mutations in the CTNS gene: predicted effect on the model of cystinosis. *Human Molecular Genetics.* 1999; 8:2507-2514
84. Town M, and Antignac C. Molecular characterization of CTNS deletions in nephropathic cystinosis: development of a PCR-based detection assay. *Am J Hum Gent.* 1999; 65:353-359
85. Shotelersuk V, Larson D, Anikster y, McDowell G, Lemons R, Bernardini I, Guo J, Thoene J, and Gahl WA. CTNS mutations in an American based population of cystinosis patients. *Am J Genet.* 1998; 63:1352-1362
86. Touchman JW, Anikster, Dietrich NL, Maduro VV, McDowell G, Shotelersuk V, Bouffard GG, Beckstrom-Sternberg SM, Gahl WA, and Green ED. The genomic region encompassing the nephropathic cystinosis gene (CTNS): complete sequencing of a 200-kb segment and discovery of a novel gene within the common cystinosis-causing deletion. *Genome Res.* 2000; 10(2):165:17
87. Rupar CA, Matsell D, Surry S, and Siu V. A G339R mutation in the CTNS gene is a common cause of nephropathic cystinosis in the south western Ontario Amish Mennonite population. *J Med Genet.* 2001; 38:615-616

88. US National Library of medicines. CTNS. [Homepage on the Internet]. USA: US Department of Health; 2008 [updated February 2008; cited 2011 May 2011]. [Available from]: <http://ghr.nlm.nih.gov/gene/CTNS>.
89. Mason S, Pepe G, Dall'Amico R, Tartaglia S, Casciani , Greco M, Bencivenga P, Murer L, Rizzoni G, Tenconi R, and Clementi M. Mutational spectrum of the CTNS gene in Italy. *European Journal of Human Genetics*. 2003; 11:503-508
90. Kelatzis V, and Antignac C. Cystinosis: from gene to disease. *Nephrol Dial Transplant*. 2002; 17:1883-1886
91. Orson WM, Donald W, Baum S, and Baum M. The Fanconi Syndrome. *Genetic Diseases of the Kidney*. 2009; 6:171-197
92. Bozdog S, Gumus K, Gumus O, and Unlu N. Formulation and in vitro evaluation of cysteamine hydrochloride viscous solutions for the treatment of corneal cystinosis. *European Journal of Pharmaceutics and Biopharmaceutics*. 2008; 70:260-269
93. Gahl WA. Early oral cysteamine therapy for nephropathic cystinosis. *European Journal of Pediatrics*. 2003; 162:S38-S41
94. Gahl WA, Reed GF, Thoene JG, Schulman JD, Rizzo WB, Jonas AJ, Denman DW, Schlesselman JJ, Corden BJ, and Schneider JA. Cysteamine Therapy for Children with Nephropathic Cystinosis. *New England Journal of Medicine*. 1987; 316(16):971-977
95. Baum M. The cellular basis of Fanconi syndrome. *Hosp Pract (Off Ed)*. 1993; 28(11):137-142, Review 147-148
96. Nesterova G, Gahl WA. Nephropathic cystinosis: late complications of a multicysteamine disease. *Pediatric Nephrol*. 2008; 23(6):863-867
97. Reznik VM et al., Treatment of Cystinosis with Cysteamine from Early Infancy. *Journal of Pediatrics*. 1991; 119(3):491-49
98. Wuhl E, Haffner D, Offner G, Broyer M, van't Hoff W, and Mehls O. European Study Group on Growth Hormone Treatment in Children with Nephropathic Cystinosis. Long term treatment with growth hormone in short children with nephropathic cystinosis. *J Pediatr*. 2001; 138:880-887

99. Besouw MT, Kremer JA, Janssen MC, and Leytchenko EN. Fertility status in male cystinosis patients treated with cysteamine. *Fertil Steril*. 2010; 93(6):1880-1883
100. Dohil R, Fidler M, Gangoiti JA, Kaskel F, Schneider JA, and Barshop BA. Twice-daily cysteamine bitartrate therapy for children with cystinosis. *The Journal of Pediatrics*. 2010; 156(1):71-75.
101. Orphan Europe 1997 European marketing Authorisation Cystagon. Available on line <http://www.orphan-europe.com> [Accessed 01 February 2012]
102. Smolin LA, and Schneider JA. Measurement of total plasma cysteamine using HPLC with electrochemical detection. *Analytical Biochemistry*. 1988; 168(2):374-379
103. Gahl WA, Tietze F, Butler JD, and Schulman JD. Cysteamine Depletes Cystinotic Leucocyte Granular Fractions of Cystine by the Mechanism of Disulphide Interchange. *Biochemistry Journal*. 1985; 228:545-550
104. Thoene JG, Oshima RG, Crawhall JC, Olson DL, and Schneider JA. Cystinosis. Intracellular Cystine Depletion by Amino thiols *In Vitro* and *In Vivo*. *Journal of Clinical Investigations*. 1976; 58(1):180-189
105. Kleta R, Gahl WA. Pharmacological treatment of nephropathic cystinosis with cysteamine. *Expert Opinion on Pharmacotherapy*. 2004; 5(11):2255-2262
106. Oberfield SE, Levine LS, Wellner D, Novogroder M, Laino P, and New MI. Ascorbic acid treatment in nephropathic cystinosis in identical twins. *Developmental Pharmacology Therapeutics*. 1981; 2(2):80-90
107. Schneider JA, Schlesselmann JJ, Mendoza SA, Orloff S, Thoene JG, Kroll WA, Godfrey AD, and Schuman JD. Ineffectiveness of ascorbic acid therapy in nephropathic cystinosis. *New England Journal of Medicine*. 1979; 300:756-759
108. Crawhall JC, Lietman PS, Schneider JA, and Seegmiller JE. Cystinosis plasma cystine and cysteine concentrations and the effect of D-penicillamine and dietary treatment. *American Journal of Medicine*. 1968; 44:330-339

109. Hambraeus L, and Brogger O. Penicillamine treatment of cystinosis. *Acta Paediatrics*. 1967; 56:243
110. Clayton BE, and Patrick AD. Used of dimercaprol or Penicillamine in the treatment of cystinosis. *Lancet*. 1961; 2:909
111. Brigger DP, Goldman H, and Scriver CR. The *in vivo* use of dithiothreitol in cystinosis. *Paediatric Research*. 1977; 11:124
112. Kleta R, Bernardini I, Ueda M, Varade, WS, Phornphutkul C, Krasnewich D, and Gahl WA. Long-term follow up of well treated nephropathic cystinosis patients. *J Pediatr*. 2004; 145:555-560
113. Cystinosis Research Network. About Cystinosis. Illinois, USA: Cystinosis Research Network. Available online: www.cystinosis.org/aboutcystinosis.html. [Accessed 20/5/09].
114. Gahl WA, Charnas L, Markello TC, Bernadini I, Ishak KG, and Dalakas MC. Parenchymal organ cystine depletion with long-term cysteamine therapy. *Biochem Med Metab*. 1992; 48:275-285
115. Kimonis VE, Troendle J, Rose SR, Yang ML, Markello TC and Gahl WA. Effects of early cysteamine therapy on thyroid function and growth in nephropathic cystinosis. *J Clin Endocrinol Metab*. 1995; 80:3257-3261
116. Bozdog S, Gumus K, Gumus O, and Unlu N. Formulation and *in vitro* evaluation of Cysteamine hydrochloride viscous solutions for the treatment of corneal cystinosis. *European Journal of Pharmaceutics and Biopharmaceutics*. 2008; 70(1):260-290
117. Choy YB, Park JH, and Prausnitz MR. Mucoadhesive microparticles engineered for ophthalmic drug delivery. *Journal of Physics and Chemistry of Solids*. 2008; 69:1533-1536.
118. Gahl WA, Kaiser-Kupfer MI, Fujikawa L, Kuwabara T, Jain S. Removal of Corneal Crystals by Topical Cysteamine in Nephropathic Cystinosis. *New England Journal of Medicine*. 1987; 316(13):775-779
119. Dufier JL. Ocular Changes in Long-Term Evolution of Infantile Cystinosis. *Ophthalmic Paediatric Genetics*. 1987; 8(2):131-137

120. Schneider JA, Fidler MC, Barshop BA, Deutsch R, Martin M, Dohil R et al. Pharmacokinetics of Cysteamine Bitartrate Following Gastrointestinal Infusion. *British Journal of Clinical Pharmacology*. 2006; 63(1):36-40
121. Dohil R, Newbury RO, Sellers ZM, Deutsch R, Schneider JA. The Evaluation and Treatment of Gastrointestinal Disease in Children with Cystinosis Receiving Cysteamine. *Journal of Pediatrics*. 2003; 143(2):224-230
122. Schneider, JA. Treatment of Cystinosis: Simple in Principle, Difficult in practice. *Journal of Pediatrics*. 2004;145(4):436-438
123. Yudkoff M, Foreman JW, Segal S. Effects of Cysteamine Therapy in Nephropathic Cystinosis. *New England Journal of Medicine*. 1981; 304(3):141-145
124. Wenner WJ, Murphy JL. The Effects of Cysteamine on the upper Gastrointestinal Tract of Children with Cystinosis. *Pediatric Nephrology*. 1997; 11(5):600-603.
125. Elenberg E. Feeding Problems in Cystinosis. *Pediatric Nephrology*. 1998; 12:365-370
126. Sonies BC, Ekman EF, Anderson HC, Adamson MD, Kaler SG, Markello TC, and Gahl WA. Swallowing Dysfunction in Nephropathic Cystinosis. *New England Journal of Medicine*. 1990; 323(9):565-570
127. Gahl WA. Coronary Artery and Other Vascular Calcifications in Patients with Cystinosis after Kidney Transplantation. *Clinical Journal of the American Society of Nephrology*. 2006; 1:555-562
128. Gahl WA, Tsilou E, Zhou m, Chan C-C, Sieving PC. Ophthalmic Manifestations and Histopathology of Infantile Nephropathic Cystinosis: Report of a Case and Review of the Literature. *Survey of Ophthalmology*. 2007; 52(1):97-105
129. Niemiec S, Ballantyne A, and, Trauner D. Cognition in Nephropathic Cystinosis: Pattern of Expression in Heterozygous Carriers. *J Med Genet*. 2012; 158A(8):1902-1908

130. Besouw MTP, Hulstijn-Dirkmaat G M, van der Rijken REA, Cornelissen EAM, van Dael CM, Vande Walle J, Lilien MR, and Levtchenko EN. Neurocognitive functioning in school-aged cystinosis patients. *J Inherit Metab.* 2010; 33(6): 787–793.
131. Ballantyne AO, Scarvie KM, and Trauner DA. Academic Achievement in Individuals With Infantile Nephropathic Cystinosis. *American Journal of Medical Genetics (Neuropsychiatric Genetics).* 1997; 74:157–161
132. Smolin LA, Clark KF, Gahl WA, Thoene JG, Schneider JA. A Comparison of the Effectiveness of Cysteamine and Phosphocysteamine in Elevating Plasma Cyseamine Concentration and Decreasing Leukocyte Free Cystine in Nephropathic Cystinosis. *Pediatric Research.* 1988; 23(6):616-620
133. Stella VJ, Charman WN, and Naringrekar VH. Prodrugs. Do they have advantages in clinical practice? *Drugs.* 1985; 29(5):455-73
134. Thomas, G. *Medicinal Chemistry. An introduction.* Second edition. 2007, London. John Wiley & Sons, Ltd
135. Stefano AD, Sozio P, and Cerasa LS. Antiparkinson prodrugs. *Molecules, Basel.* 2008; 13(1):46-68
136. Nolen H 3rd, Fedorak RN, and Friend DR. Budesonide-beta-D-glucuronide: a potential pro-drug for treatment of ulcerative colitis. *Journal of Pharmaceutical Sciences.* 1995; 84(6):677-81
137. Filho RP, Polli MC, Filho SB, Garcia M, and Ferreira EI. Prodrugs available on the Brazilian pharmaceutical market and their corresponding bioactivation pathways. *Braz. J. Pharm. Sci.* 2010; Vol.46
138. Kay G, McCaughan B, Warasiha, B, and Cairns D. The design, synthesis and biological evaluation of novel prodrugs for the treatment of cystinosis. *. Journal of Pharmacy and Pharmacology, Supplement.* 2007; 59(4):7
139. Omran Z, Kay G, Di Salvo A, Knott RM, and Cairns D. PEGylated derivatives of cystamine as enhanced treatments for nephropathic cystinosis. *Bioorganic & Medicinal Chemistry Letters.* 2011; 21(1):45-47

140. Omran Z, Moloney KA, Benylles A, Kay G, Knott RM, and Cairns D. Synthesis and in vitro evaluation of novel pro-drugs for the treatment of nephropathic cystinosis. *Bioorg Med Chem*. 2011; 19(11):3492-3496
141. Omran Z, Kay G, Hector EE, Knott RM, and Cairns D. Folate pro-drug of cystamine as an enhanced treatment for nephropathic cystinosis. *Bioorg Med Chem Lett*. 2011; 21:2502-2504
142. Anderson RJ, Cairns D, Cardwell WA, Case M, Groundwater PW, Hall AG, Hogarth L, Jones AL, Meth-Cohn O, and Suryadevara P. Design, Synthesis and Initial *in Vitro* Evaluation of Novel Prodrugs for the Treatment of Cystinosis. *Letters in Drug Design & Discovery*. 2006; 3(5):336-345
143. Cairns D, McCaughan B, Kay G, Knott RM. A Potential New Prodrug for the Treatment of Cystinosis: Design, synthesis and In-Vitro Evaluation. *Bioorganic & Medicinal Chemistry Letters*. 2008; 18(5):1716-1719
144. Bendel-Stenzel MR, Steinke J, Dohil R, Kim Y. Intravenous delivery of cysteamine for the treatment of cystinosis: association with hepatotoxicity. *Pediatric Nephrology*. 2008; 23:311-315
145. electronic Medicines Compendium (eMC). Cystagon 150mg hard capsules.[homepage on the Internet]. online: Datapharm CommunicationsLtd; 2008 [updated 16/4/08; cited 2010 29/9/10]. Available from: <http://www.medicines.org.uk/emc/medicine/>
146. Besouw M, Bowker R, Dutertre JP, MD, Emma F et al. Cysteamine Toxicity in Patients with Cystinosis. *The Journal of Pediatrics*. 2011
147. Amos J.Protective organ wash engineered. [homepage on the Internet]. London: BBC; 2010 [updated 15/9/10; cited 2010 15/9/10]. Available from: <http://www.bbc.co.uk/news/science-environment-11322197>. B60
148. Buchan BE, Kay G, Matthews KH, and Cairns D. Gel formulations for treatment of the ophthalmic complications in cystinosis. *International Journal of Pharmaceutics* . 2010; 392(1-2):192-197

149. Dohil R, Fidler M, Gangoiti JA, Kaskel F, Schneider JA, and Barshop BA. Twice-daily cysteamine bitartrate therapy for children with cystinosis. *J Pediatr.* 2010; 156:71-5
150. Belldina EB, Huang MY, Schneider JA, Brundage RC, and Tracy TS. Steady-state pharmacokinetics and pharmacodynamics of cysteamine bitartrate in paediatric nephropathic cystinosis patients. *Br J Clin Pharmacol.* 2003; 56:520-525
151. Fidler MC, Barshop BA, Gangoiti JA, Deutsch R, Martin M, Schneider JA, and Dohil R. Pharmacokinetics of cysteamine bitartrate following gastrointestinal infusion. *Br J Clin Pharmacol.* 2007; 63:36-40
152. Langman CB, Greenbaum LA, Sarwal M et al. Effectiveness on White Blood Cell Cystine Levels and Comparison of Safety. *Clin J Am Soc Nephrol.* 2013; 7:1112-1120
153. Jones W, and Trask A.V. Crystal Engineering of organic co-crystals by solid state grinding approach. *Topics in Current Chemistry.* 2005; 254:41-70
154. Vishweshwar P, McMahon JA, Bis JA, and Zaworotko MJ. Pharmaceutical Co-Crystals. *Journal of Pharmaceutical Sciences.* 2006; 95:499-516
155. Shan, N. and Zaworotko, M. The role of co-crystals in Pharmaceutical Science. *Drug Discover Today.* 2008; 13:440-446
156. Brada, D. Crystal Engineering, Where from? Where to? *Chemical Communications.* 2003:2751-2754
157. Desiraju, G. Crystal Engineering: Outlook and prospects. *Current Science.* 2001; 81:1038-1042
158. Desiraju, G. Crystals and co-crystals. *CrystEngComm.* 2003; 5:466-467
159. Attwood, D. and Florence, A. Physical Pharmacy. London: *Pharmaceutical Press*; 2008
160. Grepioni F. Themed issue: Polymorphism and crystal forms. *New J. Chem.* 2008; 32:1657-1658

161. Desiraju, G. Supramolecular Synthrons in Crystal Engineering. *Angewandte Chemie International Edition*. 1995; 34:2311-2327
162. Blagden N, de Matas M, Gavan PT, and York P. Crystal Engineering of active pharmaceutical ingredients to improve solubility and dissolution rate. *Advanced Drug Delivery Reviews*. 2007; 59(7):617-630
163. Childs S, Stahly G, and Park A. The salt-co-crystal Continuum: The influence of Crystal Structure on Ionisation State. *Molecular Pharmaceutics*. 2007; 4(3):323-338
164. Morissette S, Almarsson O, Peterson M, Remenar J, Read M, and Lemmo A. High-throughput crystallization: polymorphs, salts, co-crystals and solvate of pharmaceutical solids. *Advanced Drug Delivery Reviews*. 2003; 56:275-300.
165. Rodriguez-Hornedo N. Co-crystals: Molecular Design of Pharmaceutical Materials. *Molecular Pharmaceutics*. 2007; 4(3):299-300
166. Peresyphkin A, Variankavval N, Fertila R, Wenslow R, Smitrovich J, and Thompson K. Discovery of a Stable Molecular Complex of an API with HCL: The Long Journey to a Conventional Salt. *Journal of Pharmaceutical Sciences*. 2008; 29(9):3721-3726
167. Infantes L, Fabian L, and Motherwell W. Organic Crystal Hydrates: what are the important factors for formation. *CrystEngComm*. 2007; 9:65-71
168. Friscia, T. and Jones, W. Co-crystal architecture and properties: Design and building of chiral and racemic structures by solid-solid reactions. *Fraday Discussions*. 2007; 136:167-178
169. Jones, W. et al., Pharmaceutical Co-crystals: An Emerging Approach to Physical Property Enhancement. *MRS Bulletin*. 2006; 31:875-879.
170. Bhatt PM, Azim Y, Thakur ST, and Desiraju GR. Co-Crystals of the Anti-HIV Drugs Lamivudine and Zidovudine. *Cryst. Growth Des*. 2009; 9 (2):951-957
171. Liao X, Gautam M, Andreas Grill A, and Zhu HJ. Effect of Position Isomerism on the Formation and Physicochemical Properties of Pharmaceutical Co-Crystals. *Journal of Pharmaceutical Sciences*. 2009; 99(1):246-254

172. Mirza S, Heinnamaki J, Inna Miroshnyk I, and Yliruusi J. Co-Crystals: An emerging approach to improve properties of pharmaceutical solids. *European Journal of Pharmaceutical Sciences*. 2008; 34(1):S16-S17
173. Almarsson, O and Zaworotko, M. Crystal engineering of the composition of pharmaceutical phases. Do pharmaceutical co-crystals represent a new path to improve medicines? *Chemical Communications*. 2004; 17:1889-3645
174. Desiraju, G. Supramolecular Synthrons in Crystal Engineering. *Angewandte Chemie International Edition*. 1995; 34:2311-2327
175. Brada D and Grepioni F. Making crystals from crystals: a green route to crystal engineering and polymorphism. *Chemical Communications*. 2005; 29:3636-3645
176. EPSRC National X-Ray Crystallography Service, Department of Chemistry. Southampton University
177. Farrugia L J. *J. Appl. Cryst.* 1999; 32:837-838
178. Marvin Sketch [structure drawing tool] Available from: <http://www.chemaxon.com/products/marvin/marvinsketch/> [Accessed 13 February 2012]
179. Siuzdak G. 1996. Ion samples and ion introduction. In: G. Siuzdak. Mass Spectrometry and Biotechnology. La Jolla: *Academic Press*
180. Girgenti E, Ricoux R, and Mahy JP. Design and synthesis of a Mn(III)-porphyrin steroid conjugate used as a new cleavage affinity label: on the road to semi-synthetic catalytic antibodies. *Tetrahedron*. 2004; 60:10049-10058.
181. Supplementary Material (ESI) for Chemical Communications. The Royal Society of Chemistry 2011.
182. Tripathi A, Parmar D, Patel U, Patel G, Daslaniya d, and Bhimani B. Taste Masking: A Novel Approach for Bitter and Obnoxious Drugs. *Journal of pharmaceutical science and bioscientific research (JPSBR)*. 2011; 1(3):136-142

183. Greenwald R. B, Zhao, H Yang K, Reddy P, and Martinez A. A New Aliphatic Amino Prodrug System for the Delivery of Small Molecules and Proteins Utilizing Novel PEG Derivatives. *J. Med. Chem.* 2004; 47(3):726-734.
184. Braithwaite A, and Smith FJ. 1994. Plane Chromatography. In: A.Braithwaite, and FJ. Smith. *Chromatographic Methods*. 4th Edition. London: Chapman and Hall. pp. 24-45
185. Nicolas FL, and Gagnieu CH. Denatured thiolated collagen. *Biomaterials*. 1997; 18:807-813
186. D. McNaught and A. Wilkinson. IUPAC. Compendium of Chemical Terminology, 2nd ed. (the "Gold Book") Available from: <http://goldbook.iupac.org/A00072.html> [Accessed 02 February 2012]
187. Montabetti C.A.G.N and Falque V. Amide bond formation and peptide coupling. *Tetrahedron*. 2005; 61:10827-10852
188. Han SY, and Kim YA. Recent development of the peptide coupling reagents in organic synthesis. *Tetrahedron*. 2004;60:2447-2467
189. Bailey, P.D. 1990. An introduction to peptide chemistry. West Sussex: Wiley & Sons. pp. 125
190. Joullie MM, and Lassen KM. Evolution of amide bond formation. *ARKIVOC*. 2010;(viii):189-250.
191. Antonkine ML, Koay MS, Epel B, Breitenstein C, Gopta O, Gartner W, Bill E, and Lubitz W. Synthesis and characterisation of *de novo* designed peptides modelling the binding sites of [4Fe-4S] clusters in photosystem I. *Biocimica et Biophysica Acta (BBA) – Bioenergetics*. 2009; 1787(8):995-1008.
192. Benylles A, Cairns D, Cox PJ and Kay G. Three salts from the reactions of cysteamine and cystamine with L-(+)-tartaric acid. *Acta Crystallographica Section C, Crystal Structure Communications*. 2013; 69(6):658-664
193. Bernar J, Tietze F, Kohn LD, Bernardini I, Harper GS, Grollman EF, and Gahl WA. Characteristics of a Lysosomal Membrane Transport System for Tyrosine and Other Neutral Amino Acids in Rats Thyroid Cells. *The Journal of Biological Chemistry*. 1986; 261(36):17107-17112

Publications and Presentations

Publications

Cairns D, Benylles A, McCaughan B and Kay G. "Molecular Modelling of the Interactions between Cysteamine and Cystamine pro-drugs and β Cyclodextrin" *J. Pharm. Pharmacol.* 2007, Suppl 133.

Omran Z, Moloney KA, Benylles A, Kay G, Knott RM, and Cairns D. Synthesis and in vitro evaluation of novel pro-drugs for the treatment of nephropathic cystinosis. *Bioorg Med Chem.* 2011; 19(11):3492-3496

Benylles A, Cairns D, Cox PJ and Kay G. Three salts from the reactions of cysteamine and cystamine with L-(+)-tartaric acid. *Acta Crystallographica Section C, Crystal Structure Communications.* 2013; 69(6):658-664

Conference Proceedings

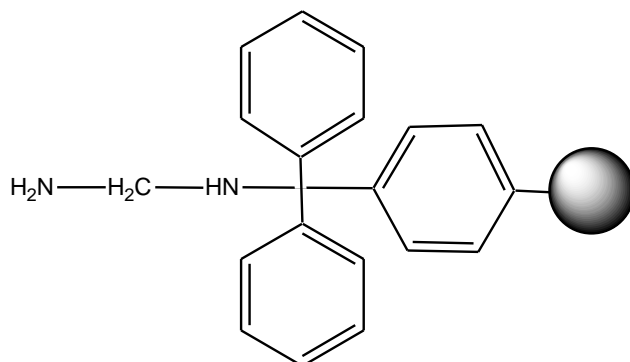
Seventh International Cystinosis Conference - Paris 2012 – Synthesis and in vitro evaluation of novel pro-drugs for the treatment of nephropathic cystinosis. Poster.

Fourth UKPharmSci conference – Edinburgh 2013 – Synthesis and in vitro evaluation of novel pro-drugs for the treatment of nephropathic cystinosis. Poster.

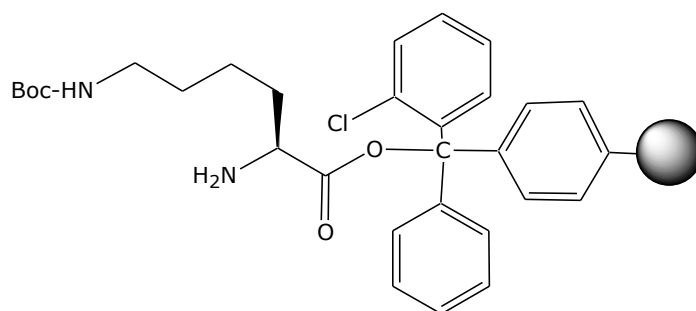
APPENDICES

Appendix 1

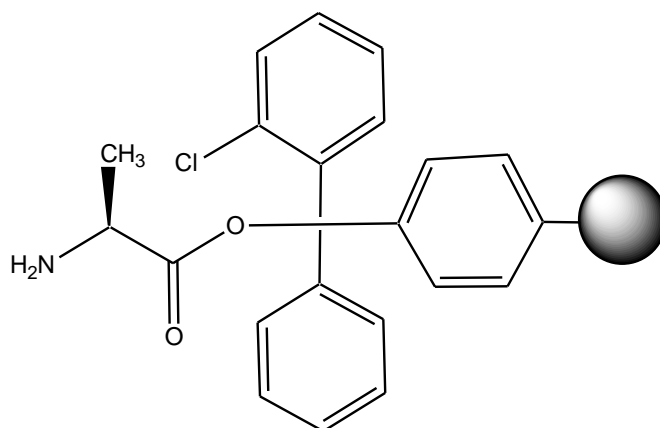
STRUCTURE LIBRARY



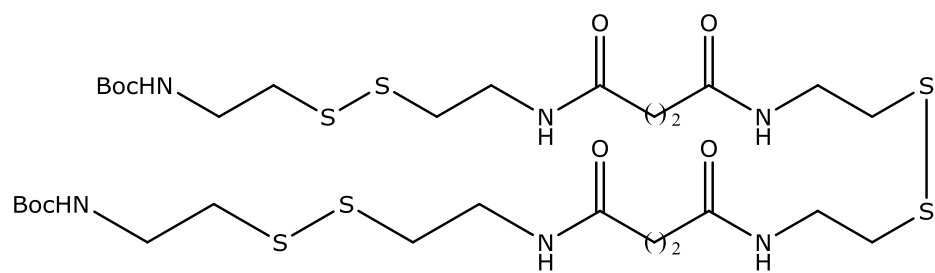
1, 3-Diaminopropane trityl resin (DAP)



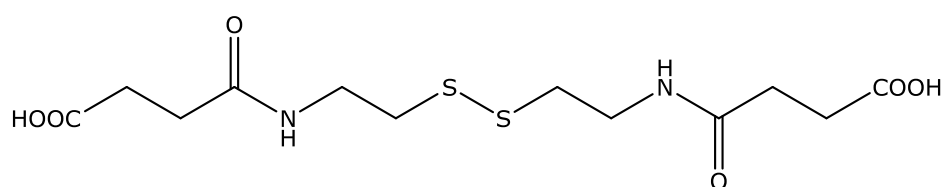
H-Lys(Boc)-2-Cl-trt resin



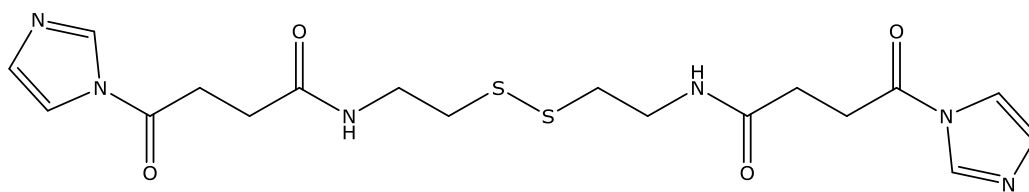
H-Ala-2 Cl-trt resin



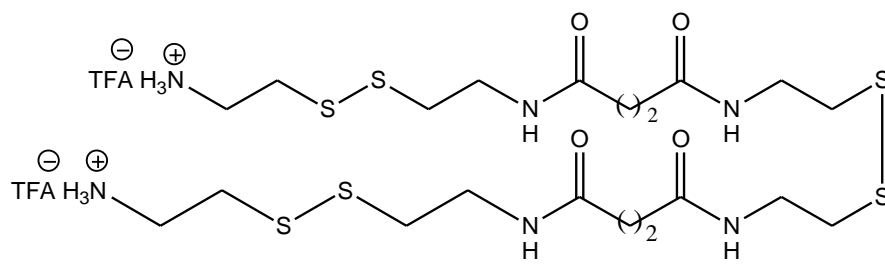
1



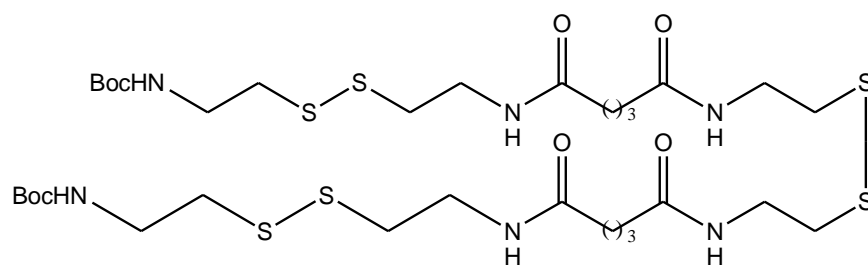
2



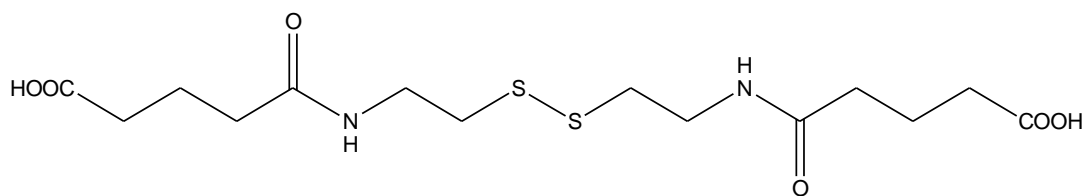
3



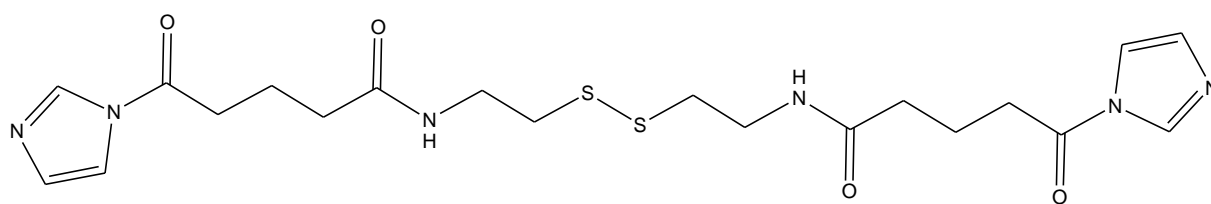
4



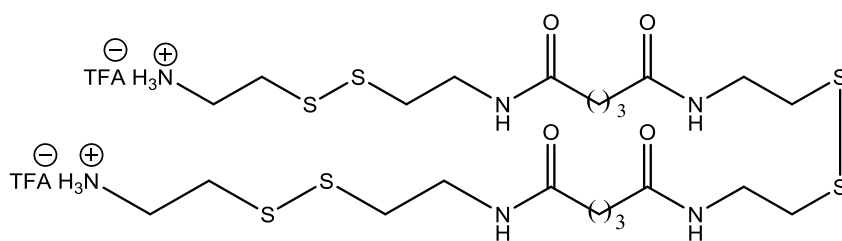
5



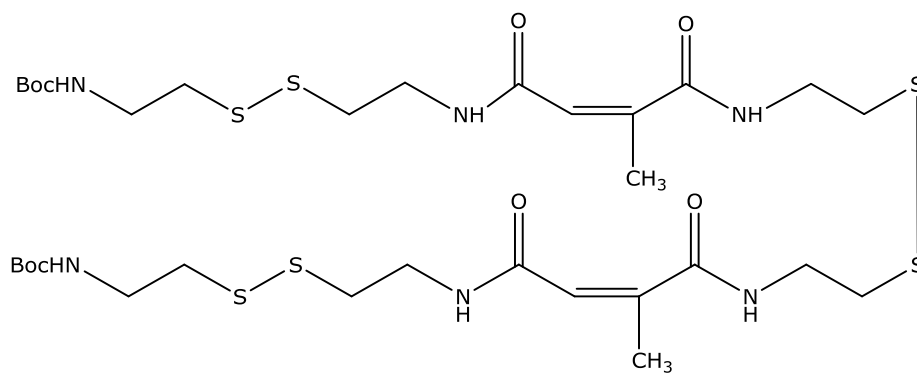
6



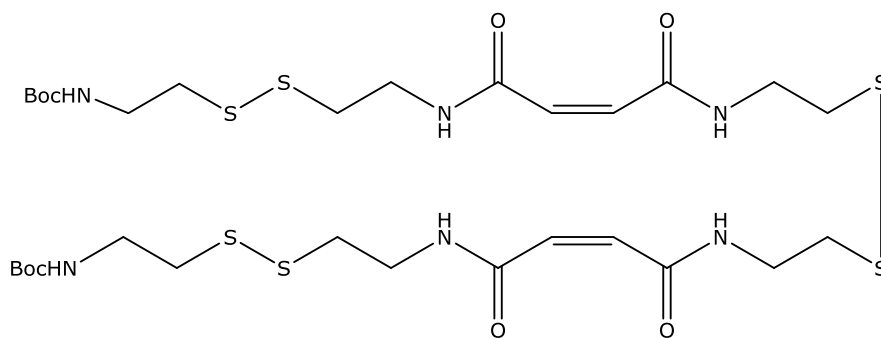
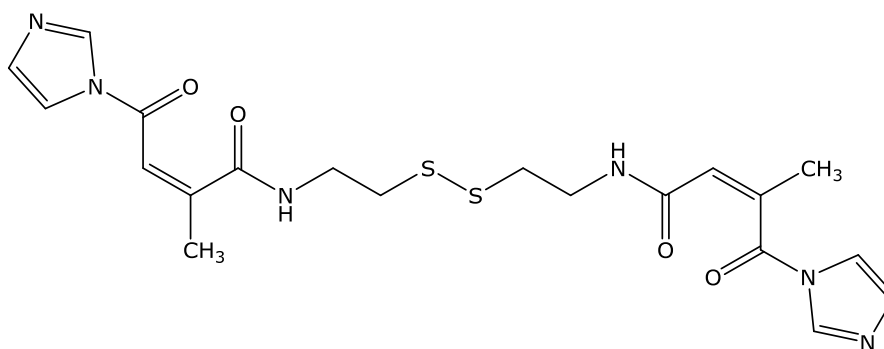
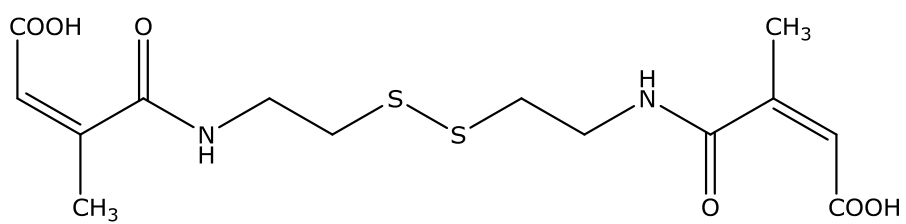
7

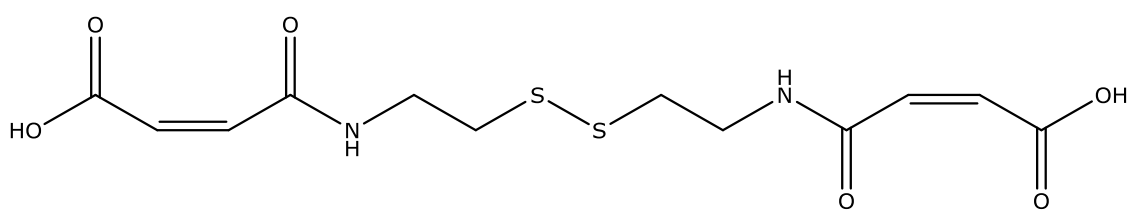


8

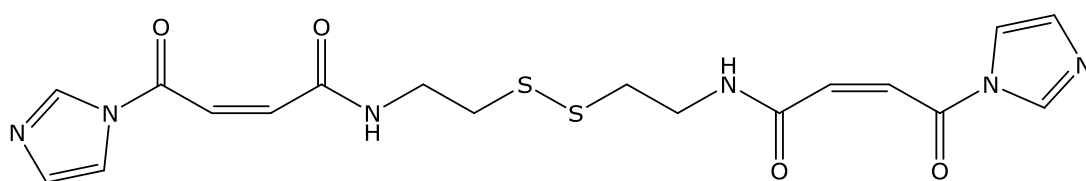


9

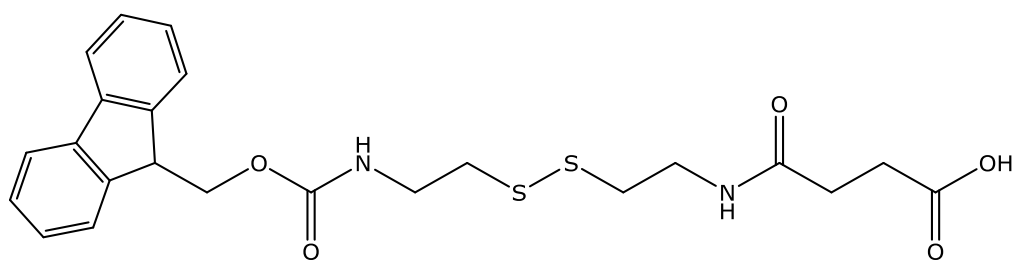




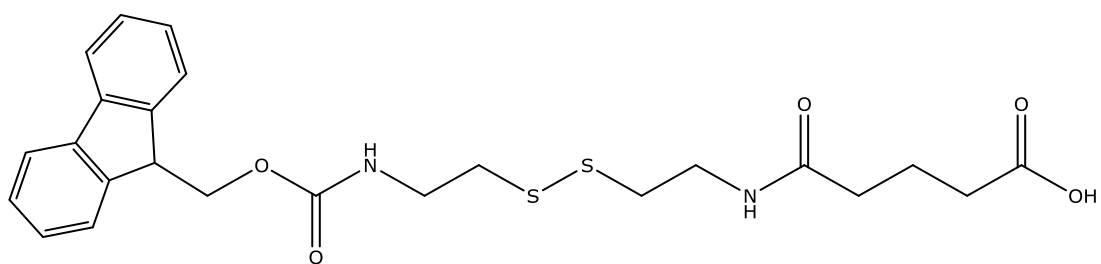
13



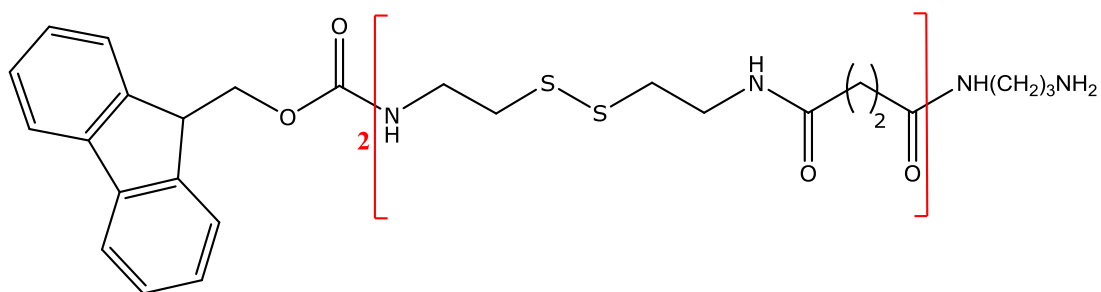
14



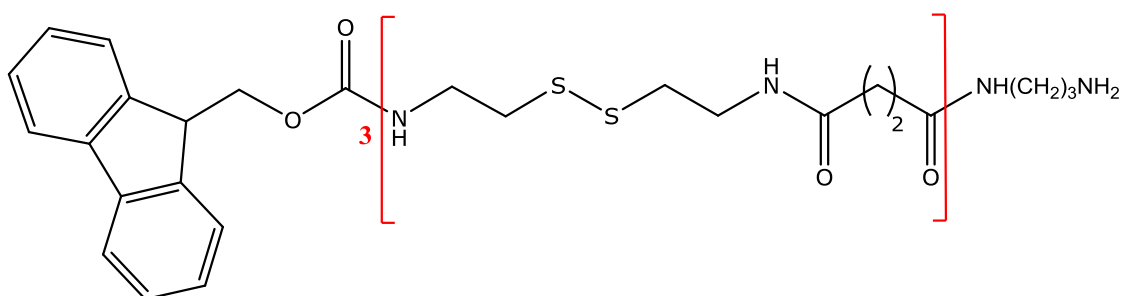
15



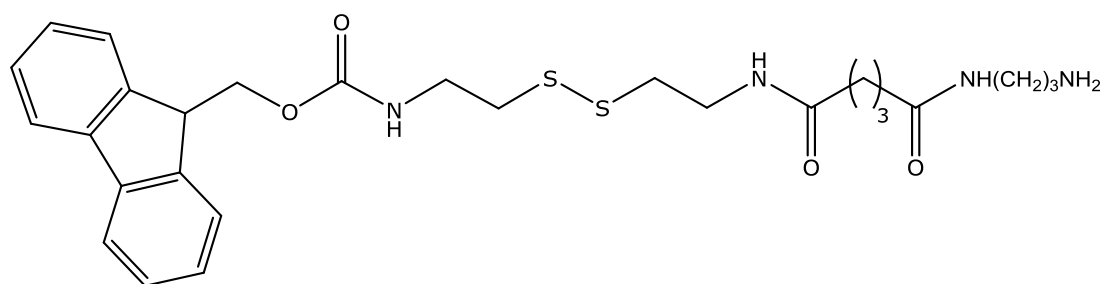
16



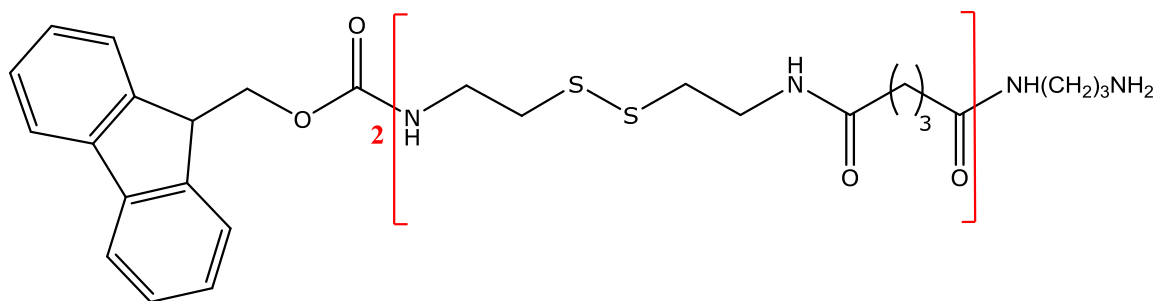
17



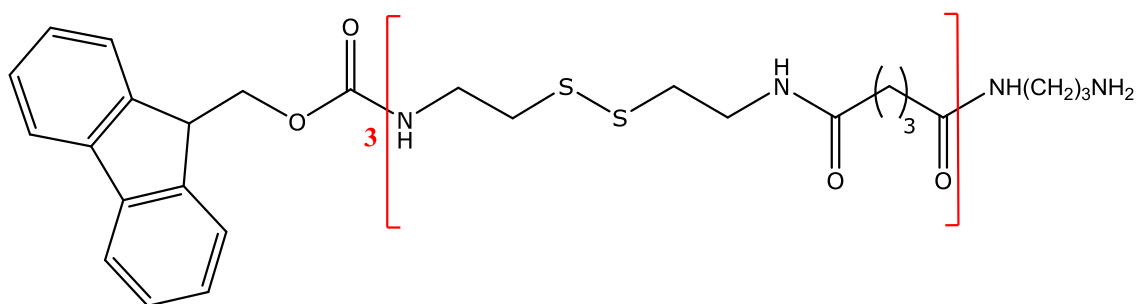
18



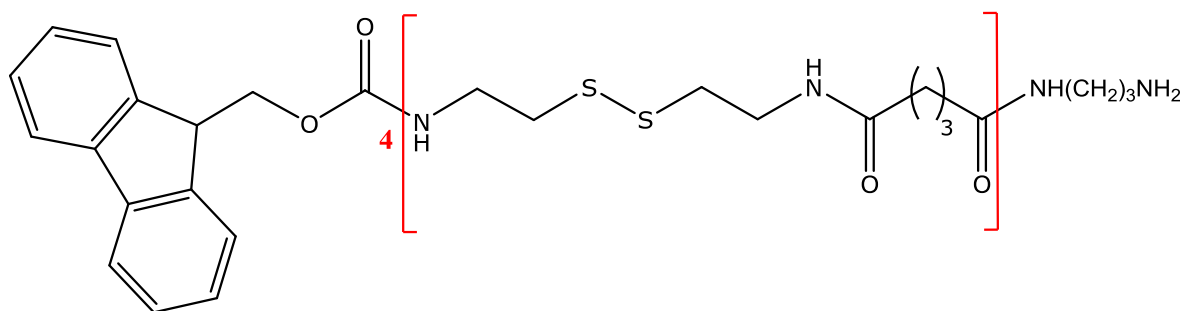
19



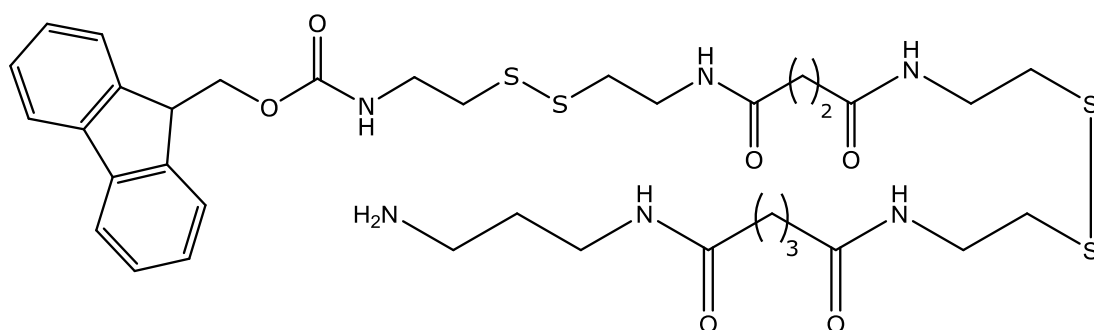
20



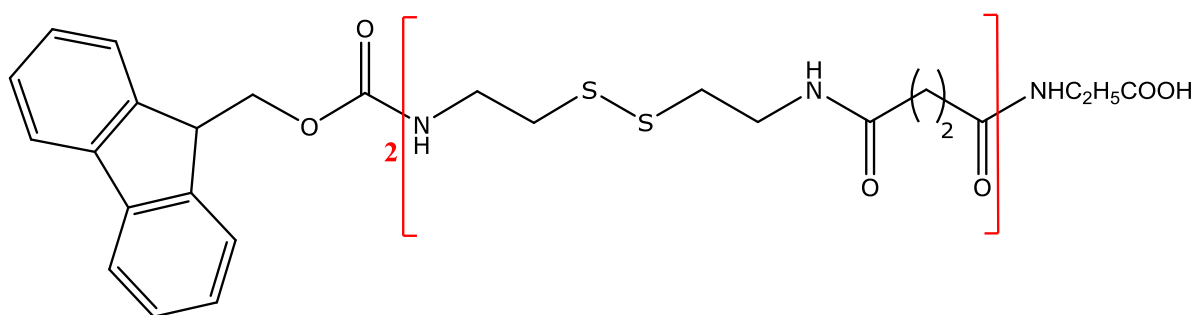
21



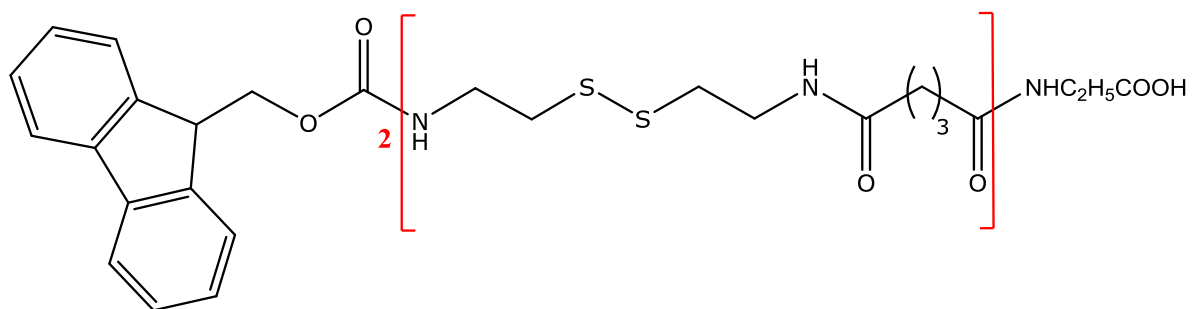
22



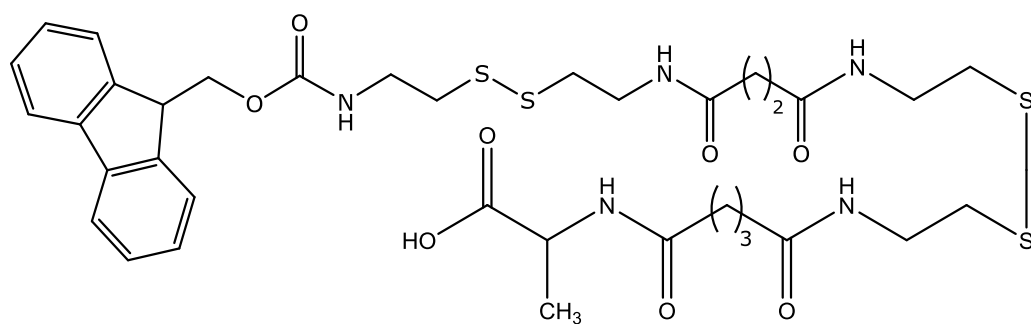
23



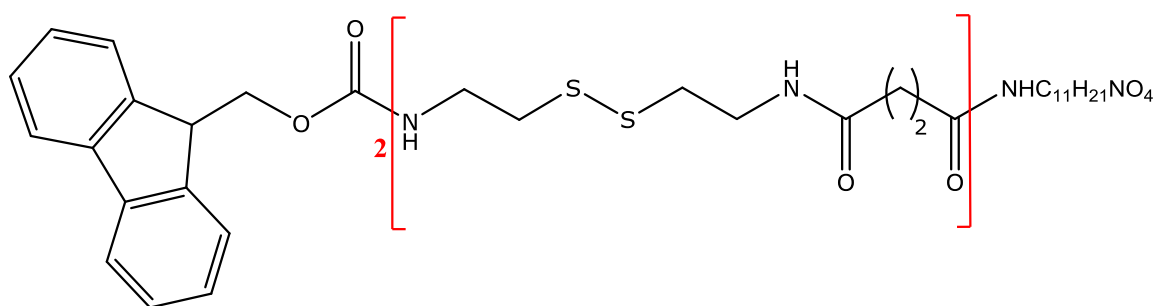
24



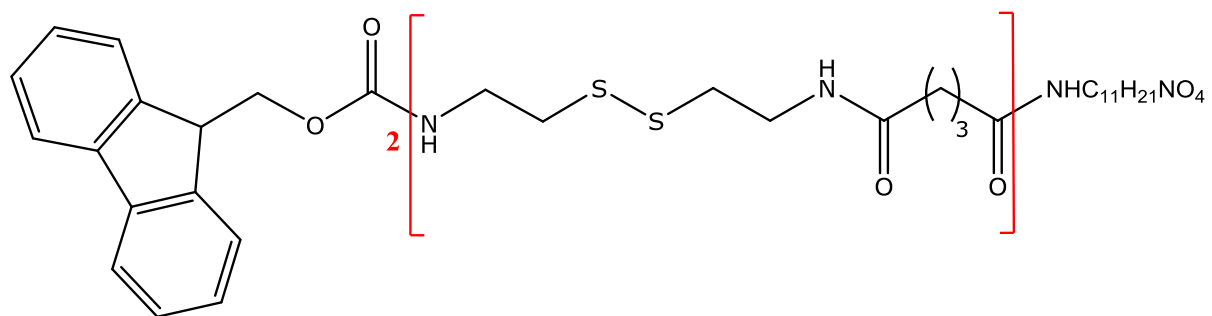
25



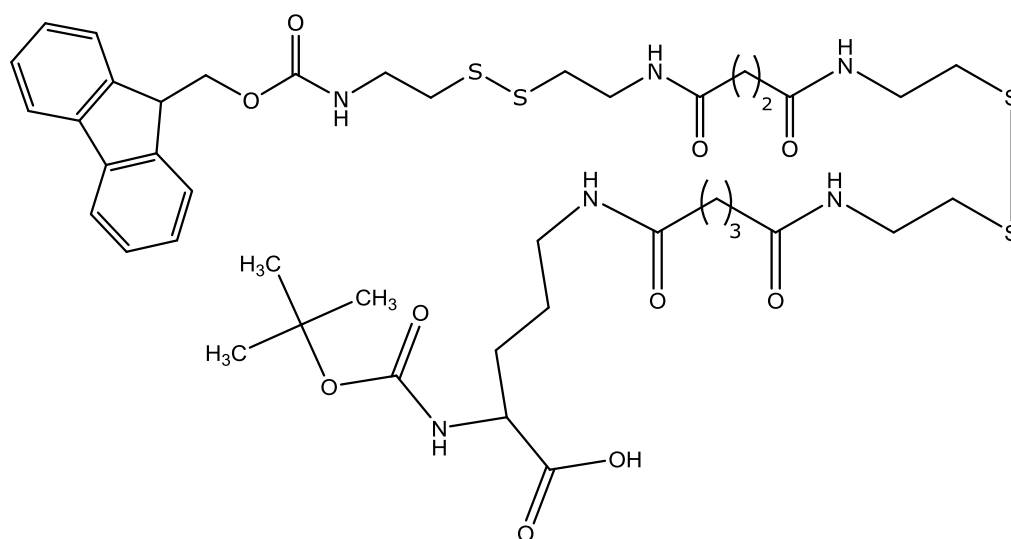
26



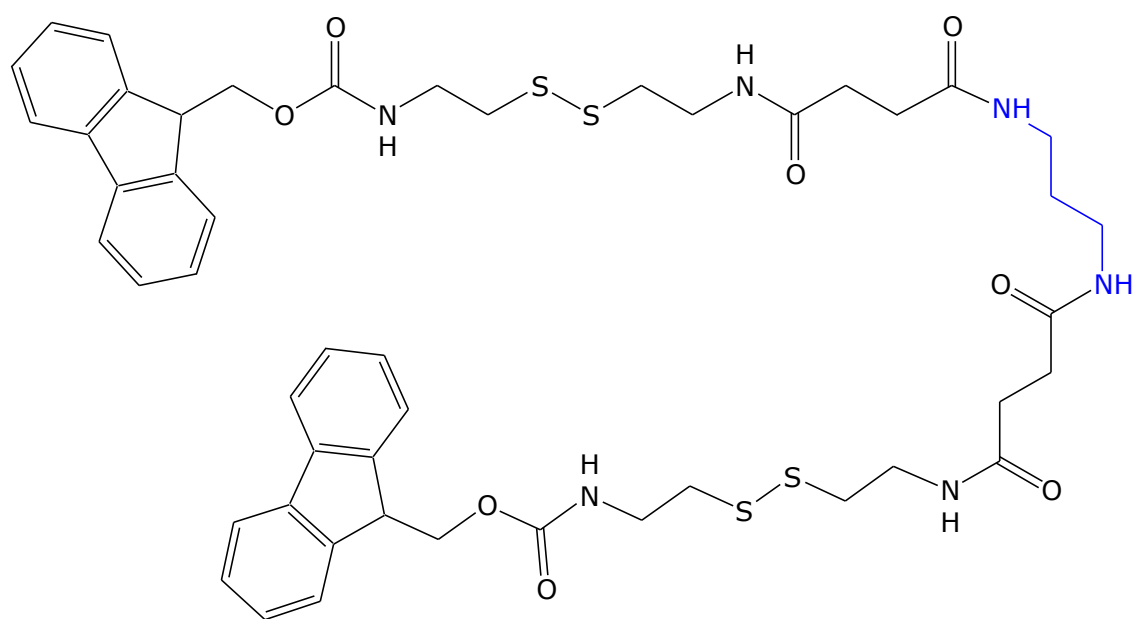
27



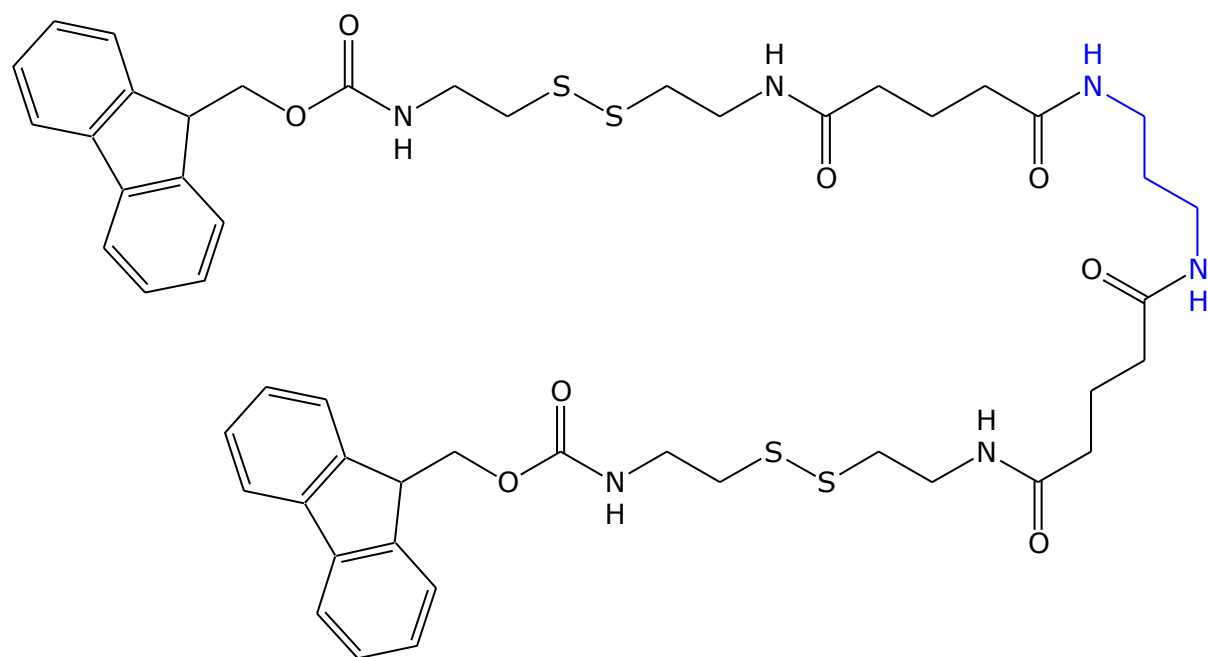
28



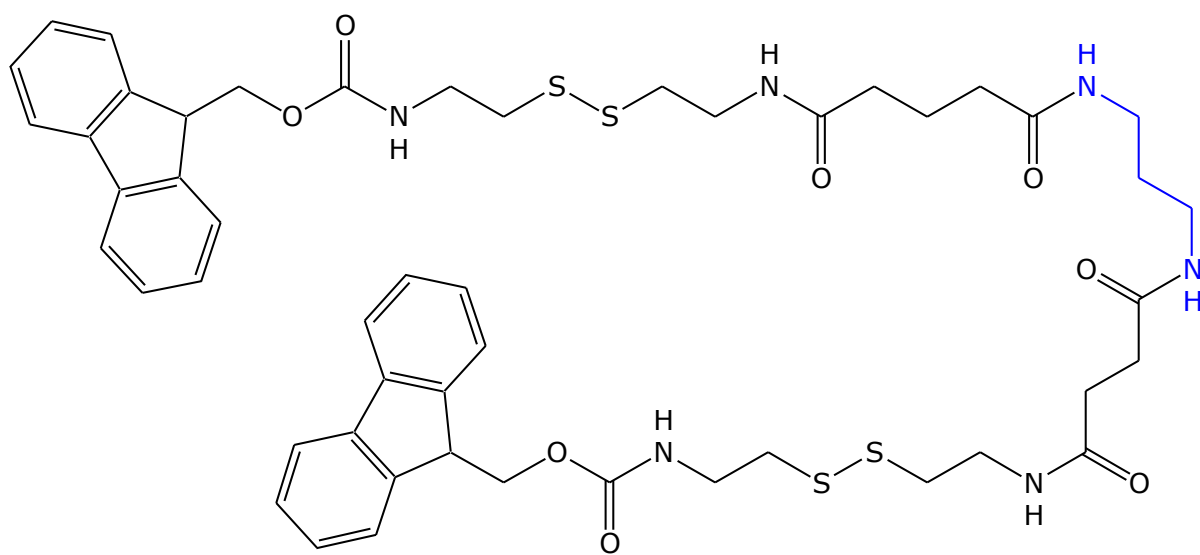
29



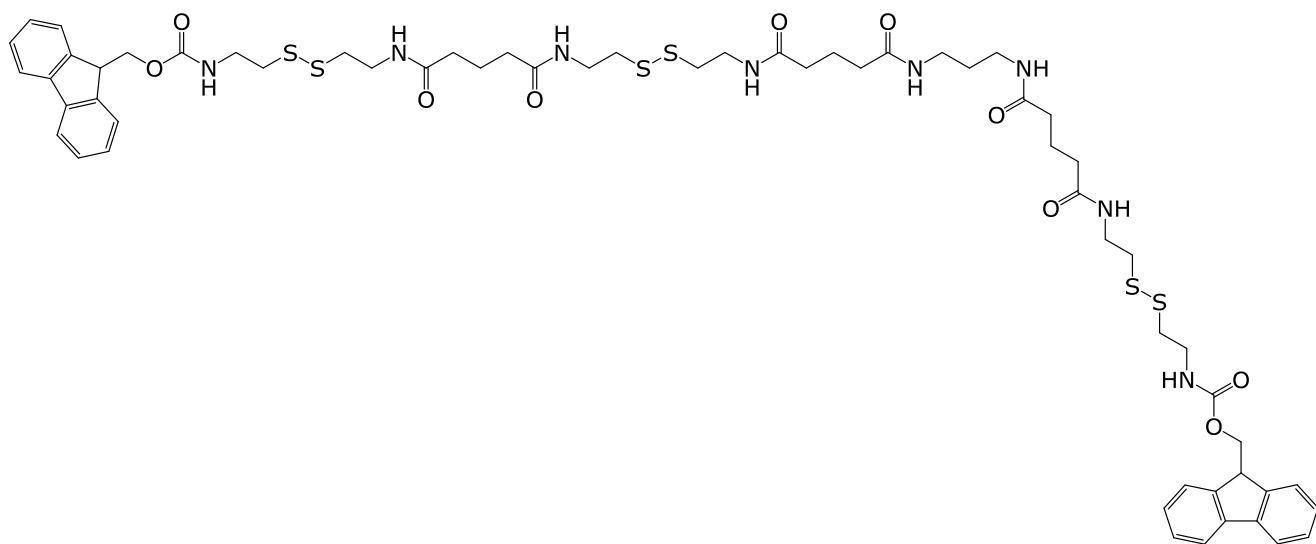
30



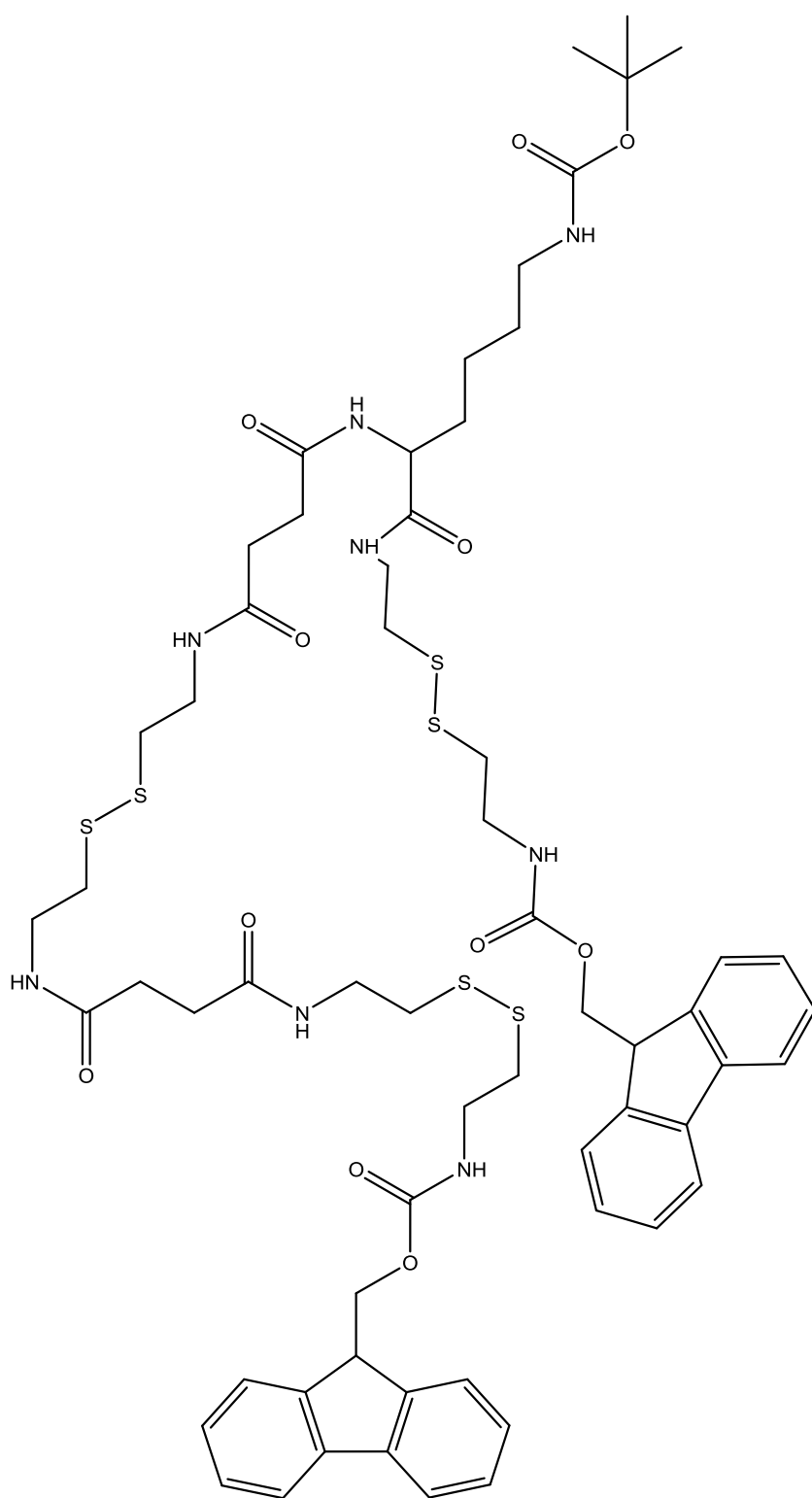
31



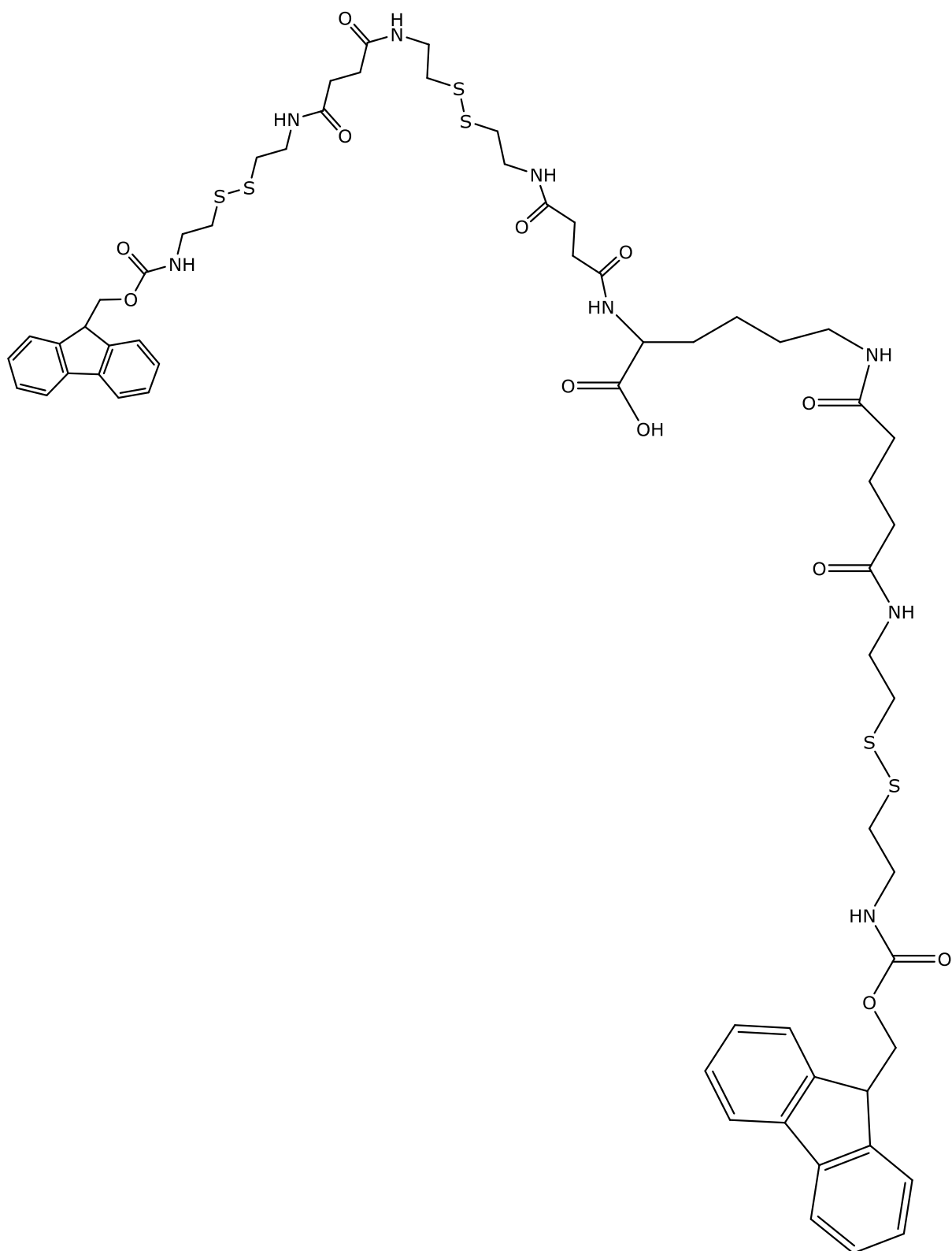
32



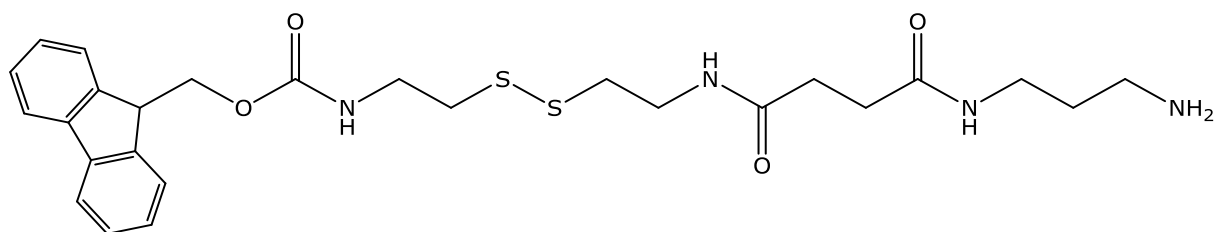
33



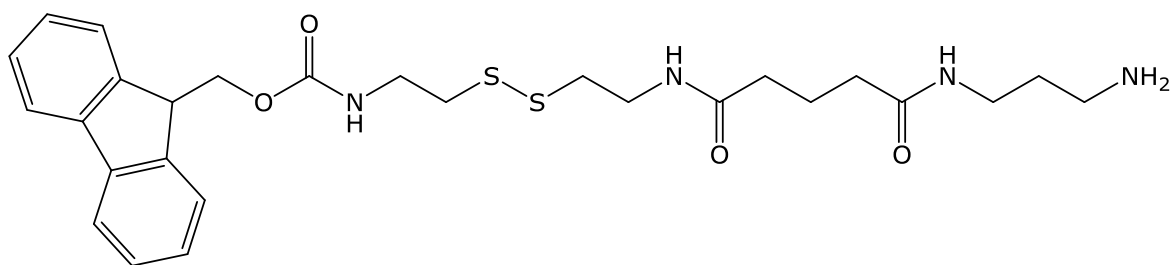
34



35



36



37

Appendix 2

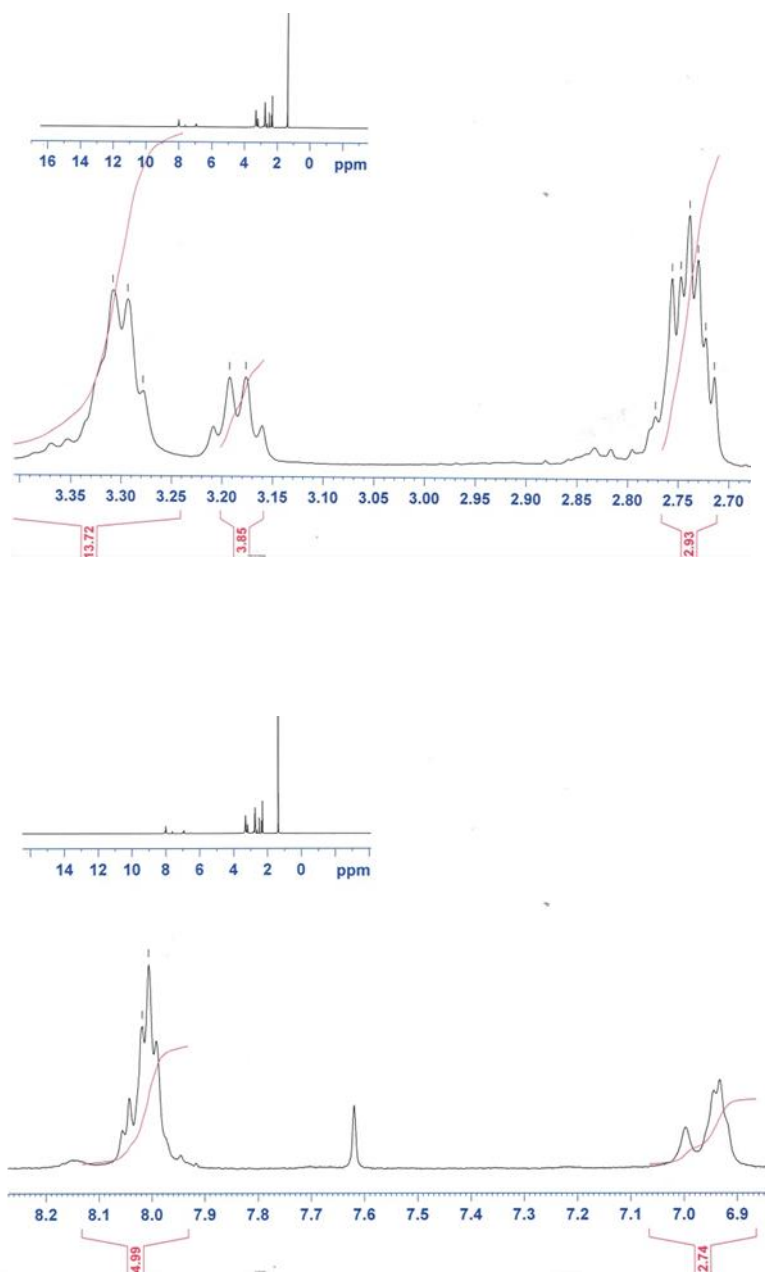


Figure A.1.: ¹H spectra of Cystamine Succinate [1]

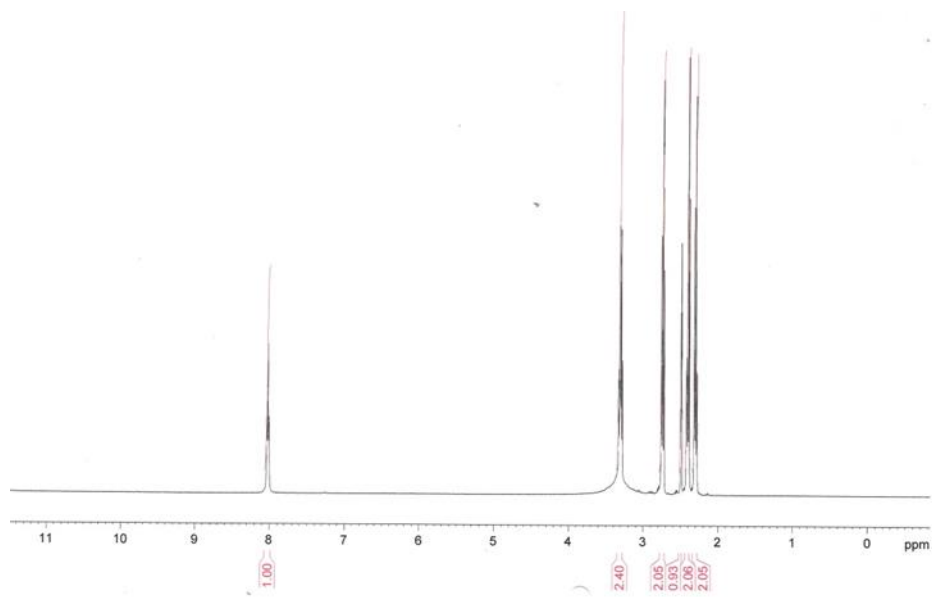


Figure A.2.: 1H spectra of N,N'-Disuccinoylcystamine [2]

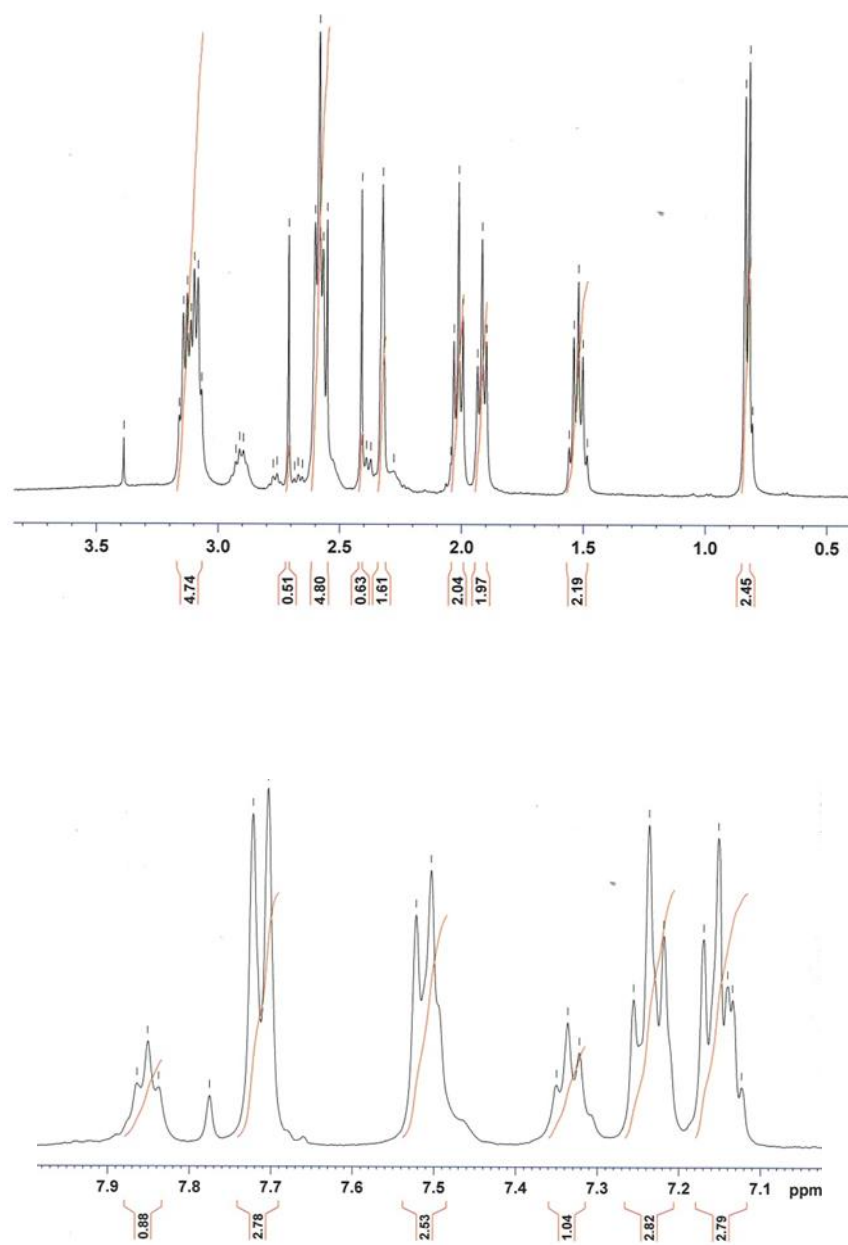


Figure A.3.: ¹H spectra of Cystamine Glutarate [5]

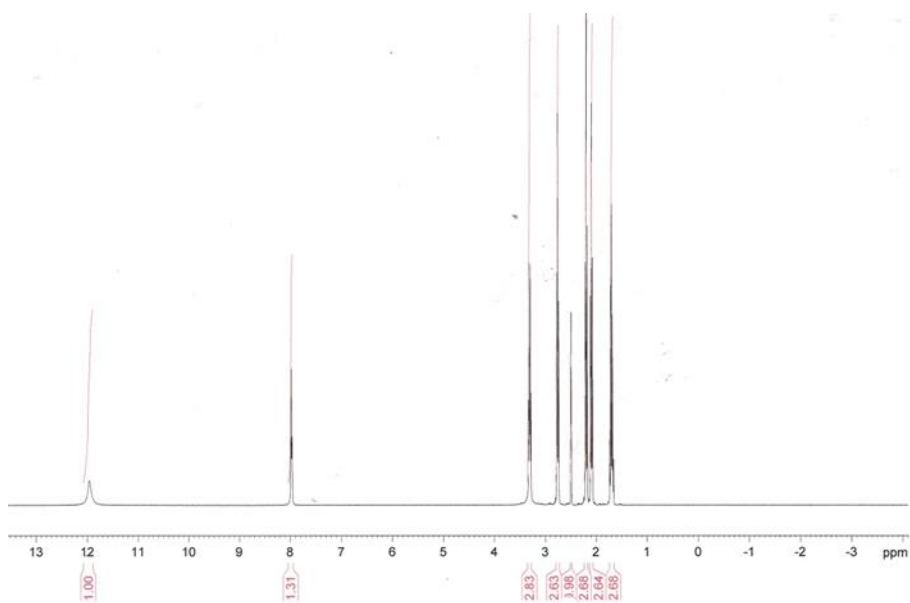


Figure A.4.: 1H spectra of N,N'-Diglutaryl-L-cystamine [6]

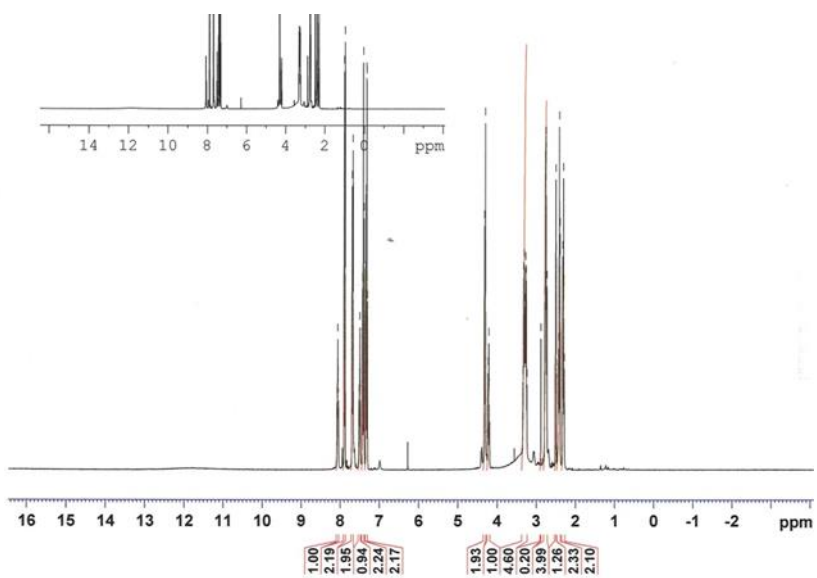


Figure A5.: 1H spectra of Fmoc-L-cystamine-succinate [15]

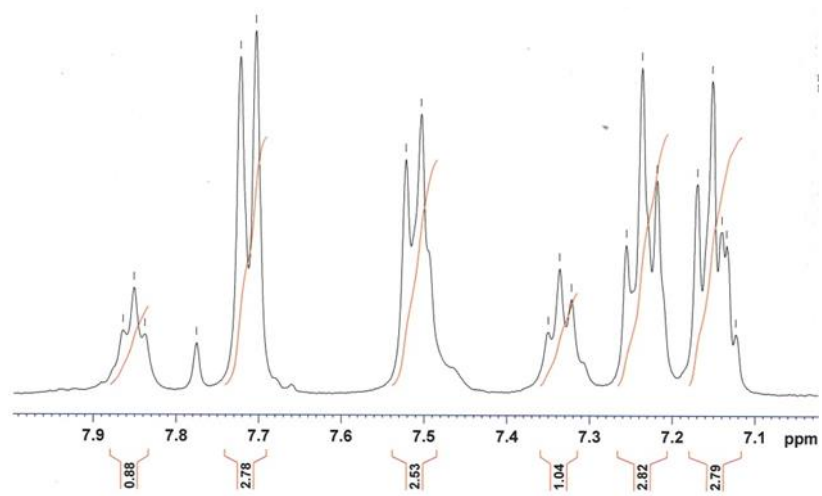
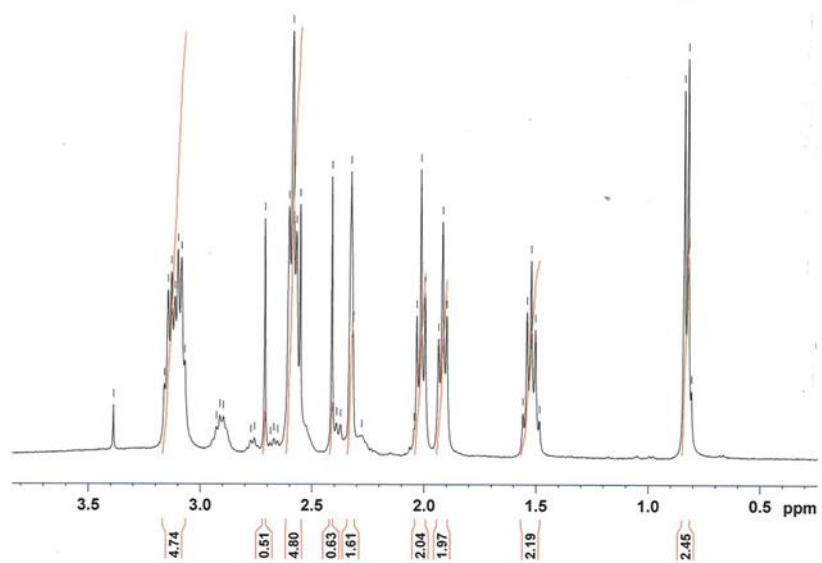


Figure A9.: 1H spectra of Fmoc-cystamine-glutarate [16]

Appendix 3

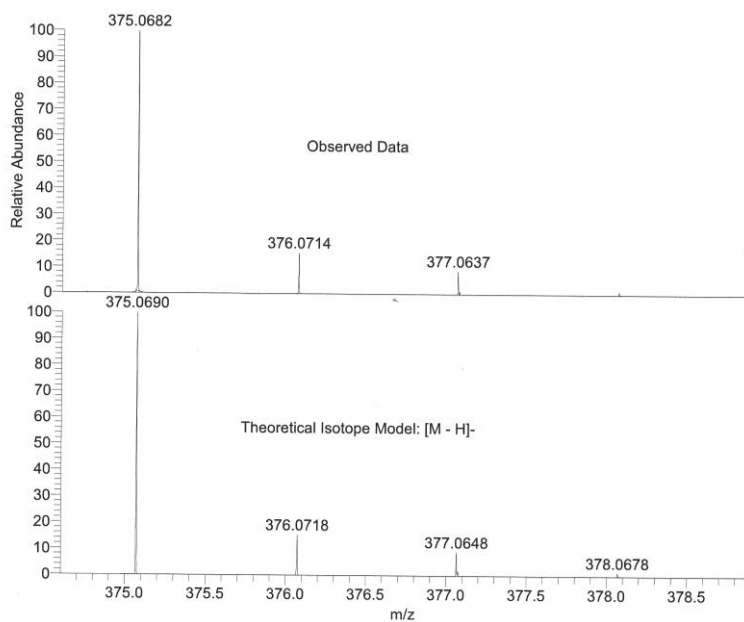


Figure B.1.: MS for N,N'-Citraconoylcystamine [10]

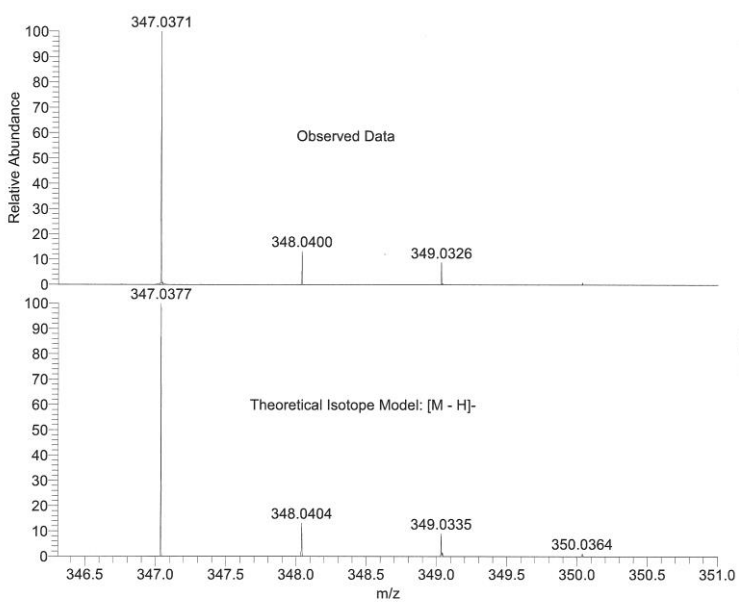


Figure B.2.: MS for N,N'-Maleioylcystamine [13]

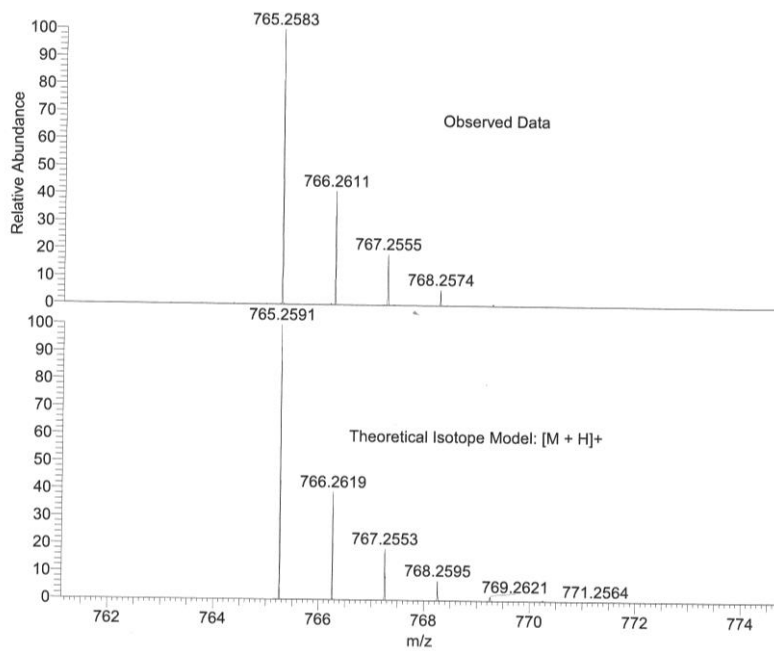


Figure B.3.: MS for Fmoc2CSDAP [17]

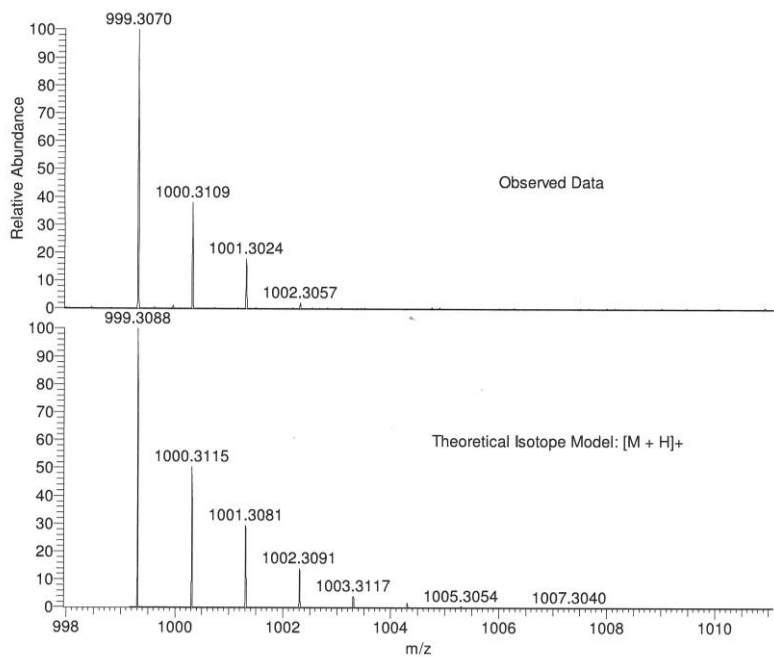


Figure B.4.: MS for Fmoc3CSDAP [18]

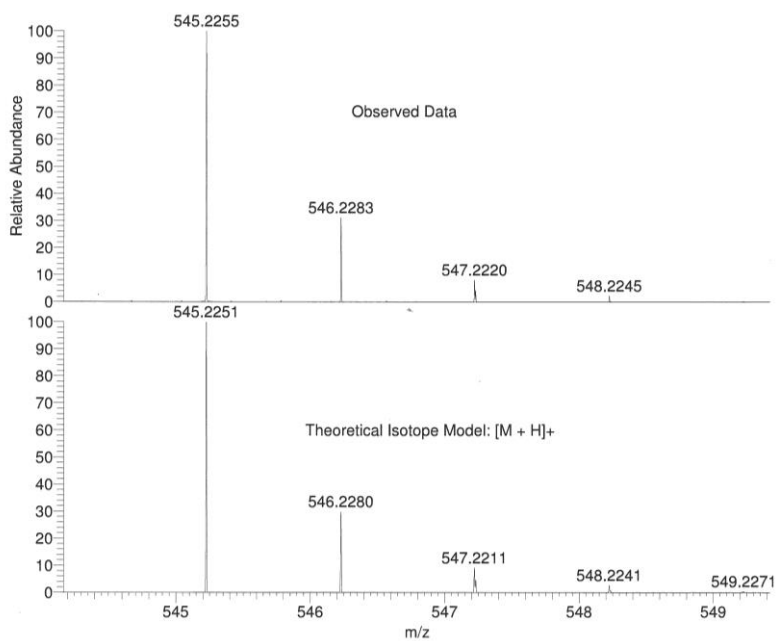


Figure B.5.: MS for FmocCGDAP [19]

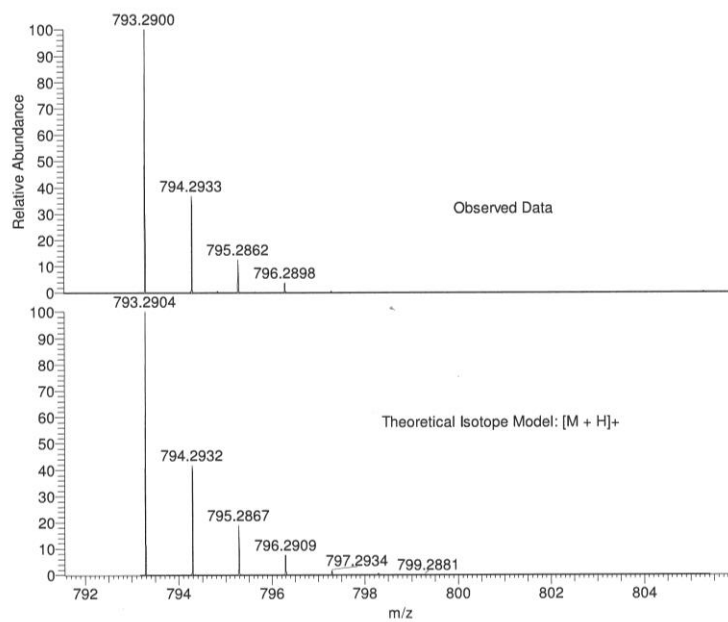


Figure B.6.: MS for Fmoc2CGDAP [20]

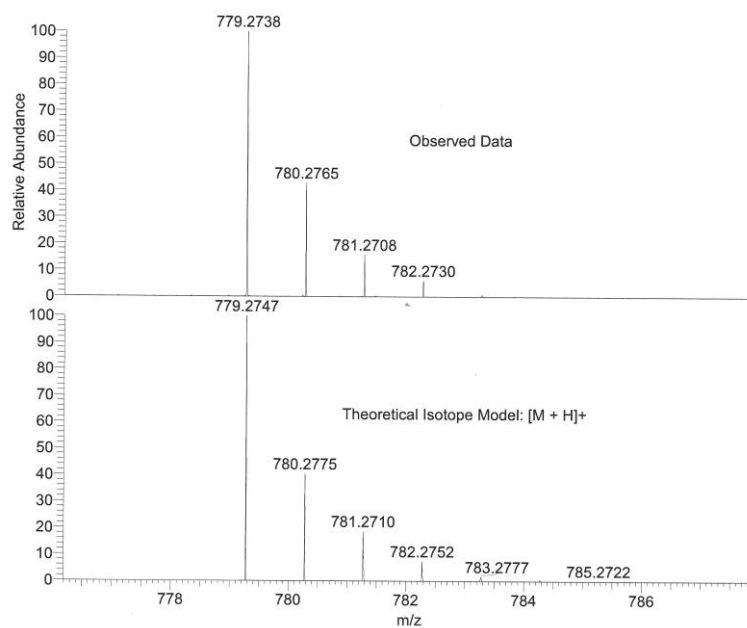


Figure B.7.: MS for FmocCSGDAP [23]

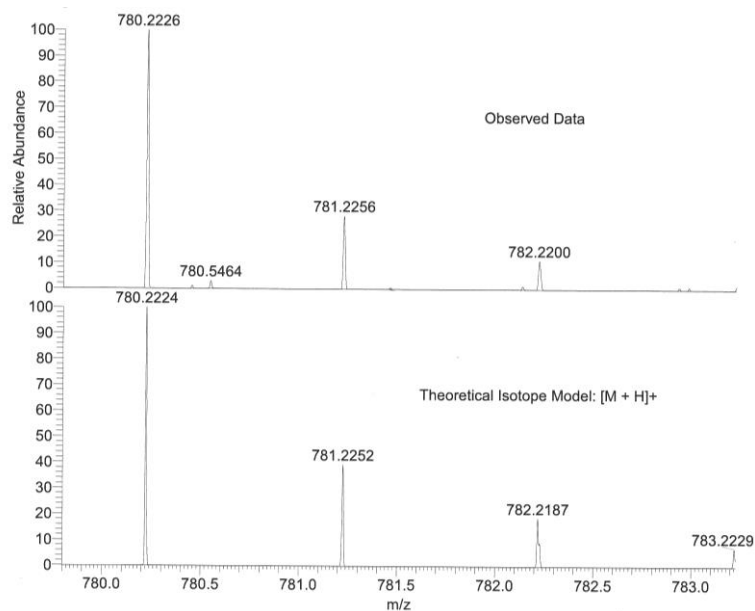


Figure B.8.: MS for Fmoc2CSAla [24]

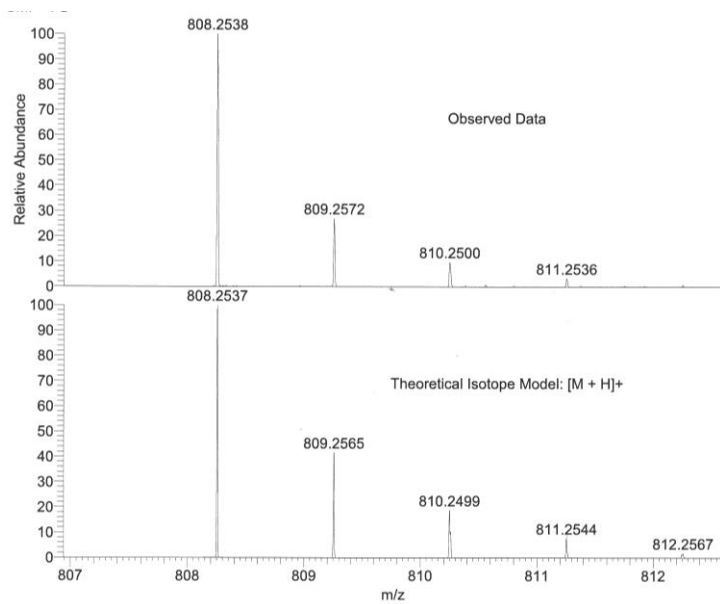


Figure B.9.: MS for Fmoc2CGAla [25]

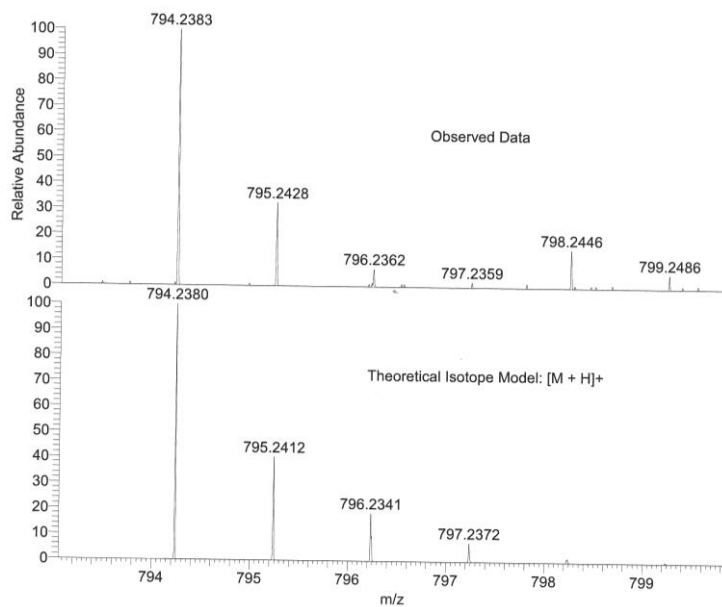


Figure B10.: MS for FmocCSCGAla [26]

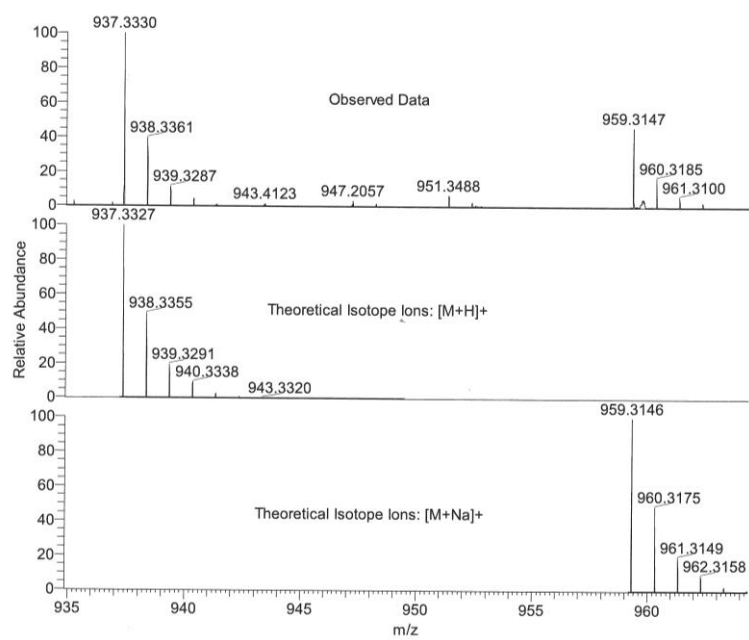


Figure B.11.: MS for Fmoc2CSBocLys [27]

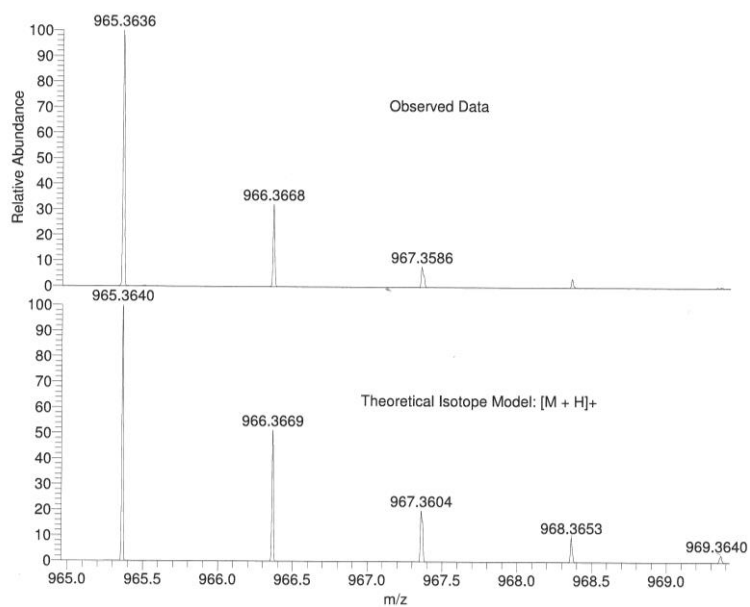


Figure B.12.: MS for Fmoc-2CG-BocLys [28]

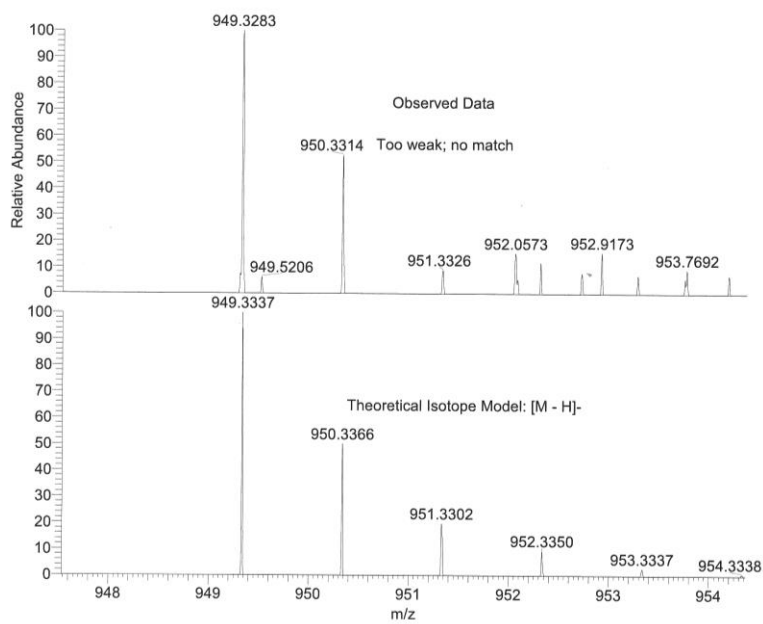


Figure B.13.: MS for FmocCSCGBocLys [29]

Public Output



Contents lists available at ScienceDirect

Bioorganic & Medicinal Chemistry

journal homepage: www.elsevier.com/locate/bmc

Synthesis and in vitro evaluation of novel pro-drugs for the treatment of nephropathic cystinosis

Ziad Omran^{a,b,*}, Kevin A. Moloney^a, Amina Benylles^a, Graeme Kay^a, Rachel M. Knott^a, Donald Cairns^a

^a School of Pharmacy and Life Sciences, Robert Gordon University, Schoolhill, Aberdeen AB10 1FR, UK

^b School of Pharmacy, The University of Nottingham, University Park, Nottingham NG7 2RD, UK

ARTICLE INFO

Article history:

Received 23 February 2011

Revised 6 April 2011

Accepted 11 April 2011

Available online 16 April 2011

Keywords:

Cystinosis

Cysteamine

Cystamine

Pro-drugs

ABSTRACT

As part of our continuing work to obtain new pro-drugs for the treatment of nephropathic cystinosis, a number of glutaric and succinic acid derivatives of cystamine have been designed, synthesised and biologically evaluated in vitro. These compounds have been designed as odourless and tasteless pro-drugs which will release multiple molecules of cysteamine upon administration. All of the synthesised compounds evaluated in this study were non-cytotoxic and displayed a greater ability than cysteamine to deplete the levels of cystine in cultured fibroblasts.

© 2011 Elsevier Ltd. All rights reserved.

1. Introduction

Nephropathic cystinosis is a rare, autosomal, recessive disease characterised by raised intracellular levels of the amino acid, cystine. Crystals of cystine are present in lysosomes, bone marrow aspirates, leucocytes, cornea, and conjunctiva. Symptoms of the disease include poor growth, renal Fanconi syndrome (impairment in proximal tubule function), renal glomerular failure and accumulation of cystine crystals in almost all cells, leading to tissue damage. Treatment begun just after birth can attenuate the rate of renal failure; however glomerular damage present at the time of diagnosis (approximately 12 months) is irreversible and may result in the need for renal transplant.¹

The disease is caused by a defect in the lysosomal transport mechanism for cystine and results from mutations in the CTNS gene, which codes for cystinosin, a membrane transport protein.² Treatment of cystinosis includes administration of electrolytes to reverse the effects of Fanconi syndrome, phosphate, vitamin D carnitine and human growth hormone in addition to corneal and renal transplant. Administration of the aminothiols, cysteamine ($\text{H}_2\text{NCH}_2\text{CH}_2\text{SH}$, marketed as the bitartrate salt, CystagonTM), acts to lower intracellular levels of cysteine by forming a cysteamine–cysteine mixed disulphide which can egress the lysosome using the lysine transporter excretion pathway which remains intact in cystinosis.³

There are major problems, however, with administration of Cystagon. The molecule possesses an offensive taste and smell and

irritates the gastrointestinal (GI) tract leading to nausea and vomiting following administration. In addition, cysteamine and its metabolites are excreted in breath and sweat, which leads to halitosis and body odour. Furthermore, some patients exhibit more serious side-effects, such as neutropenia. As a result of these problems, patient compliance can be poor.⁴ In addition, because of a combination of high first-pass metabolism and a short half-life, Cystagon only removes cystine crystals for a period of 6 h after the medication has been taken. This means that it must be given every 6 h, every day for life.^{4,5}

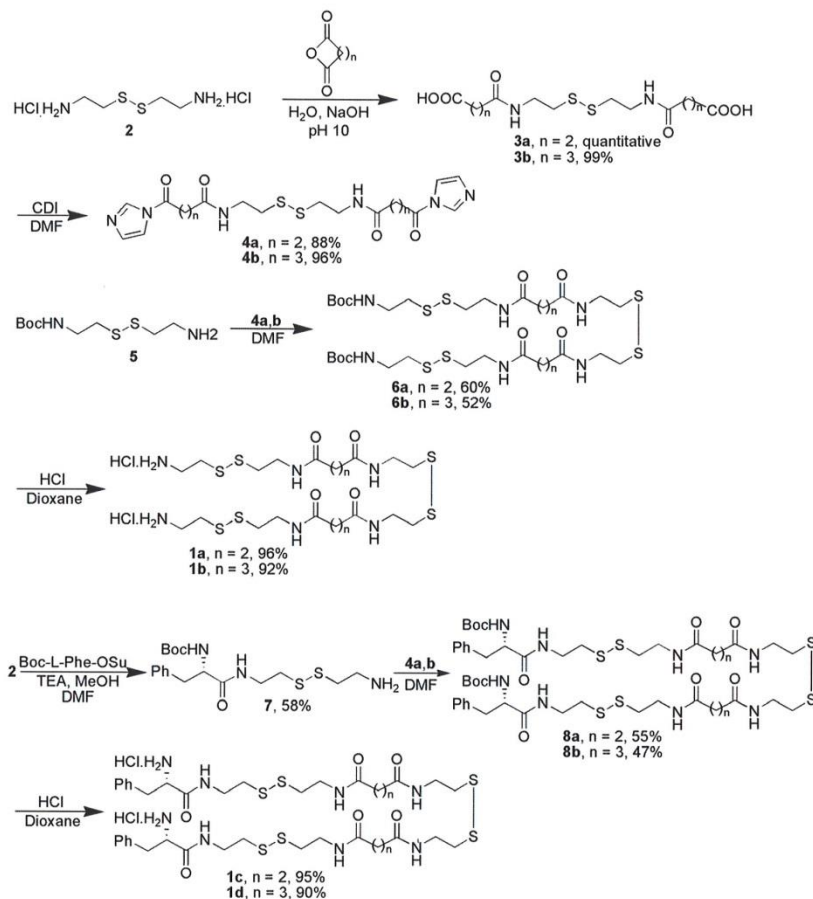
In the last few years, efforts in our laboratory have been concentrated on the design of pro-drugs of cysteamine that produce the same, or even better, cystine depleting ability than the current treatment but are devoid of the bad taste and smell of the parent drug.^{6–8} The aim of the current project is to extend previous work by synthesising novel pro-drugs that in addition to be odourless and tasteless, release multiple molecules of cysteamine (up to six per pro-drug). Furthermore, in an attempt to increase the uptake of the drug into intestinal mucosal cells⁹; we have incorporated the amino acid, phenylalanine, at the amino terminus of pro-drugs **1-c** and **1-d**.

2. Chemistry

Compounds **1a–d** were obtained from the disulphide derivative of cysteamine, cystamine dihydrochloride **2** (Scheme 1). The latter was transformed to *N,N'*-disuccinoyl¹⁰ and *N,N'*-diglutaroyl¹¹ derivatives **3a–b**, with almost quantitative yields, by reaction with the corresponding dicarboxylic anhydrides in basic aqueous solution. The activation of terminal carbonyl groups of the

* Corresponding author. Tel.: +44 1224 262552; fax +44 1224 262555.

E-mail addresses: z.omran@rgu.ac.uk, ziad.omran@nottingham.ac.uk (Z. Omran).

Scheme 1. Chemical synthesis of pro-drugs **1a–d**.

diamides **3a–b** as bisazolides was achieved by using carbonyldiimidazole (CDI).^{7,10} The imidazolide derivatives **4a–b** were then coupled with 2 equiv of mono-Boc-cystamine **5**¹² to yield the multi-cystamines derivatives **6a–b**. In the same way, the compounds **8a–b** were obtained in moderate yields by reacting the imidazolyl derivatives **4a–b** with the mono-phenylalanyl-cystamine **7**.¹³ The latter was prepared by coupling the commercially available *N*-Boc-L-phenylalanine-*N*-hydroxysuccinimide ester with cystamine dihydrochloride **2** in triethylamine–methanol–DMF mixed solvent. The Boc protecting group of the compounds **6a–b** and **8a–b** was removed by treatment with 4 M hydrogen chloride solution in dioxane¹⁴ to result in the pro-drugs **1a–d** as white odourless crystalline powders with excellent yields.

3. Biological evaluation

3.1. Toxicity profile

The cytotoxicity of pro-drugs **1a–d** was determined to confirm that any change in cystine burden observed was not a consequence

of cell death or an increase in cell proliferation. The test was carried out on human cystinotic fibroblasts using the Alamar blue cell proliferation assay.¹⁵ The cystinotic fibroblasts were subjected to 50 μM of the current treatment, cysteamine, and the compounds **1a–d**, and cell growth was measured over a 72 h period. The results are shown in Figure 1.

3.2. Measurement of intralysosomal cystine

Intralysosomal cystine was measured using the commercially available Thiol and Sulfide Quantification Kit[®] (Molecular Probes). Lysates of cystinotic fibroblasts were treated for 24 h with 50 μM of cysteamine or compounds **1a–d**. Intralysosomal cystine was isolated from the lysates, converted to cysteine and the concentration was then measured on a multiwell plate reader at 410 nm by comparison to known standards of cysteine. The effects of compounds **1a–d** on the levels of intralysosomal cystine relative to control are shown in Figure 2. The data are presented as μM cysteine per mg of protein as determined by the Bradford method.¹⁶

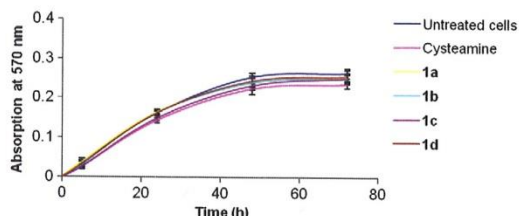


Figure 1. Net change of Alamar blue absorbance at 6, 24, 48 and 72 h intervals for compounds **1** and **1a–d**. The data shown are a mean of 6 independent experiments \pm SE, each measurement was carried out in triplicate.

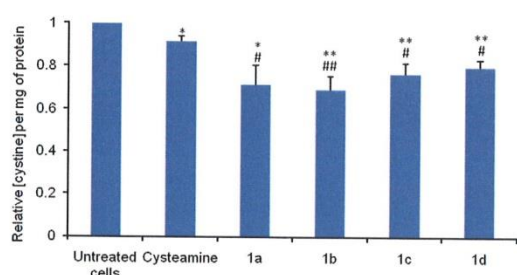


Figure 2. Relative cystine depletion in cystinotic fibroblasts measured after 24 h of incubation with compounds **1** and **1a–d**. The data shown is the mean of 4 independent experiments \pm SE. Each measurement was carried out in triplicate. The level of significance was determined using a one-tailed Student's *t*-test, and is represented as follows; comparison to untreated cells **p* < 0.05, ***p* < 0.01 and in comparison to cysteamine treated cells #*p* < 0.05, ##*p* < 0.01.

4. Discussion

It was determined from the Alamar blue study that treatment of the cystinotic fibroblasts with 50 μ M of the compounds **1a–d** or cysteamine has no significant difference in cell growth of the fibroblasts through 72 h. Figure 1 shows that cysteamine and **1a–d** have negligible toxicity at the concentrations and time frame utilised in this study.

Furthermore, the results displayed in Figure 2 shows that the synthesised pro-drugs **1a–d** significantly reduce the lysosomal cystine levels relative to control, and, more importantly, the pro-drugs deplete cystine significantly better than the current treatment, cysteamine. The observed increase in the efficacy of **1a–d** is attributed to intracellular hydrolysis of the amide linkages and subsequent release of cysteamine (up to six cysteamine molecule per pro-drug if the hydrolysis goes to completion). However, the measured depletion of intracellular cystine is not stoichiometric (i.e., pro-drugs **1a–d** are not six times more effective than cysteamine). This suggests that hydrolysis within the cells may not proceed to completion. Notwithstanding this outcome, we propose that the increased efficiency of the multi-cysteamine pro-drugs approach has been demonstrated.

5. Conclusion

The design, synthesis and biological evaluation of a series of multi-cysteamine pro-drugs have been achieved. These pro-drugs have been shown to deplete the cysteine levels in cystinotic cells with no toxicity and with a greater efficacy than the established treatment. It is anticipated that this type of pro-drug should allow less frequent administration than the current treatment and may

be better tolerated by cystinotic patients. It is hoped that in this way, patient compliance and quality of life amongst cystinotic patients will be improved.

6. Experimental section

6.1. Chemistry

6.1.1. General

All chemicals were purchased from Sigma–Aldrich (UK). ^1H NMR and ^{13}C NMR were run at 400 and 100 MHz, respectively, on Bruker 400 Ultrashield Plus machine. Coupling constants (*J*) are quoted in Hz and chemical shifts (δ) are given in parts per million (ppm) using the residue solvent peaks as reference relative to TMS. High resolution mass spectra were recorded on ThermoFisher LTQ Orbitrap XL instrument at National Mass Spectrometry Service Centre, Swansea, UK and the assistance of EPSRC is acknowledged.

6.1.2. Synthesis

6.1.2.1. 5-Imidazol-1-yl-5-oxo-pentanoic acid [2-[2-(5-imidazol-1-yl-5-oxo-pentanoylamino)-ethyl]disulfanyl]-ethyl]-amide **4b.** 1 g (2.6 mmol) of *N,N'*-diglutaryl cysteamine was dissolved in 10 ml of anhydrous DMF and 1.05 g (6.5 mmol) of CDI was added. Bubbles of CO_2 indicated the start of the reaction, and the reaction product rapidly precipitated. The reaction was allowed to continue for 3 h under reduced pressure. After dilution with 100 ml of anhydrous ethyl acetate, the product was collected by filtration, rinsed twice with 100 ml of anhydrous ethyl acetate and carefully dried in the vacuum oven at 50 °C.

Yield: 96%, ^1H NMR (400 MHz, DMSO-d_6) δ (ppm): 1.86 (quint, *J* = 7.6 Hz, 4H), 2.18 (t, *J* = 7.6 Hz, 4H), 2.73 (t, *J* = 7.6 Hz, 4H), 3.01 (t, *J* = 7.2 Hz, 4H), 3.31 (q, *J* = 7.2 Hz, 4H), 7.05 (s, 2H), 7.68 (s, 2H), 8.09 (t, *J* = 7.2 Hz, 2H), 8.39 (s, 2H). ^{13}C NMR (100 MHz, DMSO-d_6) δ (ppm): 19.74, 33.80, 33.96, 37.23, 37.88, 116.72, 130.22, 136.96, 170.22, 171.63.

6.1.2.2. General procedures for the synthesis of compounds **6a–b** and **8a–b**.

To a solution of the mono-substituted cysteamine compounds **5** or **7** (4.5 mmol) in 5 ml of dry DMF, was added the corresponding activated cysteamine derivatives **4a–b** (1.5 mmol). The reaction mixture was stirred overnight at room temperature. The solvent was then evaporated and 50 ml of distilled water were added to the residue. The white precipitate was filtered and washed by 3×50 ml of aqueous 0.1 M HCl, aqueous 0.1 M NaOH, then by 3×50 ml of AcOEt. The product was then dried in the vacuum oven at 70 °C.

6.1.2.2.1. [2-(2-[4-[2-(2-[4-[2-(2-tert-Butoxycarbonylamino)-ethyl]disulfanyl)-ethyl]carbamoyl]-propionylamino)-ethyl]disulfanyl)-ethyl]carbamoyl]-propionylamino)-ethyl]disulfanyl)-ethyl]-carbamic acid tert-butyl ester **6a.** Yield: 60%, ^1H NMR (400 MHz, DMSO-d_6) δ (ppm): 1.37 (s, 18H), 2.30 (s, 8H), 2.74 (m, 12H), 3.19 (m, 4H), 3.30 (m, 8H), 6.99 (t, *J* = 4.8 Hz, 2H), 8.04 (t, *J* = 5.2 Hz, 4H). ^{13}C NMR (100 MHz, DMSO-d_6) δ (ppm): 28.23 (6C), 30.66 (4C), 37.20 (4C), 37.24 (2C), 37.20 (4C), 37.98 (2C), 77.80 (2C), 155.52 (2C), 171.45 (4C). HR-MS calculated for $\text{C}_{30}\text{H}_{57}\text{N}_6\text{O}_8\text{S}_6$ ($\text{M}+\text{H}$): 821.2557, found: 821.2545.

6.1.2.2.2. [2-(2-[4-[2-(2-[4-[2-(2-tert-Butoxycarbonylamino)-ethyl]disulfanyl)-ethyl]carbamoyl]-butyrylamino)-ethyl]disulfanyl)-ethyl]carbamoyl]-butyrylamino)-ethyl]disulfanyl)-ethyl]-carbamic acid tert-butyl ester **6b.** Yield: 52%, ^1H NMR (400 MHz, DMSO-d_6) δ (ppm): 1.36 (s, 18H), 1.68 (quint, *J* = 7.6 Hz, 4H), 2.04 (t, *J* = 7.6 Hz, 8H), 2.74 (m, 12H), 3.17 (m, 12H), 6.98 (t, *J* = 7.2 Hz, 2H), 7.99 (t, *J* = 6.0 Hz, 4H). ^{13}C NMR (100 MHz, DMSO-d_6) δ (ppm): 21.36 (2C), 28.18 (6C), 34.65 (4C), 37.18 (4C), 37.24 (2C), 37.48 (4C),

37.83 (2C), 77.76 (2C), 155.47 (2C), 171.84 (4C). HR-MS calculated for $C_{32}H_{61}N_6O_8S_6$ (M+H)⁺: 849.2870, found: 849.2863.

6.1.2.2.3. (1-[2-[2-(3-[2-[2-(2-(S)-tert-Butoxycarbonylamino-3-phenyl-propionylamino)-ethylsulfonyl]-ethylcarbamoyl]-propionylamino)-ethylsulfonyl]-ethylcarbamoyl]-propionylamino)-ethylsulfonyl]-ethylcarbamoyl)-2-(S)-phenyl-ethyl)-carbamoyl acid tert-butyl ester **8a**. Yield: 55%. ¹H NMR (400 MHz, DMSO-*d*₆) δ (ppm): 1.28 (s, 18H), 2.31 (s, 8H), 2.73 (m, 12H), 2.92 (m, 4H), 3.34 (m, 12H), 4.10 (m, 2H), 6.90 (d, *J* = 8.4 Hz, 2H), 7.23 (m, 10H), 8.04 (t, *J* = 2.8 Hz, 4H), 8.11 (t, *J* = 4.8 Hz, 2H). ¹³C NMR (100 MHz, DMSO-*d*₆) δ (ppm): 28.15 (6C), 30.68 (4C), 37.01 (2C), 37.19 (4C), 37.67 (2C), 37.95 (2C), 37.99 (4C), 55.77 (2C), 77.98 (2C), 126.18 (2C), 128.10 (4C), 129.19 (4C), 138.15 (2C), 155.19 (2C), 171.47 (4C), 171.73 (2C). HR-MS calculated for $C_{48}H_{75}N_8O_{10}S_6$ (M+H)⁺: 1115.3925, found: 1115.3905.

6.1.2.2.4. (1-[2-[2-(4-[2-[2-(4-[2-[2-(S)-tert-Butoxycarbonylamino-3-phenyl-propionylamino)-ethylsulfonyl]-ethylcarbamoyl]-butyrylamino)-ethylsulfonyl]-ethylcarbamoyl]-2-(S)-phenyl-ethyl)-carbamoyl acid tert-butyl ester **8b**. Yield: 47%. ¹H NMR (400 MHz, DMSO-*d*₆) δ (ppm): 1.35 (s, 18H), 1.77 (quint, *J* = 7.2 Hz, 4H), 2.12 (t, *J* = 7.2 Hz, 8H), 2.81 (m, 12H), 2.98 (m, 4H), 3.41 (m, 12H), 4.18 (m, 2H), 6.98 (d, *J* = 8.8 Hz, 2H), 7.31 (m, 10H), 8.07 (t, *J* = 5.0 Hz, 4H), 8.18 (t, *J* = 5.0 Hz, 2H). ¹³C NMR (100 MHz, DMSO-*d*₆) δ (ppm): 21.36 (2C), 28.09 (6C), 34.65 (4C), 36.93 (2C), 37.15 (4C), 37.66 (2C), 37.83 (4C), 37.89 (2C), 55.72 (2C), 77.91 (2C), 126.12 (2C), 127.96 (4C), 129.13 (4C), 138.10 (2C), 155.14 (2C), 171.68 (2C), 171.84 (4C). HR-MS calculated for $C_{50}H_{79}N_8O_{10}S_6$ (M+H)⁺: 1143.4238, found: 1143.4218.

6.1.2.3. General procedures for the synthesis of the pro-drugs **1a–d**. To a solution of the compounds **6a–b** or **8a–b** (0.04 mmol) was added 5 ml of 4 M hydrogen chloride solution in dioxane, at 0 °C under a nitrogen atmosphere. The reaction mixture was stirred at 0 °C for 30 min and then for further 30 min at room temperature. The white precipitate was filtered and washed by 3 × 50 ml of AcOEt and 3 × 50 ml of CH₂Cl₂. The product was then dried in the vacuum oven at 70 °C.

6.1.2.3.1. Pro-drug **1a**. Yield: 96%. ¹H NMR (400 MHz, DMSO-*d*₆) δ (ppm): 2.31 (s, 8H), 2.76 (m, 8H), 2.94 (m, 4H), 3.07 (m, 4H), 3.31 (m, 8H), 8.11 (m, 10H). ¹³C NMR (100 MHz, DMSO-*d*₆) δ (ppm): 30.61 (4C), 34.00 (2C), 36.98 (2C), 37.14 (2C), 37.79 (2C), 37.87 (2C), 37.94 (2C), 171.48 (2C), 171.54 (2C). HR-MS calculated for $C_{20}H_{41}N_6O_4S_6$ (M+H)⁺: 621.1508, found: 621.1503.

6.1.2.3.2. Pro-drug **1b**. Yield: 92%. ¹H NMR (400 MHz, DMSO-*d*₆) δ (ppm): 1.70 (quint, *J* = 7.2, 4H), 2.07 (t, *J* = 7.2, 8H), 2.78 (m, 8H), 2.95 (m, 4H), 3.08 (m, 4H), 3.32 (m, 8H), 8.09 (m, 10H). ¹³C NMR (100 MHz, DMSO-*d*₆) δ (ppm): 21.42 (2C), 34.04 (2C), 34.09 (4C), 37.09 (2C), 37.22 (2C), 37.77 (2C), 37.82 (2C), 37.89 (2C), 171.90 (2C), 171.96 (2C). HR-MS calculated for $C_{22}H_{45}N_6O_4S_6$ (M+H)⁺: 649.1821, found: 649.1819.

6.1.2.3.3. Pro-drug **1c**. Yield: 95%. ¹H NMR (400 MHz, DMSO-*d*₆) δ (ppm): 2.31 (s, 8H), 2.63 (m, 4H), 2.74 (t, *J* = 6.4 Hz, 8H), 3.05 (m, 4H), 3.29 (m, 8H), 3.43 (m, 4H), 4.00 (m, 2H), 7.26 (m, 10 H), 8.14 (m, 4H), 8.36 (m, 6H), 8.80 (m, 2H). ¹³C NMR (100 MHz, DMSO-*d*₆) δ (ppm): 30.70 (4C), 36.70 (2C), 36.95 (2C), 37.05 (2C), 37.21 (2C), 37.81 (2C), 38.00 (2C), 38.11 (2C), 53.47 (2C), 127.13 (2C), 128.49 (4C), 129.54 (4C), 134.97 (2C), 167.95 (2C), 171.47 (2C), 171.53 (2C). HR-MS calculated for $C_{38}H_{59}N_8O_6S_6$ (M+H)⁺: 915.2876, found: 915.2878.

6.1.2.3.4. Pro-drug **1d**. Yield: 90%. ¹H NMR (400 MHz, DMSO-*d*₆) δ (ppm): 1.70 (quint, *J* = 7.6 Hz, H-7, 4H), 2.06 (t, *J* = 7.6 Hz, 8H), 2.64 (m, 4H), 2.74 (t, *J* = 6.8 Hz, 8H), 3.02 (m, 4H), 3.30 (m, 8H), 3.43 (m, 4H), 3.96 (m, 2H), 7.30 (m, 10 H), 8.04 (m, 4H), 8.20 (m, 6H), 8.64 (m, 2H). ¹³C NMR (100 MHz, DMSO-*d*₆) δ (ppm): 21.46 (2C), 35.81 (4C), 36.69 (2C), 36.96 (2C), 37.08 (2C),

37.23 (2C), 37.82 (2C), 37.90 (2C), 37.99 (2C), 53.48 (2C), 127.14 (2C), 128.50 (4C), 129.54 (4C), 134.69 (2C), 167.96 (2C), 171.93 (2C), 171.96 (2C). HR-MS calculated for $C_{40}H_{63}N_8O_6S_6$ (M+H)⁺: 943.3189, found: 943.3185.

6.2. Biology

6.2.1. General

Human cystinotic fibroblasts (GM00008) were purchased from Coriell Cell Repositories (NJ, USA) and cultured in Eagle's minimum essential media supplemented with 15% FBS, 200 U/ml penicillin, 200 µg/ml streptomycin and 2 mM glutamine at 37 °C in 5% CO₂. Alamar blue reagent was purchased from (Serotech, UK). Thiol and sulphide quantification kit (Molecular Probes T6060) was purchased from FisherScientific (UK). Bradford reagent was purchased from Sigma (UK).

6.2.2. Alamar blue assay

Cystinotic fibroblasts cultured in 96 well plates were incubated for 0–72 h in the presence of 50 µM either cysteamine, or **1a–d** in media supplemented with 10% Alamar blue. Cell growth was measured over a 72 h period on a multiwell plate reader Biotek FL6000 and is presented as the net change in absorbance at 570 nm relative to the reading at time 0 h.

6.2.3. Thiol assay

Cystinotic fibroblasts were seeded in a 25 cm³ vented flask and allowed to reach approximately 80% confluence before the addition of the test compounds; 50 µM either cysteamine, or **1a–d** in 4 cm³ Eagles minimum essential media supplemented with 15% FBS, 200 U/ml penicillin, 200 µg/ml streptomycin and 2 mM glutamine. This was then incubated at 37 °C and 5% CO₂ for 24 h. The cells were harvested, frozen in liquid nitrogen and stored at –80 °C until the cysteine concentration was determined per quantity of protein. The cells were recovered from storage at –80 °C and suspended in 100 µl 1 mM *N*-ethylmaleimide prepared in phosphate buffer (pH 7.6) followed by sonication for 10 s which was repeated three times with 20 s cooling intervals on ice. The solution was centrifuged at 800 g for 10 min at 40 °C (Biofuge primo R Heraeus centrifuge). Cell supernatant (40 µl) was then added; 4 µl of 4 M NaBH₄ in 7:3 0.1 M NaOH/DMSO. After 5 min incubation at room temperature; 800 µl of sodium acetate buffer (pH 4.7) was added. A 5 µl volume of the diluted solution was then added to 100 µl of 0.6 mg/ml solution of Papain-SSCH₃ in 96 wells plate and incubated for 1 h at room temperature. A 100 µl volume of 4.9 mM L-BAPNA solution in sodium acetate buffer (pH 4.0) was then added to each well of the 96 well plate, gently mixed and incubated for further 1 h at room temperature. The absorption at 410 nm was measured and the cysteine levels were calculated by comparison to known cysteine standards.

The protein concentration in every sample was determined according to Bradford method¹⁴ at the same time of the thiol assay. Briefly, 200 µl of Bradford reagent were added to 5 µl of the previously obtained cell supernatant in each well of a 96 well plate and incubated for 5 min at room temperature and the absorption at 595 nm was measured. The protein concentrations were calculated using a range of concentrations of bovine serum albumin as a standard. The cysteine levels are presented following normalisation to µM cysteine per mg of protein.

Acknowledgment

The authors acknowledge financial support from Cystinosis Foundation, Ireland.

References and notes

1. Gahl, W. A.; Thoene, J. G.; Schneider, J. A. Cystinosis: A Disorder of Lysosomal Membrane Transport. In *The Metabolic and Molecular Basis of Inherited Disease*; Scriver, C. R., Beaudet, A. L., Sly, W. S., Valle, D., Vogelstein, B., Eds.; McGraw-Hill: NY, 2001. eighth ed., pp 5085–5108.
2. Town, M.; Jean, G.; Cherqui, S.; Attard, M.; Forestier, L.; Whitmore, S. A.; Callen, D.; Gribouval, O.; Broyer, M.; Bates, G. P.; Van't Hoff, W.; Antignac, C. *Nat. Genet.* **1998**, *18*, 319.
3. Pisoni, R.; Thoene, J.; Christensen, H. J. *Biol. Chem.* **1995**, *260*, 4791.
4. Cardwell, W. A.; Cairns, D.; Anderson, R. J. *J. Pharm. Pharmacol.* **1997**, *49*, 99.
5. Gahl, W.; Thoene, J. G.; Schneider, J. A. *New Engl. J. Med.* **2002**, *347*, 111.
6. McCaughan, B.; Kay, G.; Knott, R. M.; Cairns, D. *Bioorg. Med. Chem. Lett.* **2008**, *18*, 1716.
7. Omran, Z.; Kay, G.; Di-Salvo, A.; Knott, R. M.; Cairns, D. *Bioorg. Med. Chem. Lett.* **2010**, *21*, 45.
8. Omran, Z.; Kay, G.; Hector, E. E.; Knott, R. M.; Cairns, D. *Bioorg. Med. Chem. Lett.* **2010**, *21*, 2502.
9. Hu, M.; Borchardt, R. T. *Pharm. Res.* **1990**, *7*, 1313.
10. Nicolas, F. L.; Gagnieu, C. H. *Biomaterials* **1997**, *18*, 807.
11. Shu, X. PCT Int. Appl. (2008), CODEN: PIXXD2 WO 2008061427.
12. Girgenti, E.; Ricoux, R.; Mahy, J. P. *Tetrahedron* **2004**, *60*, 10049.
13. Zhang, B.; Cech, T. R. *Chem. Biol.* **1998**, *5*, 539.
14. Han, G.; Tamaki, M.; Hruby, V. J. *J. Pept. Res.* **2001**, *4*, 338.
15. Ahmed, S. A.; Gogal, R. M., Jr.; Walsh, J. E. *J. Immunol. Methods* **1994**, *170*, 211.
16. Bradford, M. M. *Anal. Biochem.* **1976**, *72*, 248.



Three salts from the reactions of cysteamine and cystamine with L-(+)-tartaric acid

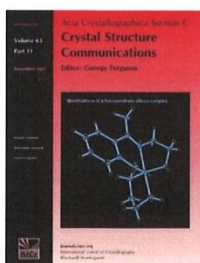
Amina Benylles, Donald Cairns, Philip J. Cox and Graeme Kay

Acta Cryst. (2013). **C69**, 658–664

Copyright © International Union of Crystallography

Author(s) of this paper may load this reprint on their own web site or institutional repository provided that this cover page is retained. Reproduction of this article or its storage in electronic databases other than as specified above is not permitted without prior permission in writing from the IUCr.

For further information see <http://journals.iucr.org/services/authorrights.html>



Acta Crystallographica Section C: Crystal Structure Communications specializes in the rapid dissemination of high-quality studies of crystal and molecular structures of interest in fields such as chemistry, biochemistry, mineralogy, pharmacology, physics and materials science. The numerical and text descriptions of each structure are submitted to the journal electronically as a Crystallographic Information File (CIF) and are checked and typeset automatically prior to peer review. The journal is well known for its high standards of structural reliability and presentation. *Section C* publishes approximately 1000 structures per year; readers have access to an archive that includes high-quality structural data for over 10000 compounds.

Crystallography Journals **Online** is available from journals.iucr.org

Three salts from the reactions of cysteamine and cystamine with L-(+)-tartaric acid

Amina Benylles,^a Donald Cairns,^a Philip J. Cox^{a*} and Graeme Kay^b

^aSchool of Pharmacy and Life Sciences, Robert Gordon University, Schoolhill, Aberdeen AB10 1FR, Scotland, and ^bInstitute for Health and Welfare Research, School of Pharmacy and Life Sciences, Robert Gordon University, Schoolhill, Aberdeen AB10 1FR, Scotland

Correspondence e-mail: ext.cox1@rgu.ac.uk

Received 27 March 2013

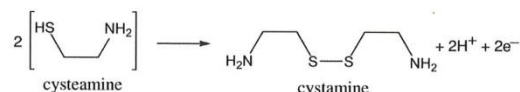
Accepted 6 May 2013

Reaction between cysteamine (systematic name: 2-aminoethanethiol, C₂H₇NS) and L-(+)-tartaric acid [systematic name: (2*R*,3*R*)-2,3-dihydroxybutanedioic acid, C₄H₆O₆] results in a mixture of cysteamine tartrate(1⁻) monohydrate, C₂H₈NS⁺·C₄H₅O₆⁻·H₂O, (I), and cystamine bis[tartrate(1⁻)] dihydrate, C₄H₁₄N₂S₂²⁺·2C₄H₅O₆⁻·2H₂O, (III). Cystamine [systematic name: 2,2'-dithiobis(ethylamine), C₄H₁₂N₂S₂], reacts with L-(+)-tartaric acid to produce a mixture of cystamine tartrate(2⁻), C₄H₁₄N₂S₂²⁺·C₄H₄O₆²⁻, (II), and (III). In each crystal structure, the anions are linked by O—H···O hydrogen bonds that run parallel to the *a* axis. In addition, hydrogen bonding involving protonated amino groups in all three salts, and water molecules in (I) and (III), leads to extensive three-dimensional hydrogen-bonding networks. All three salts crystallize in the orthorhombic space group *P*2₁2₁2₁.

Comment

Nephropathic cystinosis is a rare autosomal recessive disease that is characterized by raised lysosomal levels of cystine in the cells of most organs. If untreated, the disease results in death from renal failure by the second decade of life. The condition is characterized by poor growth, renal Fanconi syndrome, renal glomerular failure, and impairment of other tissues and organs (*e.g.* thyroid, pancreas and central nervous system). If treatment is started just after birth this can attenuate the rate of renal failure, but glomerular damage present at the time of diagnosis (usually about 12 months of age) is irreversible and may result in the need for renal transplant (Gahl *et al.*, 2000, 2001, 2002; Cairns *et al.*, 2002). Although novel prodrug strategies are being researched (Kay *et al.*, 2007; McCaughan *et al.*, 2008), the main treatment for the disorder remains the administration of the aminothioli cysteamine as the tartrate(2⁻) salt, in the commercial preparation Cystagon[®] (Orphan Europe, Paris). Cysteamine

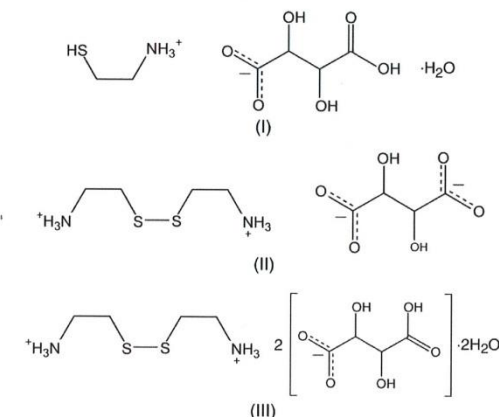
lowers intracellular levels of cystine by forming a cysteamine–cystine mixed disulfide that is spatially similar in structure to the amino acid lysine, and can egress the lysosome using the undamaged excretion pathway for lysine (Touchman *et al.*, 2000). The thiol cysteamine is known to auto-oxidize to form cystamine (Scheme 1).



Scheme 1

The known 2*R*,3*R* absolute configuration of L-(+)-tartaric acid can establish the absolute configuration of its chiral associations, where it can exist as a neutral molecule, a tartrate monoanion or a tartrate dianion. Its use in pharmaceutical salts also includes metoprolol tartrate, a β -adrenoceptor blocking agent used for migraines, and zolpidem tartrate, a hypnotic used for insomnia (Sweetman, 2011).

In this study, we have reacted cysteamine and cystamine with L-(+)-tartaric acid, and report on the formation and absolute molecular configuration of the three crystalline products, cysteamine tartrate(1⁻) monohydrate, (I), cystamine tartrate(2⁻), (II), and cystamine bis[tartrate(1⁻)] dihydrate, (III) (Scheme 2; Figs. 1–3).



Scheme 2

For (I), the cysteamine moiety remains unoxidized and salt formation results from the transfer of a proton from one of the two carboxylic acid groups in the tartaric acid molecule to the amino group of cysteamine. This results in a monohydrated tartrate monoanion (also known as a hydrogen tartrate anion or semi-tartrate anion) associated with a cysteaminium cation. In the carboxylic acid group, the single-bond character of C3–O1 [1.301 (2) Å] compares with the double-bond length of C3–O2 [1.224 (2) Å], whereas the lengths of the bonds in the carboxylate group [C6–O5 = 1.240 (2) Å and C6–O6 = 1.280 (2) Å] are closer to each other, but not equal, due to differences in hydrogen bonding. The conformation of the cation is described by a S1–C1–C2–N1 torsion angle of

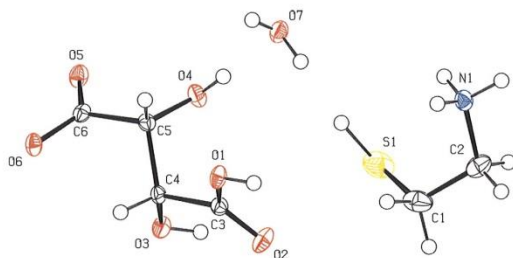


Figure 1
A view of hydrated salt (I), showing the atomic numbering scheme. Displacement ellipsoids are drawn at the 50% probability level.

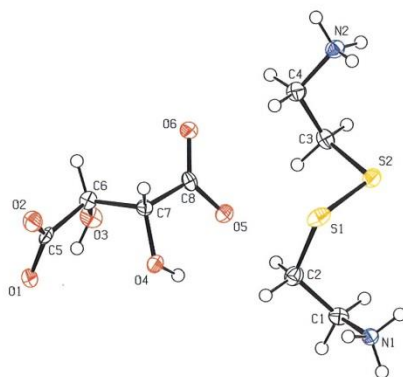


Figure 2
A view of salt (II), showing the atomic numbering scheme. Displacement ellipsoids are drawn at the 50% probability level.

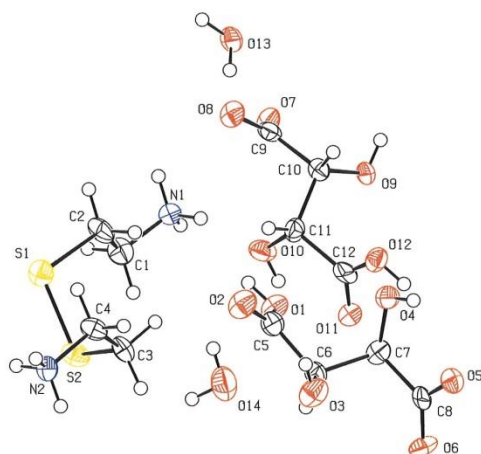


Figure 3
A view of hydrated salt (III), showing the atomic numbering scheme. Displacement ellipsoids are drawn at the 50% probability level.

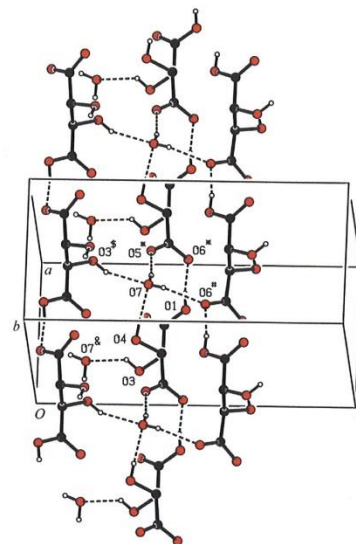


Figure 4
Part of the crystal structure of (I), showing the head-to-tail hydrogen-bonded chains of tartrate monoanions running parallel to [100] [$O1 \cdots O6^* = 2.4885(18) \text{ \AA}$] and crosslinked by water molecules, which act as double donors and double acceptors of hydrogen bonds. Atoms labelled with an asterisk (*), a hash symbol (#), a dollar sign (\$) or an ampersand (&) are at the symmetry positions $(x + 1, y, z)$, $(x + \frac{1}{2}, -y + \frac{1}{2}, -z + 1)$, $(-x + 1, y + \frac{1}{2}, -z + \frac{1}{2})$ or $(-x + 1, y - \frac{1}{2}, -z + \frac{1}{2})$, respectively. Hydrogen bonds are shown as dashed lines and H atoms not involved in the interactions have been omitted.

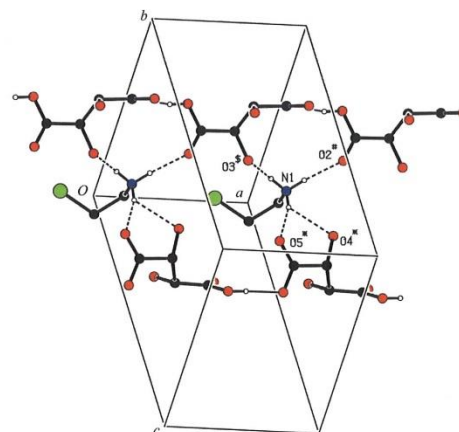


Figure 5
Part of the crystal structure of (I), showing the head-to-tail hydrogen-bonded chains of tartrate monoanions crosslinked by the protonated amino group of the cysteamine cation. One of the three hydrogen bonds is bifurcated. Atoms labelled with an asterisk (*), a hash symbol (#) or a dollar sign (\$) are at the symmetry positions $(x + 1, y, z)$, $(-x + 2, y + \frac{1}{2}, -z + \frac{1}{2})$ or $(-x + 1, y + \frac{1}{2}, -z + \frac{1}{2})$, respectively. Hydrogen bonds involving the amino groups are shown as dashed lines and H atoms not involved in the interactions have been omitted.

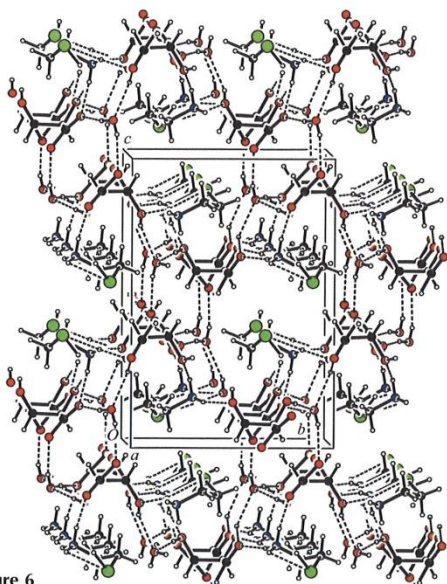


Figure 6
A view of the packing of the ions in the unit cell of (I). Hydrogen bonds are shown as dashed lines.

67.1 (2)° and differs from values of 61.7 (2), -60.3 (4) and 60.7 (4)° found in cysteamine hydrochloride (Ahmad *et al.*, 2010; Kim *et al.*, 2002), where chloride anions are engaged in hydrogen bonding. The S-H bond of 1.31 (3) Å compares with the value of 1.30 (5) Å in thiosalicylic acid (Steiner, 2000) and there are no short intermolecular contacts around the S atom. The tartrate monoanions are linked into chains running

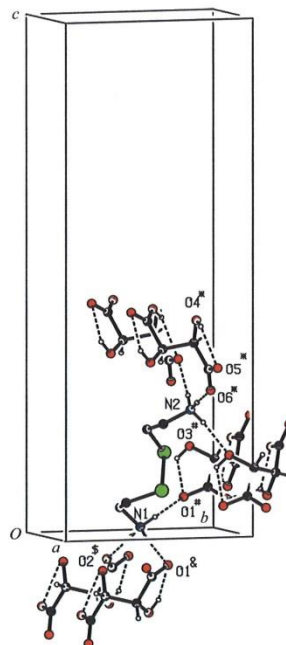


Figure 8
Part of the crystal structure of (II), showing the tartrate anions crosslinked by the protonated amino groups of the cystamine dication. Atoms labelled with an asterisk (*), a hash symbol (#), a dollar sign (\$) or an ampersand (&) are at the symmetry positions $(-x+2, y+\frac{1}{2}, -z+\frac{1}{2})$, $(x-1, y, z)$, $(x-\frac{1}{2}, -y+\frac{1}{2}, -z)$ or $(x-\frac{1}{2}, -y+\frac{1}{2}, -z)$, respectively. Hydrogen bonds are shown as dashed lines and H atoms not involved in the interactions have been omitted.

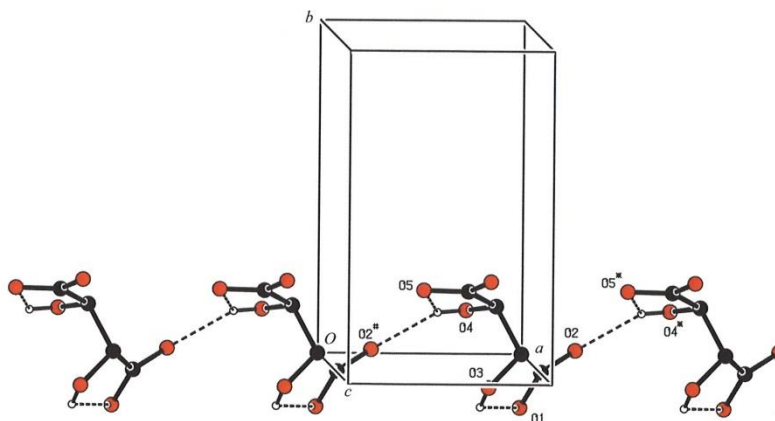


Figure 7
Part of the crystal structure of (II), showing intramolecular [O3...O1 = 2.588 (4) Å and O4...O5 = 2.613 (4) Å] and intermolecular [O4...O2# = 2.889 (4) Å] hydrogen-bonded chains of tartrate dianions running parallel to [100]. Atoms labelled with an asterisk (*) or a hash symbol (#) are at the symmetry positions $(x+1, y, z)$ or $(x-1, y, z)$, respectively. Hydrogen bonds are shown as dashed lines and H atoms not involved in the interactions have been omitted.

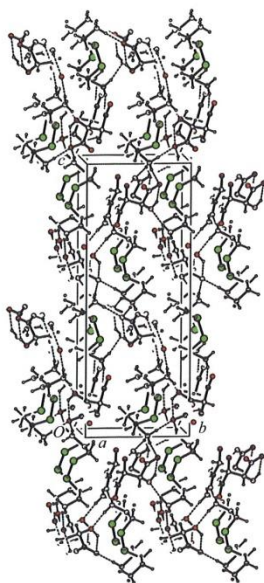


Figure 9
A view of the packing of the ions in the unit cell of (II). Hydrogen bonds are shown as dashed lines.

parallel to (100) by a strong head-to-tail $O1-H1 \cdots O6(x+1, y, z)$ hydrogen bond, with $O1 \cdots O6(x+1, y, z) = 2.489(2) \text{ \AA}$. These chains are then interlinked by water molecules (Fig. 4) and cysteamine cations (via the three H atoms of the protonated amino group; Fig. 5). One of these three H atoms, H1C, is involved in bifurcated hydrogen bonding. The resulting honeycomb or columnar packing structure (Fig. 6) is similar to those found in quinolinium hydrogen (2*R*,3*R*)-tartrate monohydrate (Smith *et al.*, 2006) and pyridinium (2*R*,3*R*)-tartrate (Suresh *et al.*, 2006). Hydrogen bonds are given in Table 1.

Product (II) is an anhydrous salt formed by the transfer of both H atoms from the two carboxylic acid groups in L-(+)-tartaric acid to the two amino groups in cysteamine. (When cysteamine is the starting material, cystamine is formed by auto-oxidation of cysteamine.) Similarities in bond character in the carboxylate groups are shown by $C5-O1 = 1.257(5) \text{ \AA}$, $C5-O2 = 1.244(5) \text{ \AA}$, $C8-O5 = 1.258(5) \text{ \AA}$ and $C8-O6 = 1.251(5) \text{ \AA}$. The disulfide bond [$S1-S2 = 2.0384(16) \text{ \AA}$] adopts a *gauche* orientation, with a $C2-S1-S2-C3$ torsion angle of $80.39(19)^\circ$, and as the five torsion angles around this bond are all positive it may be designated +RHSPiral (Schmidt *et al.*, 2006). The tartrate dianions (Fig. 7) are linked into chains running parallel to (100) by a single $O4-H4 \cdots O2(x-1, y, z)$ hydrogen bond (Table 2). In addition, each cysteamine dication is hydrogen bonded to six tartrate anions via the two protonated amino groups (Fig. 8), resulting in the overall crystal packing shown in Fig. 9. Hydrogen bonds are listed in Table 2.

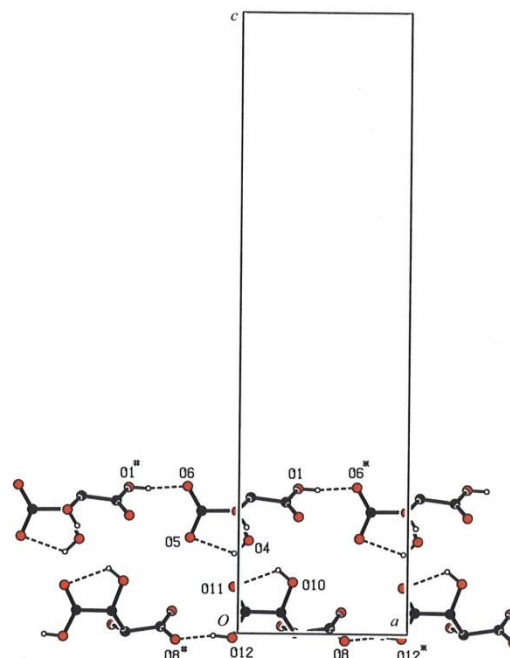


Figure 10
Part of the crystal structure of (III), showing the intra- [$O4 \cdots O5 = 2.576(7) \text{ \AA}$ and $O10 \cdots O11 = 2.572(7) \text{ \AA}$] and intermolecular [$O1 \cdots O6^* = 2.554(7) \text{ \AA}$ and $O8 \cdots O12^* = 2.476(7) \text{ \AA}$] hydrogen-bonded chains of the two independent tartrate monoanions, running parallel to [100]. Atoms labelled with an asterisk (*) or a hash symbol (#) are at the symmetry positions $(x+1, y, z)$ or $(x-1, y, z)$, respectively. Hydrogen bonds are shown as dashed lines and H atoms not involved in the interactions have been omitted.

The quality of the data set related to the crystal for (III) was not as good as those obtained for (I) and (II), and discussion of the fine details of the product structure needs to be approached with caution. As in (II), both amino groups have acquired an additional H atom. Each of these two protons appears to have transferred from separate tartaric acid molecules, leaving a single charge on each of the two symmetry-independent tartrate monoanions. Evidence for this is based on bond lengths: for the carboxylic acid group, $C5-O1 = 1.292(9) \text{ \AA}$ and $C5-O2 = 1.191(8) \text{ \AA}$, and, in the same anion, the carboxylate group has $C8-O5 = 1.261(8) \text{ \AA}$ and $C8-O6 = 1.231(8) \text{ \AA}$. In the second tartrate monoanion, the bond character is less obvious but the carboxylic acid group has $C12-O11 = 1.220(9) \text{ \AA}$ and $C12-O12 = 1.275(9) \text{ \AA}$, while in the carboxylate group these bonds are $C9-O7 = 1.229(8) \text{ \AA}$ and $C9-O8 = 1.278(8) \text{ \AA}$. In this second anion, the intermolecular $O8 \cdots O12$ separation is very short at $2.476(7) \text{ \AA}$, and although a difference Fourier map indicated that atom H12 was closer to O12 than O8, a sharing of the donor-acceptor roles of these two O atoms could explain the similarities in C—O bond lengths. Refinements of other

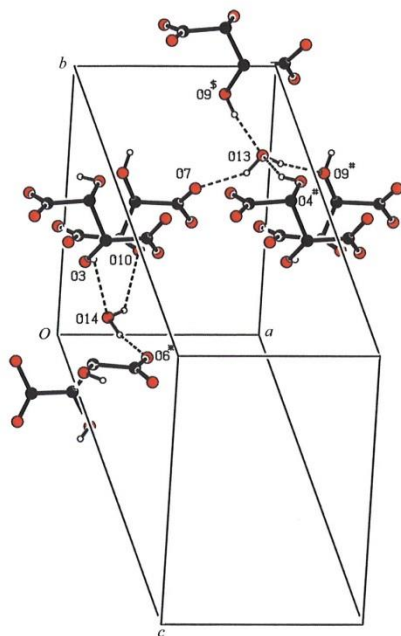


Figure 11
Part of the crystal structure of (III), showing the hydrogen-bonded tartrate monoanions crosslinked by water molecules, which act as donors and acceptors of hydrogen bonds. Atoms labelled with an asterisk (*), a hash symbol (#) or a dollar sign (\$) are at the symmetry positions $(-x, y - \frac{1}{2}, -z + \frac{1}{2})$, $(x + 1, y, z)$ or $(x + \frac{1}{2}, -y + \frac{3}{2}, -z)$, respectively. Hydrogen bonds are shown as dashed lines and H atoms not involved in the interactions have been omitted.

models involving H_3O^+ formation were unsatisfactory. The disulfide bond [$\text{S1}-\text{S2} = 2.038(3) \text{ \AA}$] adopts a *gauche* orientation, with a $\text{C2}-\text{S1}-\text{S2}-\text{C3}$ torsion angle of $75.3(2)^\circ$, and may be designated $\pm\text{RHS}$ spiral (Schmidt *et al.*, 2006). Here, the $\text{N1}-\text{C1}-\text{C2}-\text{S1}$ torsion angle is $-179.4(5)^\circ$ and this *trans*-planar arrangement is also present in cystamine hydrochloride (Vedavathi & Vijayan, 1979), whereas in (II) this arrangement is *gauche*. As in (I), each tartrate monoanion of (III) is linked into chains (Fig. 10) running parallel to (100) by a strong head-to-tail $\text{O1}-\text{H1}\cdots\text{O6}(x + 1, y, z)$ hydrogen bond, with $\text{O1}-\text{O6}(x + 1, y, z) = 2.554(7) \text{ \AA}$. These chains are crosslinked by two independent water molecules (Fig. 11) acting as acceptors and donors of hydrogen bonds. Furthermore, each protonated amino group is linked to four tartrate monoanions (Fig. 12), with one of the three protons, H4, engaged in bifurcated hydrogen-bond formation. Numerous hydrogen bonds are present and some have short donor-acceptor separations (Table 3). The resulting crystal packing is shown in Fig. 13.

Experimental

For the preparation of cysteamine tartrate(1 $-$) monohydrate (cysteamine hydrogen tartrate monohydrate), (I), millimolar

amounts (1:1 ratio) of cysteamine and L-(+)-tartaric acid were weighed and transferred into a 50 ml conical flask. A small amount (5 ml) of hot ethanol was added to the mixture, and the flask and contents were placed in a water bath, with swirling, at 323 K. After 10 min both starting materials remained solid, and so to aid dissolution the flask was stirred and heated to 333 K on a hot plate. Further quantities of solvent were added dropwise to the mixture until a clear solution was obtained. The whole process lasted for about an hour and a total volume of 15 ml of ethanol was used. The solution was then filtered, covered with Parafilm and left in the fume cupboard for crystallization to take place by slow evaporation. After 5 d, clear rod-shaped crystals of (I) separated from the product mixture. The crystals were then collected by gravity filtration and allowed to dry on filter paper. Attempts to cut crystals of (I) to a smaller size without damaging the crystals were unsuccessful.

For the preparation of cystamine tartrate(2 $-$), (II), and cystamine bis[tartrate(1 $-$)] dihydrate (cystamine hydrogen tartrate dihydrate), (III), millimolar amounts (1:1 ratio) of cystamine and L-(+)-tartaric acid were weighed and transferred into a 50 ml conical flask. Hot ethanol (5 ml) was added, resulting in the formation of a white precipitate, and the flask placed in a water bath at 323 K with swirling. Ethanol was added dropwise until a clear solution was obtained. A total volume of 20 ml of solvent was used. The solution was filtered, covered with Parafilm and left in the fume cupboard for crystallization to take place by slow evaporation. After 24 h, crystals [blades of (II) and needles of (III)] formed, and these were collected by gravity filtration and allowed to dry on filter paper. Product (III) also formed as a noncrystalline mass in the preparation of (I). Attempts to obtain high-quality crystals of (III) were only partially successful.

Compound (I)

Crystal data

$\text{C}_2\text{H}_8\text{NS}^+\cdot\text{C}_4\text{H}_5\text{O}_6^-\cdot\text{H}_2\text{O}$	$V = 1089.73(8) \text{ \AA}^3$
$M_r = 245.25$	$Z = 4$
Orthorhombic, $P2_12_12_1$	Mo $K\alpha$ radiation
$a = 7.0630(2) \text{ \AA}$	$\mu = 0.32 \text{ mm}^{-1}$
$b = 10.3833(5) \text{ \AA}$	$T = 120 \text{ K}$
$c = 14.8591(7) \text{ \AA}$	$0.84 \times 0.12 \times 0.1 \text{ mm}$

Data collection

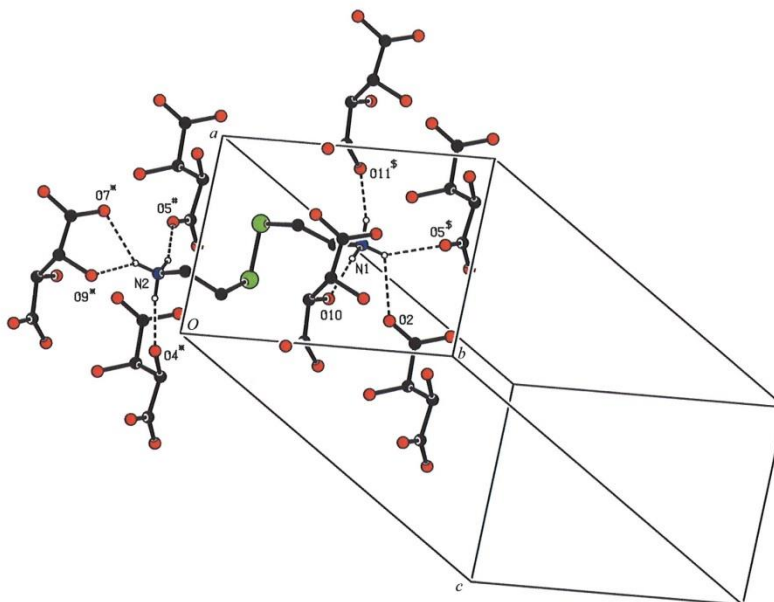
Bruker-Nonius KappaCCD area-detector diffractometer	9253 measured reflections
Absorption correction: multi-scan (SADABS; Sheldrick, 2007)	2485 independent reflections
$T_{\min} = 0.620$, $T_{\max} = 0.746$	2099 reflections with $I > 2\sigma(I)$
	$R_{\text{int}} = 0.051$

Table 1

Hydrogen-bond geometry (\AA , $^\circ$) for (I).

$D-H\cdots A$	$D-H$	$H\cdots A$	$D\cdots A$	$D-H\cdots A$
$\text{O1}-\text{H1}\cdots\text{O6}^{\text{i}}$	0.84	1.66	2.4885 (18)	169
$\text{O3}-\text{H3}\cdots\text{O7}^{\text{ii}}$	0.84	2.13	2.819 (2)	139
$\text{O4}-\text{H4}\cdots\text{O7}$	0.84	1.90	2.742 (2)	177
$\text{N1}-\text{H1A}\cdots\text{O3}^{\text{iii}}$	0.91	2.00	2.813 (2)	148
$\text{N1}-\text{H1B}\cdots\text{O2}^{\text{iv}}$	0.91	1.92	2.814 (2)	166
$\text{N1}-\text{H1C}\cdots\text{O5}^{\text{v}}$	0.91	1.89	2.772 (2)	162
$\text{N1}-\text{H1C}\cdots\text{O4}^{\text{i}}$	0.91	2.30	2.850 (2)	118
$\text{O7}-\text{H7A}\cdots\text{O5}^{\text{v}}$	0.87	1.89	2.7455 (19)	168
$\text{O7}-\text{H7B}\cdots\text{O6}^{\text{v}}$	0.77	2.14	2.8910 (19)	166

Symmetry codes: (i) $x + 1, y, z$; (ii) $-x + 1, y - \frac{1}{2}, -z + \frac{1}{2}$; (iii) $-x + 1, y + \frac{1}{2}, -z + \frac{1}{2}$; (iv) $-x + 2, y + \frac{1}{2}, -z + \frac{1}{2}$; (v) $x + \frac{1}{2}, -y + \frac{1}{2}, -z + 1$.

**Figure 12**

Part of the crystal structure of (III), showing the tartrate monoanions crosslinked by the protonated amino groups of the cystamine cation. Atoms labelled with an asterisk (*), a hash symbol (#) or a dollar sign (\$) are at the symmetry positions $(x, y - 1, z)$, $(x + 1, y - 1, z)$ or $(x + 1, y, z)$. Hydrogen bonds are shown as dashed lines and H atoms not involved in the interactions have been omitted.

Refinement

$$R[F^2 > 2\sigma(F^2)] = 0.039$$

$$wR(F^2) = 0.093$$

$$S = 1.06$$

2485 reflections

143 parameters

H atoms treated by a mixture of independent and constrained refinement

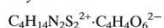
$$\Delta\rho_{\max} = 0.27 \text{ e } \text{\AA}^{-3}$$

$$\Delta\rho_{\min} = -0.25 \text{ e } \text{\AA}^{-3}$$

Absolute structure: Flack (1983),

1027 Friedel pairs

Flack parameter: -0.04 (9)

Compound (II)**Crystal data**

$M_r = 302.36$

Orthorhombic, $P2_12_12_1$

$a = 5.7281$ (3) \text{\AA}

$b = 9.3699$ (5) \text{\AA}

$c = 24.6770$ (14) \text{\AA}

$$V = 1324.46$$
 (12) \text{\AA}^3

$Z = 4$

Mo $K\alpha$ radiation

$\mu = 0.42$ mm⁻¹

$T = 120$ K

$0.36 \times 0.14 \times 0.03$ mm

Data collection

Bruker-Nonius KappaCCD area-

detector diffractometer

Absorption correction: multi-scan

(SADABS; Sheldrick, 2007)

$T_{\min} = 0.613$, $T_{\max} = 0.746$

9158 measured reflections

3020 independent reflections

2273 reflections with $I > 2\sigma(I)$

$R_{\text{int}} = 0.083$

Refinement

$$R[F^2 > 2\sigma(F^2)] = 0.060$$

$$wR(F^2) = 0.139$$

$$S = 1.05$$

3020 reflections

165 parameters

H-atom parameters constrained

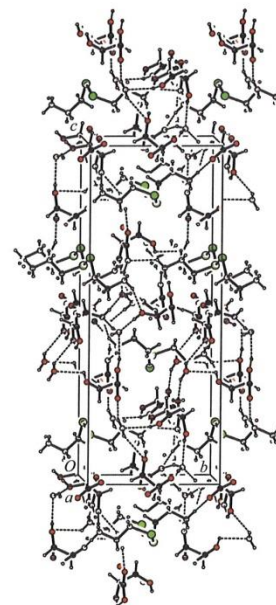
$$\Delta\rho_{\max} = 0.55 \text{ e } \text{\AA}^{-3}$$

$$\Delta\rho_{\min} = -0.43 \text{ e } \text{\AA}^{-3}$$

Absolute structure: Flack (1983),

1222 Friedel pairs

Flack parameter: 0.20 (13)

**Figure 13**

A view of the packing of the ions in the unit cell of (III). Hydrogen bonds are shown as dashed lines.

organic compounds

Table 2
Hydrogen-bond geometry (Å, °) for (II).

D—H...A	D—H	H...A	D...A	D—H...A
N1—H1A...O1 ⁱ	0.91	1.88	2.786 (4)	175
N1—H1B...O2 ⁱⁱ	0.91	1.82	2.705 (4)	162
N1—H1C...O3 ⁱⁱⁱ	0.91	1.99	2.892 (4)	170
N2—H2A...O3 ^{iv}	0.91	1.99	2.871 (4)	161
N2—H2B...O6 ^v	0.91	1.77	2.684 (4)	177
N2—H2C...O5 ^{vi}	0.91	1.87	2.727 (4)	155
O3—H3...O1	0.84	2.09	2.588 (4)	117
O3—H3...S1 ^{vii}	0.84	2.92	3.703 (3)	156
O4—H4...O5	0.84	2.13	2.613 (4)	116
O4—H4...O2 ^{viii}	0.84	2.20	2.889 (4)	139

Symmetry codes: (i) $x-1, y+1, z$; (ii) $x-\frac{1}{2}, -y+\frac{1}{2}, -z$; (iii) $x-\frac{1}{2}, -y+\frac{1}{2}, -z$; (iv) $x, y+1, z$; (v) $-x+2, y+\frac{1}{2}, -z+\frac{1}{2}$; (vi) $-x+1, y+\frac{1}{2}, -z+\frac{1}{2}$; (vii) $x, y-1, z$; (viii) $x-1, y, z$.

Table 3
Hydrogen-bond geometry (Å, °) for (III).

D—H...A	D—H	H...A	D...A	D—H...A
N1—H1A...O11 ⁱ	0.91	1.90	2.789 (8)	164
N1—H1B...O2	0.91	2.32	2.861 (8)	118
N1—H1B...O5 ^j	0.91	2.34	2.983 (8)	127
N1—H1C...O10	0.91	1.97	2.859 (7)	164
N2—H2A...O5 ⁱⁱⁱ	0.91	1.87	2.741 (8)	160
N2—H2B...O7 ⁱⁱⁱⁱ	0.91	2.16	2.948 (8)	145
N2—H2B...O9 ^v	0.91	2.27	2.987 (7)	136
N2—H2C...O4 ^{vi}	0.91	1.87	2.767 (7)	169
O1—H1...O6 ^{vii}	0.84	1.73	2.554 (7)	167
O3—H3...O14	0.84	2.39	2.819 (8)	113
O4—H4...O5	0.84	2.07	2.576 (7)	118
O4—H4...O13 ^{viii}	0.84	2.23	2.941 (7)	143
O9—H9...O13 ^{ix}	0.84	1.85	2.682 (7)	171
O10—H10...O11	0.84	2.05	2.572 (7)	119
O12—H12...O8 ^x	0.84	1.66	2.476 (7)	165
O13—H13A...O7	0.85	1.99	2.743 (7)	148
O13—H13B...O9 ^j	0.85	1.99	2.833 (7)	170
O14—H14A...O10	0.86	2.51	3.170 (8)	135
O14—H14B...O6 ^{xi}	0.87	1.97	2.786 (8)	156

Symmetry codes: (i) $x+1, y, z$; (ii) $x+1, y-1, z$; (iii) $x, y-1, z$; (iv) $x-1, y, z$; (v) $x-\frac{1}{2}, -y+\frac{1}{2}, -z$; (vi) $-x, y-\frac{1}{2}, -z+\frac{1}{2}$.

Compound (III)

Crystal data

$C_4H_{14}N_2S_2^{2+} \cdot 2C_4H_5O_6^- \cdot 2H_2O$	$V = 2084.8 (3) \text{ \AA}^3$
$M_r = 488.48$	$Z = 4$
Orthorhombic, $P2_12_12_1$	Mo $K\alpha$ radiation
$a = 7.3425 (5) \text{ \AA}$	$\mu = 0.33 \text{ mm}^{-1}$
$b = 10.5227 (8) \text{ \AA}$	$T = 120 \text{ K}$
$c = 26.983 (2) \text{ \AA}$	$0.22 \times 0.02 \times 0.02 \text{ mm}$

Data collection

Bruker–Nonius KappaCCD area-detector diffractometer	12189 measured reflections
Absorption correction: multi-scan (SADABS; Sheldrick, 2007)	3527 independent reflections
$T_{\min} = 0.363, T_{\max} = 1.000$	2471 reflections with $I > 2\sigma(I)$
	$R_{\text{int}} = 0.084$

Refinement

$R[F^2 > 2\sigma(F^2)] = 0.078$	$\Delta\rho_{\text{max}} = 0.42 \text{ e \AA}^{-3}$
$wR(F^2) = 0.152$	$\Delta\rho_{\text{min}} = -0.39 \text{ e \AA}^{-3}$
$S = 1.09$	Absolute structure: Flack, (1983),
3527 reflections	1396 Friedel pairs
271 parameters	Flack parameter: $-0.1 (2)$
H-atom parameters constrained	

Unless otherwise indicated below, H atoms were placed in geometrically idealized positions and constrained to ride on their

parent atoms, with C—H = 1.00 (methine) or 0.99 Å (methylene), O—H = 0.84 Å and N—H = 0.91 Å, and with $U_{\text{iso}}(\text{H}) = 1.2U_{\text{eq}}(\text{carrier})$. For (I), the position of the S-bound H atom was refined freely, while those of the water H atoms were refined freely initially, but then constrained to ride on their parent O atom. The water and hydroxy H atoms were assigned $U_{\text{iso}}(\text{H}) = 1.3U_{\text{eq}}(\text{O})$. For (III), the water H-atom positions were refined initially, with distance restraints of O—H = 0.85 (2) Å and H...H = 1.34 (2) Å, but were then constrained to ride on their parent O atoms. The water and hydroxy H atoms were assigned $U_{\text{iso}}(\text{H}) = 1.5U_{\text{eq}}(\text{O})$.

For all compounds, data collection: *COLLECT* (Nonius, 1998); cell refinement: *DENZO* (Otwinowski & Minor, 1997) and *COLLECT*; data reduction: *DENZO* and *COLLECT*; program(s) used to solve structure: *SHELXS97* (Sheldrick, 2008); program(s) used to refine structure: *SHELXL97* (Sheldrick, 2008); molecular graphics: *PLATON* (Spek, 2009); software used to prepare material for publication: *SHELXL97*, *PLATON*, *pubCIF* (Westrip, 2010) and *WinGX* (Farrugia, 2012).

The authors thank the EPSRC UK National Crystallographic Service at the University of Southampton for the collection of the crystallographic data (Coles & Gale, 2012).

Supplementary data for this paper are available from the IUCr electronic archives (Reference: YP3029). Services for accessing these data are described at the back of the journal.

References



- Ahmad, S., Shaheen, M. A. & Stoeckli-Evans, H. (2010). *Acta Cryst.* **E66**, o134.
- Cairns, D., Anderson, R. J., Coulthard, M. & Terry, J. (2002). *Pharm. J.* **269**, 615–616.
- Coles, S. J. & Gale, P. A. (2012). *Chem. Sci.* **3**, 683–689.
- Farrugia, L. J. (2012). *J. Appl. Cryst.* **45**, 849–854.
- Flack, H. D. (1983). *Acta Cryst.* **A39**, 876–881.
- Gahl, W. A., Kuel, E. M., Iwata, F., Lindblad, A. & Kaiser-Kupfer, M. I. (2000). *Mol. Genet. Metab.* **71**, 100–120.
- Gahl, W. A., Theone, J. G. & Schneider, J. (2001). *Cystinosis: A Disorder of Lysosomal Membrane Transport. The Metabolic and Molecular Basis of Inherited Disease*, 8th ed., edited by C. R. Scriver, A. R. Beaudet, W. Sly & D. Valle, pp. 5085–5108. New York: McGraw-Hill.
- Gahl, W. A., Theone, J. G. & Schneider, J. A. (2002). *N. Engl. J. Med.* **347**, 111–121.
- Kay, G., Cairns, D., McGaughan, B. & Warasiba, B. (2007). *J. Pharm. Pharmacol.* **59**(S1), A7–A8.
- Kim, C.-H., Parkin, S., Bharara, M. & Attwood, D. (2002). *Polyhedron*, **21**, 225–228.
- McGaughan, B., Kay, G., Knott, R. M. & Cairns, D. (2008). *Bioorg. Med. Chem. Lett.* **18**, 1716–1719.
- Nonius (1998). *COLLECT*. Nonius BV, Delft, The Netherlands.
- Otwinowski, Z. & Minor, W. (1997). *Methods in Enzymology*, Vol. 276, *Macromolecular Crystallography*, Part A, edited by C. W. Carter Jr & R. M. Sweet, pp. 307–326. New York: Academic Press.
- Schmidt, B., Ho, L. & Hogg, P. J. (2006). *Biochemistry*, **45**, 7429–7433.
- Sheldrick, G. M. (2007). *SADABS*. Bruker AXS Inc., Madison, Wisconsin, USA.
- Sheldrick, G. M. (2008). *Acta Cryst.* **A64**, 112–122.
- Smith, G., Wermuth, U. D. & White, J. M. (2006). *Acta Cryst.* **C62**, o694–o698.
- Spek, A. L. (2009). *Acta Cryst.* **D65**, 148–155.
- Steiner, T. (2000). *Acta Cryst.* **C56**, 876–877.
- Suresh, J., Krishnakumar, R. V., Rajagopal, K. & Natarajan, S. (2006). *Acta Cryst.* **E62**, o3220–o3222.
- Sweetman, S. C. (2011). *Martindale: The Complete Drug Reference*, 37th ed. London: Pharmaceutical Press. <http://www.medicinescomplete.com/mc/martindale/current/>
- Touchman, J. W., Anikster, Y., Dietrich, N. L., Maduro, V. V., McDowell, G., Shotelersuk, V., Bouffard, G. G., beckstrom-Stenberg, S. M., Gahl, W. A. & Green, E. D. (2000). *Genome Res.* **10**, 165–173.
- Vedavathi, B. M. & Vijayan, K. (1979). *Curr. Sci.* **48**, 1028–1030.
- Westrip, S. P. (2010). *J. Appl. Cryst.* **43**, 920–925.

**Poster Presentation at the Seventh International Cystinosis Conference – Paris, France - June 2012 .
Synthesis and *in vitro* evaluation of novel pro-drugs for the treatment of nephropathic cystinosis.**

Design, synthesis and evaluation of novel pro-drugs for the treatment of Nephropathic Cystinosis

A. Benylles*, G. Kay, E. Hector and D. Cairns

School of Pharmacy & Life Sciences, Robert Gordon University, Schoolhill, Aberdeen

INTRODUCTION

Cystinosis is a rare autosomal recessive disease, where raised intracellular levels of the amino acid, cystine, cause crystals to form in every organ of the body¹ (Fig. 1)

Young children are mostly affected by the disease causing a premature death due to kidney failure.

Symptoms include renal Fanconi syndrome, photophobia, growth retardation, rickets.

Treatment involves a 6 hourly administration of cysteamine usually as Cystagon. However, this drug is associated with debilitating side effects such as gastric irritation, halitosis and body odour resulting in poor patient compliance² (Fig. 2)

Increased life expectancy has been reported amongst cystinotic patients but the treatment is not curative of the disease.

Novel pro-drugs of cysteamine and cystamine have been designed and synthesised to minimise body odour and GI irritation³

Overall goal will be to produce an odourless, tasteless and orally active treatment for cystinosis and, if possible, improve on the current dosing regimen of every 6h.

Sides effects will be minimised or even entirely abolished, leading to:

Improved quality of life of both cystinotic patients and their families.

Successful pro-drug candidates are currently under evaluation for their ability to deplete cystine in cultured cystinotic cells.

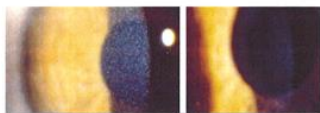
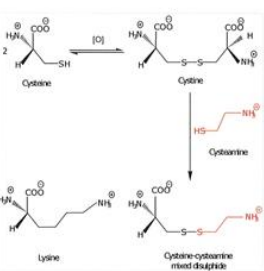
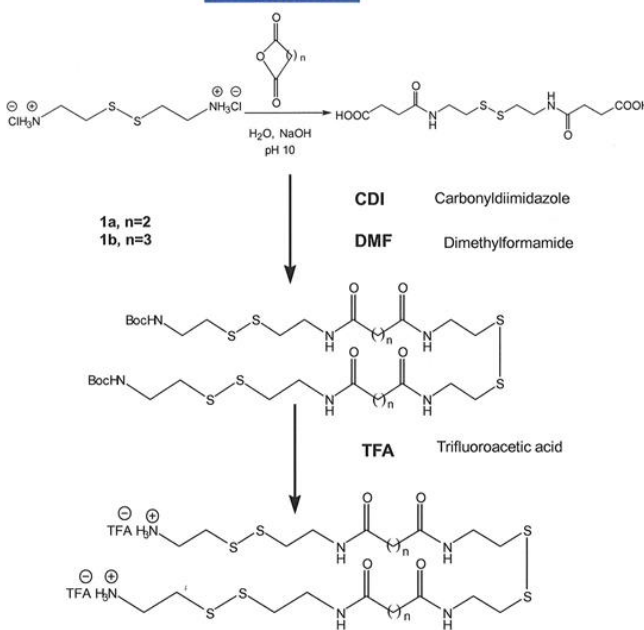


Fig.1. Corneal cystine crystals

CONCLUSION

To date, a number of cysteamine prodrugs have been synthesised and fully characterised. Compounds 1a and 1b have been evaluated *in vitro* and displayed significantly greater ability to deplete cystine in cultured cystinotic cells. (Fig. 3)

METHODS



BIOLOGICAL EVALUATION

Cystinotic fibroblasts were treated with 50 μM of compounds 1a and 1b with cysteamine as control. Cell growth was measured over a 72 h period as shown in Fig. 3.

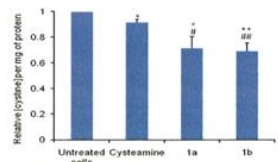


Fig. 3. Cystine depletion in cystinotic fibroblasts. Untreated cells: * p < 0.05, ** p < 0.01. Cysteamine treated cells: * p < 0.05, ** p < 0.01

1. Gahl, W.A.; Thoene, J.G.; Schneider, J.A. *N. Engl. J. Med.* 2002, 347, 111.
2. Cairns, D.; Anderson, R.J.; Coulthard, M.; Terry, J. *Pharm. J.* 2002, 269, 615.
3. Omran, Z. et al. Synthesis and *in vitro* Evaluation of novel pro-drugs for the treatment of nephropathic cystinosis. *Bioorg. Med. Chem.* 2011; 19: 3492-3496

The authors gratefully acknowledge support from The Institute of Health and Welfare Research.